DISSERTATION

CHARACTERIZING BIOMASS COMBUSTION EMISSION CONTRIBUTIONS TO AMBIENT AEROSOL CONCENTRATIONS

Submitted by

Guenter Engling

Department of Atmospheric Science

In partial fulfillment of the requirements

For the Degree of Doctor of Philosophy

Colorado State University

Fort Collins, Colorado

Spring 2006

COLORADO STATE UNIVERSITY

December 12, 2005

WE HEREBY RECOMMEND THAT THE DISSERTATION PREPARED UNDER OUR SUPERVISION BY GUENTER ENGLING ENTITLED CHARACTERIZING BIOMASS COMBUSTION EMISSION CONTRIBUTIONS TO AMBIENT AEROSOL CONCENTRATIONS BE ACCEPTED AS FULFILLING IN PART REQUIREMENTS FOR THE DEGREE OF DOCTOR OF PHILOSOPHY.

Committee on Graduate Work

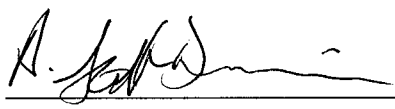

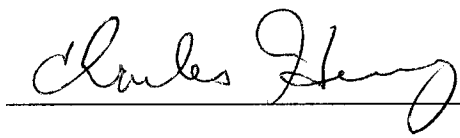

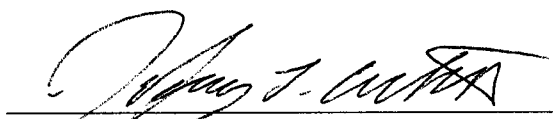

Adviser

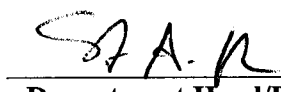

Department Head/Director

ABSTRACT OF DISSERTATION

CHARACTERIZING BIOMASS COMBUSTION EMISSION CONTRIBUTIONS TO AMBIENT AEROSOL CONCENTRATIONS

Atmospheric aerosol particles are known to exert significant effects on air quality, human health, ecosystem health, visibility, and the radiative balance of the atmosphere. Because of their relatively long lifetimes, the influence of submicron (fine) aerosol particles can be exerted far downwind of their source. Biomass combustion is a major global source of atmospheric fine particles and organic matter in particular. Quantifying the impacts of biomass combustion aerosol far from its source is difficult, but is a national priority given the frequency of fires in several parts of the U.S. and federal land manager plans to increase prescribed burning in the coming years.

In recent years the most common approach to apportioning ambient carbonaceous aerosol among different source types has involved the use of organic molecular markers which serve as source specific tracers. The most popular tracer for biomass combustion is levoglucosan, a combustion product of cellulose. Traditional methods for measuring levoglucosan involve organic solvent extraction, chemical derivatization, and Gas Chromatography-Mass Spectrometry (GC-MS) analysis of aerosol filter samples collected over periods of 24 hr or more. This analytical approach is labor intensive and expensive, precluding its widespread use in routine air quality monitoring networks. In addition, source profiles for biomass combustion, are mostly limited to residential wood combustion sources, leaving a need for new emissions profiles characteristic of wild and prescribed fires, which burn a greater mix of fuel types under a wide range of conditions. The research presented here consists of three primary efforts: (1) development of simpler, less expensive techniques for measurement of levoglucosan and other biomass

combustion products, (2) examination of the contributions of biomass combustion to ambient aerosol at a typical visually protected environment in the western U.S. (Yosemite National Park), and (3) examination of the variability in source marker emission profiles for a variety of fuel types burned under a range of conditions characteristic of those expected in wild and prescribed fires.

Three alternative measurement techniques that are sensitive and precise, yet cost effective and easy to use, were explored and optimized for the determination of biomass combustion source tracers: high performance anion exchange chromatography, micro-chip capillary electrophoresis, and an enzyme biosensor.

Sources of high summertime concentrations of organic aerosol in the western U.S. were investigated during the Yosemite Aerosol Characterization Study conducted in the summer of 2002. Primary contributions of biomass smoke to fine particle organic carbon were estimated to be as high as 100% on selected days due to the influence of local fires in addition to fires prevailing in Southern Oregon and other parts of California. High concentrations of monoterpene oxidation products and other organic compounds of secondary origin also indicated a significant contribution of secondary organic aerosol to ambient fine particle concentrations. An important portion of secondary species was likely associated with smoke from biomass combustion.

Emission signatures of carbonaceous material from the open combustion of biofuels were determined as a function of combustion conditions. Emissions of biomass combustion tracers showed a wide range of values as a function of fuel type and combustion conditions. Levoglucosan emission factors for the same combustion conditions differed between individual types of biomass by one order of magnitude, while combustion phase and burn direction generally resulted in variations between emission factors on the order of 2 to 3 for the same fuel

type. The need for more detailed emission profiles of molecular source tracers, reflecting the various combustion conditions that are characteristic of wildfires and prescribed burns, was demonstrated.

Guenter Engling
Atmospheric Science Department
Colorado State University
Fort Collins, CO 80523
Spring 2006

ACKNOWLEDGEMENTS

With great appreciation for the outstanding guidance in my research, I thank my advisor, professor Jeff Collett. Professor Collett provided excellent insights into various research topics, giving helpful advice and always being available for discussions or just a quick question, yet encouraging me to seek solutions independently.

I would also like to thank my committee members, professors Sonia Kreidenweis, Chuck Henry, and Scott Denning, for their advice. On numerous occasions, Dr. Pierre Herckes provided valuable, hands-on advice and insights to my research projects. The advice and help from various co-workers, including Dr. Kip Carrico, Dr. Jackie Carrillo, Dr. Carlos Garcia, Dr. Lynn Rinehart, Taehyoung Lee, Courtney Gorin, Gavin McMeeking, and the rest of the Collett and Kreidenweis groups, is also greatly appreciated. Special thanks are due to Connie Hale for her outstanding administrative support and providing extra help when needed.

Researchers from various institutes provided support, data, and advice critical to the results presented in this dissertation. Thanks are due in particular to Dr. Bill Malm and Derek Day from CIRA; Dr. Ron Sussott, Dr. Ron Babbitt, Dr. Wei Min Hao, Emily Lincoln, and Cyle Wold from the Forest Service Fire Science Lab; Dr. Yoshi Iinuma from IfT; Dr. Lowell Ashbaugh and Dr. Chuck McDade from the IMPROVE team; Dr. Graham Bench at Lawrence Livermore National Lab; Katie Warner in Yosemite National Park; and Air Resource Specialists. The National Park Service is acknowledged for proving the funding for most of the work presented.

Lastly, yet with utmost appreciation, I thank my wife, Shirley, for her moral support and understanding for late nights spent in the lab, as well as my parents and siblings for their encouragement and support during my graduate odyssey.

TABLE OF CONTENTS

LIST OF FIGURES

LIST OF TABLES

LIST OF ACRONYMS AND SYMBOLS

AEC	anion exchange chromatography
BC	black carbon
BSTFA	bis(trimethylsilyl)trifluoroacetamind
CC	carbonate carbon
CE	capillary electrophoresis
CMB	chemical mass balance
CPI	carbon preference index
DCM	dichloromethane
DRI	Desert Research Institute
EC	elemental carbon
ECD	electrochemical detection
EI	electron impact
ELSD	evaporative light scattering detection
EOF	electro-osmotic flow
ESI	electrospray ionization
FS	Forest Service
FSL	Fire Science Lab
GC	gas chromatography
Hi-Vol	high volume
HPAEC	high performance anion exchange chromatography
HPLC	high performance liquid chromatography
HULIS	humic-like substances
IC	ion chromatography
IfT	Institute for Tropospheric Research

IMPROVE	Interagency Monitoring of Protected Visual Environments
IS	internal standards
IUPAC	International Union of Pure and Applied Chemistry
LC	liquid chromatography
LG	levoglucosan
MDL	method detection limit
MPI	Max Plank Institute
MS	mass spectrometry
MSD	mass selective detector
m/z	mass/charge ratio
NAAQS	National Ambient Air Quality Standard
NIFC	National Interagency Fire Center
NIOSH	National Institute for Occupational Safety and Health
OM	organic matter
OC	organic carbon
PAD	pulsed amperometric detection
PAH	polynuclear aromatic hydrocarbons
PDMS	polydimethylsiloxane
PILS	particle-into-liquid-sampler
PM	particulate matter
$PM_{2.5}$	particulate matter with an aerodynamic diameter of less than 2.5 μm
PM_{10}	particulate matter with an aerodynamic diameter of less than 10 μm
QA	quality assurance
Q-TOF	quadrupole time-of-flight
RH	relative humidity
RI	refractive index

RSD	relative standard deviation
SFC	supercritical fluid chromatography
SOA	secondary organic aerosol
SOP	standard operating procedure
SVOC	semi-volatile organic compounds
TIC	total ion count
TC	total carbon
TMCS	trimethylchlorosilane
TMS	trimethyl silyl
TOR	thermal-optical reflectance
TOT	thermal-optical transmission
TSP	total suspended particles
USDA	United States Department of Agriculture
VOC	volatile organic compounds
WSOC	water-soluble organic compounds
YACS	Yosemite Aerosol Characterization Study

CHAPTER 1 INTRODUCTION

Air quality and air pollution have become topics of high public and legislative interest over the past decades, as emissions from various sources have increased dramatically with considerable impact on human health, visibility, and global climate. Aerosol particles play an important role in the processes affecting air quality, human health, ecosystems, and the radiative balance of the atmosphere (Abas et al., 2004a, Charlson et al., 1992, Crutzen and Andreae, 1990, Hobbs et al., 1997, McKenzie et al., 1995, Penner et al., 1994, Penner et al., 1992, Reid et al., 2005a, Riebau and Fox, 2001, Wu et al., 2002). Biomass combustion in particular is a major global source of atmospheric trace gases and fine particulate matter (PM), primarily composed of organic matter (OM) with estimated annual emissions of $34 \cdot 10^9$ kg (Bond et al., 2004). Hence, OM can be the major constituent of fine atmospheric particles in certain regions, such as the western U.S., with contributions to fine particle mass concentrations reaching 50% or more (Malm et al., 2004). Residential burning of wood in fireplaces and wood stoves has significant impacts on local and regional air quality; forest and brush fires, as well as slash and burn agriculture, continue to impose a significant impact on natural and man-made environments on local, regional, and global scales.

After 80 years of fire suppression in the U.S., the western states in particular have experienced wildfires of unusual magnitude over the past decade due to build-up of excessive (i.e., unnatural) amounts of fuel. Scientists and forest managers now agree that natural forest ecosystems require fire at regular intervals to maintain a healthy state. Therefore, land management agencies have

recently developed new wildland fire policies with the ultimate goal to restore natural forests in the western United States by conducting prescribed burns. These policies may be in discord with recent changes in air quality policies implemented by the US government in form of the National Ambient Air Quality Standard (NAAQS) and amendments to the Clean Air Act. In particular, the EPA regional haze rule (U.S. EPA, 1999) requires states to develop emission reduction plans with the ultimate goal of achieving natural visibility conditions within a time frame of approximately 60 years. Nevertheless, biomass burning is expected to contribute increasingly to regional ambient PM levels in the near future. It is therefore important to improve our understanding of emission characteristics of wildland fires, i.e., to investigate the chemical and physical characteristics of smoke PM, in order to assess the environmental impact of biomass combustion emissions. Smoke from prescribed fires can be a significant contributor to haze, causing substantial visibility impairment on regional scales as smoke plumes can be subject to atmospheric transport over distances of hundreds to thousands of kilometers.

Despite several recent investigations, emission characteristics of biomass burning are still not well understood, particularly in terms of the chemical composition of biomass smoke as a function of combustion conditions. Whereas several emission source profiles have been generated for wood combustion in residential wood stoves and fireplaces (e.g., Fine et al., 2004a, Hedberg et al., 2002, McDonald et al., 2000, Schauer et al., 2001), limited emissions data have been reported from open combustion of biomass (Hays et al., 2005, Hays et al., 2002, Iinuma et al., 2006, Lee et al., 2005). As fuel composition and combustion regimes are significantly different between wildfires and controlled burning in fireplaces and wood stoves, it is important to obtain detailed emission profiles under conditions representative of real-world wildfires. Numerous chemical constituents (> 300 individual chemical species), generated during the combustion of biomass by direct volatilization or thermal decomposition of plant material, have been identified in these studies. Furthermore, secondary reactions are presumed to be enhanced

during or as a result of fires (Alessio et al., 2004), leading to the formation of secondary organic aerosol (SOA). An important fraction of the SOA may be comprised of water-soluble organic compounds (WSOC). These may have significant effects on aerosol optical properties, in part due to their hygroscopic nature. However, typically only 15 to 20% of the fine organic particle mass is identified in terms of individual organic species (e.g., Schauer and Cass, 2000). Therefore, additional research, such as the efforts documented in this dissertation, is needed to better characterize OM constituents in biomass smoke directly at the source as well as in ambient PM downwind of wildland fires. The utilization of newly developed analytical approaches, in particular for molecular source tracers, may aid in this process.

An important factor in the assessment of air quality and the study of air pollution is the determination of source contributions. Various methods have been utilized to apportion source contributions to urban and remote air masses. For instance, in assessing source contributions to the organic carbon (OC) fraction, carbon-14 isotope measurements have been used to discriminate between contemporary sources and fossil fuel combustion (Bench and Herckes, 2004, Sheffield et al., 1990). Biogenic and anthropogenic sources can also be distinguished with the carbon preference index (CPI) of alkanes or carboxylic acids (Simoneit, 1989). Specific compounds emitted preferentially by certain sources or source types can be used as molecular markers to determine sources, transport, transformations, and fate of measured ambient PM. Such biomarker species (aka source tracers) have been utilized extensively in source apportionment approaches. Chemical mass balance receptor models are commonly used to determine the contributions of different emission sources to atmospheric fine-particle samples, utilizing a set of specific marker species (Schauer et al., 1996, Zheng et al., 2002). An overview of commonly used molecular markers for a variety of emission sources is given in Table 1-1.

Table 1-1. Overview of source-specific molecular markers, including selected key references.

Source	Molecular Markers	References
Vehicle Emissions	Hopanes and steranes	(Fraser et al., 1998, Schauer et al., 2002a)
Meat Cooking	Cholesterol	(Kleeman et al., 1999, Rogge et al., 1991)
Cigarette Smoke	Iso- and ante-iso alkanes	(Kavouras et al., 1998b, Kleeman et al., 1999, Rogge et al., 1994)
Biomass Combustion	Methoxyphenols	(Fine et al., 2001, Hawthorne et al., 1988, Simoneit, 2002, Simoneit et al., 1993, Simpson et al., 2005)
	Resin acids	(Fine et al., 2001, Schauer et al., 2001, Simoneit, 2002, Simoneit et al., 1993)
	Retene	(Ramdahl, 1983)
	Anhydrosugars	(Fraser and Lakshmanan, 2000, Hornig et al., 1985, Simoneit et al., 1999, Zdrahal et al., 2002)
Secondary Organic Aerosol	Dicarboxylic acids	(Glassius et al., 2000)
	Pinene oxidation products	(Grosjean et al., 1993, Jang and Kamens, 1999, Jaoui and Kamens, 2003, Schrader et al., 1999, Warscheid and Hoffmann, 2001)

Traditionally, water-soluble potassium (K^+), not of soil or sea salt origin, has been used as a biomass combustion tracer (Andreae, 1983, Leslie, 1981, Lewis et al., 1986, Morales et al., 1996, Zweidinger et al., 1990), although several additional sources for K^+ have been reported, including meat cooking and vegetation (Lawson and Winchester, 1979, Morales et al., 1996, Schauer et al., 1999, 2002). As some of these sources may produce K^+ associated with fine particles as well (similar to biomass smoke particles), K^+ observed in ambient fine particles may not be an exclusive indication of biomass combustion sources.

Over the past decade organic biomarker compounds have been extensively used as source tracers, as they provide more precise information about specific sources. Biomass combustion in particular results in the emission of a variety of compounds associated with the different chemical

constituents of biomass. The major components of plant biomass include three classes of biopolymers: cellulose (40 - 50%), hemicellulose (20- 35%), and lignin (15 - 35%). Thermal degradation of cellulose results in the generation of anhydrosugars, including levoglucosan (1,6-anhydro-β-D-glucopyranose), the single most abundant constituent in biomass smoke (Hornig et al., 1985, Simoneit et al., 1999). Consequently, levoglucosan has been observed as a major component in ambient aerosol particles influenced by biomass combustion (Abas et al., 2004b, Engling et al., 2006b, Fraser and Lakshmanan, 2000, Gao et al., 2003, Palma et al., 2004, Poore, 2002, Schkolnik et al., 2005, Simoneit et al., 2004, Simoneit et al., 1999, Yttri et al., 2005, Zdrahal et al., 2002). Likewise, thermal decomposition products of hemicellulose include the isomers of levoglucosan, mannosan (1,6-anhydro-β-D-mannopyranose) and galactosan (1,6-anhydro-β-D-galactopyranose). Lignin breakdown products include a variety of substituted aromatic compounds, referred to as methoxyphenols, containing one or more methoxy groups and in most cases additional functional groups, such as carboxyl, carbonyl, or alkyl groups (Hawthorne et al., 1987, Simpson et al., 2005). The combustion of softwood also produces resin acids and retene, present in the extractives of softwood (Ramdahl, 1983, Simoneit et al., 1993, Standley and Simoneit, 1994).

Organic constituents in atmospheric aerosol particles are commonly determined by gas chromatography with mass spectrometric detection (GC-MS). However, as mentioned above, the combined mass of all individual quantified species typically accounts for less than 20% of the carbonaceous particle mass. Therefore, additional analytical methods are needed for a more comprehensive characterization of OM by providing complementary information to GC-MS analyses. Moreover, simpler and less expensive alternative methods are necessary for applications in routine and semi-continuous measurements, particularly in monitoring networks. Alternative analytical methods are specifically needed for polar, thermally labile, and non-volatile

compounds present in atmospheric aerosol. These methods also need to be sufficiently sensitive, as many organic PM constituents are present at rather low concentrations (pg to ng/m^3). While several complementary methods to GC-MS have been utilized for the determination of selected compound classes, additional more sensitive and selective methods need to be developed for certain aerosol species, in particular tracer compounds for biomass combustion emissions. The methods investigated here (as described below in sections 2.3. to 2.5.) are attempts to develop and optimize alternative measurement techniques for biomass combustion molecular markers that are sensitive and reliable, yet cost effective and easy to use. Such methods would allow monitoring of carbonaceous aerosol species at high time resolution, providing a better understanding of chemical and transport processes that occur on rather short time scales in the troposphere.

In response to the needs outlined above, including the need for alternative analytical methods for biomass combustion source tracers and better characterization of organic constituents in biomass smoke or ambient particles influenced by biomass combustion, the current research was based on the following key objectives:

• The first general objective was to develop and optimize alternative analytical methods for the separation, identification, and quantification of biomass combustion source tracers. Three methods based on liquid chromatography (LC), capillary electrophoresis (CE), and a biosensor were investigated. The results of these efforts are presented below in chapter 2. More concise descriptions of two of these methods (HPAEC-PAD and CE-PAD) can be found in peer-reviewed journal articles (Engling et al., 2006a, Garcia et al., 2005).

• The second main objective was to investigate the sources of high OM concentrations in summertime aerosol in the western U.S. This was addressed during the Yosemite Aerosol

Characterization Study (YACS) conducted in the summer of 2002. Contributions to the ambient aerosol were determined from different source types, with a particular focus on biomass combustion and biogenic secondary organic aerosol (SOA). Results from this study are discussed in chapter 3 and have been summarized in a journal article (Engling et al., 2006b).

• The third main objective was to characterize the emission signatures of carbonaceous material from the open combustion of biofuels as a function of combustion conditions. Emission factors of molecular tracers for biomass smoke were determined for various fuel types and combustion conditions. The findings from this study, conducted at the US Forest Service Fire Science Laboratory, are presented in Chapter 4, while a summary of the results can be found in Engling et al. (2006a).

CHAPTER 2 SMOKE MARKER MEASUREMENT METHODS

2.1. INTRODUCTION

Organic constituents in atmospheric aerosol particles are typically quantified by gas chromatography with mass spectrometric detection (GC-MS). Over the past three decades GC-MS has been successfully utilized for the characterization of ambient and source samples, providing simultaneously qualitative and quantitative information regarding aerosol components (e.g., Fraser et al., 2003, Schauer and Cass, 2000, Schauer et al., 1996, Zheng et al., 2002). As many as 300 individual organic compounds have been identified and quantified by GC-MS in fine atmospheric PM during recent field studies. However, the combined mass of these individual species typically accounts for only up to 20% of the carbonaceous particle mass due to three main reasons: (1) only a fraction of the organic carbon is extracted from PM collected on filters because of the limited choice of GC-MS compatible solvents which results in the discrimination against more polar organic compounds in the aerosol; (2) some of the compounds present in the solvent extracts may interact with GC columns too strongly or they are not sufficiently volatile to elute from the column; (3) those compounds that are extractable and elute may not be resolved well enough for unambiguous identification by mass spectrometry. Therefore, additional analytical methods are necessary for a more comprehensive characterization of carbonaceous aerosol particles. Moreover, simpler and less expensive alternative methods are needed for potential applications in semi-continuous measurements and for possible use in large

monitoring networks. Such methods are most likely not going to replace established techniques, such as GC-MS, but rather provide complementary analytical information.

2.1.1. Alternative Analytical Methods

Alternative analytical methods are particularly required for more polar, thermally labile, and non-volatile, i.e., higher molecular weight, compounds present in atmospheric aerosol. These methods also need to be sufficiently sensitive, since many organic PM constituents are present at rather low concentrations in ambient aerosol particles. In addition, such methods should be less expensive and easy to use. While several complementary methods to GC-MS have been utilized for the determination of selected compound classes, new methods that are more sensitive and selective for additional aerosol species, in particular tracer compounds for biomass combustion emissions, need to be developed, such as those methods investigated here and described below (sections 2.3. to 2.5.).

High performance liquid chromatographic (HPLC) and supercritical fluid chromatographic (SFC) methods have shown promising results, particularly for the characterization of polar organic compounds, since aqueous extracts can be injected onto most HPLC columns. In addition, chemical derivatization, as required for polar compound determinations by GC-MS, is not necessary in HPLC and SFC analyses. Nevertheless, HPLC and SFC methods have not been widely used for the characterization of organic aerosol particles, except for preparative LC separations according to compound polarity or according to certain compound classes prior to analysis by GC-MS or other methods (Bushby et al., 1993, Chang et al., 2005, Decesari et al., 2000, Shimmo et al., 2002, Shimmo et al., 2004). The few analytical applications of HPLC in atmospheric aerosol analyses reported in the literature are mainly limited to determinations of polycyclic aromatic hydrocarbons (PAH) and organic acids (Anttila et al., 2005, Eiguren-Fernandez and Miguel, 2003, Glasius et al., 2000, Kiss et al., 1997, Koeber et al., 1999, Lewis et

al., 1995, Lintelmann et al., 2005, Schnelle et al., 1996, Schuetzle et al., 1982). The limited use of HPLC and SFC methods in organic aerosol analysis is mainly due to two reasons. First, HPLC columns are typically designed to separate only selected compound classes, therefore requiring several different columns for a more comprehensive characterization of atmospheric PM extracts. Second, common detectors, including UV absorption or fluorescence detectors, are not suitable for the detection of many organic compounds due to the lack of chromophoric or fluorophoric groups in the analyte molecules, unless the sample is chemically derivatized which again adds complexity and potential artifacts to the analysis. Other detection techniques, such as refractive index (RI) or evaporative light scattering detection (ELSD) have been used for the determination of polar compounds, such as carbohydrates in food and other matrixes (Calull et al., 1992, Herbreteau et al., 1999, Lopez Hernandez et al., 1998, Morin-Allory and Herbreteau, 1992), but they lack sensitivity and selectivity helpful for atmospheric aerosol analysis. Electrochemical detection methods coupled with HPLC provide higher sensitivity and selectivity, particularly for carbohydrate analyses (Baldwin, 1999, Cataldi et al., 2003, Jandik et al., 2004, Lu and Cassidy, 1993, O'Shea and Lunte, 1993, Zook and LaCourse, 1995). For example, anion exchange chromatography (AEC) coupled with pulsed amperometric detection (PAD) is a superior method for the determination of carbohydrates (Cataldi et al., 2000, Jandik et al., 2004). This method has recently been used for the analysis of anhydrosugars, including levoglucosan, mannosan, and galactosan, present in biomass combustion aerosol (Engling et al., 2006a, Gao et al., 2003). Recently developed mass spectrometric detection methods coupled with HPLC show promising capabilities for the determination of additional carbonaceous species in atmospheric aerosol particles, such as humic-like substances (HULIS) and oxidation products of primary biogenic emissions (Anttila et al., 2005, Glasius et al., 1999, Gora and Hutta, 2005, Jaoui and Kamens, 2003, Larsen et al., 2001, Reemtsma and These, 2005, Samburova et al., 2005, Schkolnik et al., 2005, Schrader et al., 2001).

Electrically driven micro-column separation methods, such as capillary electrophoresis (CE), have several intrinsic advantages over HPLC. The high resolving power of these methods and short analysis times, in addition to requiring only small sample amounts, allow for very fast and selective separations. Furthermore, no sample pre-treatment is necessary and the operation of CE systems is relatively simple. Similar to HPLC, CE is based on aqueous separation, and thus suitable for the analysis of water-soluble compounds. Therefore, CE has been successfully used for the determination of various inorganic and organic compounds, including carbohydrates (Honda, 1996, O'Shea and Lunte, 1993, Oefner et al., 1994, Paulus and Klockow, 1996), carboxylic acids (Dabek-Zlotorzynska et al., 2005, Dabek-Zlotorzynska et al., 2001, Kiss et al., 1997, Krivacsy et al., 1997), and higher-molecular weight compounds, such as HULIS (Havers et al., 1998, Krivacsy et al., 2000). However, only a limited number of CE applications to atmospheric aerosol samples have been reported. Nevertheless, several compound classes, including carbohydrates, carboxylic acids, methoxyphenols, and HULIS, have been successfully determined in atmospheric particles by various CE methods (Dabek-Zlotorzynska et al., 2005, Garcia et al., 2005, Havers et al., 1998, Iinuma et al., 2004, Iinuma and Herrmann, 2003, Krivacsy et al., 2000, Krivacsy et al., 1997).

The recent developments of microchip-based analysis systems, also referred to as "lab-on-a-chip" or micro total analysis systems (μ-TAS), have taken CE and LC separations to another level of performance (e.g., Baldwin et al., 2002, Fanguy and Henry, 2002, Figeys and Pinto, 2000, Garcia et al., 2005, Garcia and Henry, 2003, Keynton et al., 2004, Kutter, 2000, Lacher et al., 2001, Mogensen et al., 2004, Wang, 2002, Zamfir et al., 2004). Microfabricated CE systems in particular offer superior performance to conventional techniques, including higher chromatographic resolution, faster separations, and smaller sample sizes. Electrokinetic fluid flow eliminates the need of pumps and the resulting compact design, minimal solvent use, and reduced waste regeneration simplify the operation and allow for *in situ* field use (Wang, 2002).

Furthermore, when coupled with electrochemical detection (ECD), microchip-CE separation provides highest sensitivity and a high degree of integration, combining separation and detection on a single chip at low cost (Wang, 2002). A microchip-CE method coupled with PAD has been extended to atmospheric aerosol applications as part of this research. The method is described below (section 2.4.) and recently reported in more detail in the literature (Garcia et al., 2005).

Three alternative/complementary methods to GC-MS have been investigated here, including high performance anion-exchange chromatography (HPAEC) with pulsed amperometric detection (PAD), microchip-CE-PAD, and an enzyme biosensor method. While potential applications of these methods may be extended to several other compounds, their primary utilization will be for measurement of the biomass combustion marker compounds levoglucosan and its isomers (mannosan and galactosan). Results from method development and applications of these methods are presented below (sections 2.3. to 2.5.). The GC-MS method that was utilized for the analysis of samples from two field studies (Yosemite Aerosol Characterization Study and Missoula biomass combustion study) is described below as well (section 2.2.)

2.1.2. Potential Applications of Alternative Methods

Based on promising initial results from testing these new methods, multiple applications can be envisioned that have not been possible with current instrumental techniques. The low cost and fast measurement possible with these methods would allow their implementation into routine monitoring programs, such as the Interagency Monitoring of Protected Visual Environments (IMPROVE) network. These methods could also be used on a routine basis by states and other agencies to assess the contribution of biomass combustion smoke and other sources to $PM_{2.5}$. Furthermore, the high sensitivity and fast measurement would allow coupling of some of these methods with semi-continuous sampling systems for monitoring of carbonaceous aerosol species at high time resolution. This would potentially provide a better understanding of chemical and

transport processes that occur on rather short time scales (on the order of a few hours or less) in the troposphere.

2.2. GC-MS METHOD

2.2.1. Background

The most commonly used method for speciation of organic compounds in aerosol samples is GC-MS. GC-MS has been widely utilized in the characterization of ambient and source samples, providing simultaneously qualitative and quantitative information regarding the aerosol components (Fine et al., 2004b, Glasius et al., 2000, Helmig et al., 1990, Jaoui et al., 2005, Limbeck and Puxbaum, 1999, Mazurek et al., 1989, Pashynska et al., 2002, Pereira et al., 2001, Shimmo et al., 2002, Simoneit, 1992, Zdrahal et al., 2002, Zheng et al., 2000). Hundreds of individual organic compounds, including alkanes, alkenes, alcohols, carbonyls, carboxylic acids, PAH, and biomarkers, have been identified and quantified by GC-MS in fine atmospheric PM.

However, method-specific limitations of GC-MS limit its applicability to polar and higher molecular weight, i.e., non-volatile, organic compounds. Furthermore, separation and detection of organic aerosol constituents by GC-MS typically requires a series of sample preparation steps that are labor intensive and potentially introduce artifacts into the analytical sequence. Nevertheless, GC-MS has been successfully utilized in the characterization of important aerosol components as well as gas-phase species in the atmosphere, and several studies have applied GC-MS to quantify molecular markers for source apportionment of ambient aerosol (e.g., Fraser et al., 2003, Schauer and Cass, 2000, Schauer et al., 1996, Zheng et al., 2002).

2.2.2. Internal Standards

While quality control measures are important in any analytical procedure, they are particularly critical in GC-MS analyses because of the large number of steps involved, including sample preparation and analysis. In addition to taking various precautions, the use of internal standards has been successful in accounting for irregularities during sample preparation and analysis, including incomplete extraction, volatilization, adsorption to surfaces, varying injection volumes, and other losses of sample components. Isotopically labeled compounds, such as perdeuterated compounds in which hydrogen atoms were substituted by deuterium (^{2}D) atoms, are most commonly used as internal standards (IS). Ideally, a labeled analog of each analyte would be added to a sample prior to extraction. However, the cost of such practice would be prohibitive. Therefore, a suite of representative labeled compounds is typically used, covering a broad range of polarities and molecular weights. Five different perdeuterated compounds were used as recovery standards and for quantification of organic aerosol constituents in the studies described below (chapters 3 and 4). Table 2-1 gives an overview of the individual IS species, including the corresponding retention times, concentrations of stock solutions, amounts used per sample (filter extract), and the molecular MS fragments (i.e., mass-to-charge ratios (m/z)) used for quantification. While six different IS species are listed in the table, only five of them were used at a time by eliminating either benzaldehyde-D5 or vanillin-D2. Benzaldehyde-D6 was initially used as IS for quantification of the more volatile analytes, such as methoxyphenols. Due to irregular chromatographic behavior (e.g., peak shape), benzaldehyde-D6 was later replaced by benzaldehyde-D5 with ring deuterium atoms that were assumed to be more stable. However, both species have rather high vapor pressure, reflected in short retention times (ca. 6 min.), thus rendering them less useful as IS for most analytes of interest (with retention times > 16 min.). Therefore, custom synthesized vanillin-D2 was used in selected filter extracts from the Yosemite Aerosol Characterization Study instead of the perdeuterated benzaldehyde. The physico-chemical properties (vapor pressure in particular) of the labeled vanillin are much closer to those

of the methoxyphenols investigated here as wood smoke markers. However, the characteristic mass fragments (m/z) of the non-deuterated vanillin coincided with those of the labeled species. Therefore, vanillin was not quantified in those samples. The perdeuterated vanillin was consequently no longer used in future extractions.

Table 2-1. Perdeuterated compounds used as internal standards for filter extracts.

Compound	Retention Time (min.)	Concentration (µg/mL)	Volume (µL)	m/z
Benzaldehyde-D5	6.8	250	50	82, 110, 112
Vanillin-D2	19.9	250	50	152, 153, 154
Decanoic acid-D19	18.0	250	50	77, 91, 155
Levoglucosan-D7	23.3	250	25	206, 220, 339
Chrysene-D12	30.4	25	100	240
Octacosane-D58	32.3	250	50	66, 82, 98

A general overview of compounds or compound classes identified here and the corresponding IS species used for their quantification is presented in Table 2-2. While the number of IS available in our laboratories was limited, the suite of five labeled compounds covers a wide range of functionalities as well as molar masses. Nevertheless, some compounds were not ideally represented by the chosen IS, such as in the case of the n-alkanes where one perdeuterated alkane (octacosane-D58) was used for determination of the entire homologous series (C_{16} - C_{38}), introducing additional uncertainty to the quantifications.

Table 2-2. Overview of compounds or compound classes and corresponding IS species chosen for quantification.

IS	Compound Classes
Benzaldehyde-D5	methoxy phenols
Octacosane-D58	n-alkanes, alkanols, carbonyls, biogenic SOA species
Decanoic acid-D19	n-alkanoic acids, dicarboxylic acids, resin acids, SOA acids
Chrysene-D12	PAH, hopanes, steranes
Levoglucosan-D7	anhydrosugars, sterols

2.2.3. Chemical Derivatization

Many organic compounds present in atmospheric fine aerosol particles have polar character, as they contain various functional groups that add a dipole moment to the molecule. Common polar functionalities observed in organic aerosol constituents include carboxyl, hydroxyl, and carbonyl groups. Most GC and GC-MS methods are not capable of adequately resolving polar compounds for unambiguous identification and quantification due to the inability of common analytical GC columns to resolve polar compounds. Therefore, it is necessary to chemically derivatize samples in order to decrease the polarity of compounds for determination by common GC or GC-MS methods. Two different chemical derivatization techniques were applied to all samples (calibration standards and filter extracts) in this study: carboxylic acids were methylated with diazomethane to produce methyl esters of the individual acids; compounds containing hydroxyl groups, such as carbohydrates (including anhydrosugars) and sterols, were silylated with bis(trimethylsilyl)trifluoroacetaminde (BSTFA) and trimethylchlorosilane (TMCS), added as catalyst, to form trimethyl silyl esters of the respective compounds. In addition to being less polar, the resulting products have increased volatility and higher thermal stability compared to

their non-derivatized analogs. The procedure for the two types of derivatization applied here is outlined below (section 2.2.4.).

While the methylation reaction is fairly straightforward, several factors influence the success of a silylation reaction, including reaction time, temperature, nature of the equipment used, and the presence/absence of water or other potentially interfering species. Due to inconsistent results using the method previously reported by Brown and coworkers (Brown et. al, 2002), a series of silylation experiments was performed in order to optimize the current silylation procedure. The conversion efficiency was monitored while varying reaction time, temperature, and reagent characteristics. BSTFA readily reacts with water and alcohols. Therefore, it is critical to minimize the contact of these compounds with BSTFA. As certain standard solutions had been prepared with a small amount of methanol (to increase solubility of more polar compounds in DCM), it was presumed that the presence of the alcohol may have caused inconsistent calibration data. Therefore, alcohols were completely omitted from those standard solutions to be silylated. Furthermore, in order to minimize the time that BSTFA is exposed to ambient air (containing a certain amount of water vapor) a combined BSTFA-TMCS reagent mix was purchased that significantly reduced the handling time. In addition, the use of BSTFA-TMCS reagent mix contained in smaller (1 mL) ampules (to be used for a single set of samples to be silylated) reduces the risk of contamination with water, as storage of an opened reagent is eliminated. Finally, the reaction time was increased to five hours (at 65 °C), since silylation experiments (using known amounts of a test compound) as a function of time showed incomplete conversion for reaction periods of less than three hours. Future improvement of the silylation procedure should include the use of high-purity nitrogen (with lower water content) for the concentration step of filter extracts.

2.2.4. Experimental Procedures

Sample media, chemicals (authentic standards and solvents), and supplies were obtained from various suppliers. Quartz fiber filters (type QM-A; 20.3 x 25.4 cm) were manufactured by Whatman (Maidstone, England). Dichloromethane (DCM), used for filter extraction and as solvent for standard solutions, was obtained from Fisher Scientific (Optima grade), as was isopropanol, used for cleaning of glassware. Authentic standards were purchased from several different companies (listed in Appendix A, including information about compound purity and molar mass).

Aerosol samples were typically collected on quartz fiber filters with high-volume (Hi-Vol) samplers at a nominal flow rate of 1130 L/min according to standard operating procedures (SOP). The sample collection process is described in more detail in sections 3.2.1. and 4.2.3., as well as in the Hi-Vol SOP (Appendix B). For speciation of the organic aerosol component by GC-MS, sample filters were solvent extracted according to protocols reported previously (Brown et. al, 2002). Sample preparation included spiking of a portion of each filter (typically ¼) with the above mentioned suite of perdeuterated standards (IS) prior to extraction. Filters were extracted three times with 25 mL of DCM for 15 minutes under ultrasonic agitation, using a Branson model 5210 ultrasonic bath. The combined extracts were filtered through a pre-fired quartz filter (using a stainless steel syringe filter) and subsequently reduced in volume to 250 μL.

Two aliquots of each concentrated filter extract were subjected to chemical derivatization (methylation and silylation), described in more detail by Brown and coworkers (Brown et. al, 2002). Methylations were performed with freshly produced diazomethane by combining equal volumes (50 μL) of diazomethane solution (in benzene) and sample extract or standard solution. Diazomethane was generated by adding 600 μL of 5 M KOH solution to approximately 100 mg of 1-methyl-3-nitro-1-nitroguanadine (suspended in 500 μL of D.I. water). The evolving

diazomethane gas was captured in benzene. The optimized silylation procedure consisted of combining 50 μL of concentrated extract or standard solution in an amber 1 mL ampule with 50 μL of BSTFA (containing 1% of TMCS). The ampule was sealed immediately and the reaction was allowed to proceed for 5 hours at 65 °C.

A HP 6890 GC (Hewlett Packard) coupled with a HP 5973 mass selective detector (MSD) (Hewlett Packard) was used for all GC-MS analyses, except for those conducted at the Institute for Tropospheric Research (IfT) in Leipzig, Germany (section 2.3.4.). Separation was accomplished using either a Supelco Equity 5 capillary column (30 m x 250 μm x 0.25 μm 5% phenyl-methyl-siloxane film) or a HP-5MS column (Hewlett Packard) with the same dimensions and stationary phase. Helium (ultra-high purity) was used as carrier gas. Injections of 1 μL aliquots were performed in splitless mode. The GC temperature profile consisted of an initial hold time of 10 minutes at 65 °C, followed by a temperature gradient of 10 °C /min to a final temperature of 300 °C that was held constant for 20 minutes. Thus, a typical GC-MS run lasted 53.5 minutes. The MSD was operated in ion scan mode and ions were produced by electron impact (EI) ionization with a source temperature of 230°C. Mass to charge ratios of 50 to 500 were scanned at 2.94 scans/second. HP (Hewlett Packard) Chemstation software for GC-MS (G1701BA; version B.01.00) was used to control GC-MS instrument parameters and to perform data acquisition, as well as process the data. A total-ion mass spectrum was obtained with each chromatogram. Authentic standards were used for identification and to obtain response factors for the majority of the quantified organic compounds. A typical GC-MS total ion count (TIC) chromatogram of a DCM filter extract ($PM_{2.5}$ sample collected during YACS, as discussed in chapter 3) is shown in Figure 2-1.

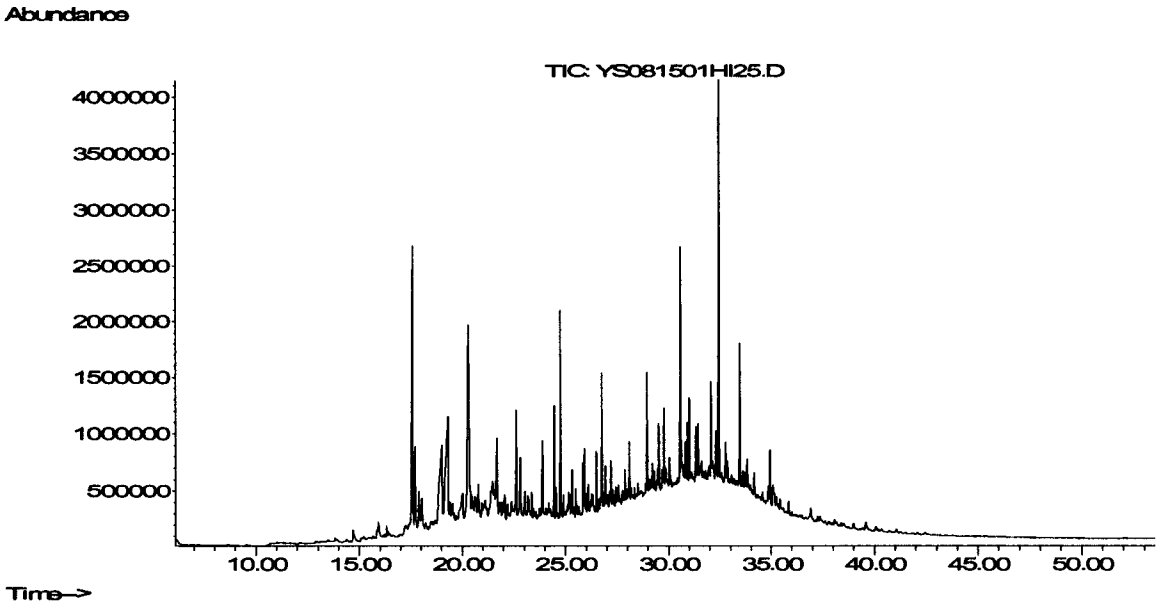

Figure 2-1. GC-MS TIC chromatogram of an ambient $PM_{2.5}$ extract from the Yosemite Aerosol Characterization Study (chapter 3).

Quality assurance (QA) measures included various precautions and particular quality control practices. Prior to using any glassware or other equipment that would come in contact with a sample extract or standard, a strict cleaning protocol was applied that included pre-firing of glassware at 450 °C for at least 6 hours. Quartz filters were pre-fired at 600 °C for at least 6 hours, handled only with clean non-serrated tweezers, and stored in pre-fired aluminum envelopes placed in a freezer (< −10 °C). In addition, various types of blanks, including instrument, field, and total process blanks, were analyzed according to the standard analytical procedure. Quantified concentrations of individual analytes in aerosol extracts were blank corrected with correction factors obtained from corresponding field blanks.

2.2.5. Analyte Quantification

Absolute concentrations of individual organic species in aerosol extracts were determined by using relative response factors and peak area counts of individual analytes and corresponding IS on a per-sample basis. Relative response factors were calculated for every compound based on the compound to IS peak area ratio. These ratios were determined with the summed peak areas of three characteristic mass fragments (i.e., m/z ratios) for each analyte and IS, instead of the TIC peak areas, in order to minimize uncertainties in the quantification. In case of a few compounds, only two characteristic fragment ions were present in the mass spectrum. The m/z ratios used for quantification of the individual analytes are listed in Tables 2-3 to 2-6. Calibration curves were generated for each individual compound by plotting the peak area ratio of compound to IS versus nominal concentration and fitting a least squares linear regression curve (with the intercept forced to zero). Each calibration curve was split into a lower-concentration range (1.0 to 10 μg/mL) and the full range (typically 1.0 to 100 μg/mL) for more accurate quantifications. The calibration factor for a certain analyte was obtained from the most appropriate calibration curve, once the peak area ratio was determined in a given extract. An example calibration curve is shown for the biomass combustion marker levoglucosan in Figure 2-2. Response factors for compounds for which no authentic standards were available were estimated from compounds with similar chemical properties (e.g., polarity and vapor pressure). This was particularly the case for compounds within homologous series, such as n-alkanes or n-alkanoic acids.

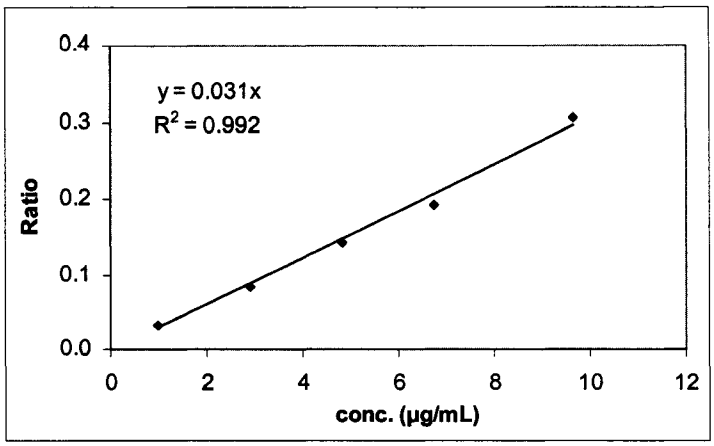

Figure 2-2. Example GC-MS calibration curve levoglucosan.

Quantification of individual compounds was performed on an Excel spread sheet, using detector response (peak area counts) of the analyte and corresponding IS, the characteristic response factor, and sample volume. A typical quantification sheet is attached in Appendix C. The following equation encompasses the mathematical operations carried out on the spread sheet, where c_x is the concentration of an individual compound, A_x is the peak area of that compound, A_{IS} is the IS peak area, and m is the response factor (i.e., slope from the calibration curve):

$$c_x = \frac{A_x}{A_{IS}} \cdot \frac{1}{m} \qquad (2\text{-}1)$$

An overview of biomass combustion markers investigated in the extracts of ambient and source PM samples collected as part of this research is given in Tables 2-3 to 2-6. Indicators for atmospheric processing of primary biogenic emissions (aka biogenic SOA species) are listed in Table 2-6. In addition to the common (trivial) compound name, the tables contain the molar mass of each compound, sources, analytical method (non-derivatized, methylated, or silylated), and the characteristic MS ion fragments (m/z) used for quantification. Molecular structures of selected

compound. Additional organic compounds quantified in the aerosol extracts, such as n-alkanes, n-alkanoic acids, dicarboxylic acids, PAH, hopanes, and steranes, are listed in Appendix A-6, including their molar masses, origin, and m/z ratios used for quantification.

Table 2-3. List of authentic standards used for compound identification and quantification: 1. methoxyphenols.

Compound	Molar Mass (g/mol)	Biomass Type	Method [a]	Ret. Time (min.)	m/z
vanillin	152.15	softwood		19.4	151, 152
acetovanillone	166.17	softwood		20.6	151, 166
vanillic acid	168.15	softwood	methylated	21.1	151, 182
homovanillic acid	182.18	softwood	methylated	21.7	122, 137, 196
homovanillyl alcohol	168.19	softwood		21.2	137, 168
eugenol	164.20	softwood		18.8	77, 149, 164
isoeugenol	164.20	softwood		20.1	77, 149, 164
guaiacol	124.14	hard + softwood		17.2	81, 109, 124
4-ethyl guaiacol	152.19	hard + softwood		17.5	137, 152
4-methyl guaiacol	138.16	hard + softwood		15.8	95, 123, 138
cinnamaldehyde	132.16	hard + softwood		17.3	77, 103, 131
cannamic acid	148.16	hard + softwood	methylated	19.1	103, 131, 162
syringol	154.16	hardwood		18.7	96, 139, 154
4-methyl syringol	168.19	hardwood		20.0	125, 153, 168
syringe aldehyde	182.17	hardwood		22.3	181, 182
acetosyringone	196.20	hardwood		23.6	153, 181, 196
syringic acid	198.18	hardwood	methylated	23.9	181, 197, 212

Notes: a.) If no method is specified, GC-MS analysis was performed with neutral, i.e., non-derivatized, extracts.

Table 2-4. List of authentic standards used for compound identification and quantification: 2. resin acids and diterpenoids.

Compound	Molar Mass (g/mol)	Biomass Type	Method [a]	Ret. Time (min.)	m/z
abietic acid	302.46	softwood	methylated	29.8	121, 256, 316
pimaric acid	302.45	softwood	methylated	28.6	121, 180, 316
isopimaric acid	302.45	softwood	methylated	29.1	241, 257, 316
sandaracopimaric acid	302.45	softwood	methylated	28.7	121, 257, 316
dehydroabietic acid	300.44	softwood	methylated	29.4	239, 299, 314
7-oxo-dehydroabietic acid	314.42	softwood	methylated	31.2	187, 253, 328
retene	234.34	softwood		28.4	178, 219, 234

Notes: a.) If no method is specified, GC-MS analysis was performed with neutral, i.e., non-derivatized, extracts.

Table 2-5. List of authentic standards used for compound identification and quantification: 3. anhydrosugars and sterols.

Compound	Molar Mass (g/mol)	Biomass Type	Method	Ret. Time (min.)	m/z
levoglucosan	162.14	all biomass	silylated	23.3	204, 217, 333
mannosan	162.14	all biomass	silylated	23.0	204, 217, 333
galactosan	162.14	all biomass	silylated	22.8	204, 217, 333
b-sitosterol	414.71	all biomass	silylated	37.7	357, 396, 486
stigmasterol	412.70	all biomass	silylated	37.0	255, 394, 484
ergosterol	396.65	all biomass	silylated	36.5	337, 363, 468
cholesterol	386.65	meat cooking	silylated	35.6	329, 368, 458

Table 2-6. List of authentic standards used for compound identification and quantification: 4. biogenic SOA species.

Compound	Molar Mass (g/mol)	Source Type	Method [a]	Ret. Time (min.)	m/z
pinonaldehyde	168.1	α-pinene oxidation		17.4	83, 98, 109
pinic acid	186.21	α-pinene oxidation	methylated	19.4	83, 114, 128
trans-norpinic acid	172.18	α-pinene oxidation	methylated	17.9	83, 114, 140
cis-pinonic acid	184.23	α-pinene oxidation	methylated	19.2	83, 96, 125
(1R)-(+)-nopinone	138.21	β-pinene oxidation		14.5	83, 95, 123
trimethyl-2-pentadecanone	268.48	phytol oxidation		24.6	58, 71, 85

Notes: a.) If no method is specified, GC-MS analysis was performed with neutral, i.e., non-derivatized, extracts.

2.3. HPAEC-PAD METHOD

2.3.1. Background

Various chromatographic techniques have been used for carbohydrate analysis, including GC-MS and LC methods (Gao et al., 2003, Pashynska et al., 2002, Schkolnik et al., 2005, Simoneit et al., 2004). The intrinsic chemical characteristics of sugars, including their polarity and lack of chromophores or fluorophores, render many common analytical methods ineffective or require additional time-consuming and expensive sample preparation prior to analysis. Consequently, recent efforts have been directed towards alternative analytical methods that are simple and fast, yet sensitive, precise and accurate. As mentioned above, electrochemical detection methods, such as PAD, coupled with HPLC provide high sensitivity and selectivity, particularly for the determination of carbohydrates (Baldwin, 1999, Cataldi et al., 2003, Cataldi et al., 1999, Jandik et al., 2004, Lu and Cassidy, 1993, O'Shea and Lunte, 1993, Zook and LaCourse, 1995).

Carbohydrates, including the anhydrosugars examined here, are amenable to anion exchange chromatography (AEC) due to their (weak) acidic nature that allows for ionization in highly basic media. Separations of carbohydrates are mainly dependent upon the difference between their pK_a values. While high performance (HP) AEC coupled with PAD has been utilized for carbohydrate analysis in various matrices, its application to aerosol chemistry is limited to only a few recent efforts (Gao et al., 2003, Puxbaum, 2004). A HPAEC-PAD method was developed as part of this research effort for the analysis of anhydrosugars, including levoglucosan, mannosan, and galactosan, in atmospheric aerosol samples. The method was successfully applied for the determination of these biomass combustion markers in PM samples from an ambient aerosol characterization study (chapter 3) and a biomass combustion source sampling study (chapter 4).

2.3.2. Experimental

Sample preparation for HPAEC-PAD analysis included extraction of portions of quartz fiber filters twice with 15 mL portions of de-ionized water. Typical extraction efficiencies for levoglucosan were 100% based on extraction experiments of quartz fiber filters spiked with levoglucosan, using ultrasonic agitation. The combined extracts were passed through a syringe filter containing a pre-fired 25 mm quartz fiber filter to remove insoluble material, such as filter fragments and water-insoluble aerosol constituents. Sample aliquots and calibration standards were injected (100 μL sample loop) without concentration or chemical derivatization into the chromatograph.

The HPAEC-PAD system utilized here was a Dionex DX-500 series ion chromatograph (IC), consisting of a Dionex LC25 Chromatography Oven, Dionex GP50 Gradient Pump, and Dionex ED50 Electrochemical Detector. The electrochemical detector was equipped with a Dionex ED50/ED50A Electrochemical Cell, utilizing disposable gold electrodes. Separation of the individual anhydrosugars was achieved using a Dionex CarboPac PA 10 Analytical Column (4 x

250 mm) with an 18 mM aqueous sodium hydroxide (NaOH) eluent at a flow rate of 0.5 mL/min. The eluent was prepared from a carbonate-free 50% (wt/wt) stock solution of NaOH (Fisher Scientific) and degassed D.I. water. Typical analytical run times were 60 minutes, including isocratic elution for 10 min., followed by a linear gradient, increasing the eluent concentration from 18 mM (at 10 min.) to 54 mM (at 24 min.). Immediately following the separation period (24 min.), the analytical column was regenerated for 15 minutes with 180 mM NaOH, followed by a 15-minute re-equilibration period (with 18 mM NaOH). Authentic standards were used for identification and to obtain response factors for all quantified anhydrosugars and other sugars.

Following chromatographic separation, upon entering the electrochemical detection cell, the analytes (carbohydrates) are electroanalytically oxidized on the surface of the (gold) working electrode by application of a positive potential (voltage). The oxidation products would "poison" the surface of the electrode over time, if they were not removed. Therefore, the electrode surface needs to be continuously cleaned which is achieved by application of a different potential for a defined period of time after the detection step, followed by a surface regeneration step. Pulsed (or integrated) amperometric detection is based on the repeated application of such a series of potentials. This sequence is referred to as a waveform. For the experiments performed here waveform "A" (Dionex, Sunnyvale, CA: Technical Note 21) was determined to be appropriate without further modification. Figure 2-3 shows the series of voltage steps comprising waveform A. After a short delay period (200 ms) at 0.1 V, the detection potential (0.1 V) is maintained for 200 ms. Cleaning of the working electrode takes place for 10 ms at -2.0 V, followed by the brief (few ms) application of a positive potential (0.6 V) to form a small amount of gold oxide. Finally, a negative potential (-0.1 V) is applied for 60 ms to regenerate the electrode surface. Thus, one cycle of the entire waveform lasts 500 ms.

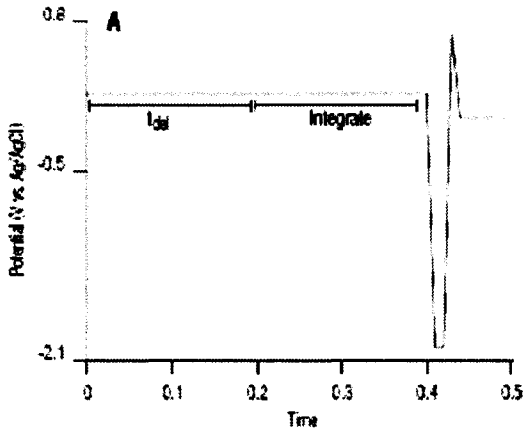

Figure 2-3. Diagram of "waveform A" for pulsed amperometric operation, used in the current HPAEC-PAD method.

Regardless of the regeneration of the working electrode during each cycle of the waveform, the working electrodes employed here had a limited lifetime, as they were disposable-type electrodes. An indication for the need to replace a working electrode was an increase in background signal (2 to 3 times the current measured with a new electrode) and a larger solvent dip at the beginning of a chromatogram. Typical background currents were approximately 20 nC for a new reference electrode (original type) with a new working electrode and 10 nC for the new (2^{nd} generation polymer-type) reference electrode. Useful lifetimes of the working electrodes varied with the number of injections performed and would thus range from one month to several months. Typical lifetimes of the reference electrode were on the order of 9 to 12 months.

2.3.3. Method Development

The HPAEC-PAD method developed here requires minimal sample preparation. Aqueous standard solutions and extracts of filter samples were separated on an anion exchange column, without prior chemical derivatization. Chromatographic conditions were optimized for the separation of levoglucosan, mannosan, and galactosan. Additional carbohydrates, including glucose, mannose, xylose, maltose, and sucrose, were detected as well.

Chromatographic separation was optimized for the sugars of interest, in particular the three anhydrosugars, by varying eluent parameters, such as eluent concentration, flow rate, isocratic versus gradient elution, and type of gradient. A commonly used eluent (NaOH) concentration for sugar analysis by HPAEC is 18 mM. Variation of the eluent concentration from 9 to 54 mM did not have any significant effect on the separation efficiency or speed. Therefore, 18 mM NaOH was accepted here as the typical eluent concentration. While at an eluent flow rate of 1.0 mL/min. (common in HPAEC separations) the resolution of the anhydrosugars was not sufficient, all three species were well resolved at a lower flow rate of 0.5 mL/min. (simultaneously reducing the amount of solvent used and the volume of chemical waste generated), as shown for a sugar standard mix in Figure 2-4. An eluent gradient was not necessary for the separation of the anhydrosugars. Therefore, a typical separation was isocratic for the initial 10 minutes (during which all three anhydrosugars eluted), followed by an eluent gradient (from 18 to 54 mM over 14 min.) during the remaining run time in order to increase the elution rates of glucose, mannose, and sucrose. The retention time of glucose, for instance, was reduced from approximately 30 min. (with isocratic elution) to 24 min. with a gradient (starting at 10 min.). These additional sugars, including glucose, mannose, and sucrose, were separated reasonably well under these conditions (optimized for anhydrosugar separation), as demonstrated in Figure 2-4. All of these sugars also produced calibration curves with high correlation factors ($R^2 > 0.999$) for linear regressions. In addition to the anhydrosugars discussed above, some of these other sugars may be important aerosol constituents as well, as they have recently been detected in ambient aerosol samples, particularly those impacted by biomass combustion smoke (Decesari et al., 2005, Gao et al., 2003, Graham et al., 2002, Simoneit et al., 2004).

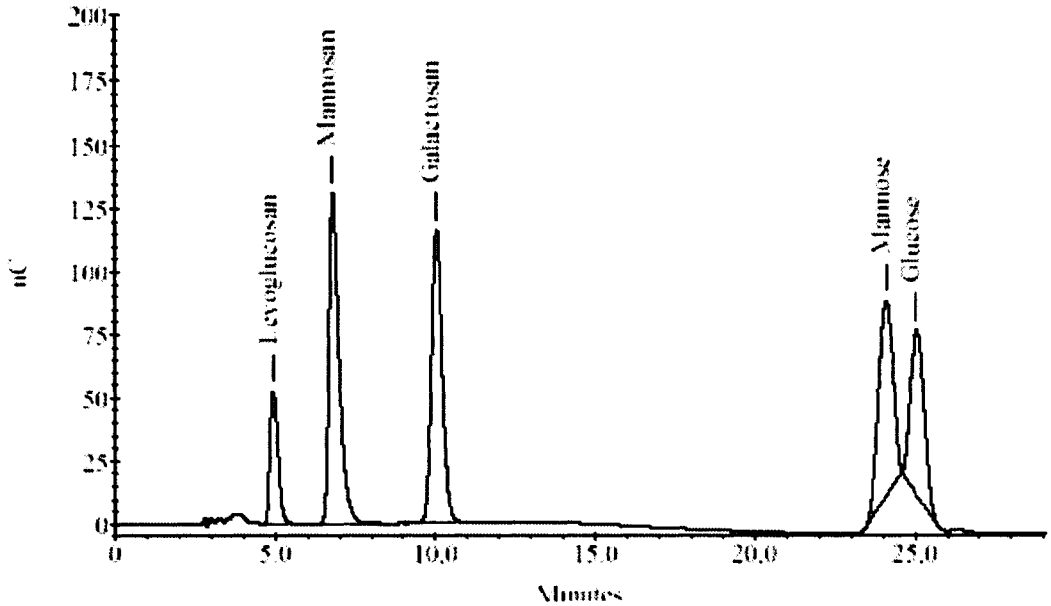

Figure 2-4. Typical HPAEC-PAD chromatogram illustrating the separation of five sugars (each at 3.0 μg/mL), using a Dionex CarboPac PA 10 column. Elution was isocratic with a flow rate of 0.5 mL/min. (18 mM NaOH) for the first 10 minutes, followed by a linear eluent gradient, increasing the NaOH concentration to 54 mM at 24 minutes.

In order to maintain consistent performance, the column needs to be washed with higher concentration NaOH (e.g., 180 mM) between analyses, mainly to remove any carbonate ions that may occupy active sites on the stationary phase of the analytical column. This regeneration requires an additional re-equilibration step with eluent of regular concentration (i.e., 18 mM). While the separation time for the three anhydrosugars is relatively short (ca. 10 min.), these steps, even though automated, contribute additional time to each chromatographic run. Therefore, an optimal sequence of regeneration and re-equilibration steps that are long enough to sufficiently regenerate the column, while minimizing the total analytical run time, was examined. It was determined that 10 minutes of regeneration, followed by 10 minutes of re-equilibration, may suffice in many cases. However, due to varying composition (particularly in terms of carbonate content) of samples and different batches of eluent, each step was chosen to have a duration of 15 minutes. In addition, it is crucial to use degassed solvents and to maintain a head space of ultra-

high-purity helium over all eluent reservoirs and NaOH stock solutions in order to protect NaOH from air exposure and thus to minimize the introduction of carbonate ions.

All separations were conducted at ambient column temperatures (22 - 24 °C). The effect of temperature on separation efficiency was not investigated due to a malfunctioning column heater. While temperature effects in LC are not as large as in GC, where the separation of analytes depends in part on the temperature profile of the chromatographic process, the column temperature in HPAEC does influence the separation efficiency to a certain extent. Therefore, future method optimization should include evaluation of column temperature effects.

Measurement uncertainty for levoglucosan was 5.3% (one relative standard deviation (RSD)), based on detector response (peak area) from replicate analyses (n = 12) of the same filter extract (burn #88 from the Missoula biomass combustion study, discussed in chapter 4). The measurement precision for replicate injections of a levoglucosan standard solution (3.0 μg/mL) was 3.6% (one RSD; n = 11). The corresponding uncertainties for mannosan were 6.9% and 3.9%, and those for galactosan were 7.7% and 4.4%, respectively. Retention times of all anhydrosugars were extremely stable under identical eluent conditions. For a given concentration of levoglucosan, retention times varied by ± 0.05 min. between calibrations conducted over a timeframe of several weeks, while the retention time variability over a concentration range of two orders of magnitude within one calibration series was only 0.02 min. The analytical limit of detection was estimated to be better than 0.002 μg/mL based on a signal-to-noise ratio of 3 which corresponds to an ambient air concentration of 0.1 ng/m^3 based on a typical 24-hour Hi-Vol sample (using ¼ of the Hi-Vol filter). Calibration curves for all anhydrosugars (levoglucosan, mannosan, and galactosan) typically showed correlation coefficients (R^2) of 0.9999 for quadratic regressions, as illustrated in Figures 2-5 a, b, and c. In accordance with common anion and cation IC procedures, calibrations were performed at the beginning of each analytical schedule

(consisting of up to 50 injections) and calibration checks were conducted approximately every 10 injections. However, less frequent calibrations would be sufficient, as the detector response was shown to be stable for at least 10 days without re-calibration based on a series of standard injections performed in intervals of two to three days over a period of 10 days, even when the amperometric cell was turned off in-between for two to three days. More frequent calibrations may be necessary if analytical conditions change, such as after eluent re-fills. The HPAEC-PAD method was capable of detecting and accurately quantifying anhydrosugars as well as other carbohydrates, over a concentration range of at least 3 orders of magnitude.

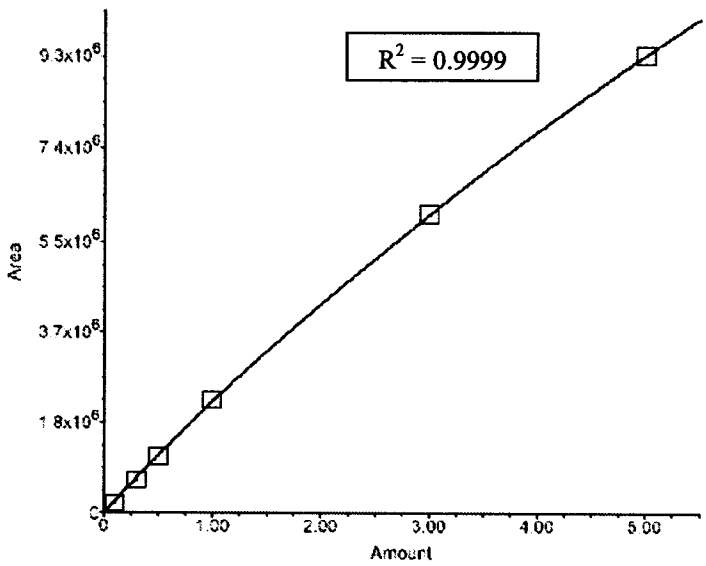

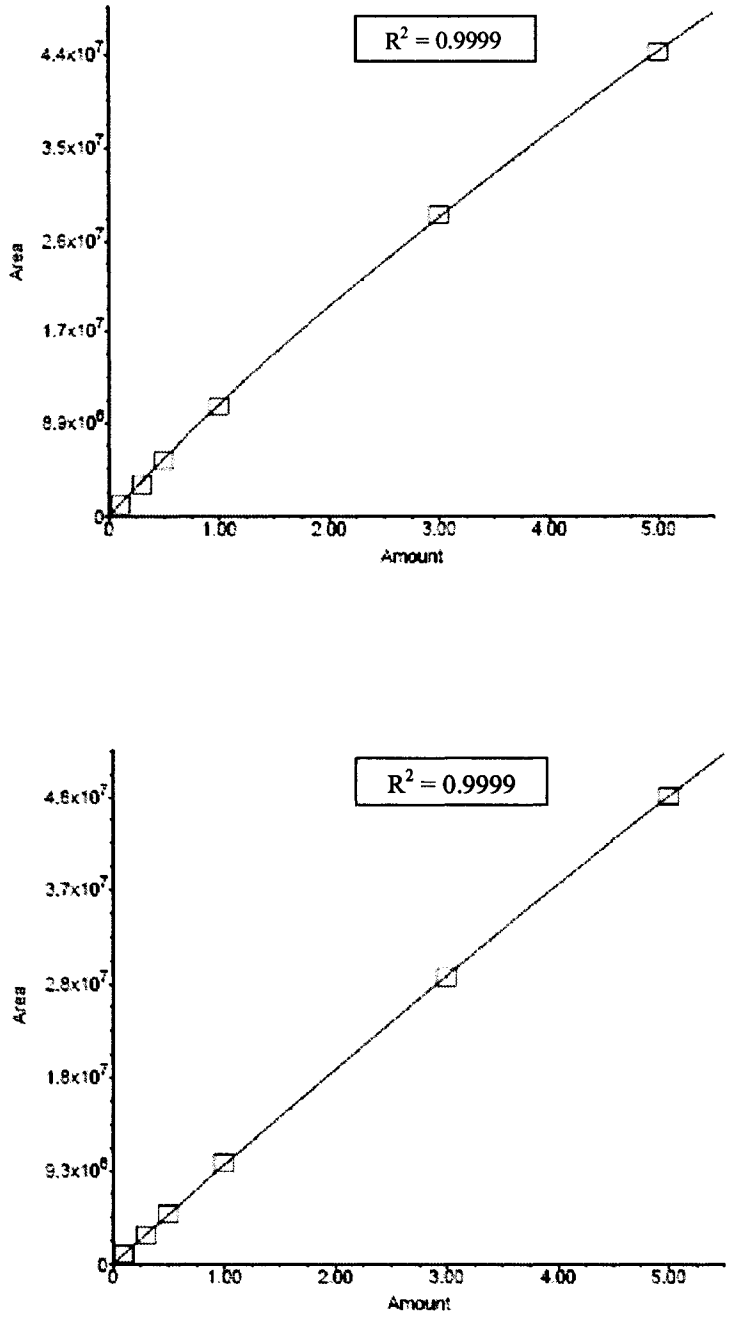

Figure 2-5. Calibration curves for levoglucosan (top), mannosan (middle), and galactosan (bottom), using quadratic regressions. Amounts (concentrations) were measured in μg/mL and ranged from 0.02 to 5.0 μg/mL.

Various other organic compounds, containing one or more hydroxyl groups in the molecule, were evaluated in terms of their PAD response under the optimized detection conditions for the anhydrosugars. Representative species of several compound classes were investigated, including polyols (e.g., arabitol, erythritol, threitol, and xylitol), methoxyphenols (e.g., vanillin), amines (e.g., ethanolamine), alcohols (e.g., hexanol), dicarboxylic acids (e.g., adipic, azelaic, and pinic acids), hydroxy acids (e.g., glycolic, malic, and gluconic acids), keto acids (7-oxooctanoic acid), poly(acrylic acid), humic acid, and fulvic acid. The majority of these compounds were not detected or had minute PAD response, possibly either due to their limited ionization at the given eluent pH or the ineffective oxidation at the applied working electrode potential. On the other hand, arabitol, xylitol, erythritol, and threitol (straight-chain sugar alcohols, i.e., polyols) were observed with relatively strong PAD signals. While the D and L isomers of these polyols had similar retention times, they did not interfere with the peaks of any of the anhydrosugars, as shown in Figure 2-6, except for arabitol that co-eluted with levoglucosan.

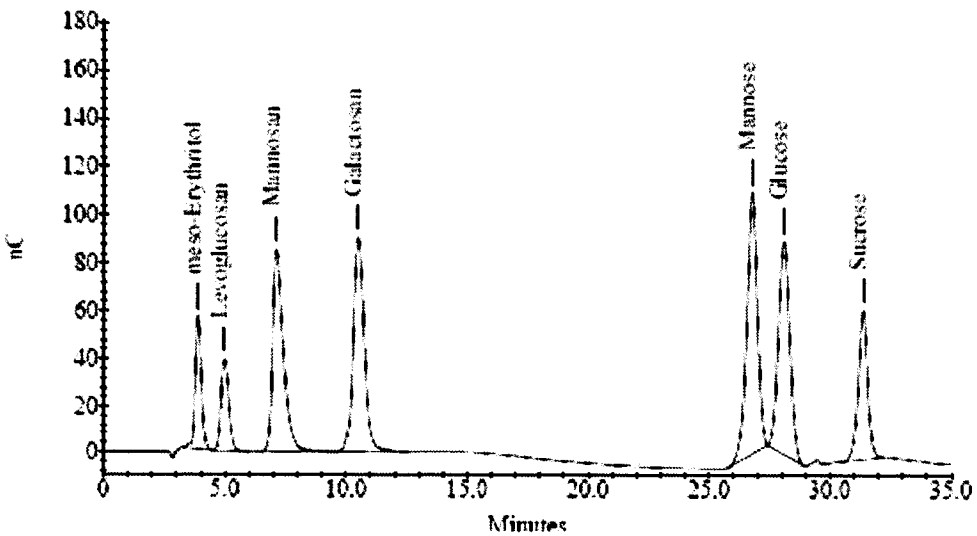

Figure 2-6. HPAEC-PAD chromatogram illustrating the separation of several sugars and sugar alcohols (each at 3.0 μg/mL), using a Dionex CarboPac PA 10 column..

Future research may be directed at improving the chromatographic resolution of these species, for instance by optimizing the eluent gradient. Furthermore, the investigation of additional polyols constitutes an important application of this method, as recent observations in atmospheric aerosol particles suggest such compounds to be novel indicators for SOA formed from biogenic precursors (Claeys et al., 2004a, Claeys et al., 2004b).

2.3.4. Method Intercomparison

Anhydrosugar mass concentrations obtained by HPAEC-PAD were compared to data generated by an independent HPLC-MS method conducted by Y. Iinuma at IfT in Leipzig, Germany (Engling et al., 2006a). The two methods differ significantly in separation and detection principles, and utilize different sample preparation procedures (see sections 4.2.6. and 4.2.7.), yet show fairly good agreement in concentrations (emission factors based on mass of OC) of levoglucosan determined independently by the two methods, as demonstrated in Figures 2-7 and 2-8. The agreement between the methods for mannosan and galactosan was not as good as for levoglucosan (Figure 2-9), possibly due to lower concentrations and larger measurement uncertainties in the HPLC-MS method. Selected $PM_{2.5}$ filter sample extracts from this study were also analyzed by GC-MS, according to protocols reported above (section 2.2.4.). Comparison of the two data sets again revealed rather good correlation for levoglucosan emission factors determined by GC-MS and by HPAEC-PAD, as shown in Figure 2-10 and in form of a scatter plot of levoglucosan emission factors obtained by the different methods (Figure 2-11). Generally, GC-MS and HPLC-MS emission factors appear to be somewhat lower than the corresponding values obtained by HPAEC-PAD, perhaps reflecting inadequate quantification of losses by internal standards employed during the more complex sample preparation procedures for those methods.

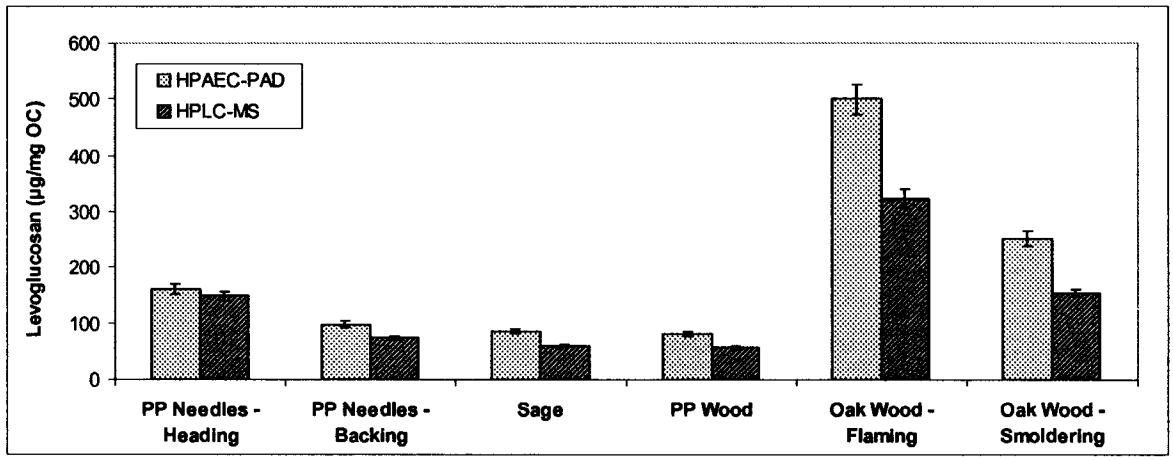

Figure 2-7. Emission factors of levoglucosan determined independently by HPAEC-PAD and HPLC-MS for various biofuels. Error bars indicate measurement uncertainties of 5.3% and 5.1% (one RSD) for the HPAEC-PAD and HPLC-MS data, respectively. Samples were water and methanol extractions, respectively, of separate pieces of individual quartz filters used to collect biofuel smoke in experiments described below (chapter 4).

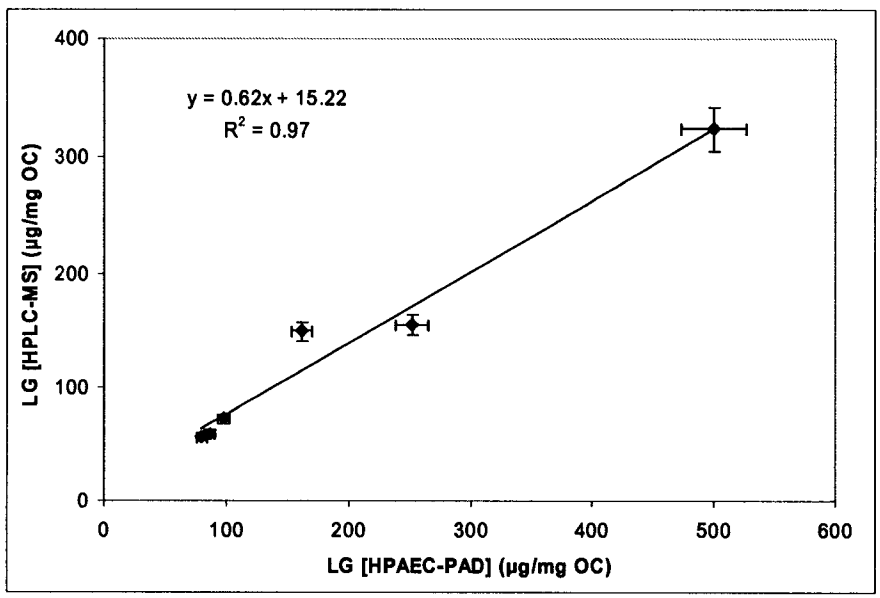

Figure 2-8. Scatter plots of levoglucosan (LG) emission factors determined independently by HPAEC-PAD and HPLC-MS.

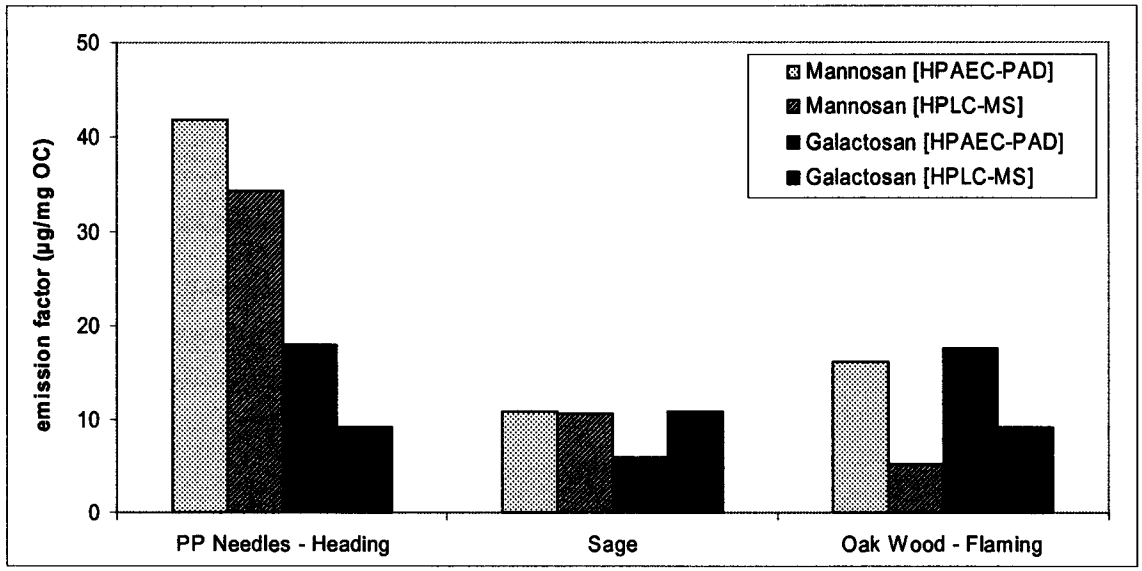

Figure 2-9. Mannosan and galactosan emission factors determined independently by HPAEC-PAD and HPLC-MS for various biofuels, as described in the caption for Figure 2-7.

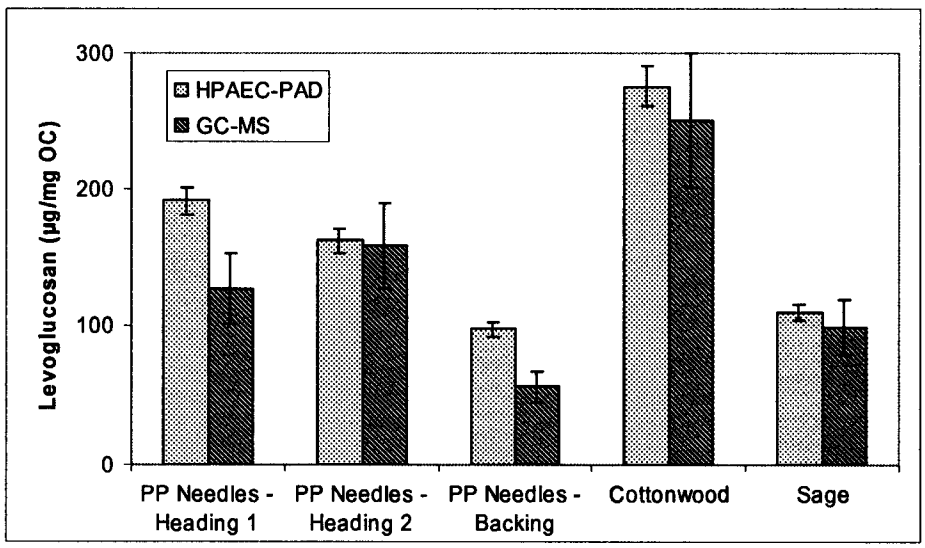

Figure 2-10. Levoglucosan emission factors determined independently by HPAEC-PAD and GC-MS in $PM_{2.5}$ smoke samples from selected fuel types and combustion conditions.

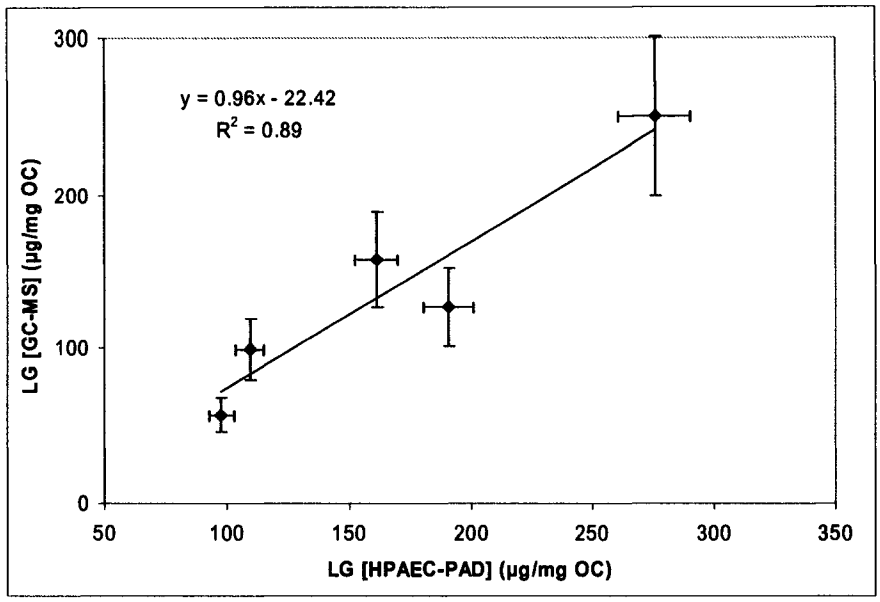

Figure 2-11. Scatter plots of levoglucosan (LG) emission factors determined independently by HPAEC-PAD and GC-MS.

Additional method intercomparisons were done with filter samples collected during biomass combustion experiments at the Max Plank Institute (MPI) for Chemistry in Mainz, Germany. Extracts of selected quartz filter samples were analyzed by HPAEC-PAD and compared to data obtained independently by GC-MS at the Institute for Tropospheric Research (IfT) in Leipzig, Germany, where the HPLC-MS analyses were performed as well. Again, levoglucosan mass concentrations show rather good agreement between these two methods, as demonstrated in Figure 2-12. Mannosan and galactosan concentrations determined by the two methods also agree well, as shown in Figure 2-12.

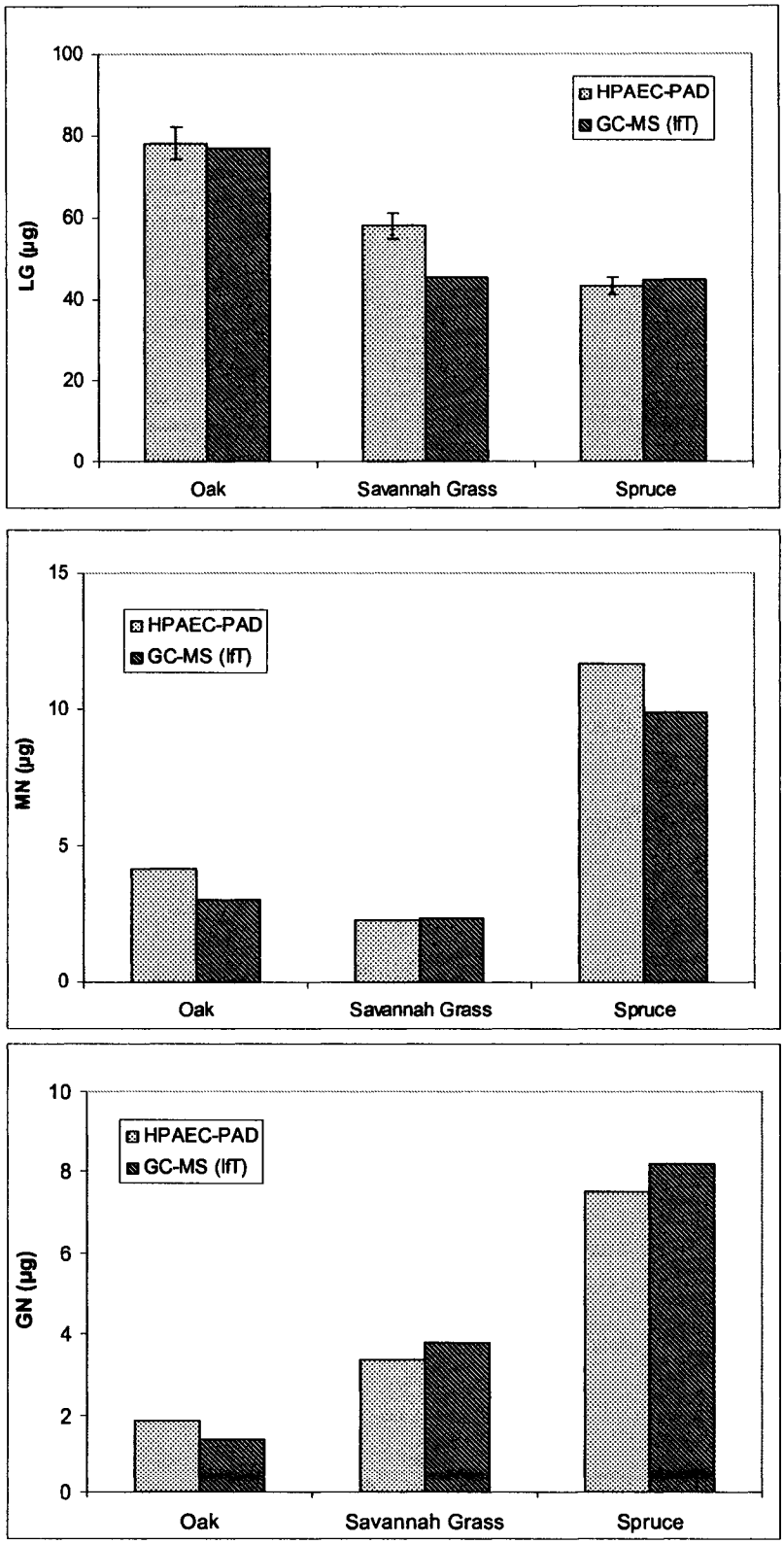

Figure 2-12. Levoglucosan (LG) (top), mannosan (MN) (middle), and galactosan (GN) (bottom) mass determined independently by HPAEC-PAD and GC-MS (conducted at IfT) in smoke PM extracts from selected fuel types.

Aside from simpler extraction and sample preparation procedures, an additional advantage of the HPAEC-PAD method over GC-MS analysis of aerosol extracts is a significantly shorter chromatographic run time. Separations of levoglucosan, mannosan, and galactosan by HPAEC-PAD are typically achieved within 12 minutes, while a typical GC-MS analysis of a corresponding solvent extract requires nearly 60 min. Furthermore, HPAEC-PAD shows great potential for detecting other sugars in aerosol extracts, including glucose, mannose, sucrose, and xylose, as indicated above. Chromatographic fractionation of biomass combustion aerosol extracts obtained during a biomass combustion study conducted at MPI in Mainz, Germany, yielded additional carbohydrate species (with characteristics similar to levoglucosan) that were also detected by HPAEC-PAD, but not identified due to the lack of authentic standards.

2.3.5. Levoglucosan Stability

The measurement of levoglucosan in various types of samples, such as ambient aerosol extracts, biomass combustion source samples, and fog water samples, revealed new insight into the stability of levoglucosan. While a series of exposure tests of levoglucosan (deposited on quartz fiber filters) to ambient sunlight indicated that levoglucosan may not be subject to photochemical degradation (at least over a period of 3 to 4 weeks), significant losses were observed in certain aqueous samples over a relatively short period of time. Levoglucosan appeared reasonably stable in biomass combustion $PM_{2.5}$ source sample extracts. On the other hand, ambient $PM_{2.5}$ extracts from Yosemite National Park showed a large decrease in levoglucosan content over a period of several months. Similar observations were made in fog water samples, collected in Fresno, CA, as part of a fog study during winter 2003/2004. Comparison of untreated samples to those that had been treated with chloroform (for organic acid preservation) showed a sizeable decrease in levoglucosan concentrations two and a half months after collection, as demonstrated in Figure 2-13. However, reduced levoglucosan response was observed after analyzing several preserved samples by HPAEC-PAD, indicating some type of interaction of chloroform or its hydrolysis

product (HCl) with levoglucosan or with the detection scheme. In order to maintain good performance of the HPAEC system, no more samples preserved with chloroform were analyzed from thereon.

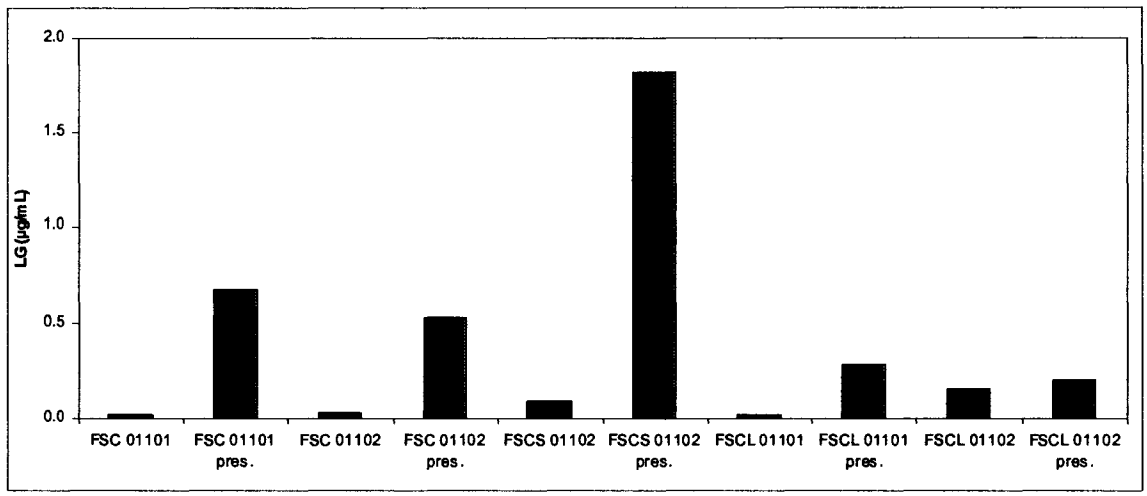

Figure 2-13. Comparison of levoglucosan (LG) concentrations in fog water samples (untreated versus preserved with chloroform) from Fresno, CA, determined by HPAEC-PAD 2.5 months after sample collection.

These observations were surprising, particularly since Fraser and coworkers determined levoglucosan to be reasonably stable even in acidic solutions (down to pH 2) (Fraser and Lakshmanan, 2000). Degradation in ambient aerosol extracts and fog water may be due to microbial activity. Alternatively (or in addition), the presence of acidic and possibly even basic constituents in the aqueous samples may cause degradation over longer periods of time (compared to Fraser's experiments). Additional research is necessary to determine the degradation mechanisms. Moreover, alternative sample preservation techniques need to be investigated, such as buffering or treatment with UV light to destroy microorganisms potentially present in the aerosol extracts/fog water. This phenomenon may have serious implications, as potential degradation of levoglucosan in aqueous media may lead to significant atmospheric

losses when levoglucosan is scavenged in fog or clouds. For instance, the validity of source apportionment estimates utilizing levoglucosan as a biomass combustion tracer would be questionable. Further research is certainly necessary to better understand the atmospheric stability of levoglucosan.

2.3.6. Conclusions

HPAEC-PAD is a rather new analytical approach for the analysis of carbohydrates in aerosol samples. The method is capable of measuring various sugars, including isomeric anhydrosugars used as biomass combustion markers, over a wide range of concentrations, without chemical derivatization or other complex sample preparation prior to analysis. The HPAEC-PAD method was shown to be highly sensitive and selective for the separation and quantification of anhydrosugars and other sugars in aqueous extracts of ambient aerosol particles as well as biomass combustion source samples. Due to the high sensitivity of the method, HPAEC-PAD may also be suitable for semi-continuous (on-line) measurements of fine-particle levoglucosan and other sugars, for instance by direct coupling with a particle-into-liquid-sampler (PILS) (Orsini et al., 2003, Weber et al., 2001).

2.4. MICROCHIP-CE-PAD METHOD

2.4.1. Background

Separation in CE takes place inside a narrow capillary (I.D. < 100μm) filled with an electrolyte (buffer) solution. A potential applied across the capillary and the formation of a charged ionic double layer at the interface of buffer and capillary initiate bulk flow inside the capillary through electro-osmotic flow (EOF). Migration of the analytes through the capillary depends on several factors, including the mass/charge ratio of individual compounds, magnitude of the applied

potential, and the composition of the electrolytic solution. The main advantage of CE over many other analytical methods is its very high separation efficiency. However, there are a few difficulties associated with electrophoretic analysis that need to be addressed prior to successful application of CE methods. These limitations include the absence of chromophoric or fluorophoric groups in many analytes, limiting the choice of detection methods, as in HPLC. Furthermore, separation in CE is based on differential migration of charged species through the capillary. However, most organic compounds are neutral and thus not amenable for electrophoretic separation. Electromigration can be induced by various methods, including ionization of hydroxyl groups at high pH, complex formation with charged species, or derivatization with reagents forming ionizable products.

Detection methods applicable for CE are essentially the same as those used with HPLC. While UV-light absorption and fluorescence detection are highly sensitive methods, many compounds are not detectable by these methods without prior chemical derivatization due to the lack of chromophores or fluorophores in the analyte molecules. However, a derivatization step adds complexity to the analytical procedure and potentially introduces artifacts. Electrochemical detection methods provide high sensitivity and selectivity, particularly in carbohydrate analysis, while eliminating the need for chemical derivatization (Baldwin, 2000, Lu and Cassidy, 1993, O'Shea and Lunte, 1993, Voegel and Baldwin, 1997). Recent advances in CE detection methods also include various MS techniques, such as ion-trap and quadrupole time-of-flight (Q-TOF) MS (Iinuma and Herrmann, 2003, Zamfir and Peter-Katalinic, 2001).

The intrinsic design of electrophoretic devices, using micro-columns (capillaries) without the need for active pumping, lends itself well to further miniaturization of the instrumentation, resulting in the recent development of microchip CE systems (Baldwin et al., 2002, Fanguy and Henry, 2002, Keynton et al., 2004, Kutter, 2000, Lacher et al., 2001, Wang, 2002). The method

developed here is based on electrophoretic separation of aqueous samples on a microfluidic chip, using a borate buffer to provide electromigration, coupled with electrochemical detection. Development of the method was led by Garcia and coworkers and is described in more detail elsewhere (Garcia et al., 2005). A brief summary of the experimental conditions and initial results are presented below to complement information presented in this chapter on analysis of biomass combustion markers.

2.4.2. Experimental

A custom-designed and lab-built microchip CE device was optimized for the separation and detection of anhydrosugars and other simple carbohydrates. The microchip was fabricated from a polymeric material, polydimethylsiloxane (PDMS), and consisted of a capillary, potential electrodes (platinum), and working electrode (gold wire). Figure 2-14 shows a schematic of the microchip.

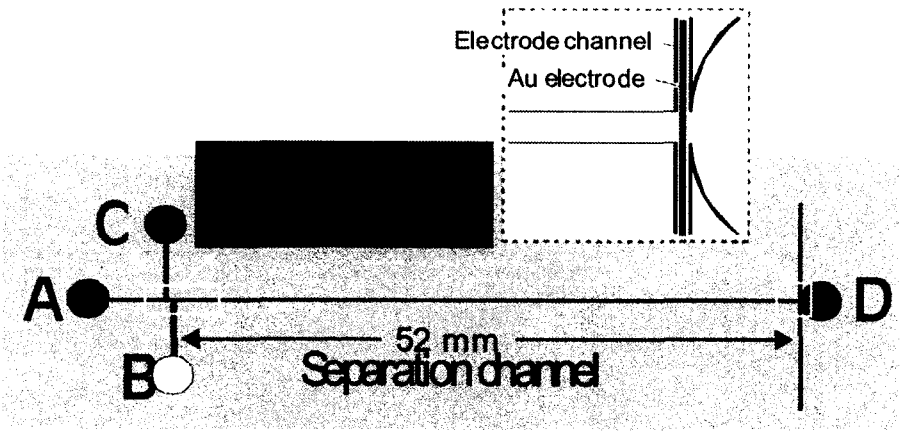

Figure 2-14. Diagram of the CE microchip, showing the various reservoirs, separation channel, and electrodes.

Separation potentials between +600 and +1500 V were evaluated; +1000 V provided a reasonable compromise between analysis time and signal/noise ratio. A range of detection potentials was also examined, with +0.9 V chosen as the optimal value. Effective separations were achieved with 5 mM borate ($Na_2B_4O_7$) buffer (pH = 12.3) while simultaneously enhancing the electrochemical detection of the analytes.

2.4.3. Initial Results

Results from preliminary CE separations of several simple carbohydrates are promising. Levoglucosan was readily separated from other isomeric anhydrosugars (e.g., mannosan and galactosan) and regular sugars (e.g., glucose) without prior chemical derivatization, as demonstrated in Figure 2-15 by a typical microchip-CE-PAD electropherogram. The sensitivity of the CE-PAD method is at least as good as current levoglucosan measurement by GC-MS. Furthermore, separations are significantly faster than by GC-MS or HPAEC-PAD (1 min. versus 52 min. for GC-MS or 15 min. by HPAEC-PAD).

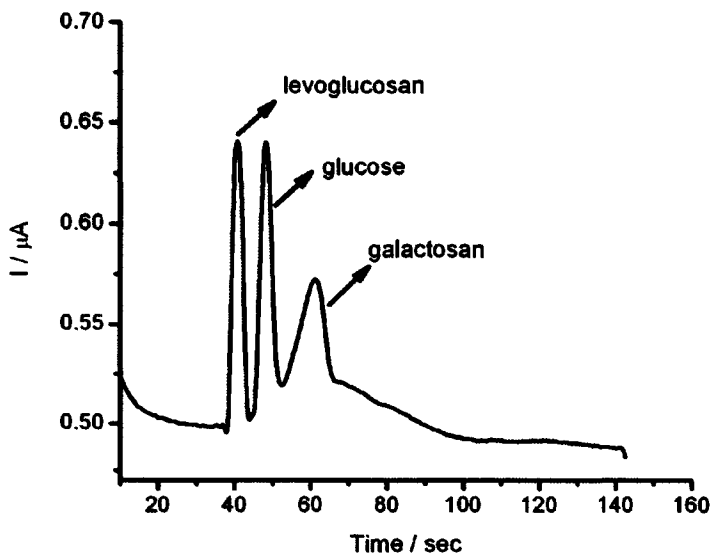

Figure 2-15. Microchip-CE-PAD electropherogram showing the separation of the anhydrosugars levoglucosan and galactosan, as well as glucose.

Several challenges that need to be addressed in future research include potential interference with levoglucosan detection from high ion concentrations in aerosol extracts (or fog water). Possible approaches include varying the buffer composition, for instance by adding a modifier that would result in a change of mobility, viscosity, or other separation parameters. Alternatively, the filter extraction could be performed in a polar solvent (other than water) or even in buffer solution.

2.4.4. Conclusions

Microchip-CE-PAD is capable of separating several sugars, including levoglucosan, mannosan, and galactosan, effectively in less than two minutes. The instrumentation is easy to operate and it is less expensive than GC-MS and HPAEC-PAD systems. Furthermore, microchip-CE-PAD is highly sensitive, requiring absolute amounts of mass on the order of picograms or less. Therefore, this approach also has the potential to be utilized for semi-continuous, automated measurements of biomass combustion tracers. Coupling a microchip-based CE system to an on-line aerosol collection system, such as PILS (Orsini et al., 2003, Weber et al., 2001), would allow for near-real-time monitoring of airborne fine particle concentrations of anhydrosugars or other chemical species.

2.5. BIOSENSOR METHOD

2.5.1. Background

In another attempt to develop alternative measurement techniques for biomass combustion molecular markers that are cost effective, easy to use, and portable, and thus suitable for field applications, biosensor methods were explored. Biosensors are chemical sensors that employ an immobilized biological component, such as enzymes, in conjunction with an electrical transducer to produce an analytical signal (Pearson et al., 2000). Major advantages of biosensors include the

ability to measure specific analytes even in a complex sample matrix because of the high selectivity of the biological recognition element. The biological element in the devices explored here is the glucose oxidase enzyme which selectively catalyzes the oxidation reaction of glucose (Wang, 2001, Wilson and Turner, 1992). Biosensors typically have fast response times, allowing for real-time and continuous measurements (Wang, 2002). Electrochemical biosensors are the most common types, using amperometric or potentiometric transducers (Heller, 1996, Wang, 2002). Initial experiments as part of the investigations reported here were conducted with two simple sensors: a commercial amperometric blood glucose sensor and a home-made sensor, consisting of a pH electrode in conjunction with an enzyme solution. The biosensor method that was investigated further for the detection of levoglucosan is based on an established procedure for the detection of glucose which is formed during hydrolysis of levoglucosan, as described below.

2.5.2. Exploratory Experiments

The goal of this work was to explore the applicability of simple biosensor methods to the measurement of levoglucosan in aqueous solutions, representing aerosol extracts influenced by biomass combustion. Two approaches to the proposed method were initially investigated: amperometric detection of glucose via its oxidation products and measurement of the pH change due to the formation of gluconic acid during the oxidation of glucose. The first approach utilized a commercial glucose meter (Medisense Precision QID) designed for glucose monitoring in human blood. The enzyme-catalyzed oxidation produces a signal based on the electric current that is generated by the oxidation reaction. The amperometric approach may be limited by the presence (or absence) of electrolytes in the solution to be measured. Since commercial blood glucose meters are designed and calibrated for the determination of glucose in human blood, containing a variety of ions, test solutions were prepared with an electrolyte composition that approximately simulated blood in terms of its salinity. The test solutions contained the major ionic components of blood, including sodium (Na^+), potassium (K^+), calcium (Ca^{2+}), bicarbonate

(HCO_3^-), and chloride (Cl^-) ions. In the simple test procedure a drop of the test solution was applied to a Medisense Precision QID test strip which was inserted into the glucose meter and readings were obtained within 20 seconds.

Reasonably accurate results were obtained from solutions of known glucose concentrations with the Precision QID meter, provided a certain electrolyte composition of the test solutions was maintained. A series of tests showed the need to include a buffer, such as bicarbonate ion, in the solution rather than merely a certain ion content for accurate measurement, as demonstrated in Table 2-7. The solution used in test 2 contained a higher concentration of total ionic species than test mixture 1, yet the true glucose concentration was underestimated. Test solutions 3 and 4, containing sodium bicarbonate and sodium chloride, provided relatively accurate QID sensor readings. The necessity to add ionic compounds to an aerosol extract complicates application of this approach for the detection of glucose and/or levoglucosan in atmospheric aerosol particles. Another disadvantage of the commercial sensor was the limited range of detection (200 - 6000 μg/mL) that would not allow the determination of levoglucosan concentrations observed in ambient aerosol samples. Typical ambient levoglucosan concentrations vary roughly between 2 and 500 ng/m^3 (corresponding to approximately 0.04 - 10 μg/mL in aqueous solution based on a typical 24-hour Hi-Vol sample) (Engling et al., 2006b, Fine et al., 2004c, Fraser and Lakshmanan, 2000, Zdrahal et al., 2002), while samples impacted by smoke from biomass combustion have been observed with levoglucosan concentrations as high as 7.6 μg/m^3 (Schauer and Cass, 2000). However, the limited detection range is not a limitation that is intrinsic to the technique but rather the specific instrument that was designed for measurement of (relatively high) glucose concentrations within a certain range typically observed in human blood. In fact, amperometry is one of the most sensitive instrumental analytical techniques.

Table 2-7. Results from Precision QID glucose sensor experiments.

Composition	Test 1	Test 2	Test 3	Test 4
NaCl (mg/mL)	7.3	98.0	23.0	23.0
$NaHCO_3$ (mg/mL)	8.0		8.6	8.5
Glucose (mg/mL)	1.05	1.30	0.49	1.00
QID - theoretical	105	130	49	100
QID - actual	117	42	52	108

The second approach was based on pH measurements with a sensor constructed from a pH electrode and an aqueous solution of glucose oxidase (Sigma) embedded in a semi-permeable membrane (Spectrum Spectra/Por molecular-porous regenerated cellulose membrane). A decrease in pH was observed due to the formation of gluconic acid during the oxidation of glucose. A commercial pH meter (Orion model 250A) was used to measure the change in pH. Test solutions with various glucose concentrations were measured by taking periodic pH readings. Plots of pH versus time showed qualitatively that the rate of formation of the oxidation products (gluconic acid) decreased over time, as shown in Figure 2-16. Furthermore, the reaction rate was a function of the initial glucose concentration.

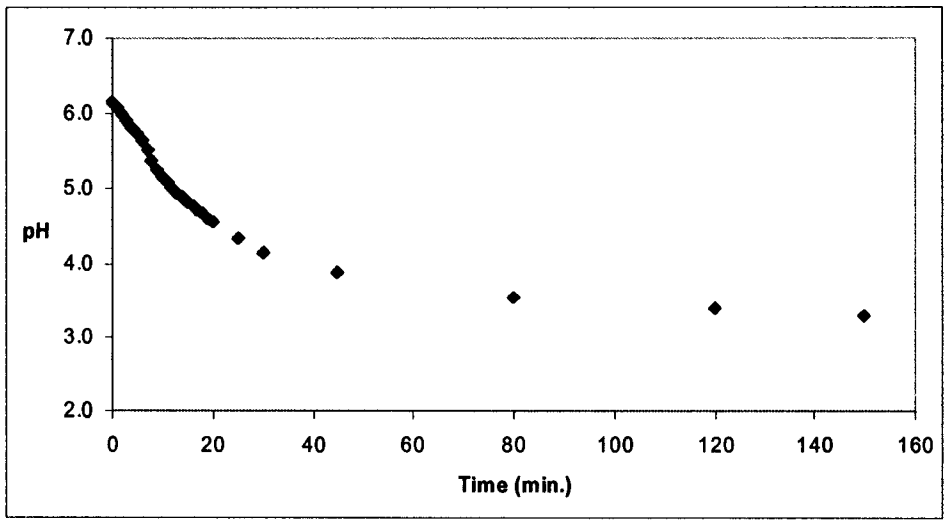

Figure 2-16. pH as a function of time from pH-electrode-based glucose biosensor.

The pH biosensor method has the advantage of a simple experimental setup and very low cost. On the other hand, major drawbacks of this approach include long analysis times due to acquisition of sufficient data for kinetic data reduction. These exploratory biosensor experiments prompted the investigations with a universal amperometric biosensor that measures glucose either via the amount of oxygen consumed or hydrogen peroxide generated during the oxidation process, as described in the following section.

2.5.3. Experimental

This biosensor method for levoglucosan detection utilizes an amperometric glucose sensor. Glucose is formed during hydrolysis of levoglucosan upon acidification (pH = 1 or less) of the aqueous sample or standard solution, as shown in Figure 2-17. No hydrolysis was observed at higher pH values, at least not over periods of several hours.

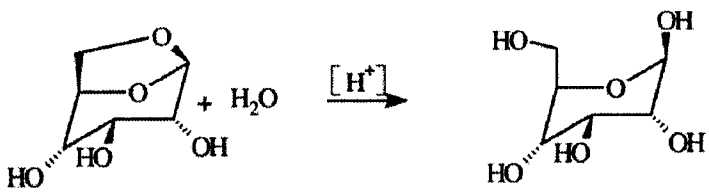

Figure 2-17. Acid hydrolysis of levoglucosan to glucose.

While biosensors are typically custom prepared by immobilizing the enzyme in a polymer film, the glucose sensors used in this study were based on Clark-type oxygen electrodes, obtained from Universal Sensors, Inc. ("USensors", Metairie, LA). A schematic of the electrodes is shown in Figure 2-18. Two types of glucose electrodes were investigated, both using glucose oxidase chemically immobilized in a membrane that is in contact on one side with the analyte solution and on the other side with the amperometric electrode: the oxygen system uses an oxygen membrane and a negative potential to reduce oxygen. Glucose diffuses into the enzyme layer where it is oxidized under the catalytic action of the enzyme to produce hydrogen peroxide and D-glucono-d-lactone. The consumption of oxygen at the electrode surface is directly proportional to the concentration of glucose present in the analyte solution; the peroxide system is based on the production of hydrogen peroxide at the electrode surface during the oxidation reaction which is also proportional to the glucose concentration in the analyte solution. The sensing method (oxygen or peroxide) can readily be changed by substituting the enzyme jacket designed for a particular method (shown in white in Figure 2-18) on the electrode. The reactions taking place at the electrode, including the biocatalytic oxidation of glucose, are shown below.

$$\text{glucose} + O_2 \rightarrow H_2O_2 + \text{D-glucono-d-lactone}$$

$$H_2O_2 \rightarrow O_2 + 2\,H^+ + 2\,e^-$$

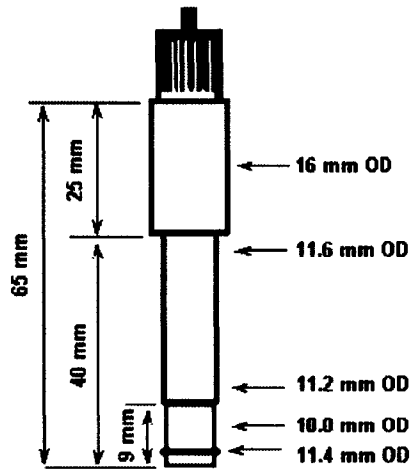

Figure 2-18. Schematic of Universal Sensors' Glucose Sensor.

In addition to the electrode, a potentiostat (USensors model 3002) and a digital volt-meter (Extech model M570 high-resolution multimeter) were needed for the operation of the biosensor. The signal produced in the oxidation reaction is an electric current that is converted to a voltage by the potentiostat and displayed on the volt meter. All required equipment to operate the glucose biosensor occupies little space, as demonstrated in Figure 2-19.

Figure 2-19. Image of the complete experimental set-up of the glucose biosensor.

Two protocols were used: the "buffer" and "drop" methods. Initial experiments (buffer method) were carried out in 2.0 mL of buffer solution that was continuously stirred at a constant rate to aid mass transfer, therefore improving reproducibility. Once the voltage of the electrode response in the buffer solution reached steady state, that reading was recorded as background value. A small, precisely measured, volume of sample or standard solution was added to the stirring buffer solution and a voltage reading was taken two minutes later following the sample injection. The second protocol (drop method) was developed to improve the sensitivity of the method. A 200 μL drop of buffer solution was equilibrated with the ambient air. Again, a small volume of sample or standard was injected into the buffer drop and readings were taken two, four and six minutes following the injection.

In the case of the oxygen sensor (that is based on the consumption of oxygen during the oxidation of glucose), it was important to maintain a constant temperature during the measurements. The equilibrium amount of oxygen dissolved in water (or buffer solution) depends on the solution temperature. As the surrounding air was in direct contact with a relatively small volume of buffer solution, the ambient temperature significantly affected the buffer temperature and thus the oxygen content, as demonstrated by a timeline of ambient temperature and measured voltage in Figure 2-20. Use of a constant-temperature bath during measurements effectively minimized the temperature effect. In addition to maintaining a steady temperature during the measurements for improved precision and accuracy, a RC filter was used to minimize electronic noise from the instrument output. Finally, corrections were made to account for the dilution effect due to the addition of analyte solution to a relatively small volume of buffer, particularly in the case of the drop method.

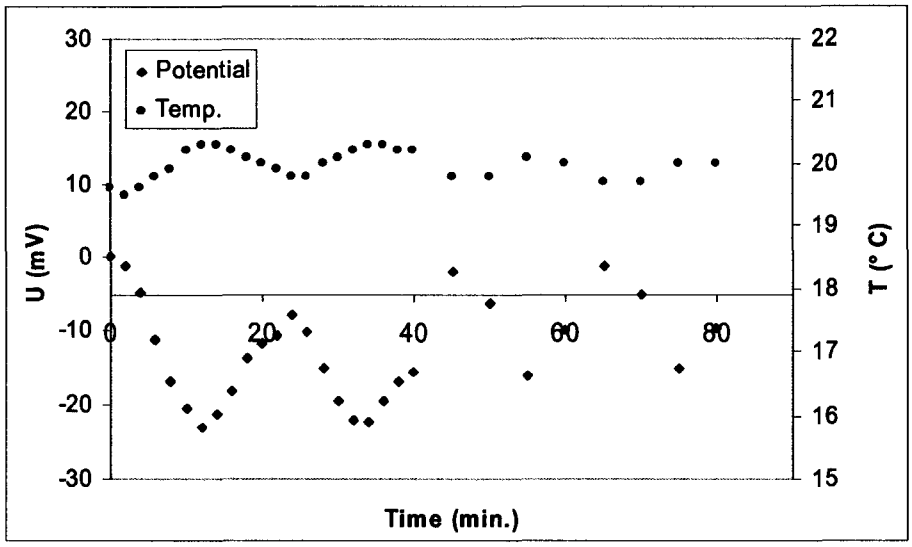

Figure 2-20. Biosensor signal as a function of time and temperature.

Ambient $PM_{2.5}$ aerosol samples collected on quartz fiber filters were extracted with known amounts of DI water and acidified with hydrochloric acid (HCl) to pH 0.5. The resulting solutions were then measured with the glucose sensor by the drop method.

2.5.4. Method Development and Optimization

Glucose oxidase selectively catalyzes the oxidation of glucose (Wilson and Turner, 1992). However, tests with mannosan, a stereoisomer of levoglucosan, showed that there is a small response of the glucose sensor to mannose (formed upon acidification of mannosan) as well. While the sensor response to mannose was relatively small (< 25% of the levoglucosan response), there was no response observed from galactosan, i.e., galactose. In addition, ambient aerosol concentrations of mannosan are typically lower than those of levoglucosan by approximately one order of magnitude. Therefore, artifacts caused by interfering reactions of mannosan can be considered negligible. On the other hand, glucose potentially present in an aerosol extract (prior to the formation of glucose by hydrolysis of levoglucosan) would be detected by the sensor as

well and thus constitute a positive artifact in the quantification of levoglucosan. To account for this portion of glucose, a differential measurement is necessary by determining the original concentration of glucose prior to acidification which will be subtracted from the value obtained upon acidification (conversion of levoglucosan to glucose), i.e., the total glucose.

Under the optimized conditions, outlined above (section 2.5.3.), the glucose (oxygen) sensor typically reached steady state within two minutes after injection of the sample or standard solution into the buffer solution. Measurements of biosensor signal (expressed in mV) as a function of time were conducted for different sugar concentrations, such as shown for a 100 μg/mL glucose standard in Figure 2-21, using the buffer method. The sensor response reached steady state for all concentrations in two minutes or less.

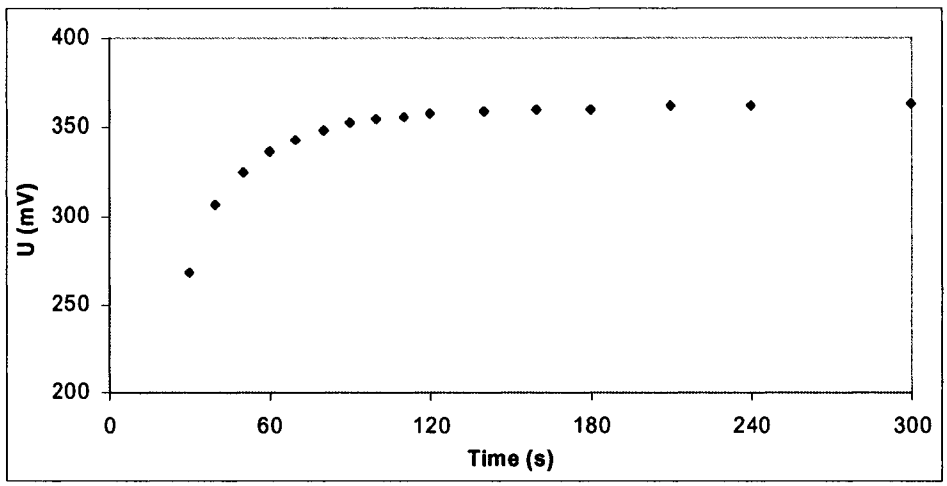

Figure 2-21. Biosensor signal as a function of time for a 100 μg/mL glucose solution (buffer method).

Glucose calibration curves, using the buffer method, were linear over more than three orders of magnitude (0.2 to 250 μg/mL), including the lower part of the concentration spectrum that is more representative of ambient levels, as shown in Figures 2-22 and 2-23. Good correlation was

observed for the lower concentration range as well, with correlation factors (R^2) of 0.99 or higher (Figure 2-23). Calibration curves obtained by the drop method showed a lower degree of linearity compared to buffer method calibrations, possibly due to the smaller volumes used in the drop method (200 μL). Likewise, correlation factors (R^2) for the linear regressions are lower than those for calibrations obtained by the buffer method. A typical glucose calibration curve using the drop method is shown in Figure 2-24.

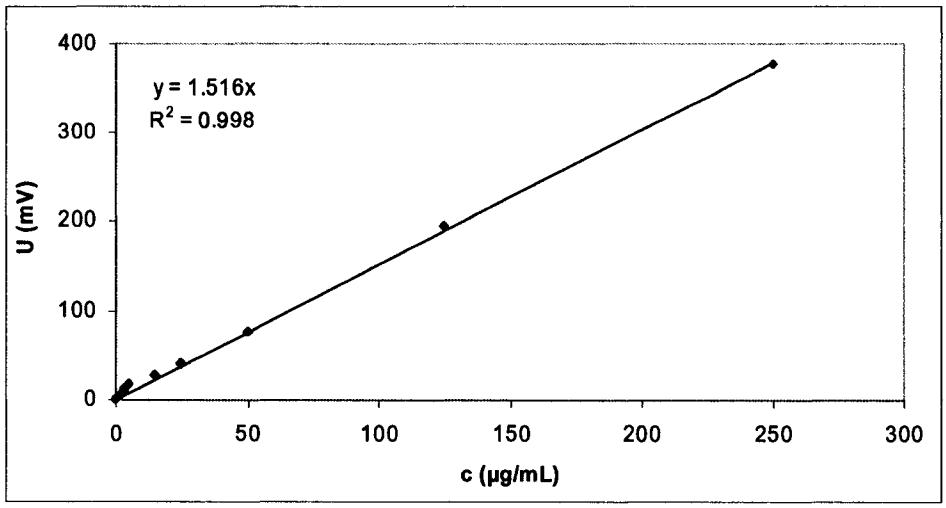

Figure 2-22. Glucose calibration curve (buffer method).

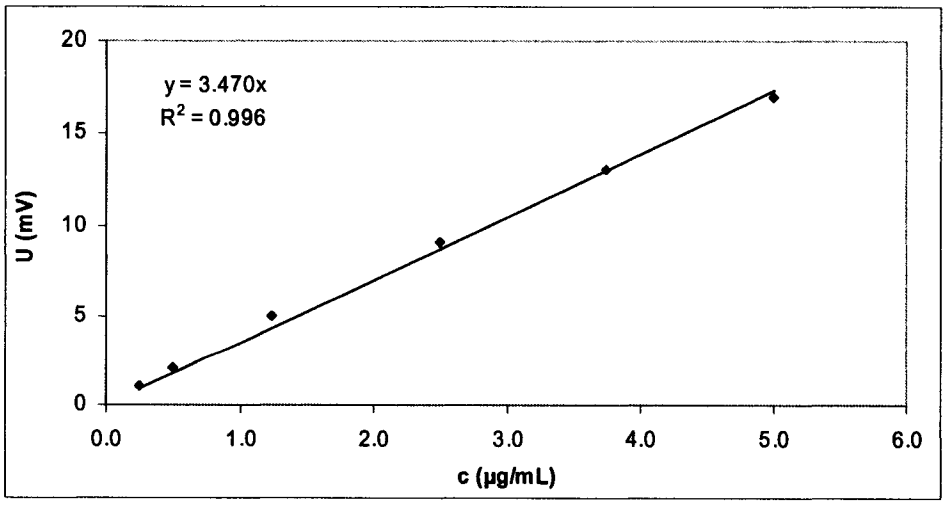

Figure 2-23. Glucose calibration curve (lower concentration range - buffer method).

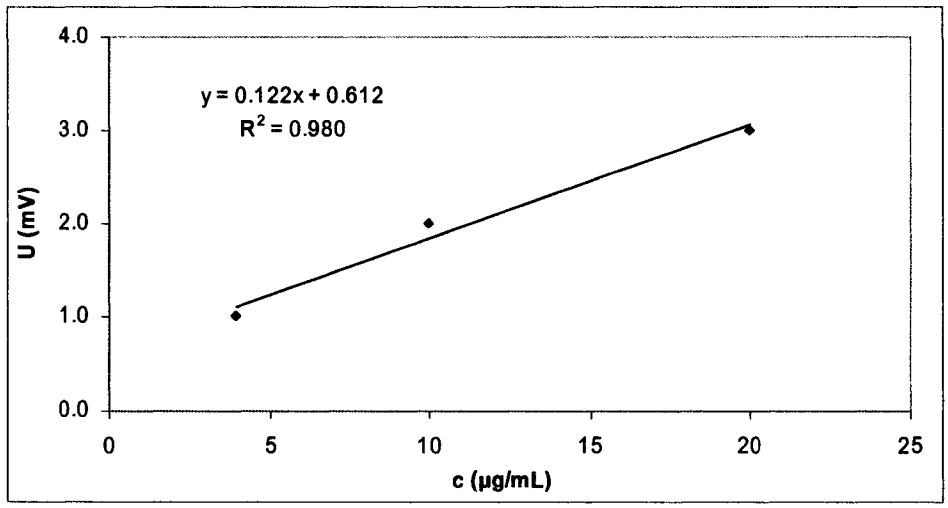

Figure 2-24. Glucose calibration curve (drop method).

Calibration solutions for levoglucosan were prepared by acidifying standard solutions, containing three different concentrations of levoglucosan, with HCl to pH 0.5. Levoglucosan calibration curves were obtained only by the drop method, as shown in Figure 2-25.

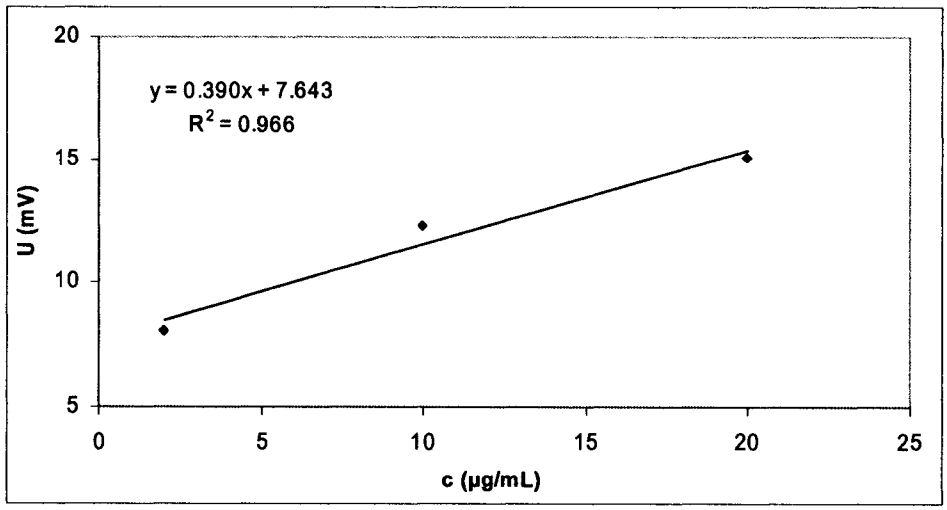

Figure 2-25. Levoglucosan (pH = 0.5) calibration curve (drop method).

Exploratory experiments were also carried out with the glucose sensor using the hydrogen peroxide enzyme jacket. While more research is needed to explore the capabilities of this sensing method, initial results are promising, as demonstrated by the glucose calibration in Figure 2-26 and method comparison in Figure 2-27. The peroxide method may allow for more precise measurements, since the signal is independent of the oxygen content in solution and thus less dependent on temperature compared to the oxygen method.

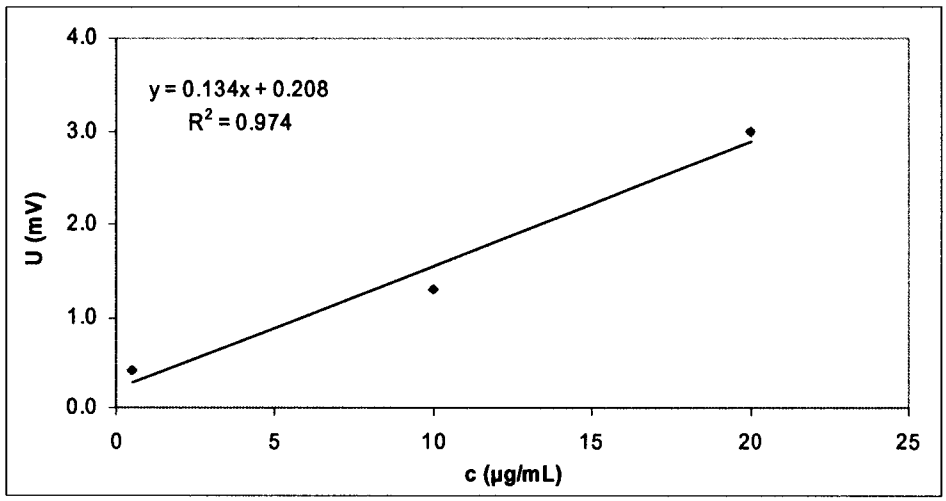

Figure 2-26. Glucose calibration curve obtained with the peroxide-based sensor (drop method).

The method detection limit (MDL) for glucose, using the buffer method, was estimated to be 5 µg/mL (corresponding to a final concentration of 0.25 µg/mL in the buffer solution) based on the lowest standard concentration measured. This value also corresponded to a measured voltage approaching the lowest resolution of the volt meter (0.1 mV). The biosensor signal is based on a differential measurement of the voltage of a sample (containing glucose) and the buffer solution. Thus, blank measurements (0 V) can not be used to determine detection limits. Detection limits for the drop method are lower by approximately a factor of two. The measurement uncertainty for the buffer method was typically approximately 20% (one RSD), based on replicate measurements of glucose standards, as demonstrated in Figure 2-27 for a 0.9 µg/mL glucose

standard (n = 7). Due to the smaller volume of buffer used with the drop method compared to the buffer method (200 μL versus 2.0 mL), measurement precision was lower when using the drop method.

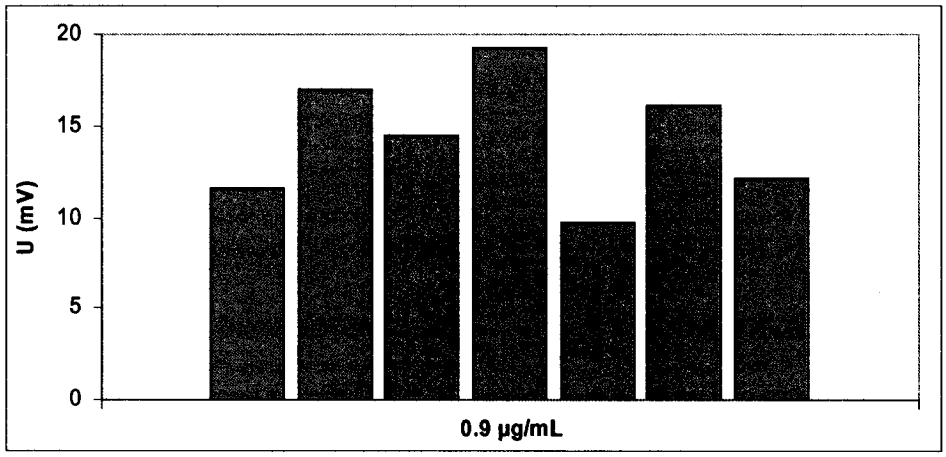

Figure 2-27. Replicate measurements of a 0.9 μg/mL glucose standard solution (oxygen-based buffer method).

Extracts of selected ambient $PM_{2.5}$ aerosol samples collected on quartz fiber filters were measured with the glucose (peroxide) sensor by the drop method, following acid hydrolysis of levoglucosan to glucose. These results were compared to concentrations in the same samples determined independently in DCM extracts by GC-MS or in aqueous extracts by HPAEC-PAD, as shown in Figure 2-28. The correlation between the methods was reasonably good, especially considering the intrinsic uncertainty of organic compound analysis by GC-MS.

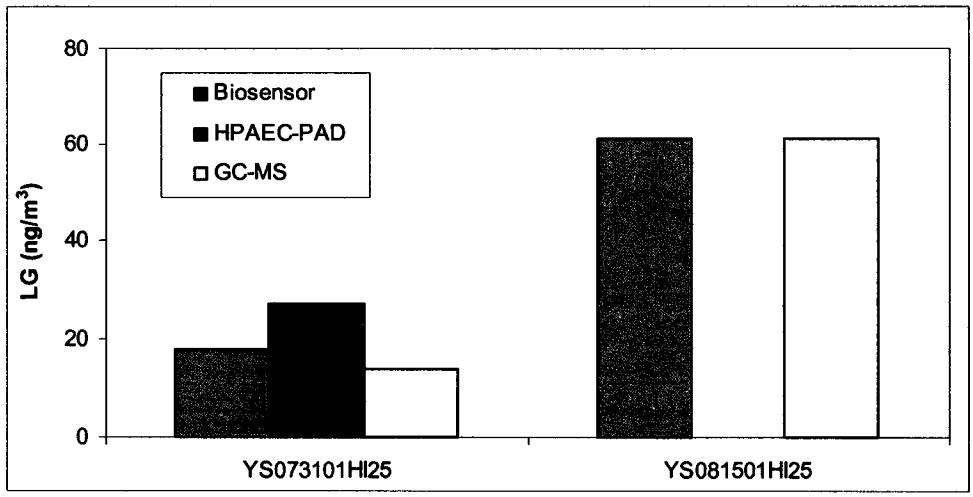

Figure 2-28. Comparison of levoglucosan (LG) concentrations obtained by three independent methods: biosensor (peroxide-based drop method), GC-MS, and HPAEC-PAD.

2.5.5. Applications

Due to the simple operation and fast measurement of aqueous samples, the biosensor method could be used for initial evaluations of aerosol samples before selecting specific filters for more detailed (and expensive as well as time consuming) chemical analysis. The low cost of the method also suggests its possible application as a screening tool for large numbers of aerosol samples, such as those collected from monitoring networks (e.g., IMPROVE network), in order to identify periods of significant biomass combustion influence.

2.5.6. Conclusions

The main advantages of the glucose biosensor technique developed here are selective enzyme-catalysis, linear response over a wide range of concentrations, short response times, and inexpensive instrumentation (ca. $1500 for the entire set-up, including electrode, potentiostat, volt meter, and adapters) that allow for field applications or screening of large sample numbers. Limitations of the technique are given by the nature of the enzyme sensor and include a certain attainable level of precision and sensitivity as well as possibly limited long-term stability of the

enzyme. The low sensitivity of the sensor in its current development state and rather high measurement uncertainty pose serious limitations to the applicability of the method to samples with low biomass smoke influence. However, the potential of this method appears to be broader than the results presented here, indicating that additional modifications to the system may expand the range of detectable concentrations especially at the lower end. For instance, the use of more sensitive custom-made electrodes may further lower the limits of detection. Nevertheless, the method developed here using a Universal Sensors glucose sensor is a promising supplemental technique to common detection methods for levoglucosan in atmospheric aerosols.

2.6. CONCLUSIONS

Despite several inherent limitations, GC-MS methods provide both qualitative and quantitative information about organic aerosol constituents. An important strength of GC-MS methods is the high sensitivity that allows for accurate measurements of trace-level organics. Unlike most other instrumental methods, GC-MS is capable of simultaneously analyzing numerous species within various compound classes. Nearly two hundred individual organic compounds have been identified and quantified as part of the studies discussed here.

HPAEC-PAD, a rather new analytical approach for aerosol samples, is capable of measuring various sugars over a wide range of concentrations in ambient and source samples. The HPAEC-PAD method was shown to be a highly sensitive, yet relatively simple analytical technique for the separation and quantification of anhydrosugars and other sugars in aqueous extracts of aerosol particles from different sources. Unlike with traditional GC and LC methods, there is no need for chemical derivatization or other complex sample preparation prior to analysis. Due to the high sensitivity of the method, HPAEC-PAD may also be suitable for semi-continuous measurements

of fine-particle levoglucosan and other sugars. The sensitivity and simplicity of the method also allow for routine analysis of biomass combustion tracers in samples collected in aerosol monitoring networks, such as IMPROVE.

The CE-PAD technique is characterized by fast analysis times and high sensitivity. The method is capable of separating several sugars, including the biomass combustion tracers levoglucosan, mannosan, and galactosan in less than two minutes. Furthermore, the instrumentation is easy to operate and it is less expensive than GC-MS and HPAEC-PAD systems. Future optimization of this technique should focus on potential matrix interferences during analysis of ambient aerosol samples. In addition, interfacing CE-PAD with an on-line aerosol collection system, such as PILS, for semi-continuous aerosol characterization, promises to provide important information about chemical constituents in the atmosphere that are subject to rapid changes which can not be measured by current methods.

The biosensor method developed here promises to be a useful supplemental technique to conventional detection methods for levoglucosan in atmospheric aerosols. The selective enzyme-catalysis, fast response times, and inexpensive instrumentation of this method would allow for field applications or screening of large sample sets. However, the rather low precision and sensitivity of the method in its current state of development certainly requires further improvement for the biosensor to be utilized as viable screening tool for aerosol with influence from biomass combustion. The CE-PAD and HPAEC-PAD methods, on the other hand, provide relatively simple and fast measurement at a high level of sensitivity and precision, rendering them as superior alternative methods for the detection of biomass combustion tracers in ambient aerosol.

CHAPTER 3 YOSEMITE AEROSOL CHARACTERIZATION STUDY

3.1. INTRODUCTION

3.1.1. Motivation

As discussed in chapter 1, particulate OM is an important component of atmospheric aerosol and can be the predominant constituent of fine atmospheric particles in the Western U.S., with contributions to fine particle mass concentrations reaching 50% or more (Malm et al., 2004). National Parks in the western U.S., such as Yosemite, are examples of Class I areas that are strongly impacted by particulate OM (Malm et al., 2004). Emissions from biomass burning are a major global source of OM (Bond et al., 2004). Smoke from wildfires and prescribed burns can therefore have significant impacts on visibility and regional air quality. Since the effect of atmospheric particles on visibility strongly depends on their chemical and physical characteristics, the primary goal of the 2002 Yosemite Aerosol Characterization Study (YACS) was to investigate the chemical composition as well as the physical and optical properties of the ambient aerosol in Yosemite National Park. In particular, contributions from biomass burning to the regional haze were to be determined.

The chemical composition of aerosol particles, particularly in rural and pristine areas, is generally not well characterized. Typically, only 15 to 20% of the fine organic particle mass is identified in terms of individual organic species (e.g., Schauer and Cass, 2000). Furthermore, it is known that

the aerosol chemical composition varies with particle size, reflecting the formation processes and determining atmospheric lifetimes (Seinfeld and Pandis, 1998). However, only a limited number of studies have investigated particle size distributions of carbonaceous aerosol in general (e.g., Alves et al., 2002, Plewka et al., 2004, Temesi et al., 2001). Likewise, size distributions of individual organic compounds have been determined for only a few selected compound classes, including PAH and oxidation products of biogenic organic compounds (e.g., Allen et al., 1997, Allen et al., 2001, Alves et al., 2000, Kavouras and Stephanou, 2002, Kavouras et al., 1998b, Miguel et al., 2004, Plewka et al., 2004, Sicre et al., 1990). Particle size distributions of biomass burning markers have not been reported to date, with the exception of a select number of compounds, including levoglucosan (Fine et al., 2004c, Schkolnik et al., 2005, Yttri et al., 2005). Therefore, the focus of the investigations reported here was speciation of the organic aerosol component, including the determination of carbonaceous aerosol species as a function of particle size, and the assessment of source contributions to summertime aerosol in Yosemite National Park.

3.1.2. Air Quality in Yosemite National Park

Yosemite National Park has traditionally been subject to poor visibility due to high PM concentrations, as illustrated by photographs taken during YACS at Turtleback Dome, situated on the south rim above the entrance to Yosemite Valley (Figure 3-1). Unlike most other pristine (Class I) areas in the US, the ambient aerosol in Yosemite is primarily carbonaceous in nature, with OM contributions to fine PM of 50 to 60% (Malm et al., 2000). It has also been demonstrated by long-term IMPROVE measurements that biogenic and pyrogenic sources have significant contributions to the ambient aerosol in western National Parks, like Yosemite (Malm et al., 2000), resulting in a large seasonal variability in aerosol loadings. Ambient PM concentrations are elevated during the summer months due to increased wildfire activity, while being subject to monthly or weekly variability because of the dynamic nature of wildfires. The

summer of 2002 was a particularly active fire season in most of the western U.S., with more than one hundred thousand acres of land burned in Oregon and California during the time frame of YACS (National Interagency Fire Center (NIFC) (NIFC, 2005). Satellite images and back trajectory analyses indicated that smoke from some of these fires was transported to Yosemite National Park during YACS (McMeeking et al., 2005c). As described below, other measurements carried out during the study confirmed a strong influence of wildfire smoke on the visibility in Yosemite, both on a regional and local scale. In addition, Yosemite National Park is influenced by air masses transported from California's Central Valley and the San Francisco Bay Area.

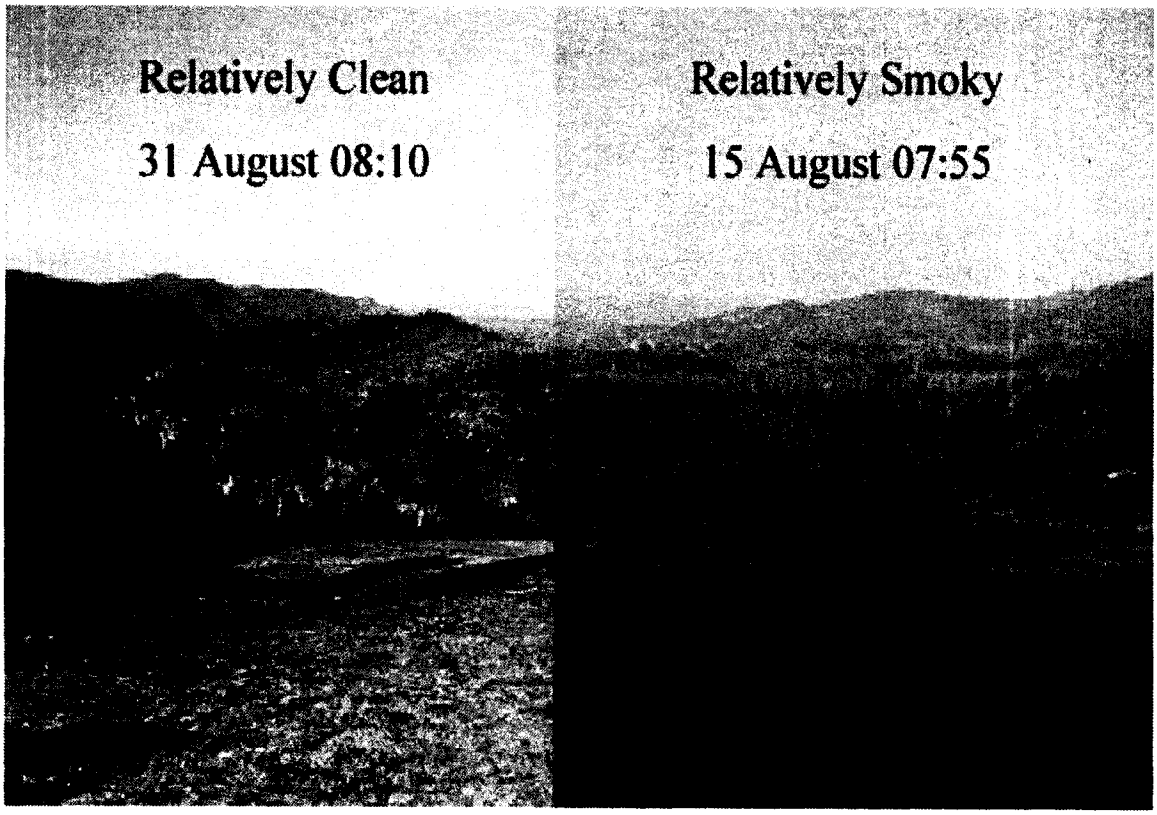

Figure 3-1. View from the Turtleback Dome sampling site in Yosemite National Park on two days during YACS, demonstrating different visibility conditions in the park.

3.1.3. Study Overview

The study was conducted from July 13, 2002, to September 5, 2002, at three sites in Yosemite National Park, California, as described in more detail below. The locations of the park and the major fires (larger than 500 acres in size) that were active during the time of YACS are shown in Figure 3-2. Two intensive sampling periods (July 28 – 31 and August 14 – 16) were selected during the study based on a number of observations, including elevated carbon levels, a diverging signal on a dual-wavelength aethalometer (operated with 5-minute time resolution), and an increase in visible haze (McMeeking et al., 2005c). Light scattering measurements with two nephelometers were performed to monitor the haze during YACS as well (Malm et al., 2005a). A timeline of fine-particle light scattering demonstrated the different haze levels throughout YACS (Figure 3-3). Cleaner periods (i.e., periods with better visibility) were observed at the beginning of the study and again at the end, while heavy haze caused increased scattering during two periods, towards the end of July and in the middle of August, 2005 (Figure 3-3). These periods coincide with the intensive haze episodes (identified above) that were classified as "regional" haze episodes due to the influence of smoke advected from Southern Oregon and other parts of California (McMeeking et al., 2005c). Light scattering by $PM_{2.5}$ dominated (~ 80%) the total light extinction during YACS (Malm et al., 2005a).

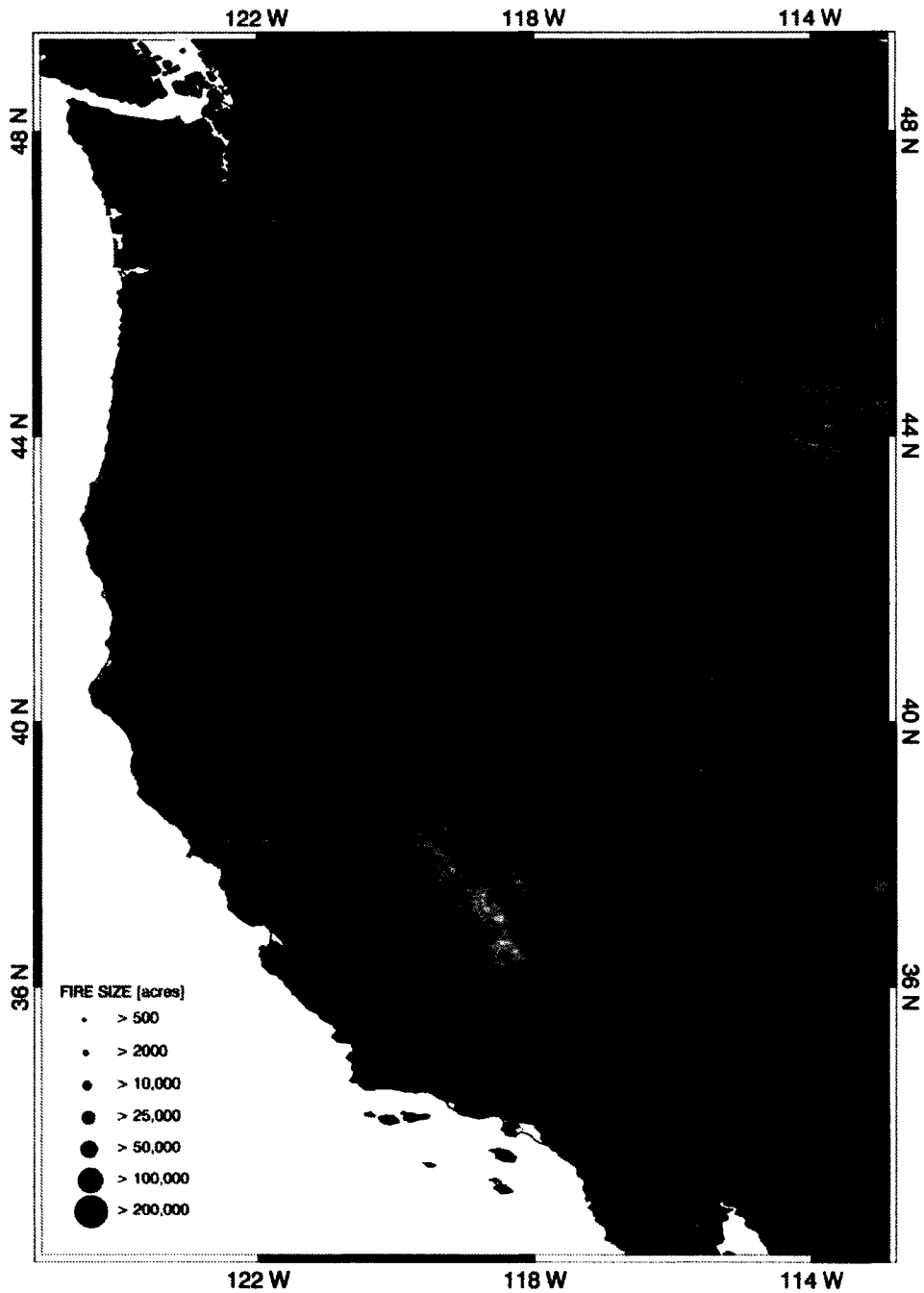

Figure 3-2. Location of the Turtleback Dome (Yosemite National Park) sampling site and of wildfires greater than 500 acres in size occurring in Washington, Oregon and California during the period from July 10th, 2002, to September 5th, 2002, as reported by the National Interagency Fire Center (NIFC).

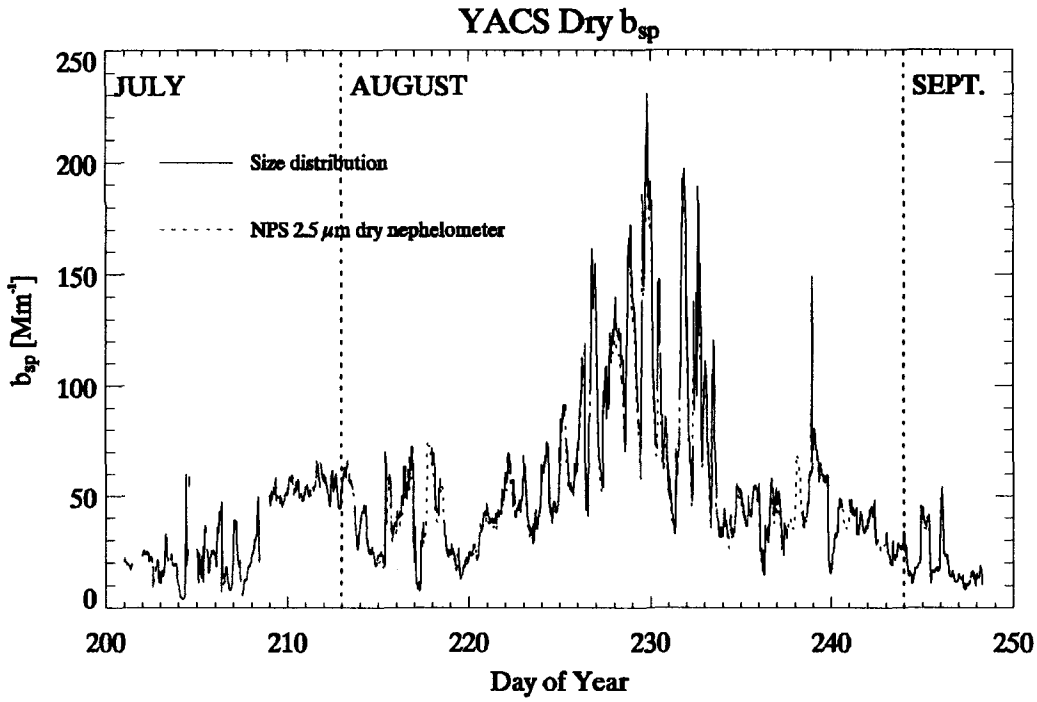

Figure 3-3. Timeline of light scattering measured at Turtleback Dome. Data provided by Derek Day.

The meteorological conditions during YACS were characterized by dry and warm air masses with an average temperature of 21.1 °C and an average relative humidity (RH) of 33% (the day-time averages were 25.0 °C and 26%, respectively). While westerly (up-slope) flow to the sampling site prevailed during the day, initiating transport of polluted boundary layer air from the direction of California's Central Valley in the morning, winds calmed in the evening and the wind direction changed to easterly, associated with down-slope drainage flow (McMeeking et al., 2005c).

The fine particle composition was dominated by OM during the study period, representing more than 70% of the total particulate matter with an aerodynamic diameter of 2.5 μm or less ($PM_{2.5}$) measured at Turtleback Dome. In addition, carbon isotope measurements indicated that the fine OM was derived mainly (in excess of 90% on average) from contemporary carbon sources, rather

than fossil fuel combustion (Bench and Herckes, 2004). Total carbon (TC) was shown to be directly proportional to contemporary carbon with a correlation factor of 0.99 and a slope of 0.9997, implying that variations in the TC concentrations in the ambient $PM_{2.5}$ were primarily a function of changes in the concentrations of contemporary carbon (Bench and Herckes, 2004). Fossil carbon did not vary with TC, constituting a small but nearly constant contribution of 0.7 $\mu g/m^3$ to the ambient $PM_{2.5}$ throughout the study (Bench and Herckes, 2004).

Several other publications provide additional information about YACS, including a general overview of the study (McMeeking et al., 2005c), physical and optical properties of the ambient aerosol in Yosemite National Park (Carrico et al., 2005, Hand et al., 2005, Malm et al., 2005a, Malm et al., 2005b, McMeeking et al., 2005a, McMeeking et al., 2005b), and a classification of fine PM as modern versus fossil-fuel derived (Bench and Herckes, 2004). This chapter focuses on the chemical composition of summer-time fine particulate OM during YACS and examines in particular source contributions to ambient $PM_{2.5}$ measured at Yosemite's Turtleback Dome from biomass combustion and other source types.

3.2. EXPERIMENTAL METHODS

3.2.1. Sample Collection

Samples were collected from July 13, 2002, to September 5, 2002, at three sites in Yosemite National Park, CA, USA: on Turtleback Dome (37.7125° North; 119.7042° West; 1615 m above sea level), on the roof of the visitors center in Yosemite Valley (37.7486° North; 119.5869° West; 1213 m above sea level), and at the park's ozone monitoring site near the Merced River in Yosemite Valley (37.7431° North; 119.5842° West; 1219 m above sea level). The Turtleback

Dome site, which also serves as a monitoring site for the Interagency Monitoring of Protected Visual Environments (IMPROVE) program, was chosen to capture regional influences in the Park, as it is located above the entrance to Yosemite Valley. The Yosemite Valley sites were utilized to help determine whether higher OM concentrations occur in this active visitor area. Samples at Turtleback Dome were collected using two different samplers: a ThermoAndersen (Smyrna, GA) GI200-2.5 high-volume (Hi-Vol) collector, equipped with an impactor to give a nominal size cut of 2.5 μm aerodynamic particle diameter, and a ThermoAndersen TA 235 Hi-Vol sampler, equipped with a 5-stage cascade impactor with nominal size cuts at 7.2, 3.0, 1.5, 0.95 and 0.49 μm, plus a back-up filter, collecting particles smaller than 0.49 μm (Willeke, 1975). Figure 3-4 shows the two samplers at the Turtleback Dome site beside the $PM_{2.5}$ sampler that was used to collect filters for ^{14}C analysis (Bench and Herckes, 2004). At the Merced River site samples were collected with a ThermoAndersen TA 235 Hi-Vol sampler, equipped either with a 5-stage cascade impactor or without size-selective inlet, generating total suspended particle (TSP) samples. The valley visitors center samples were collected with a Hi-Vol sampler equipped with a PM_{10} inlet. $PM_{2.5}$, PM_{10}, and the sub 0.49 μm particles from the cascade impactor were collected on Whatman (Maidstone, England) QM-A quartz fiber filters (20.3 x 25.4 cm). Coarse particles (larger than 2.5 μm aerodynamic diameter) and stages 1 through 5 from the cascade impactor were collected on slotted filters, custom-cut from Whatman QM-A quartz fiber filters. All samples were collected at a nominal flow rate of 1.13 m^3/min. Actual flow rates, reflecting ambient pressure and temperature, ranged from 1.03 to 1.13 m^3/min, as shown in Appendix E (Tables E-1 to E-3). Typical sampling times for $PM_{2.5}$ samples at the Turtleback Dome site were 24 hours (approximately 08:00 to 08:00 local time) or 12 hours (08:00 to 20:00 or 20:00 to 08:00) during intensive study periods. Sampling times for multi-stage samples, collected at Turtleback Dome or in Yosemite Valley, ranged from 24 to 72 and 48 to 91 hours, respectively. PM_{10} samples collected at the Yosemite visitors center had sampling times from 22 to 38 hours. An overview of all samples, including flow rates and corresponding sample volumes, is given in

Appendix E. Quality control measures included field blanks collected once per week. Prior to sampling, filters were pre-fired at 600 °C for at least 8 hours. Exposed filters were placed into individual pre-fired aluminum envelopes and stored frozen (< -15 °C) until analysis.

Figure 3-4. Hi-Vol samplers at the Turtleback Dome sampling site: $PM_{2.5}$ sampler for ^{14}C analysis (left), $PM_{2.5}$ sampler for organic speciation (center), and multi-stage impaction sampler (right).

3.2.2. Sample Preparation

Sample filters were solvent extracted for speciation of the organic aerosol component by GC-MS, as described in more detail in section 2.2. above and analogous to protocols reported previously (Brown et al., 2002). In summary, the collected filters were spiked with deuterated internal standards prior to extraction. A portion of the filter (typically one quarter) was extracted three

times with 25 mL of dichloromethane (DCM) for 15 minutes under ultrasonic agitation. The combined extracts were passed through a pre-fired quartz filter and subsequently reduced in volume by N_2 blow down to 250 μL. The concentrated extracts were divided into three portions for direct analysis by GC-MS and for chemical derivatization. One aliquot of each extract was methylated, using diazomethane, in order to convert carboxylic acids to their respective methyl esters. Another fraction was silylated to generate trimethylsilyl esters of alcohols, sterols, sugars and other organic species containing hydroxyl groups. In a typical silylation procedure 50 μL of concentrated sample extract were combined with 50 μL of BSTFA and 10 μL of TMCS, and the mixture was allowed to react for 2 hours at 70 °C. Composite samples were prepared prior to extraction by combining 1/8 of an original (20.3 x 25.4 cm) exposed quartz filter from each sampling period (24 or 12 hours) within a given week. Thus, eight weekly composite samples were prepared, consisting of seven to ten 1/8 filter portions of the corresponding 12 or 24 hour samples, as shown in Appendix E (Table E-4). Sample preparation of filters for HPAEC analysis is described below (section 3.2.4.).

3.2.3. GC-MS Analysis

Filter extracts were analyzed on a HP 6890 Gas Chromatograph coupled with a HP 5973 mass selective detector (MSD). Separation was accomplished using either a Supelco Equity 5 capillary column (30 m x 250 μm x 0.25 μm 5% phenyl-methyl-siloxane film) or a HP-5MS column with the same dimensions and stationary phase. Injections of 1 μL aliquots were performed in splitless mode. The GC temperature profile included an initial hold time of 10 minutes at 65 °C, followed by a temperature gradient of 10 °C/min to a final temperature of 300 °C that was held constant for 20 minutes. The MSD was operated in ion scan mode and ions were produced by electron impact ionization. Authentic standards were used for identification and to obtain response factors for the majority of the quantified organic compounds.

3.2.4. HPAEC-PAD Analysis

A portion of each filter (typically one quarter) was extracted twice with 15 mL of de-ionized water. The combined extracts were passed through a syringe filter containing a pre-fired 25 mm quartz fiber filter to remove insoluble material. Sample aliquots were injected without concentration or chemical derivatization into the chromatograph, using a 100 μL sample loop. The HPAEC-PAD system utilized here was a Dionex DX-500 series ion chromatograph, as described in section 2.3. above, consisting of a Dionex LC25 Chromatography Oven, GP50 Gradient Pump, and ED50 Electrochemical Detector. The electrochemical detector was equipped with a Dionex ED50/ED50A Electrochemical Cell, utilizing disposable gold electrodes and was operated in integrating amperometric mode. Separation of the individual anhydrosugars was achieved using a Dionex CarboPac PA 10 Analytical Column (4 x 250 mm) with an 18 mM aqueous NaOH eluent at a flow rate of 0.5 mL/min. Authentic standards were used for identification and to obtain response factors for all quantified anhydrosugars.

3.2.5. Carbon Analysis

Carbonaceous material in the ambient aerosol was determined by several independent methods (Malm et al., 2005a). Two of the methods provided a split between organic carbon (OC) and elemental carbon (EC) in addition to measuring TC. Samples were collected on quartz filters over 24 hr periods with the IMPROVE sampler, installed at the Turtleback Dome site, and subsequently analyzed by the Desert Research Institute (DRI) for TC, OC and EC according to the IMPROVE protocol, using the thermal-optical reflectance (TOR) method (Chow et al., 1993, McDade et al., 2004). In addition, portions (2.3 cm^2 punches) of the filters collected with the $PM_{2.5}$ Hi-Vol sampler were analyzed in our laboratory with a Sunset Laboratories continuous carbon analyzer in off-line mode, using the modified NIOSH thermal-optical transmission (TOT) method for pyrolysis correction (Birch, 1999, Birch and Cary, 1996). In order to examine artifact adsorption of volatile organic compounds on the pre-fired quartz filters, selected filters were cut

in half horizontally, followed by measurement of OC and EC on the front and back filter portions with the Sunset analyzer. While particulate carbonaceous matter and gas-phase organic compounds were assumed to be collected on the front portion, the carbonaceous material measured on the back portion of these filters was attributed to gas-phase organic compounds only. It was also assumed that the front and back filter portions collected equal amounts of gas-phase organic compounds. The analysis of eight sliced filters representing different conditions throughout the study showed varying amounts of vapor-phase OC on the back filter portion, suggesting the need of "seasonal" correction factors. In general, filters collected during periods with low OC concentrations showed significantly higher adsorption artifacts (in excess of 50%) compared to samples collected during hazy periods (characterized by high OC concentrations). Therefore, "seasonal" correction factors were determined based on the evaluation of the adsorption artifact on these selected filters. In addition, a gravimetric analysis of 15 sliced filters revealed a slight cutting bias: on average the front filter portion represented 44% of the total filter mass, while the back half was typically thicker (56% of total mass). Consequently, an additional correction factor to account for the cutting bias was determined. The seasonal correction factor for vapor adsorption together with the cutting correction factor were applied to all OC data obtained with the Sunset analyzer, including $PM_{2.5}$ and size-segregated samples, using equation 3-1, where OC_{F+B} denotes the combined OC mass measured on the front and back filter portions, OC_{BLK} is the blank value, OC_B is the OC measured on the back half of each filter (i.e., the vapor-phase OC), and 0.786 is the correction factor to account for the cutting bias.

$$OC = (OC_{F+B} - OC_{BLK}) - (2 \cdot OC_B \cdot 0.786) \qquad (3\text{-}1)$$

Possible negative sampling artifacts due to evaporation of semi-volatile organic compounds (SVOC) from fine particles collected on the quartz fiber filters were not accounted for. $PM_{2.5}$ filters collected with an additional Hi-Vol sampler at Turtleback Dome were analyzed for TC and $^{14}C/^{12}C$ ratios by accelerator mass spectrometry in order to determine the content of modern versus fossil carbon (Bench and Herckes, 2004). Finally, a dual-wavelength Aethalometer (Magee Scientific) was used to measure black carbon (BC) by absorbance at 880 nm and 360 nm with 5-minute time resolution (Allen et al., 2004, Hansen et al., 1984).

3.3. RESULTS and DISCUSSION

3.3.1. $PM_{2.5}$ Composition

The composition of fine particulate matter during the time frame of YACS was dominated by carbonaceous material. Average $PM_{2.5}$ components for the period of July 14 through September 5, 2002, at Turtleback Dome are shown in Figure 3-5. While OM constituted nearly three quarters (70%) of the total fine particle mass, BC (i.e., light absorbing carbon) contributed on average only 4% to the ambient $PM_{2.5}$. Inorganic ions comprised 20% of $PM_{2.5}$, with the major ionic species observed at Turtleback Dome being ammonium sulfate (15%) and sodium nitrate (4%), the latter indicating influence from marine air masses (Pacific Ocean).

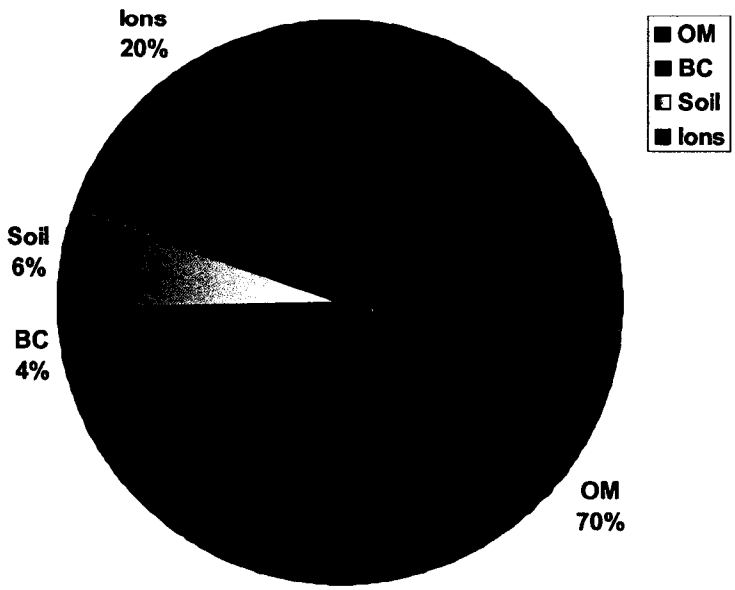

Figure 3-5. Average $PM_{2.5}$ composition at Turtleback Dome during the time frame of YACS. OM was determined by applying a conversion factor of 1.8 (based on mass closure calculations) to the measured average OC concentration.

3.3.2. Carbonaceous Content

The average OM fraction in the fine aerosol during YACS was 70%, as shown in Figure 3-5 (Malm et al., 2005a). On individual days during a haze episode in mid August, OM contributed up to 90% to the fine particle mass. Using a multiplier of 1.8 for the conversion of OC to total organic mass, the fine OM mass concentration at Turtleback Dome averaged 6.3 $\mu g/m^3$ during the study period (based on TOT carbon data obtained with the Sunset analyzer). While traditionally a factor of 1.4 has been used at IMPROVE sites for the conversion of OC to organic mass, a higher factor of 1.8 was chosen here due to the observation that biogenic sources, including biomass burning and SOA, made large contributions to the ambient OM during YACS, as will be described below (and also see: Bench and Herckes, 2004). In addition, a factor of 1.8 was determined from mass closure calculations of total fine mass for YACS (Malm et al., 2005a). A

recent evaluation of average molecular mass per carbon mass for a non-urban aerosol suggests that even higher factors may be appropriate in certain environments, particularly in the case of wood smoke impact on the ambient OM (Turpin and Lim, 2001). The TOT carbon data were corrected for the vapor adsorption artifact with a "seasonal" correction factor, as described in section 3.2.6. The amount of vapor-phase carbonaceous material observed in the $PM_{2.5}$ samples from Turtleback Dome was surprisingly high (44% on average, based on eight representative samples). A timeline of fine particle OM over the course of the entire study is presented in Figure 3-6, using OM data obtained by two independent methods: the IMPROVE (TOR) protocol and the Sunset modified NIOSH (TOT) method. $PM_{2.5}$ OM 24-hour average concentrations ranged between approximately 2 and 17 $\mu g/m^3$ (based on TOT data) or between 1.5 and 22 $\mu g/m^3$ (based on TOR data), peaking in mid-August. While OM concentrations obtained from IMPROVE samples show a similar pattern to the TOT data, ambient OM concentrations determined by the TOR method are higher during the haze episode in mid-August. This discrepancy may be due to multiple factors associated with the differences in sampling protocols and analysis methods between the IMPROVE and the modified NIOSH method. For instance, the filters analyzed by the modified NIOSH method were collected with Hi-Vol samplers, whereas the IMPROVE sampler was operated at lower flow rates collecting particles on smaller filters. While vapor-phase organic compounds present in the sample air stream were not removed by either sampling method, the Hi-Vol samples were more likely affected by the adsorption artifact due to the larger filter surface area. Moreover, while the IMPROVE carbon data were blank and artifact corrected by subtracting monthly network median artifact values obtained from after-filters (McDade et al., 2004), the TOT data were corrected for the vapor adsorption artifact in addition to blank correction by the "slicing" method (section 3.2.5.). However, the correction factor was determined from eight samples that may not have been truly representative for all samples, particularly those collected during the intensive haze period in mid August, characterized by rather high OM concentrations. Furthermore, the loss of SVOC due to

volatilization, not accounted for by either protocol, may have resulted in negative artifacts of different magnitude for one method versus the other due to differences in sampling conditions (e.g., filter size, flow rate, pressure drop).

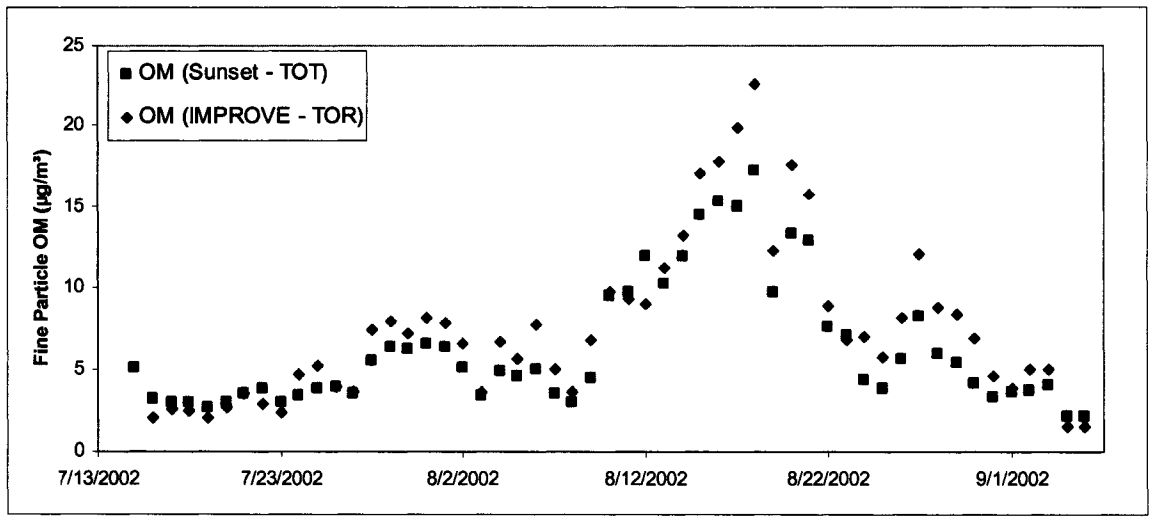

Figure 3-6. Timeline of fine particle OM at Turtleback Dome, determined by the Sunset Labs (TOT) method and the IMPROVE (TOR) protocol.

Numerous organic compounds were identified and quantified in the samples, including PAH, n-alkanes, n-alkanoic acids, and dicarboxylic acids. In addition, several source-specific molecular markers, including tracers for smoke from biomass burning and vehicular emission tracers, as well as SOA species, were quantified. An overview of ambient aerosol concentrations of various organic species was obtained from weekly composites of the daily samples collected throughout the study.

Specific trends in concentrations of homologous hydrocarbon series can be utilized to characterize ambient aerosol as predominantly anthropogenic or biogenic in origin. A commonly used method is the carbon preference index (CPI) that is defined, for instance in the case of n-

alkanes, as the sum of the concentrations of odd carbon number species divided by the sum of the even carbon number species concentrations (Simoneit, 1989). Enzyme-regulated biosynthetic pathways in plants involve reduction reactions of alkanoic acids that yield odd-carbon number n-alkanes. Thus, a CPI greater than 2 is typically considered indicative of predominantly biogenic sources. Several studies have used CPI values in the past to distinguish urban source contributions, dominated by fossil fuel combustion, from biogenic sources (e.g., Brown et al., 2002, Didyk et al., 2000, Gogou et al., 1996, Simoneit, 1989). Analogously, the CPI of n-alkanoic acids is defined as the sum of the concentrations of even carbon number acids over the sum of the odd carbon number acids, since biogenic sources preferentially emit even carbon number acids.

Concentrations of straight-chain alkanes (from C_{16} through C_{38}) were relatively steady throughout the study period, but increased to some extent during intensive haze periods. The average weekly n-alkane concentration, summed over C_{16} through C_{38} alkanes, was 14.7 ng/m^3 with a minimum of 9.5 ng/m^3 during the last week of the study and a maximum concentration of 22.8 ng/m^3 during week 5 (second smoke period), as shown in Table 3-1. The highest concentration of summed n-alkanes on an individual day was observed on July 30 (first smoke period) with 70 ng/m^3. CPI values for the n-alkanes were rather steady over the entire study period (Table 3-1). Values in weekly composites at Turtleback Dome ranged from 3.0 to 3.5 with an average value of 3.3, classifying the alkanes at this site as primarily biogenic in origin. A predominance of the C_{29} n-alkane, typical of plant waxes (Simoneit, 1989), also reinforced the important contributions of biogenic emissions. CPIs of n-alkanoic acids (C_8 through C_{34}) in the weekly composites ranged from 4.5 to 7.0 with an average value of 6.2 (Table 3-1), indicating a predominance of biogenic sources as well, although relatively high n-alkanoic acid CPI values have also been observed at urban locations, i.e., areas primarily influenced by anthropogenic sources (Simoneit, 1989).

Table 3-1. Ambient concentrations of total n-alkanes (summed over $C_{16} - C_{38}$) and total n-alkanoic acids ($C_8 - C_{34}$), their corresponding CPIs, and C_{max} values, observed in weekly composite samples from Turtleback Dome.

	July 14 - 20	July 21 - 27	Jul 28 - Aug 03	Aug. 04 - 10	Aug. 10 - 16	Aug. 17 - 23	Aug. 24 - 30	Aug. 31 - Sep. 05	Study Average
C_{16} - C_{38} n-alkanes (ng/m^3)	12.3	12.2	17.4	13.5	22.8	18.3	11.8	9.5	**14.7**
CPI	3.5	3.5	3.1	3.2	3.4	3.5	3.2	3.0	**3.3**
C_{max}	29	29	29	29	29	29	29	29	**29**
C_8 - C_{34} n-acids (ng/m^3)	45.3	45.9	58.1	82.8	153.5	215.6	96.4	64.6	**95.3**
CPI	4.5	5.2	7.0	6.5	6.5	6.5	6.8	6.3	**6.2**

Concentrations of n-alkanes in Yosemite Valley were considerably higher than those at Turtleback Dome (55 ng/m^3 at the visitors center vs. 15 ng/m^3 at Turtleback Dome on average). Moreover, the alkane CPI was significantly lower at the valley site (e.g.: CPI = 1.5 on August 15), indicating a stronger influence from anthropogenic sources. Likewise, concentrations of the n-alkanoic acids (C_8 through C_{34}) were significantly higher at the visitors center compared to Turtleback Dome (235 ng/m^3 for the summed n-acids at the visitors center vs. 95 ng/m^3 at Turtleback Dome on average based on weekly composite data) , while the n-alkanoic acid CPI in the valley was 6.7 on average. The visitor center region is subject to significant local emissions from gasoline vehicles and diesel buses; therefore, higher concentrations and lower CPI values (i.e., greater anthropogenic influence) are expected at this site.

3.3.3. Biomass Burning Smoke Contribution to $PM_{2.5}$

Various molecular markers for biomass combustion were identified and quantified in fine and coarse particles. An overview of the ambient aerosol concentrations of these molecular markers was generated from weekly composite samples, with additional 12 and 24 hr samples from the intensive haze periods providing further information about concentrations of these species on shorter timescales. Smoke tracers identified in this study include levoglucosan, a thermal degradation product of cellulose, previously used in several studies for source apportionment of smoke from biomass combustion (Brown et al., 2002, Elias et al., 2001, Fraser and Lakshmanan, 2000, Hornig et al., 1985, Simoneit et al., 1999), as well as two isomers of levoglucosan: mannosan and galactosan. A selection of resin acids and retene were quantified as well (Ramdahl, 1983, Simoneit et al., 1993). In addition, several methoxyphenols, including vanillin, acetovanillone, and 4-ethyl guaiacol, derived from lignin combustion, were used as tracers particularly for softwood combustion (Hawthorne et al., 1988, Schauer et al., 2001). All of these compounds are markers of primary particle emissions from biomass combustion. As will be discussed below, it is likely that aged smoke plumes also contain significant amounts of SOA matter associated with oxidation of biogenic volatile organic compounds (VOC) which may experience enhanced emissions in fires (Alessio et al., 2004).

Timelines of the quantified primary smoke tracers are shown in Figures 3-7 through 3-9. Included are ambient mass concentrations of the methoxyphenols vanillin, acetovanillone, and methyl guaiacol (Figure 3-7), retene, and the resin acids, pimaric, isopimaric, sandaracopimaric, 7-oxo-dehydroabietic, and dehydroabietic acids (Figure 3-8), which are softwood-specific tracers. Also included in Figure 3-9 are timelines of levoglucosan, mannosan, and galactosan, molecular markers for combustion of biomass in general, including softwood, hardwood, grasses, and foliar fuels (Simoneit et al., 1999). Elevated weekly average concentrations of biomass burning smoke tracers were observed during the second half of the study; the highest levels of most biomass

burning smoke tracers, including levoglucosan, occurred between August 10 and 16. This time frame encompasses an intensive measurement period between August 14 and 16. Vanillin was observed with the highest concentration of the methoxyphenols during that week with an average value of 0.6 ng/m^3 (Figure 3-7). Dehydroabietic acid had the highest average concentration of all quantified resin acids with 17 ng/m^3 during the same week (Figure 3-8). The average concentration of levoglucosan was 50 ng/m^3 during that period (Figure 3-9). Concentrations of smoke tracers were significantly higher on individual days, particularly during the intensive periods, with peak levels as high as 234 ng/m^3 for levoglucosan.

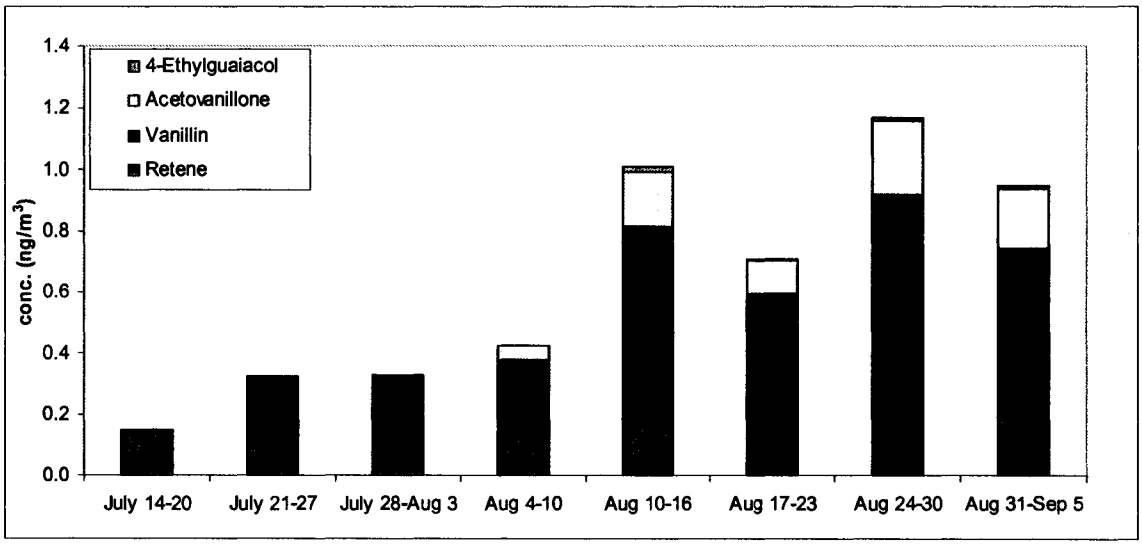

Figure 3-7. Timelines of retene and various methoxyphenol concentrations, including vanillin, acetovanillone, and 4-ethylguaiacol, contained in weekly composite samples from Turtleback Dome.

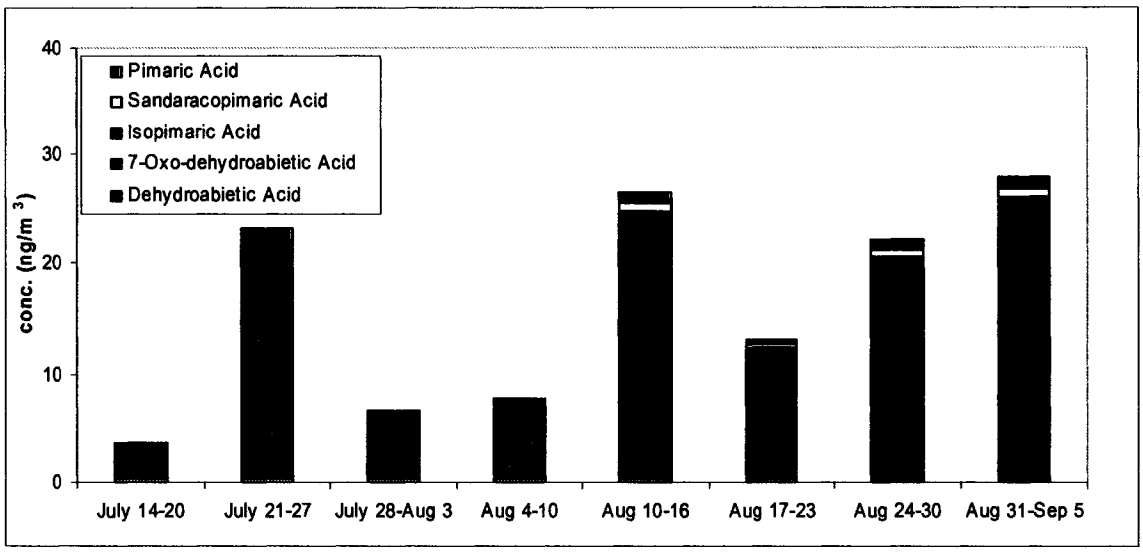

Figure 3-8. Timeline of various resin acids observed in weekly composite samples from Turtleback Dome.

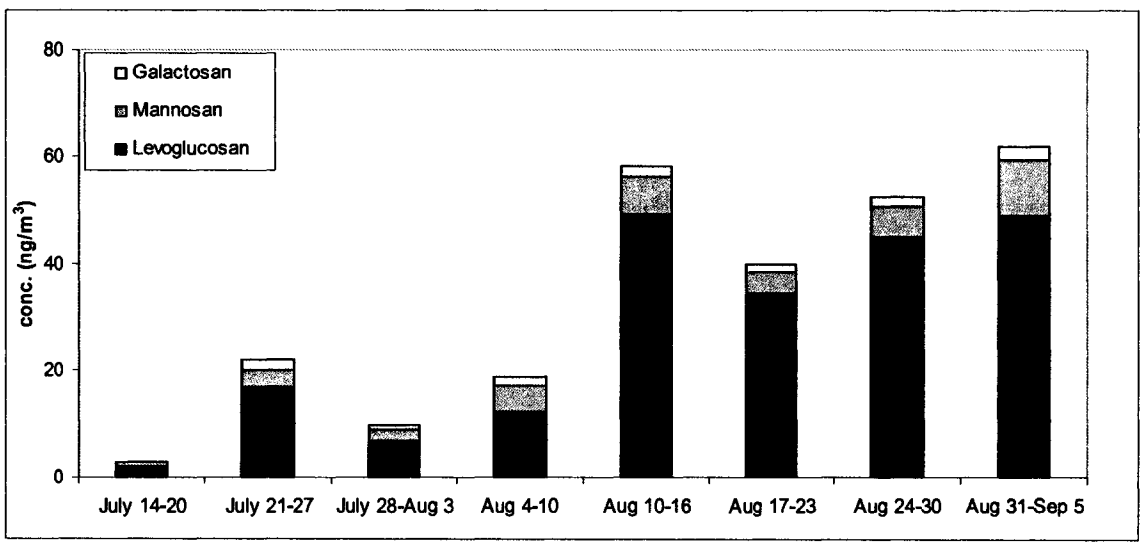

Figure 3-9. Timeline of the anhydrosugars, levoglucosan, mannosan, and galactosan, observed in weekly composite samples from Turtleback Dome.

A diverging signal on the dual-wavelength (UV and visible) aethalometer supports the presence of smoke from biomass combustion during the hazy study periods. The measurement of BC at two wavelengths (360 and 880 nm) allows a distinction between purely black carbon and BC that contains additional UV light-absorbing organic compounds (Allen et al., 2004). While absorption at 880 nm is primarily due to BC, certain lower molecular weight organic compounds derived from biomass or diesel fuel combustion enhance absorption at 360 nm. Thus, a divergence between BC concentrations derived from absorbance measurements at 880 and 360 nm can signal contributions of smoke from biomass burning and/or diesel emissions. Since more than 90% of the OM in Yosemite National Park during YACS was of non-fossil nature (Bench and Herckes, 2004), the majority of the BC observed with a diverging signal by the dual-channel method is assumed to be attributable to biomass combustion. During the second haze episode, qualitative evidence for the presence of smoke from biomass burning is given by the diverging BC signals, as shown in Figure 3-10 for the period 08/13 – 08/16. MODIS satellite data and back trajectory analyses confirmed regional smoke contributions from wildfires in Oregon and California during the time frame of YACS as well (McMeeking et al., 2005c).

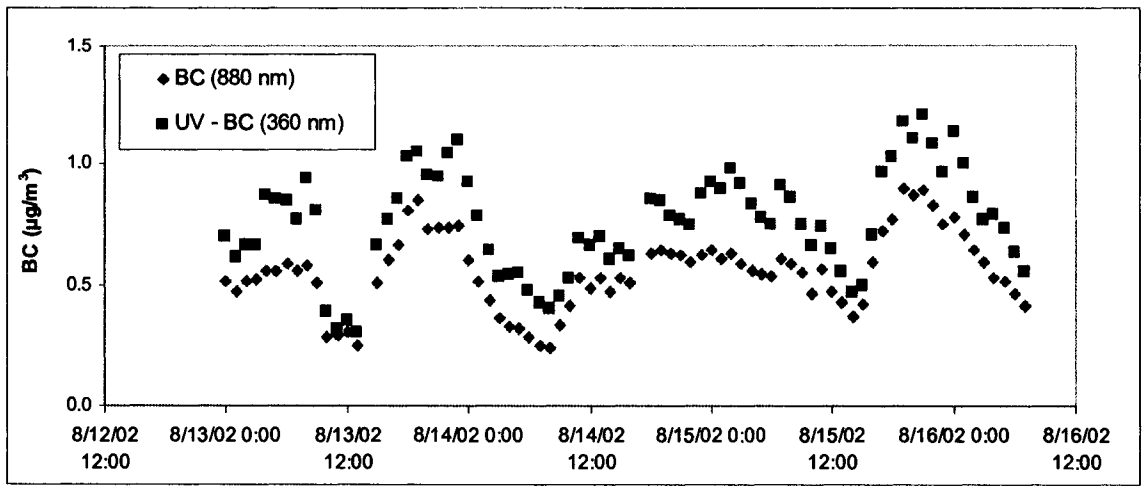

Figure 3-10. Differential BC concentrations (880 nm and 360 nm UV channel) during the second regional haze period in mid-August at Turtleback Dome.

Water soluble potassium (K^+), not of soil or sea salt origin, has been widely used as biomass combustion tracer (Andreae, 1983). However, weak correlations of biomass burning tracer concentrations with K^+ concentrations (not corrected for sea-salt contributions) were observed during YACS, as shown in Figure 3-11 in form of a scatter plot of K^+ versus levoglucosan concentrations based on 12-hour samples collected during the two intensive haze episodes. Likewise, no correlation was evident between K^+ and levoglucosan concentrations based on daily average data from the entire study period (Figure 3-12). These unexpected observations are possibly due to additional non-soil source contributions to fine-particle K^+, such as meat cooking and emissions from vegetation (Lawson and Winchester, 1979, Morales et al., 1996, Schauer et al., 1999a, 2002b). Moreover, K^+ and levoglucosan emission factors may vary independently with type of biomass burned and combustion conditions, resulting in non-linear correlations between the two tracer species, as discussed in more detail in section 4.3.3.

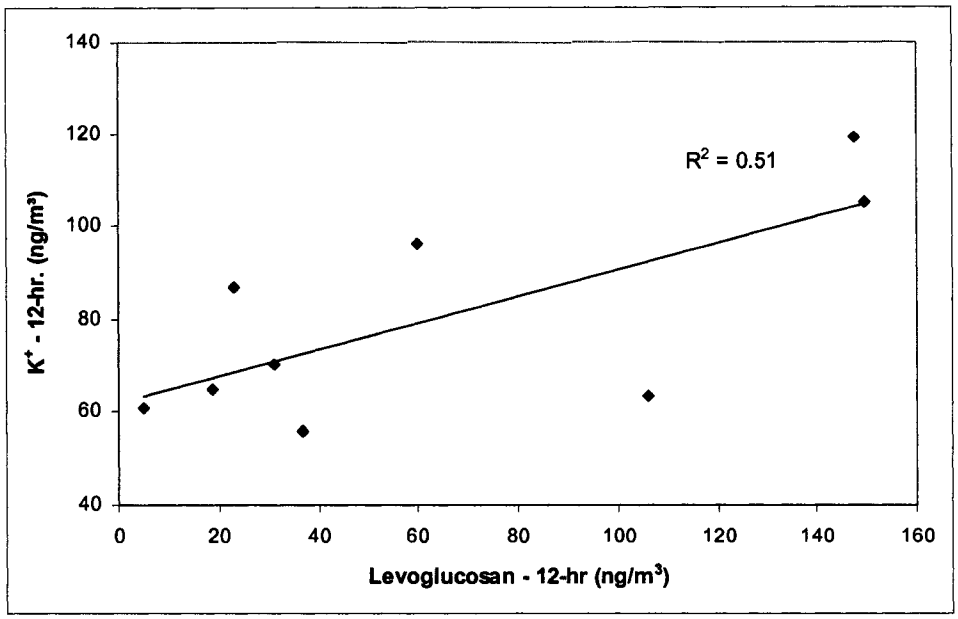

Figure 3-11. Scatter plot of soluble potassium (K^+) versus levoglucosan concentrations at Turtleback Dome, based on 12-hour samples collected during the two intensive haze periods (levoglucosan data obtained by HPAEC-PAD). K^+ was measured by ion chromatography on Teflon filter samples collected with a URG annular denuder-filter pack sampler.

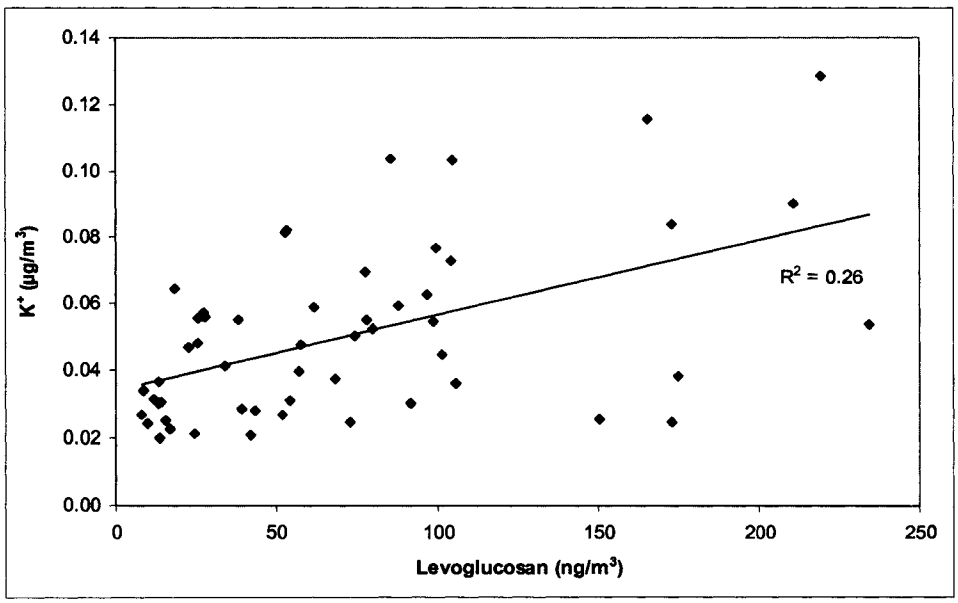

Figure 3-12. Scatter plot of average daily soluble potassium (K^+) versus levoglucosan concentrations at Turtleback Dome (levoglucosan data obtained by HPAEC-PAD).

Many biomass burning smoke tracer concentrations (based on weekly composites) show good correlation to each other (with correlation coefficients as high as 0.98), as seen in Table 3-2 and Figure 3-13. Weaker correlations in some cases may be due to different fire source regions emitting varying marker profiles during different time periods. Further, since some tracer species are less stable in the atmosphere, there is the potential for degradation, especially in smoke plumes subject to long-range transport as observed in this study. For instance, some methoxyphenols are suspected to undergo degradation during their atmospheric lifetimes (Hawthorne et al., 1992, Simpson et al., 2005).

Table 3-2. Correlations (R^2) of primary biomass burning smoke tracer concentrations based on weekly composite data.

	Levoglucosan	Retene	Vanillin	Pimaric Acid	Isopimaric Acid	Dehydroabietic	OC
Levoglucosan	1.00	0.64	0.93	0.60	0.81	0.66	0.19
Retene		1.00	0.89	0.16	0.35	0.19	0.16
Vanillin			1.00	0.38	0.59	0.45	0.07
Pimaric Acid				1.00	0.83	0.98	0.00
Isopimaric Acid					1.00	0.83	0.16
Dehydroabietic A.						1.00	0.01
OC							1.00

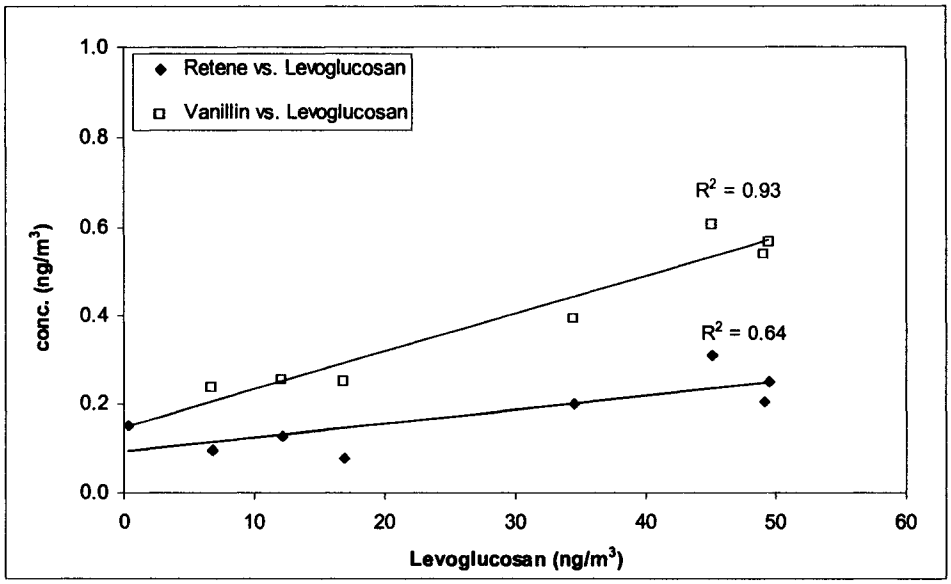

Figure 3-13. Scatter plots of vanillin versus levoglucosan (red) and retene versus levoglucosan (black) concentrations, based on weekly composite data at Turtleback Dome.

All biomass burning smoke tracer concentrations show a diurnal trend, with higher concentrations during the night (Figure 3-14). For instance, levoglucosan was observed with concentrations as high as 180 ng/m^3 during the night of 08/16 and only 23 ng/m^3 during the day. This observation coincides with a persistent diurnal wind pattern: at night easterly, down-slope winds prevailed, while during the day thermally driven up-slope flows transported air to Yosemite from the foothills and perhaps the Central Valley of California. Smoke concentrations may have increased at night as a result of subsidence of a regional, elevated smoke plume in the down-slope drainage flow. A similar diurnal pattern was observed in BC concentrations and the differential BC signal (BC minus UV-BC), as shown for the period 08/13 – 08/16 in Figure 3-12. OC concentrations show a different diurnal trend, peaking in late afternoon (Malm et al., 2005a). This might reflect increased SOA concentrations due to daytime increases in biogenic emissions from the local forest and higher photochemical activity. OC concentrations remain high during the night, but

decrease in the early morning hours, based on carbon measurements with the Rupprecht & Pattashnick (R&P) 5400 Ambient Carbon Particulate Monitor.

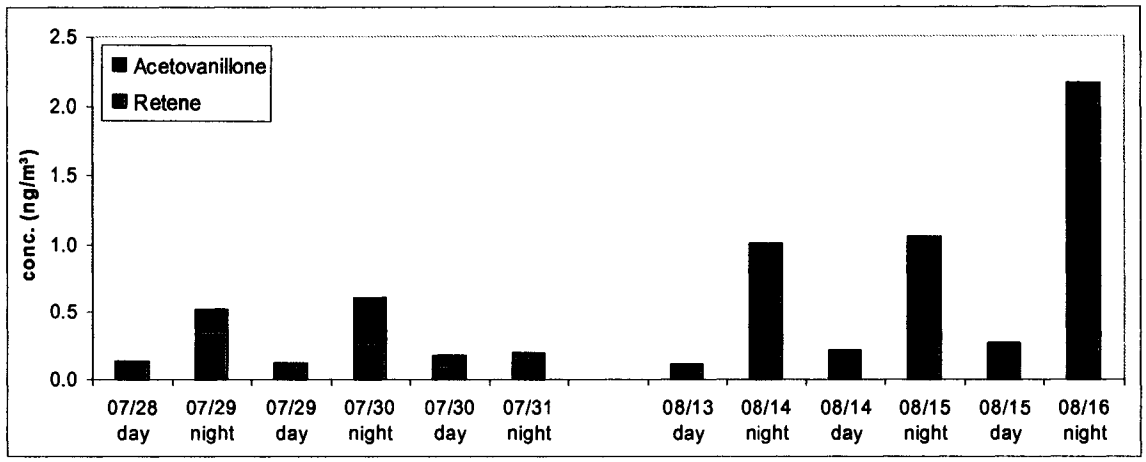

Figure 3-14. Timeline of selected biomass burning smoke tracer concentrations observed in 12-hour samples during the two haze episodes.

Levoglucosan concentrations were also obtained by HPAEC-PAD. The diurnal pattern shown for retene and acetovanillone above was observed for levoglucosan as well, as demonstrated in Figure 3-15. A timeline of levoglucosan daily average concentrations (obtained by HPAEC-PAD) for the entire study period, as shown in Figure 3-16, mirrors the timeline based on weekly average (composite) levoglucosan concentrations, measured by GC-MS (Figure 3-9).

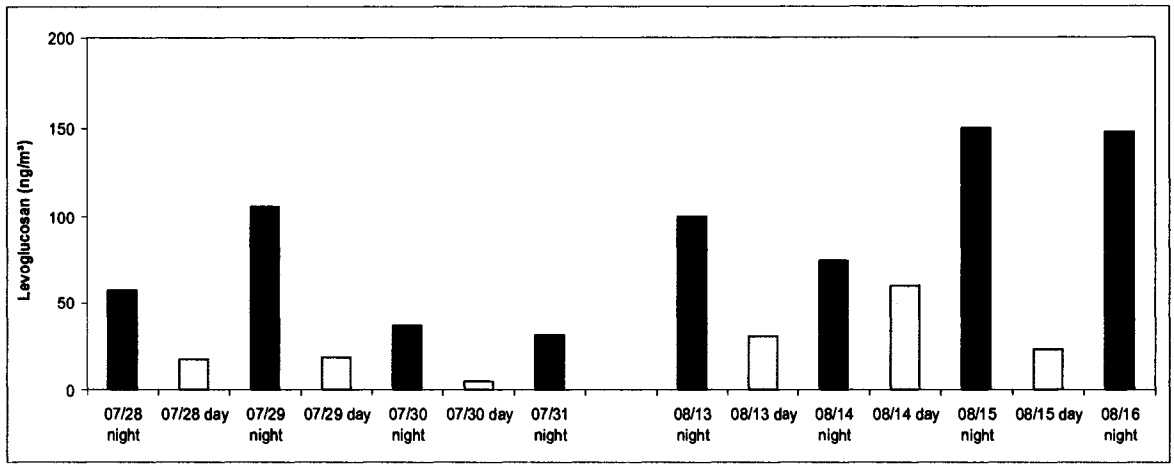

Figure 3-15. Timeline of levoglucosan concentrations observed in 12-hour samples during the two haze episodes (measured by HPAEC-PAD).

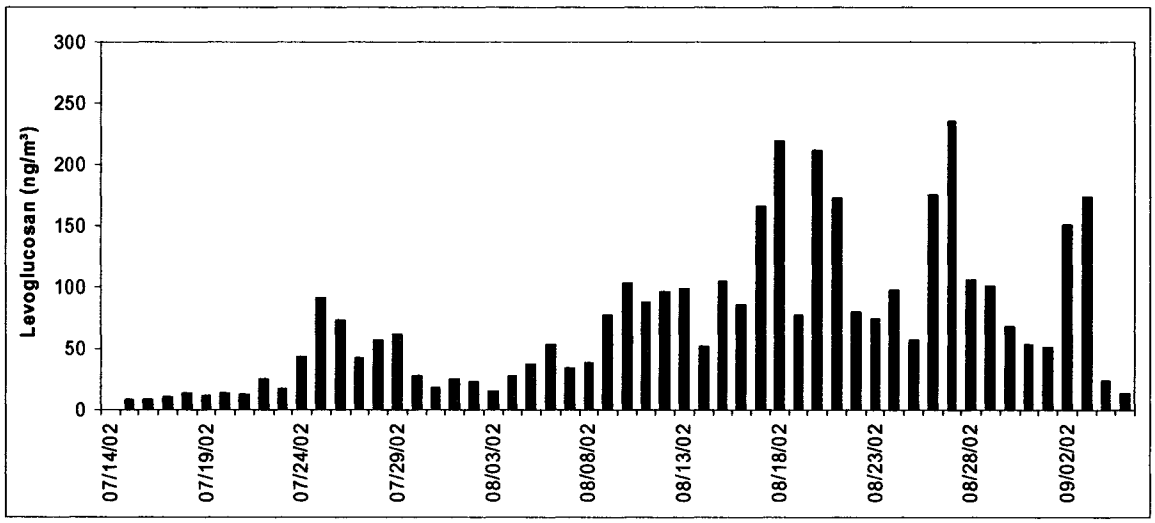

Figure 3-16. Timeline of daily average levoglucosan concentrations at Turtleback Dome for the duration of YACS (measured by HPAEC-PAD).

The contribution of smoke from biomass combustion to primary fine particle OC was estimated from the ambient $PM_{2.5}$ concentrations of selected biomass burning smoke tracers, using source profiles from the literature. While this approach sometimes involves the utilization of chemical mass balance (CMB) models (e.g., Manchester-Neesvig et al., 2003, Schauer et al., 1996, Ward

and Smith, 2005, Zheng et al., 2002), the apportionment of biomass burning sources to the ambient aerosol in Yosemite was determined here with a simplified receptor-based molecular marker method. This simpler approach was chosen due to the expectation that primary sources would not fully explain the observed carbon concentrations. The CMB approach generally works best when known sources account for at least 80% of ambient particulate carbon (G. Cass, personal communication). As fuel composition and combustion regimes are significantly different between wildfires and controlled burning in fireplaces and wood stoves, the source profiles utilized here were generated by combustion of foliar fuels, including branches and leaves, under open burning conditions (Hays et al., 2002). These conditions are more representative of the sources and burning conditions of the wildfires that were believed to produce the smoke observed in this study. Utilizing these source profiles, ratios of individual source tracer concentrations to the ambient OC concentrations were used to determine contributions of primary smoke from biomass combustion to fine particle OC for a given sampling period, as shown in Figure 3-17. Estimated contributions based on ratios of retene, vanillin, or levoglucosan to OC show reasonably good agreement, whereas source contributions based on acetovanillone/OC ratios were consistently lower. This may be in part due to lower stability of acetovanillone during atmospheric transport. In addition, $PM_{2.5}$ concentrations of this marker were relatively low, resulting in higher measurement uncertainties. While the highest concentrations of individual smoke tracers and associated primary biomass combustion smoke were observed during the second intensive haze period (August 14 – 16), relative contributions to fine particle OC from primary biomass burning emissions appear largest during the last two weeks of the study (as high as 65% during the 08/31 – 09/05 period).

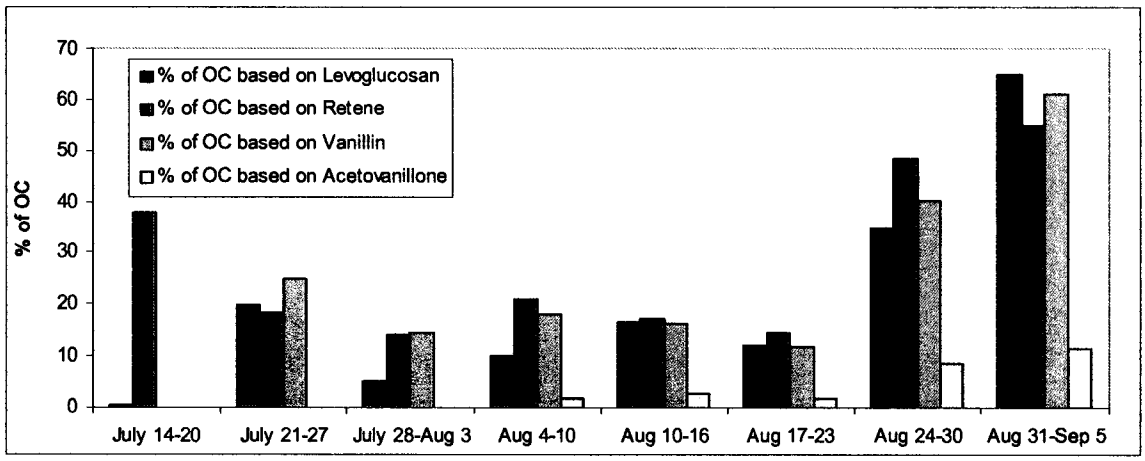

Figure 3-17. Estimated primary biomass burning smoke contributions to fine-particle OC (in % of OC), using different molecular markers, based on weekly composites.

Source contributions from biomass combustion were also estimated with 12 hr and 24 hr observations as shown in Figures 3-18 and 3-19. A diurnal pattern is observed analogous to that shown above for BC and absolute biomass smoke tracer concentrations (Figures 3-12, 3-14, 3-15, and 3-19). Contributions of primary smoke emissions during the two haze episodes were estimated as high as 53% on individual days and even higher (in excess of 100%) during periods influenced by local fires (Figure 3-18). SOA generated in the smoke plume may constitute an additional, substantial portion of carbonaceous aerosol observed during these periods that is not reflected in these estimates.

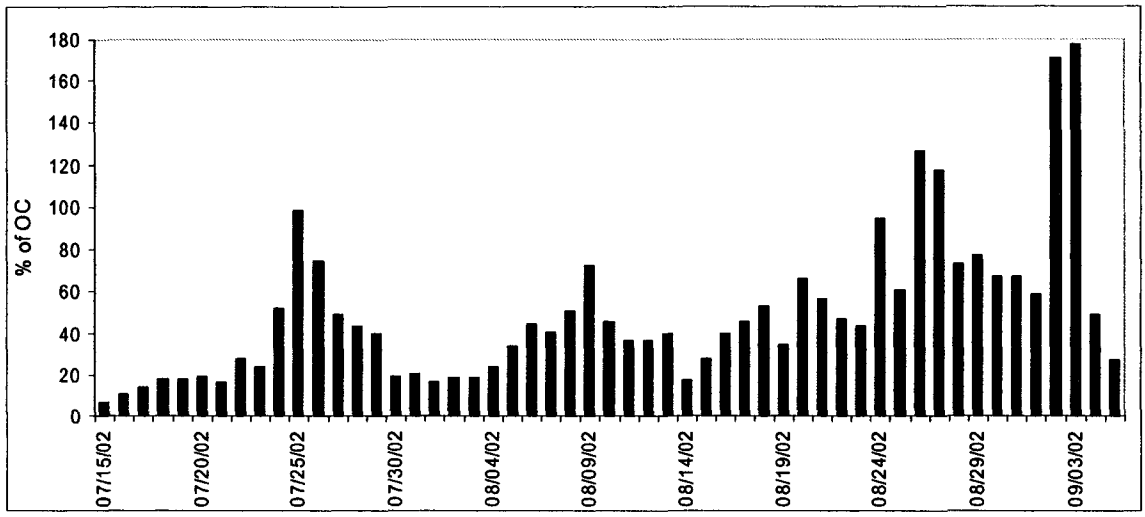

Figure 3-18. Estimated primary biomass burning smoke contributions to fine-particle OC (in % of OC), using daily HPAEC-PAD levoglucosan concentrations.

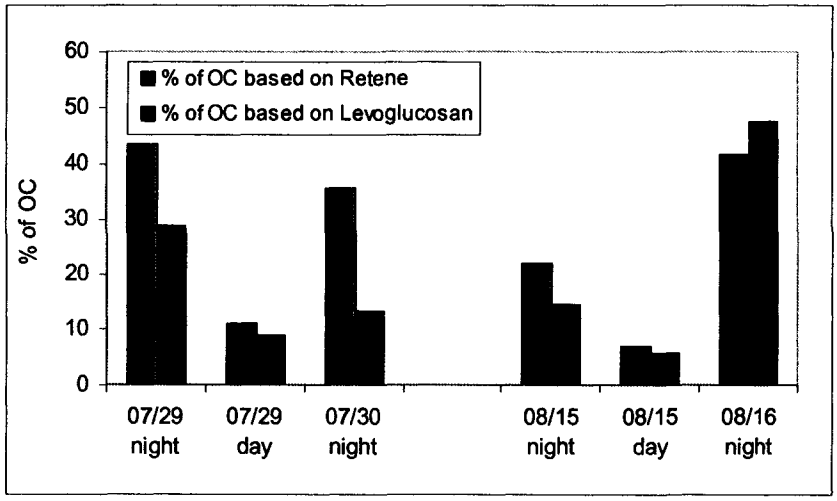

Figure 3-19. Estimated primary biomass burning smoke contributions to fine-particle OC (in % of OC), using retene and levoglucosan, based on 12 hr samples.

OC concentrations between August 10 and 16 were the highest of the entire study period, partially due to contributions of smoke from biomass burning, but heavily influenced by SOA as well, as discussed below. The observed OC probably includes SOA produced in the smoke plume

(Alessio et al., 2004). This second intensive period was characterized by regional haze with aged smoke from long-range transport, allowing much more time for SOA production compared to the latter part of the study, when fresh smoke from local fires impacted the sampling site.

3.3.4. Anthropogenic Contributions to $PM_{2.5}$

Polycyclic aromatic hydrocarbons (PAH) were observed at very low concentrations (on the order of pg/m^3) in the weekly Turtleback Dome composite samples and in many cases were below the detection limits (Figure 3-20). Slightly higher concentrations were detected in selected daily samples. The most abundant PAH species during cleaner periods as well as during periods with local smoke impact was benzo[k]fluoranthene with a maximum concentration of 45 pg/m^3 in week 7 (August 24 – 30). Benzo[e]pyrene was the dominant PAH during regional haze periods with the highest concentration of 37 pg/m^3 observed in week 5 (August 10 – 16). Higher PAH concentrations were observed at the valley site, apparently reflecting the heavier vehicle traffic near that collection site. For instance, ambient benzo[k]fluoranthene concentrations measured at the valley site were 140 pg/m^3 on August 15 and benzo[e]pyrene was detected at 95 pg/m^3 on the same day. PAH concentrations at Turtleback Dome showed little correlation with detected hopanes and steranes (discussed below), suggesting that PAH there may be associated to a larger extent with wood smoke rather than fossil fuel (diesel) combustion.

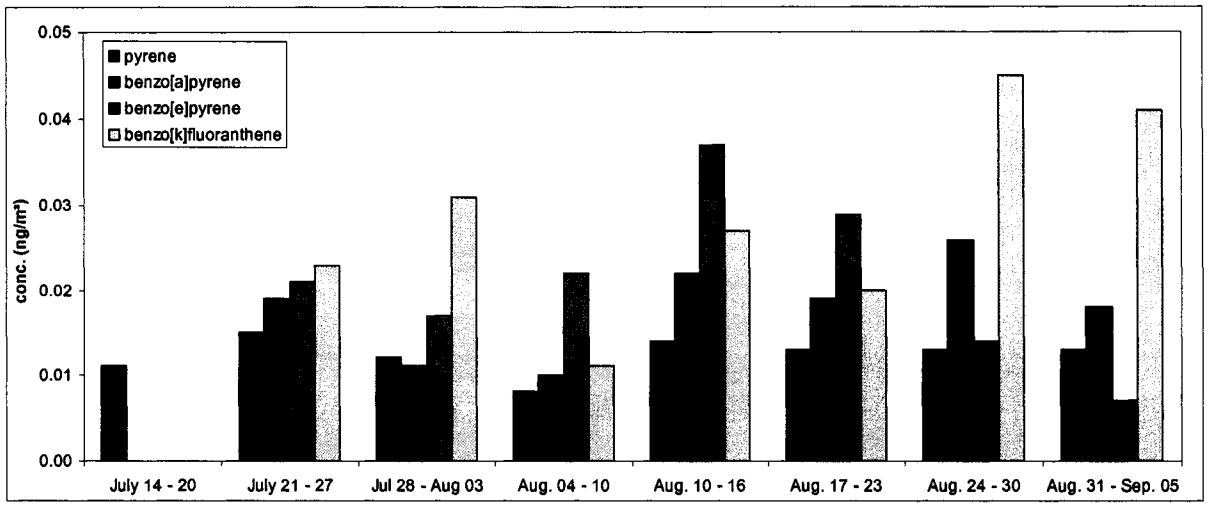

Figure 3-20. Timeline of selected PAH concentrations at Turtleback Dome based on weekly composites.

Meat cooking contributions to $PM_{2.5}$ OC were estimated based on the measured ambient concentrations of cholesterol and OC in conjunction with emission factors from the literature, using a combination of published source profiles (Rogge et al., 1991, Schauer et al., 1999a), analogous to the method applied by Brown and coworkers (Brown et al., 2002). Briefly, the emission factors applied here were based on a 1:1 ratio of charbroiling to frying of hamburger meat, using an average value of the two emission factors reported by Rogge et al. (1991) and Schauer et al. (1999a) for charbroiling. Equation 3-2 was used to determine source contributions from meat cooking, where $\%OC_{meat}$ is the fraction of the measured OC attributed to meat cooking, $c_{cholesterol}$ is the observed $PM_{2.5}$ concentration of cholesterol, c_{OC} is the OC concentration, and EF_{Ch} and EF_F are the emission factors for charbroiling and frying of meat, respectively.

$$\%OC_{meat} = \left(\frac{c_{cholesterol} \cdot EF_{Ch} \cdot 0.5}{c_{OC}} + \frac{c_{cholesterol} \cdot EF_{F} \cdot 0.5}{c_{OC}} \right) \cdot 100 \qquad (3\text{-}2)$$

Concentrations of cholesterol at Turtleback Dome were low (ranging from 55 pg/m^3 to 450 pg/m^3), resulting in average $PM_{2.5}$ source contributions of approximately 3% from meat cooking (see Table 3-3). Cholesterol levels were higher at the Yosemite Valley site (as high as 4 ng/m^3), probably due to more extensive cooking activities in that part of the park.

Table 3-3. Average fine particle OC concentrations (Sunset TOT method) and estimated contributions of biomass burning smoke, meat cooking, vehicle emissions, and SOA (and unidentified sources) to OC at Turtleback Dome.

	July 14 - 20	July 21 - 27	Jul 28 - Aug 03	Aug. 04 - 10	Aug. 10 - 16	Aug. 17 - 23	Aug. 24 - 30	Aug. 31 - Sep. 05	Study Average
Average OC (μg/m^3)	1.76	1.85	3.00	2.61	6.45	6.11	2.82	1.64	**3.28**
Biomass Smoke (%) [a]	0.51	20	5.0	10	17	12	35	65	**21**
Meat Cooking (%)	4.9	5.0	4.2	1.3	0.7	3.9	1.0	3.1	**3.0**
Vehicle Emissions (%)	19	18	8.5	8.3	4.6	3.8	8.3	11	**10**
SOA/Unidentified (%)	76	57	82	80	78	80	56	21	**66**

Notes: a.) Biomass burning source contributions were determined with measured levoglucosan concentrations.

Selected hopanes and steranes were measured in weekly and daily samples for use as vehicle emission tracers. Concentrations were on the order of pg/m^3, as shown in Table 3-4, and exhibited small variability throughout the study period, similar to the low variability in fossil fuel carbon levels reported by Bench and Herckes (Bench and Herckes, 2004). Source contribution estimates from vehicle emissions were made analogous to the method used by Brown et al. (Brown et al., 2002), utilizing source profiles from the literature (Rogge et al., 1993a, Schauer et al., 1999b). In summary, emission factors of 17α(H),21β(H)-hopane were applied based on a 8:1:1 ratio of catalyst-equipped to non-catalyst to diesel vehicles, using the average of the diesel emission factors from the source profiles by Rogge et al. (1993a) and Schauer et al. (1999b).

Primary contributions to $PM_{2.5}$ at Turtleback Dome from vehicle emissions were estimated to be approximately 10% on average, based on weekly composite data (Table 3-3). These observations are consistent with results from ^{14}C analysis that showed a contribution to fine-particle OC from fossil fuel combustion of less than 10% on average (Bench and Herckes, 2004).

Table 3-4. Hopane and sterane concentrations observed in weekly composite samples (expressed in ng/m^3).

	July 14 - 20	July 21 - 27	Jul 28 - Aug 03	Aug. 04 - 10	Aug. 10 - 16	Aug. 17 - 23	Aug. 24 - 30	Aug. 31 - Sep. 05
5α,14,17β R cholestane	0.029	0.013	0.021	0.006	0.025	0.015	0.017	0.007
5α,14β,17β S cholestane	0.027	0.017	0.019	0.008	0.024	0.015	0.011	0.004
5α,14α,17α R cholestane	0.085	0.063	0.053	0.043	0.075	0.056	0.049	0.042
5α,14β,27β R S+R ergostane	0.009	0.012	0.008	0.007	0.011	0.004	0.010	0.008
5α,14β,27β R S+R ergostane	0.007	0.009	0.013	0.007	0.014	0.009	0.014	0.006
5α,14β,17β sitosane S+R	0.048	0.040	0.029	0.027	0.035	0.029	0.023	0.024
22, 29, 30 trisnorneohopane	0.090	0.100	0.068	0.077	0.106	0.066	0.056	0.051
17α,21β-29-hopane	0.261	0.241	0.189	0.183	0.276	0.202	0.173	0.163
17α,21β-hopane	0.274	0.274	0.213	0.181	0.245	0.192	0.195	0.151
22 S+R 17α,21β-30-homohopane	0.055	0.065	0.049	0.043	0.063	0.054	0.045	0.040
22 S+R 17α,21β-30-homohopane	0.044	0.046	0.031	0.030	0.050	0.038	0.029	0.032
22 S+R 17α,21β-30-bishomohopane	0.020	0.022	0.018	0.022	0.016	0.020	0.020	0.022
22 S+R 17α,21β-30-bishomohopane	0.031	0.024	0.023	0.017	0.019	0.023	0.017	0.023

3.3.5. Secondary Organic Aerosol

Several oxidation products of biogenic precursors, particularly monoterpenes, were detected in weekly composites as well as daily samples. Figure 3-21 gives an overview of some of these species quantified in weekly samples. While relatively high concentrations of pinic acid, cis-

pinonic acid, pinonaldehyde, and (1R)-(+)-nopinone were observed during clean periods as well, the maximum concentrations of all measured SOA species were observed during weeks 5 and 6 (August 10 – 23). The α-pinene oxidation product pinonaldehyde was measured with an average concentration of 21 ng/m^3, ranging from 7 to 51 ng/m^3. Pinic and cis-pinonic acids were measured with average ambient concentrations of 12 and 21 ng/m^3, respectively, while the β-pinene oxidation product, (1R)-(+)-nopinone, was observed at relatively low levels (0.9 ng/m^3 on average). In general, conditions were favorable for SOA formation during YACS because of the abundance of biogenic precursors and strong solar radiation, resulting in enhanced photochemical activity. High concentrations of biogenic VOC in the presence of oxidants, such as ozone and hydroxyl radical, and solar radiation have been shown to produce a variety of SOA species (Grosjean et al., 1993, Hatakeyama et al., 1987, Jang and Kamens, 1999, Jenkin and Clemitshaw, 2000, Kavouras et al., 1999a, Kuckelmann et al., 2000, Plewka et al., 2003). The ambient concentrations of pinic and cis-pinonic acids measured in this study are slightly higher than those reported at other rural sites. For example, the sum of pinic and cis-pinonic acids quantified in the particle phase above a boreal forest in Finland ranged from 1 to 4 ng/m^3 (Spanke et al., 2001). While similar concentrations were measured above a coniferous forest in Greece (Kavouras et al., 1999b), higher cis-pinonic acid concentrations (one order of magnitude higher) were observed over a eucalyptus forest in Portugal (Kavouras et al., 1998a). A relatively strong correlation between individual biogenic SOA species and fine-particle OC indicates an important influence of fine-particle carbon produced by secondary processes throughout the study period. The correlation of selected monoterpene oxidation product concentrations with OC concentrations gave correlation (R^2) coefficients of 0.76 or higher, as demonstrated in Figure 3-22.

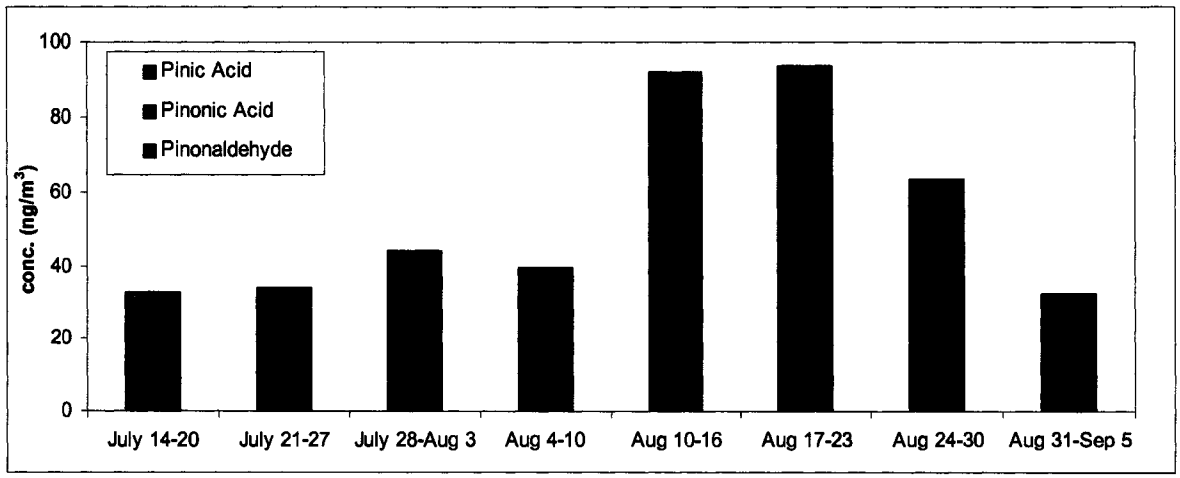

Figure 3-21. Timeline of selected biogenic SOA concentrations based on weekly composites.

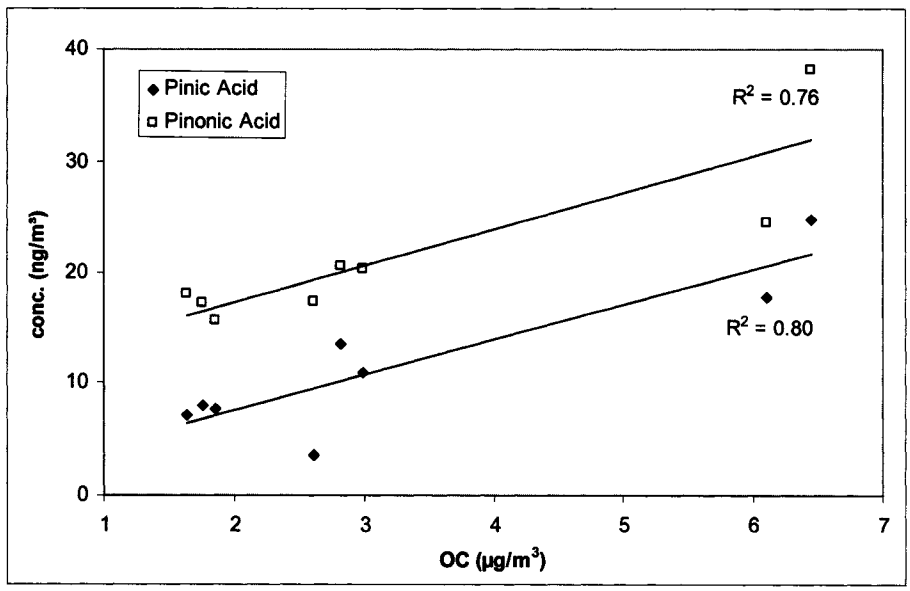

Figure 3-22. Scatter plots of cis-pinonic acid and pinic acid concentrations versus OC (Sunset TOT method) based on weekly composite data at Turtleback Dome.

In addition to the monoterpene oxidation products, several other indicators of atmospheric processing of primary emissions and the generation of secondary species were examined. For instance, 6,10,14-trimethyl-2-pentadecanone, a branched unsaturated ketone that is the photo-

oxidation product of phytol (present in chlorophyll), has been used as an indicator of biogenic SOA formation (Alves et al., 2001, Simoneit and Mazurek, 1982). The observed concentrations of 6,10,14-trimethyl-2-pentadecanone during this study were the second highest of all the carbonyl species quantified, ranging from 5 to 15 ng/m^3 with an average of 8.6 ng/m^3. While dicarboxylic acids can be of primary or secondary origin, several studies have shown contributions to SOA by dicarboxylic acids formed *in situ* during atmospheric aerosol processing (Ervens et al., 2004, Glassius et al., 2000, Kavouras et al., 1998a, Kavouras et al., 1999a, Kawamura et al., 1996). The dicarboxylic acids measured during YACS show a relatively large variability in concentrations throughout the study based on the weekly composite samples (1.3 - 11 ng/m^3 for the sum of C_4 through C_{14} dicarboxylic acids) and as demonstrated for individual diacid species in Figure 3-23. As with most other organic species, the highest concentrations were observed during the second half of the study, particularly during and after the second intensive period (Figure 3-23). The C_2 dicarboxylic acid, oxalic acid, was quantified by ion chromatography and reported elsewhere with inorganic ion concentrations (Malm et al., 2005a). A rather large average $PM_{2.5}$ oxalate concentration of 120 ng/m^3 was observed with additional oxalic acid in the gas phase. The most abundant species in the C_4-C_{14} range during hazy periods (August 10 – 30) were succinic acid (C_4) and glutaric acid (C_5); during cleaner periods azelaic acid (C_9) was most abundant (Figure 3-23). This trend was observed in the daily samples as well. Oleic acid may be degraded to nonanoic acid and a C_9 diacid (azelaic acid) during the atmospheric lifetime of an aerosol particle (Kawamura and Gagosian, 1987, Rogge et al., 1993b). Therefore, an abundance of azelaic acid may indicate aerosol that has been subject to significant atmospheric processing. Dicarboxylic acid trends and concentrations at the Yosemite Valley site were similar to observations at Turtleback Dome.

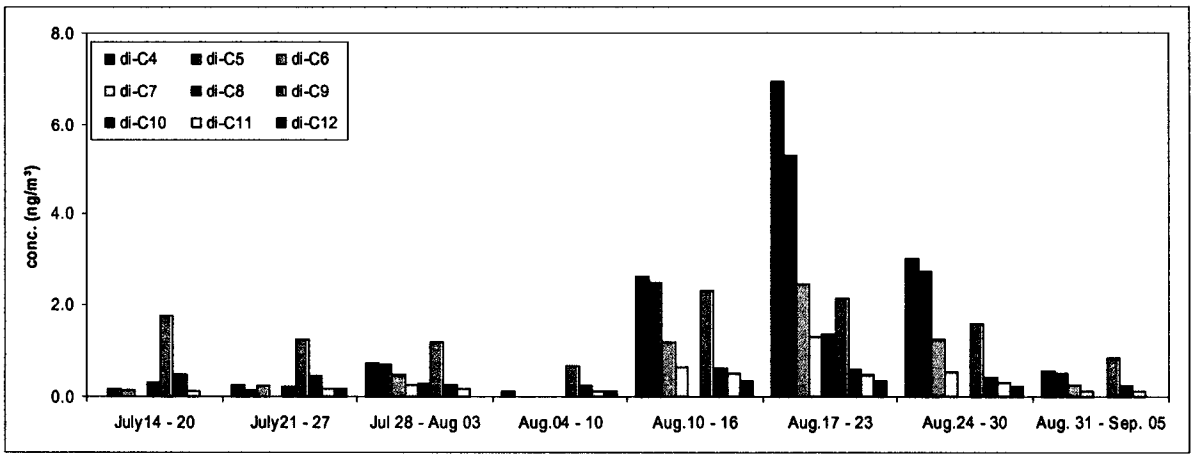

Figure 3-23. Timeline of dicarboxylic acid concentrations measured at Turtleback Dome based on weekly composites.

Estimates of primary aerosol contributions to OC from biomass burning smoke (discussed above) and other important anthropogenic sources (also described above), explain approximately 20 to 80% of the observed OC concentrations during different weeks of the study (see Table 3-3 and Figure 3-24). Although there is considerable uncertainty in this fraction, it is clear that SOA must be a significant contributor to local aerosol concentrations, consistent with our observations of appreciable concentrations of particular SOA species. The source of the SOA precursors is uncertain, but local biogenic emissions and emissions associated with smoke plumes impacting the site are likely both important. Under the assumption that the unidentified OC fraction roughly represents contributions from SOA, SOA contributions are high both early in the study and during the second intensive period, but lower at the end of the study. During the early part of the study, OC concentrations were low and production of SOA from locally produced biogenic VOC emissions was probably an important contributor to observed aerosol concentrations. During early to mid August high OC concentrations were observed in conjunction with long range transport of wildfire smoke plumes. High apparent SOA contributions during this period suggest

that a significant portion of the aerosol burden in the smoke plume was formed by reactions during transport. By contrast, in the last week of the study when local fires impacted the measurement site, apparent contributions of SOA are relatively low.

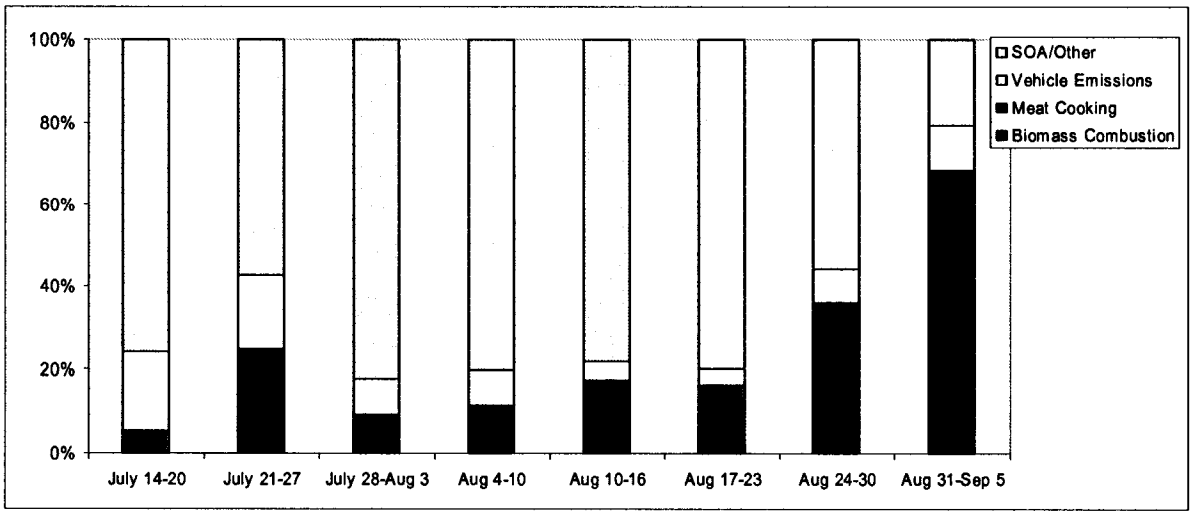

Figure 3-24. Estimated average contributions of biomass burning smoke, meat cooking, vehicle emissions, and SOA (and unidentified sources) to OC at Turtleback Dome.

3.3.6. Size Distributions

The chemical composition as a function of particle size can be an indicator for the formation processes of the aerosol. For instance, particle generation by nucleation generally results in sub-micron particles, while condensation of vapors onto existing particles results in larger particle sizes. While the majority of organic compounds (> 75% of OM) measured at Turtleback Dome was typically observed in fine particles (i.e., $PM_{2.5}$), a certain OM fraction was also present in particles of larger sizes. Most molecular marker species for biomass combustion were predominantly contained in submicron particles (see Figure 3-25), although on certain smoke-influenced days levoglucosan was observed in slightly larger particles as well, as demonstrated by

the levoglucosan size distribution at Turtleback Dome on August 16, 2002, one of the days during the second intensive haze episode (Figure 3-26).

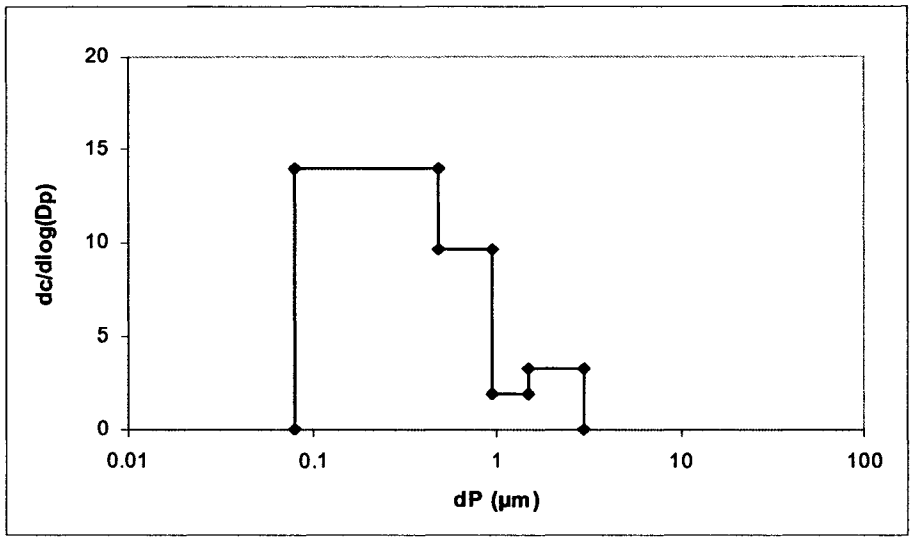

Figure 3-25. Size distribution of levoglucosan at Turtleback Dome on July 25, 2002.

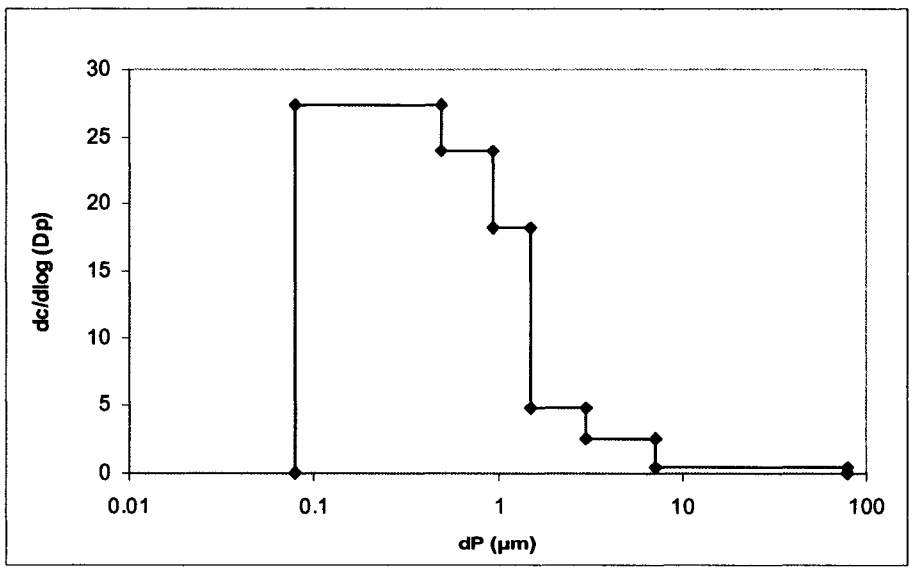

Figure 3-26. Size distribution of levoglucosan at Turtleback Dome on August 16, 2002.

Secondary biogenic compounds, including pinic and pinonic acids, were associated predominantly with smaller particles, while pinonaldehyde exhibited broader size distributions, possibly due to its higher volatility and resulting ability to redistribute across a range of particle sizes, as shown in Figure 3-27. Size distributions of additional organic species observed during YACS can be found in a paper accepted for publication (Herckes et al., 2005).

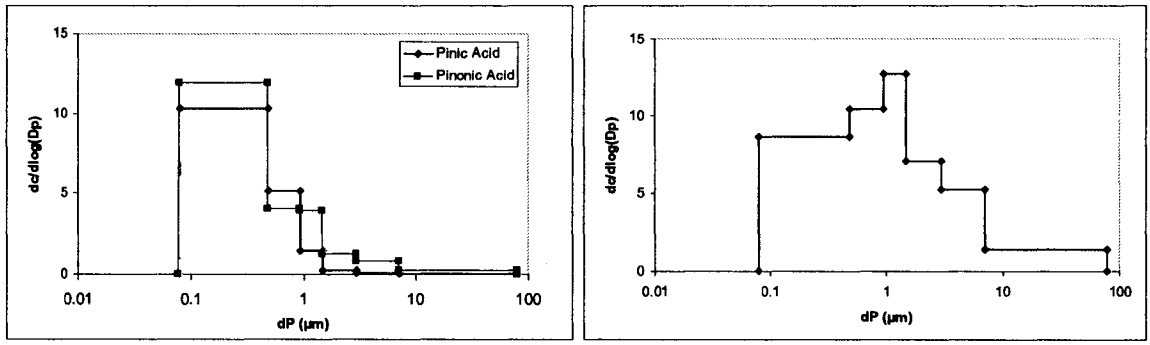

Figure 3-27. Size distributions of pinic and pinonic acids (left) and pinonaldehyde (right) at Turtleback Dome on August 16, 2002.

3.4. SUMMARY and CONCLUSIONS

During the summer of 2002 more than one hundred thousand acres of land were burned by wildfires or prescribed burns in the western United States. Smoke from wildfires in California and southern Oregon was transported to Yosemite National Park during the time frame of YACS. In particular, two regional haze episodes during YACS were strongly influenced by smoke from biomass burning. Molecular source tracers were used in conjunction with measurements of OC and BC, water-soluble potassium, satellite data, and back trajectories to identify sources and source regions of the smoke (McMeeking et al., 2005c).

The composition of $PM_{2.5}$ at Turtleback Dome during YACS was dominated by carbonaceous material with an average OM content of 70.6%, corresponding to a study-average OM concentration of 6.3 $\mu g/m^3$ (using an OC/OM multiplier of 1.8), and a peak concentration of 17 $\mu g/m^3$. More than 90% of the fine OM was derived from contemporary, i.e., biogenic, carbon sources rather than fossil fuel combustion, according to radiocarbon measurements (Bench and Herckes, 2004). In addition, n-alkane and n-alkanoic acid average CPI values of 3.3 and 6.2, respectively, indicated a predominance of biogenic carbon sources. Low fossil carbon contributions were further reinforced by estimates of vehicle emission contributions to fine particle OC that averaged approximately 10%. Meat cooking was estimated to contribute approximately 3% to fine particle OC.

Several classes of primary biomass burning smoke tracers, including anhydrosugars, methoxyphenols, and resin acids, were quantified in weekly composite and 24-hour or 12-hour samples. Levoglucosan concentrations up to 180 ng/m^3 were measured during the second intensive haze period during night-time drainage flow. Primary biomass combustion smoke contributions to $PM_{2.5}$ organic carbon were estimated to be as high as 65% on a weekly average and as high as 100% on selected individual days during intensive haze episodes. In addition to smoke from biomass combustion, high concentrations of monoterpene oxidation products and other organic compounds of secondary origin, such as dicarboxylic acids, indicated a significant contribution of SOA to fine OM. Pinene oxidation products, such as pinonaldehyde were observed with concentrations as high as 51 ng/m^3 on individual days and showed good correlation with fine particle OC. A significant contribution of secondary species was likely associated with smoke from biomass burning due to enhanced VOC emissions.

CHAPTER 4 BIOMASS COMBUSTION STUDY

4.1. INTRODUCTION

Fire has been an integral part of land use and culture throughout the history of mankind. In addition to residential burning of biomass in fireplaces and wood stoves, forest and brush fires, as well as slash and burn agriculture continue to impose a significant impact on natural and man-made environments on local and global scales. Biomass combustion is a major global source of fine PM in the atmosphere with substantial impacts on regional air quality, visibility, ecosystems, human health, and global climate (Abas et al., 2004a, Charlson et al., 1992, Crutzen and Andreae, 1990, Hobbs et al., 1997, McKenzie et al., 1995, Penner et al., 1994, Penner et al., 1992, Reid et al., 2005a, Riebau and Fox, 2001, Wu et al., 2002). It is important to understand the chemical and physical characteristics of smoke PM in order to asses the environmental impact of biomass combustion emissions. Furthermore, the contribution of biomass smoke to the ambient aerosol in a given location can be estimated, if certain chemical characteristics are known.

4.1.1. Source Apportionment

Various methods have been developed to apportion source contributions to ambient fine particle concentrations, including those from biomass combustion. Among these, molecular markers have been used extensively in source apportionment studies as well as to evaluate the transport, transformation, and fate of atmospheric constituents (e.g., Cass, 1998, Fraser et al., 2003, Gogou et al., 1996, Schauer et al., 1996, Simoneit, 1989, 2002, Yttri et al., 2005). A common approach

is based on measuring the ratios of selected organic marker compounds to either fine PM mass or OC mass concentrations at a receptor (i.e., sampling) site. These methods require accurate and representative source emission profiles. If such profiles are available, primary contributions to fine PM (or OC) mass at the receptor site from a specific source, such as wildfires or prescribed burns, can be estimated by comparing the marker/PM or marker/OC ratios with the ratios measured at the source (reported in the emission source profiles). While several source profiles for wood combustion in residential wood stoves and fireplaces have been generated in previous studies (e.g., Fine et al., 2004a, Hedberg et al., 2002, McDonald et al., 2000, Schauer et al., 2001), limited smoke emissions data have been reported from open combustion of biomass (Hays et al., 2005, Hays et al., 2002, Iinuma et al., 2006, Lee et al., 2005).

4.1.2. Biomass Combustion Source Tracers

Compounds intended for use as molecular markers should be representative of a specific source type. In addition, source tracers need to be present at the receptor site at measurable concentrations. Furthermore, they need to be conserved during transport to the receptor site, i.e., source tracers need to be stable in the atmosphere for a sufficient period of time and not subject to removal from the atmosphere, such as by chemical reactions. Thus, ideal tracer compounds are predominantly present in the condensed (i.e., particle) phase with particle sizes smaller than 2.5 μm aerodynamic diameter (i.e., $PM_{2.5}$) in order to have sufficiently long lifetimes (on the order several days).

Tracers for biomass combustion sources include a variety of compounds associated with the different chemical constituents of biomass. Wood is the dominant type of biomass burned in the western hemisphere. The three major constituents of wood are cellulose (40 - 50% of dry mass), hemi-cellulose (20 - 35%), and lignin (15 - 35%). Wood smoke contains thermal break-down

products of all three types of biopolymers. Table 4-1 gives an overview of common biomarkers that have been used in previous studies as biomass combustion source tracers.

Table 4-1. Molecular markers for combustion of various types of biomass.

Type of Biomass	Source Material	Source Tracers	References
Biomass (all)	Cellulose	Levoglucosan	(Hornig et al., 1985, Simoneit et al., 1999)
	Hemicellulose	Galactosan	(Nolte et al., 2001, Simoneit and Elias, 2000)
	Hemicellulose	Mannosan	(Nolte et al., 2001, Simoneit and Elias, 2000)
Softwood	Lignin	Vanillin	(Hawthorne et al., 1987, Kjallstrand et al., 2000)
	Lignin	Eugenol, Guaiacols	(Simpson et al., 2005)
	Extractives	Retene	(Ramdahl, 1983)
	Extractives	Resin Acids	(Simoneit et al., 1993)
Hardwood	Lignin	Syringols	(Simpson et al., 2005)

Thermal degradation of cellulose results in the generation of various anhydrosugars, including levoglucosan (1,6-anhydro-β-D-glucopyranose) with the highest emission factors of any single compound in biomass combustion smoke (Hornig et al., 1985, Simoneit et al., 1999). Levoglucosan is therefore a major component of aerosol particles emitted by biomass combustion (Abas et al., 2004b, Engling et al., 2006b, Fraser and Lakshmanan, 2000, Gao et al., 2003, Palma et al., 2004, Poore, 2002, Schkolnik et al., 2005, Simoneit et al., 2004, Simoneit et al., 1999, Yttri et al., 2005, Zdrahal et al., 2002). The production of levoglucosan is essentially limited to pyrolysis of cellulose in wood and other types of biomass. Temperatures are typically not sufficiently high to pyrolize carbohydrates (resulting in the formation of levoglucosan) in thermal processes such as cooking and baking (Simoneit et al., 1999). Likewise, pyrolysis reactions occurring during smoking of cigarettes typically favor the production of furans and lower

molecular weight carbonyls rather than levoglucosan (Sanders et al., 2003). Moreover, the production (i.e., synthesis) of levoglucosan is not likely to occur as a result of microbial activity or other processes (Hornig et al., 1985, Locker, 1988, Simoneit et al., 1999). In addition, levoglucosan is sufficiently stable in the atmosphere and can thus be used as biomass burning tracer even for smoke subject to long-range transport (Engling et al., 2006b, Fraser and Lakshmanan, 2000, and the discussion in section 2.3.5. of this dissertation). Therefore, due to (1) its source-specific emission with (2) relatively high concentrations, (3) its association with fine (accumulation mode) particles, and (4) presumed atmospheric stability, levoglucosan is an important molecular source tracer for fine particle emissions from biomass combustion.

Because of the lower content of hemicelluloses in wood relative to cellulose and variable composition in terms of sugar monomers (including mannose, galactose, arabinose, and xylose) emission factors of hemicellulose break-down products, such as mannosan and galactosan, are typically lower than those of levoglucosan. Nevertheless, these anhydrosugars can be utilized as biomass combustion source tracers as well, as they are exclusively emitted by biomass combustion (Nolte et al., 2001, Simoneit and Elias, 2000).

Lignin breakdown products include a variety of aromatic compounds. These compounds are commonly referred to as methoxyphenols, because their molecular structures include a methoxy and hydroxyl (phenyl) group. Methoxyphenols may contain additional functional groups, including carboxyl, carbonyl, alkyl, or additional methoxy and hydroxyl groups (Hawthorne et al., 1987, Simpson et al., 2005). Certain methoxyphenols are preferentially emitted by one type of wood versus another one. For instance, softwood combustion results in the formation of primarily (mono) methoxyphenols, such as vanillin, acetovanillone, and eugenol, whereas hardwood combustion generates dimethoxy compounds. The combustion of softwood also

produces resin acids and retene, present in the extractives of wood, while these tracers are absent in hardwood smoke (Ramdahl, 1983, Simoneit et al., 1993, Standley and Simoneit, 1994).

4.1.3. Study Overview

This study was designed to provide additional insight into primary aerosol emissions from the open combustion of various types of biomass under different combustion conditions. Resulting information can be used to constrain biomass combustion emission profiles for important fire emission categories to improve assessment of contributions of biomass combustion to ambient fine PM (i.e., $PM_{2.5}$) concentrations. Laboratory experiments to simulate wildfires under various combustion conditions were conducted at the U.S. Department of Agriculture (USDA) Forest Service (FS) Fire Sciences Laboratory (FSL) in Missoula, Montana, in collaboration with the Desert Research Institute (DRI). Smoke from the fires was captured near the source after dilution and cooling with ambient air. Emissions from 44 combustion experiments, burning 10 different types of biomass, were characterized with a large suite of instruments, both in real-time and by various laboratory methods following the combustion experiments.

4.2. EXPERIMENTAL METHODS

4.2.1. Combustion Facility

All combustion experiments were conducted at the USDA-Forest Service Fire Sciences Laboratory in Missoula, Montana. The facility, described in detail elsewhere (Christian et al., 2004), consists of a chamber that measures 12.5 x 12.5 m and 22 m in height (Figure 4-1a). An exhaust stack inside the chamber begins approximately 2 m above the floor and extends through the ceiling (Figure 4-1b). The stack has an inner diameter of 1.6 m and a base opening in the shape of an inverted funnel (3.6 m in diameter). A continuously weighed fuel bed (80 x 210 cm)

was positioned directly under the stack. Smoke emissions from fires burning underneath the stack were completely entrained in the stack flow due to positive air pressure inside the chamber that was continuously vented through the stack. Sampling equipment was located on a measurement platform approximately 16 m above ground. Typical stack flow rates were on the order of 3 m^3/sec and residence times of smoke from generation to sampling were approximately 5 seconds. Horizontal temperature and concentration profiles at the height of the sampling platform were assumed to be uniform, based on previous experiments (Christian et al., 2004).

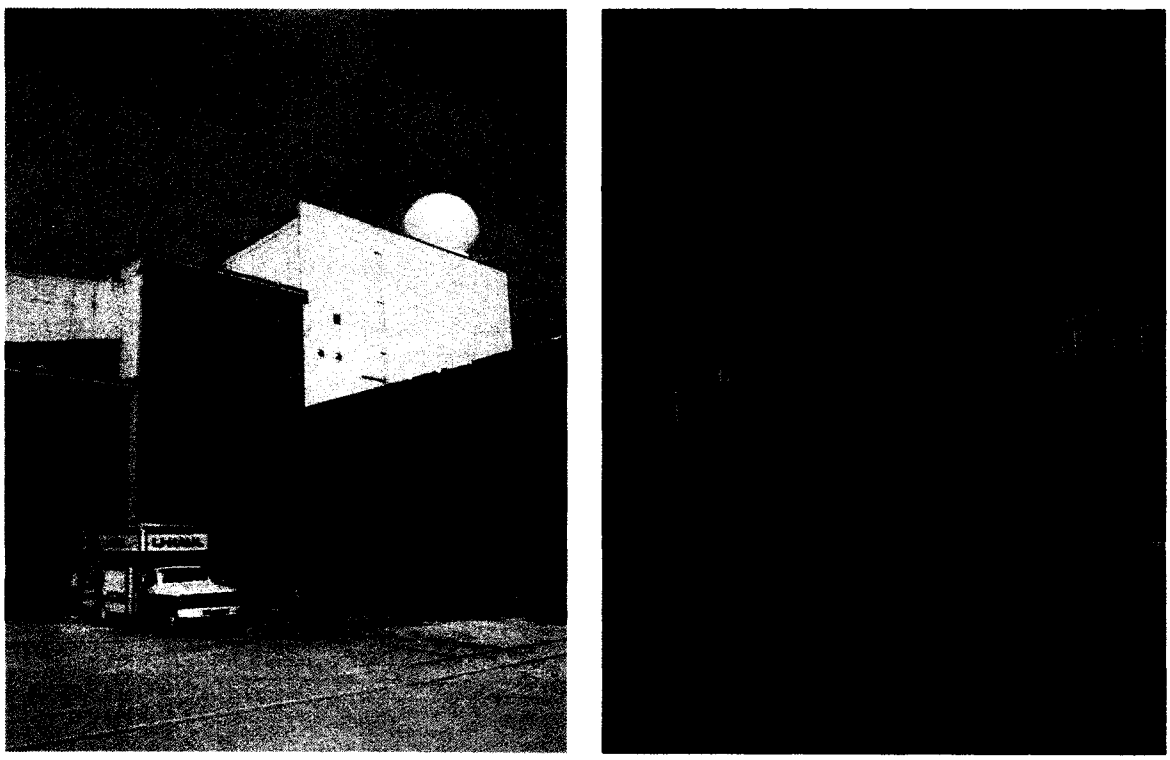

Figure 4-1. Images of the FSL combustion chamber (left) and exhaust stack (right).

4.2.2. Combustion Experiments

Two types of combustion experiments were carried out during the study. "Stack" burns were conducted by burning a pre-weighed amount of biomass on the fuel bed under the stack. In addition, seven "chamber" burns were performed inside the combustion chamber by burning

biomass on a mobile fuel bed located approximately 5 m from the stack inlet. There was no stack flow during these experiments, allowing smoke to fill the entire chamber. While all chamber burns were conducted on a flat surface, stack burns were carried out either as "heading" burns (upslope fire progression at an angle of 22 °) (Figure 4-2), "backing" burns (downslope fire progression at 22 °), or on a flat surface. Sampling of selected stack burns (# 83 and 86) was conducted to distinguish emissions during flaming versus smoldering fires by collecting separate samples during the flaming and smoldering stages. Sampling during the remaining stack and chamber burns included the flaming and smoldering phase combined in one sample. Types of biomass burned included hardwoods (cottonwood, oak wood, and Excelsior, a poplar product), softwood (ponderosa pine), needles (white pine and ponderosa pine), sage brush, grasses (African Savannah and wet Montana grass), and duff (Alaskan tundra feather moss), as depicted in Figure 4-3.

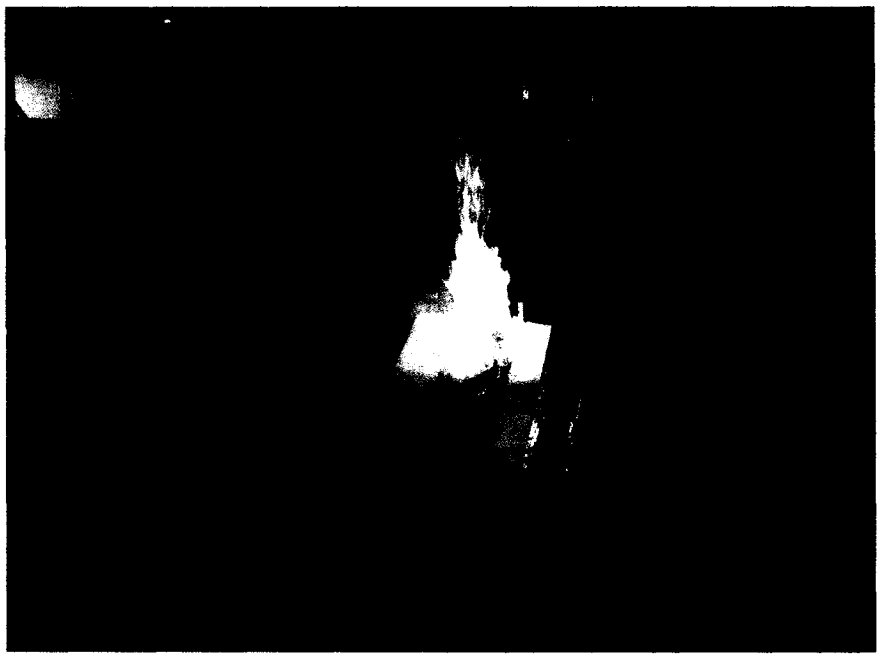

Figure 4-2. Heading "stack" burn of white pine needles.

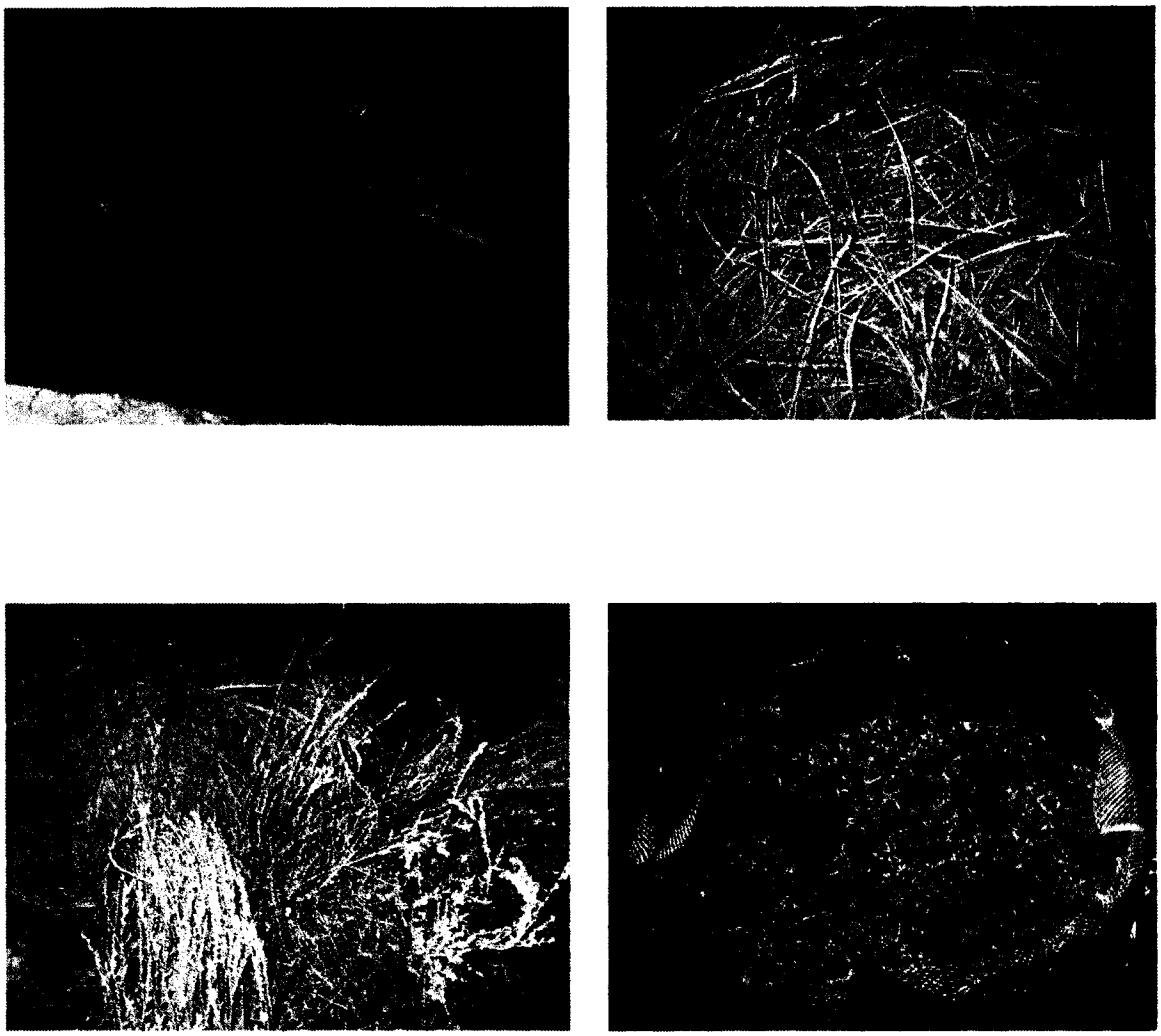

Figure 4-3. Examples of fuel types burned during the study: cottonwood (a), ponderosa pine needles (b), sage brush (c) and Tundra duff (d).

4.2.3. Sample Collection

Smoke particle samples were collected with two types of Hi-Vol samplers: fine particles ($PM_{2.5}$) were collected with a ThermoAndersen (Smyrna, GA) GI200-2.5 sampler, attached to the stack with a custom manifold and operated at a nominal flow rate of 1130 L/min. Size-segregated aerosol samples were collected during the "chamber" burns with a ThermoAndersen TA 235 Hi-Vol sampler, equipped with a 5-stage impactor with nominal size cuts at 7.2, 3.0, 1.5, 0.95 and 0.49 μm, plus a back-up filter, collecting smaller particles (Willeke, 1975). $PM_{2.5}$ samples and

sub 0.49 μm particles from the cascade impactor were collected on Whatman (Maidstone, England) QM-A quartz fiber filters (20.3 x 25.4 cm). Coarse particles (larger than 2.5 μm aerodynamic diameter) and stages 1 through 5 from the cascade impactor were collected on slotted filters, custom-cut from Whatman QM-A quartz fiber filters. Smoke temperatures inside the stack were continuously monitored at the height of the sampling platform. Temperatures were typically close to the ambient chamber temperatures, ranging from 18 to 26 °C. In order to ensure sufficient sample loadings, sampling with quartz fiber filters for organic speciation was sometimes conducted for the duration of two to four burns (of the same fuel and under the same combustion conditions). Typical sampling times for $PM_{2.5}$ composite samples were approximately 30 to 35 minutes, while sampling times for individual stack burns ranged from 10 to 15 minutes. Corresponding total sample volumes were approximately 35 - 40 m^3 or 15 - 20 m^3, respectively. Chamber burns were conducted over longer periods of time (up to 200 min.), resulting in sample volumes of 70 to 230 m^3. An overview of collected samples and the corresponding combustion experiments selected for discussion is given in Table 4-2.

Table 4-2. Overview of combustion experiment and corresponding samples.

Burn I.D.	Type of Biomass	Fuel Moisture [c]	Surface	Type of Fire	Sample Type
46 - 48	WP Needles [a]	8.79	Slope [e]	Backing	$PM_{2.5}$
49 - 51	WP Needles [a]	8.24	Slope [e]	Heading	$PM_{2.5}$
52 - 54	Sage	7.75	Slope [e]	Heading	$PM_{2.5}$
55 - 58	Sage	7.75	Slope [e]	Backing	$PM_{2.5}$
59 - 61	Savannah Grass	6.42	Slope [e]	Heading	$PM_{2.5}$
62 - 64	Savannah Grass	5.92	Slope [e]	Backing	$PM_{2.5}$
65	PP Needles [b]	8.09	Slope [e]	Heading	$PM_{2.5}$
66	PP Needles [b]	7.68	Slope [e]	Heading	$PM_{2.5}$
67 - 68	PP Needles [b]	7.58	Slope [e]	Heading	$PM_{2.5}$
69 - 71	PP Needles [b]	7.35	Slope [e]	Backing	$PM_{2.5}$
73	Duff	15.9 - 289 [d]	Flat (Cylinder)	Smoldering	$PM_{2.5}$
74 - 75	Montana Grass	17.53	Slope [e]	Heading + Backing	$PM_{2.5}$
77	Sage	9.30	Flat	Chamber Burn	$PM_{2.5}$
79	PP Wood [b]	6.60	Slope [e]	Heading	$PM_{2.5}$
80	PP Wood [b]	5.77	Slope [e]	Backing	$PM_{2.5}$
81	Excelsior (Poplar)	6.33	Flat	Chamber Burn	$PM_{2.5}$
82	Cottonwood	4.94	Flat	Chamber Burn	$PM_{2.5}$
83	Oak Wood	13.64	Flat	Flaming/Smoldering	$PM_{2.5}$
84	Oak Wood	16.92	Flat	Chamber Burn	$PM_{2.5}$ + MULT [f]
85	Duff	6.9 - 72 [d]	Flat (Cylinder)	Chamber Burn	$PM_{2.5}$ + MULT [f]
86	PP Wood [b]	11.41	Flat	Flaming/Smoldering	$PM_{2.5}$
87	Sage	15.14	Flat	Chamber Burn	$PM_{2.5}$ + MULT [f]
88	PP Needles [b]	8.47	Flat	Chamber Burn	$PM_{2.5}$

Notes: a.) WP ... white pine; b.) PP ... ponderosa pine; c.) Fuel moisture: expressed as dry weight %; d.) Fuel moisture of duff: the range of moisture contents corresponds to measurements made at three different depths within a particular duff core (top to bottom); e.) the angle of the slope was 22 °; f.) MULT: multi-stage cascade impactor sample.

Quality control measures included field blanks and a chamber air background sample analyzed according to the same protocols as smoke samples. Prior to sampling, filters were pre-fired at 600 °C for at least 8 hours to remove any organic carbon present on the filters. Sample filters were placed into individual pre-fired aluminum envelopes following collection and stored cold (< 0 °C) until analysis. A total of 29 $PM_{2.5}$ and 3 multi-stage impactor samples were collected from the chamber and stack burns.

4.2.4. Carbon Analysis

Carbonaceous material in the smoke samples was determined with a Sunset Laboratories continuous carbon analyzer in off-line mode, using TOT measurement for pyrolysis correction (Birch and Cary, 1996). Portions (2.3 cm^2 punches) of filters collected with the $PM_{2.5}$ Hi-Vol sampler during chamber and stack burns were analyzed for OC and EC. Selected filters were cut in half horizontally, followed by measurement of OC and EC on the front and back portions of each filter, in order to examine artifact adsorption of gas-phase organic compounds on the pre-fired quartz filters. As described in more detail in section 3.2.5., particulate carbonaceous matter and gas-phase organic compounds were assumed to be collected on the front portion, while the carbonaceous material measured on the back portion of these filters was attributed to gas-phase organic compounds only. Accordingly, a correction factor to account for the vapor adsorption artifact was determined and applied to all OC data obtained with the Sunset carbon analyzer using equation (4-1), where OC_{F+B} denotes the combined OC mass measured on the front and back portions, OC_{BLK} is the blank value, OC_B is the OC measured on the back half of each filter (i.e., the vapor-phase OC), and 0.786 is a correction factor to account for the cutting bias (determined by gravimetric analysis of a series of cut filter slices (n = 15), as described in section 3.2.5.).

$$OC = \left(OC_{F+B} - OC_{BLK}\right) - \left(2 \cdot OC_B \cdot 0.786\right) \qquad (4\text{-}1)$$

A typical thermogram from a filter sample (analyzed by Sunset Labs) containing OC, carbonate (CC), and EC obtained from pulverized beet pulp, rock dust, and diesel particulate is shown in Figure 4-4. PC is pyrolytically generated carbon (i.e., "char"). The final (blue) peak is from methane used for instrument calibration. Figure 4-4 also shows the temperature and oxidant profiles for the duration of an analytical cycle (12 min. in total length).

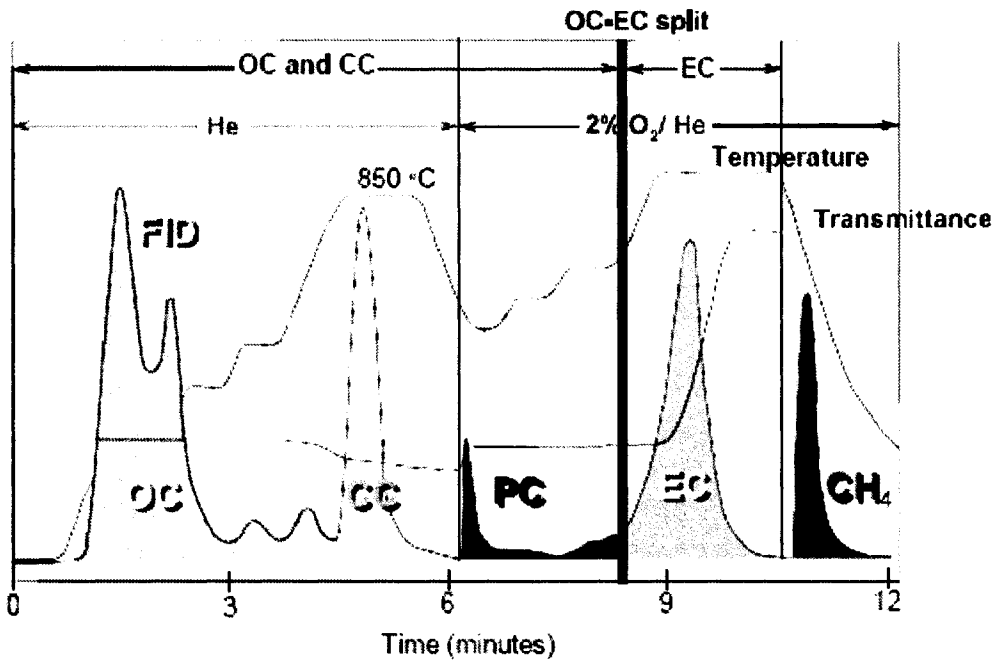

Figure 4-4. Typical thermogram for a filter sample containing OC, carbonate (CC), and EC obtained with the Sunset Labs Carbon Analyzer (Birch, 1999).

4.2.5. GC-MS Analysis

Filter extracts (using DCM) were analyzed on a HP 6890 Gas Chromatograph coupled with a HP 5973 MSD, as described in more detail in section 2.2. In summary, chromatographic separation of the individual organic species was accomplished using a HP-5MS capillary column (30 m x 250 μm x 0.25 μm 5% phenyl-methyl-siloxane film). Injections of 1.0 μL aliquots were performed in splitless mode. The GC temperature profile consisted of an initial hold time of 10

minutes at 65 °C, followed by a temperature gradient of 10 °C /min to a final temperature of 300 °C maintained for 20 minutes. Authentic standards were used for compound identification and to obtain response factors for the majority of the individual quantified organic species.

4.2.6. HPAEC-PAD Analysis

A more detailed summary of the HPAEC method is given in section 2.3. Briefly, a portion of each filter (typically one eighth) was extracted twice with 15 mL of de-ionized water. Typical extraction efficiencies for levoglucosan were 100% based on extraction experiments, using ultrasonic agitation, of quartz fiber filters spiked with a known amount of levoglucosan. The combined extracts were passed through a syringe filter containing a pre-fired 25 mm quartz fiber filter to remove insoluble material. Sample aliquots were injected (100 μL sample loop) without concentration or chemical derivatization into the chromatograph. Separation of the individual anhydrosugars was achieved using a Dionex CarboPac PA 10 Analytical Column (4 x 250 mm) with an 18 mM aqueous NaOH eluent at a flow rate of 0.5 mL/min. Authentic standards were used for identification and to obtain response factors for all quantified anhydrosugars.

4.2.7. HPLC-MS Analysis

Another portion of selected filters was analyzed by Y. Iinuma at IfT in Leipzig, Germany, using HPLC coupled with MS detection. Filter portions (1 x 6.3 cm) were cut into small pieces using ceramic scissors. These filter pieces were extracted in 1.0 mL of methanol under ultrasonication for 15 minutes. The extracts were filtered using membrane filters. The extraction vials and filters were washed with an additional 0.5 mL of methanol to remove residual analytes. The resulting extracts were dried under a gentle stream of nitrogen and recovered in 0.5 mL of methanol. Extracts were further diluted with methanol, if necessary. The separation was carried out using an Agilent 1100 series HPLC instrument with a Phenomenex Luna amino column (250 mm

length x 4.6 mm inner diameter, 5 μm particle size). The eluent composition was 92.5% acetontrile/7.2% H_2O/0.3% acetic acid and the column temperature was held constant at 7.5 °C. A Bruker Esquire 3000 plus ion trap mass spectrometer equipped with an electrospray ionization (ESI) source was used as a detector. Detection of anhydrosugars was achieved by the formation of anhydrosugar acetate adducts $[M + CH_3COO]^-$ in the negative electrospray mode.

4.3. RESULTS and DISCUSSION

A large array of measurements made by the participating laboratories provides important information regarding the chemical, physical and optical properties of smoke emissions from the combustion experiments conducted during this study (e.g., Carrico et al., 2006, Chakrabarty et al., 2006, Chen et al., 2006, Day et al., 2006, and the data reported in this chapter). In addition to extensive characterization of the smoke emissions, important fuel characteristics, such as moisture content, and combustion parameters, including combustion time and flame duration (vs. smoldering time), were measured.

4.3.1. $PM_{2.5}$ Composition

On average, 93% of the $PM_{2.5}$ mass was attributed to carbonaceous material, based on carbon measurements in smoke emissions from four chamber burns, #81, 82, 83, and 87, (Day et al., 2006). Carbonaceous material was determined as the sum of particulate OM and EC. OM was determined from $PM_{2.5}$ mass closure calculations using emissions data from the chamber burns. The OM content in $PM_{2.5}$ emissions from these chamber burns varied from 87% (sage) to 96% (chestnut oak). The EC content in $PM_{2.5}$ from the selected chamber burns ranged from 3% (sage) to 6% (poplar). Inorganic ions constituted an additional 2% (chestnut oak) to 6% (sage) of fine mass. The balance (1 - 3%) of the $PM_{2.5}$ mass was attributed to soil minerals (Day et al., 2006).

4.3.2. Carbonaceous Content

Emissions for OC and EC varied with type of biomass and combustion conditions, as demonstrated in Figure 4-5 and Table 4-3. The emission rates shown in Figure 4-5 are average values for each type of biomass (including various combustion conditions) expressed as mass of OC or EC per mass unit of fuel burned and normalized by the volume of air sampled. OC emissions ranged from 23 $\mu g/m^3$ (heading Savannah grass fire) to 316 $\mu g/ m^3$ (backing white pine needles), while EC emissions were observed from near zero (wet Montana grass) to 1049 $\mu g/m^3$ (heading ponderosa pinewood fire). However, when taking into account both the amount of biomass burned and the volume of air sampled, the biomass species with highest OC and EC emissions was the poplar product Excelsior, while Savannah grass still had the lowest OC emissions. EC to OC ratios also showed large variations with type of biomass and combustion conditions (Table 4-3).

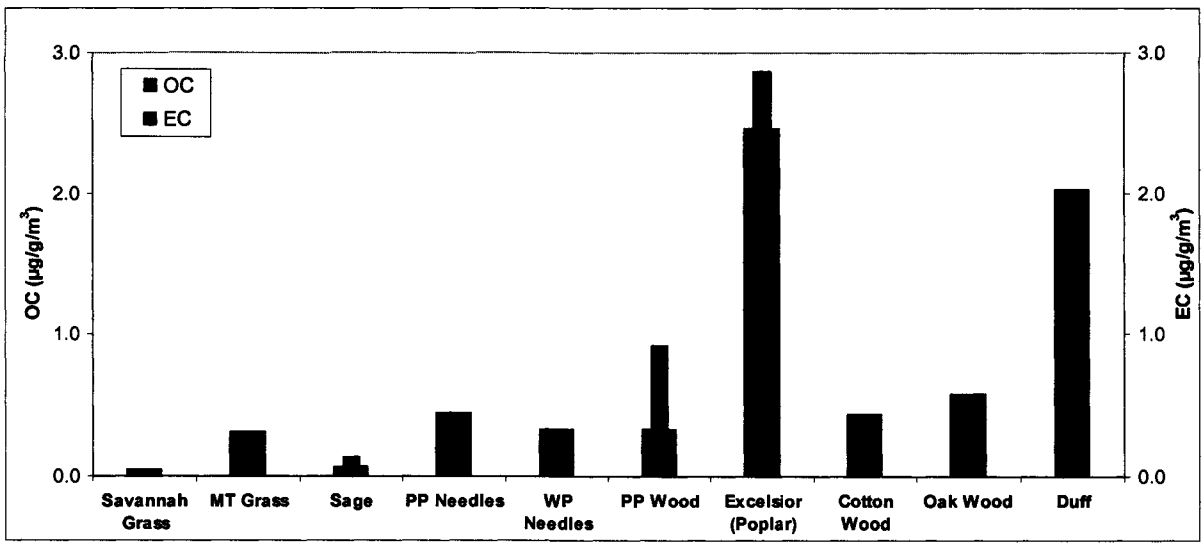

Figure 4-5. Average emissions for OC and EC from the combustion of various types of biomass based on carbon data obtained with the Sunset Labs Carbon Analyzer (TOT protocol).

Table 4-3. Summary of OC, EC, and $PM_{2.5}$ emission rates, as well as EC/OC ratios.

Type of Biomass	Type of Fire	OC ($\mu g/m^3$)	OC (µg/g fuel)	EC ($\mu g/m^3$)	EC (µg/g fuel)	EC/OC
Savannah Grass	Heading	23	1.1	31	1.5	1.3
Savannah Grass	Backing	48	2.1	20	0.9	0.4
Montana Grass	Heading + Backing [a]	129	18.8	0.004	0.0006	0.00003
Sage	Heading	64	2.7	92	3.9	1.4
Sage	Backing	49	2.7	144	8.0	2.9
PP Needles	Heading	170	7.2	75	3.2	0.4
PP Needles	Backing	51	2.3	111	4.9	2.2
WP Needles	Heading	127	16.3	6	0.3	0.02
WP Needles	Backing	316	6.2	28	1.3	0.2
PP Wood	Heading	126	4.2	1049	35.4	8.3
PP Wood	Backing	51	0.7	23	0.3	0.5
PP Wood	Flaming	114	4.8	479	20.2	4.2
PP Wood	Smoldering	196	11.1	17	1.0	0.1
Cottonwood	Flaming + Smoldering [b]	87	9.0	0.6	0.07	0.01
Excelsior (Poplar)	Flaming + Smoldering [b]	26	36.3	30	42.4	1.2
Oak Wood	Flaming	228	8.1	6	0.2	0.03
Oak Wood	Smoldering	32	2.3	8	0.6	0.3
Duff	Smoldering	94	4.5	1.4	0.06	0.07

Notes: a.) Sample comprised heading and backing fires; b.) Sampling was conducted during flaming and smoldering fire stages

The carbon data reported here were compared to measurements conducted independently, using DRI TOR and TOT protocols. While OC emissions, expressed in mass of OC per mass unit of fuel burned and normalized by the volume of air sampled, show good agreement between the two DRI protocols, the Sunset Labs (TOT) OC values are consistently lower by a factor of approximately two, as demonstrated in Figures 4-6 and 4-7. Neither the DRI sampler nor the CSU sampler were equipped with denuders to remove gas-phase organic species. Therefore, OC emissions obtained from the DRI samples may be overestimated due to adsorption of gas-phase

organic species on the quartz filters in contrast to the Sunset OC data that have been corrected for the adsorption artifact, as described above (section 4.2.4.). In fact, the agreement between all three methods is significantly improved when the uncorrected Sunset Labs OC data are compared to the DRI OC data, as shown in Figure 4-8. Linear regressions of the uncorrected OC data have slopes of near unity and correlation factors (R^2) of 0.99. The average vapor-phase carbon contribution was estimated to be 50% based on OC content on the back filter portions determined by the Sunset Labs analyzer. This fraction roughly corresponds to the difference in emissions obtained by the DRI and CSU methods, expressed by slopes of approximately 2.4 from the linear regressions (Figure 4-7).

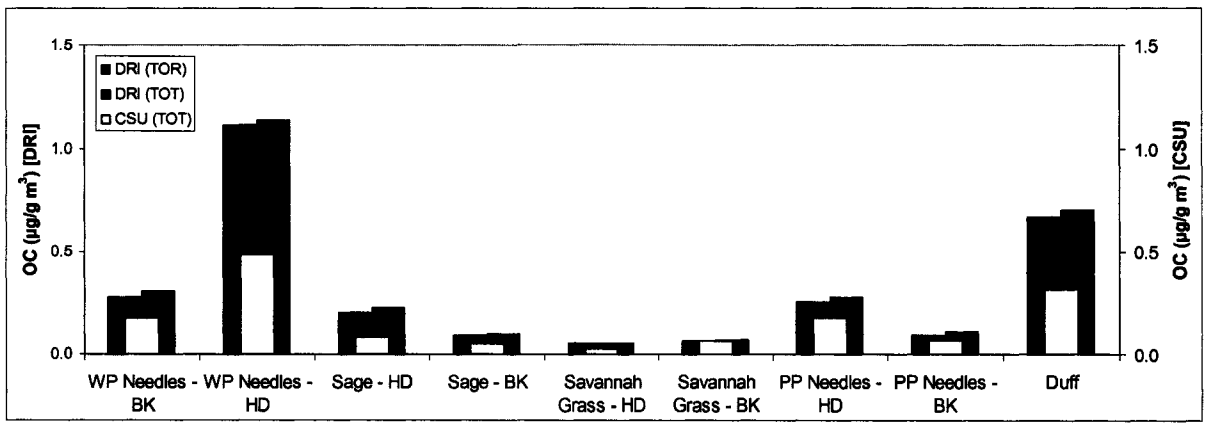

Figure 4-6. OC emissions for the combustion of various types of biomass obtained by three independent methods: DRI TOR and TOT protocols, as well as the Sunset Labs TOT (modified NIOSH) protocol.

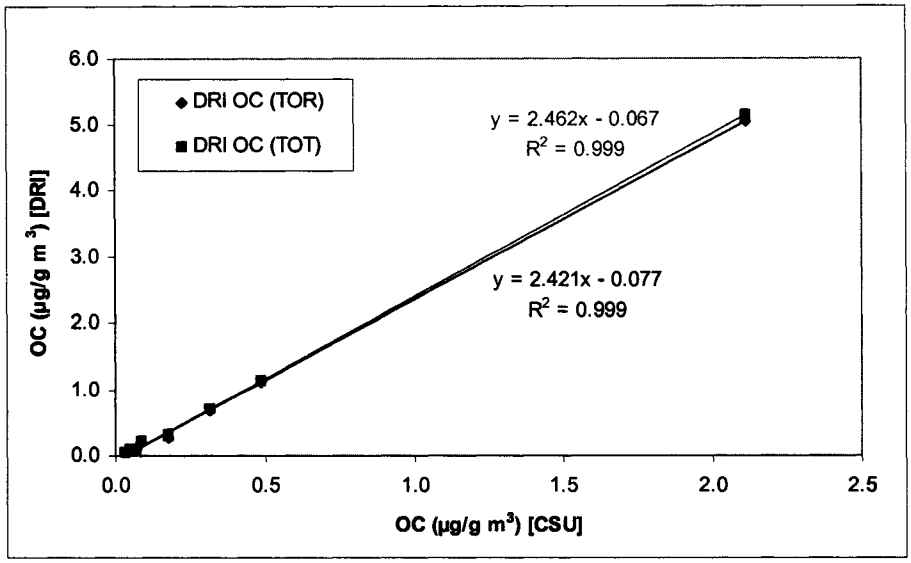

Figure 4-7. Correlation of normalized OC emissions for the combustion of various types of biomass obtained by three independent methods (DRI TOR, DRI TOT, and Sunset Labs TOT protocols).

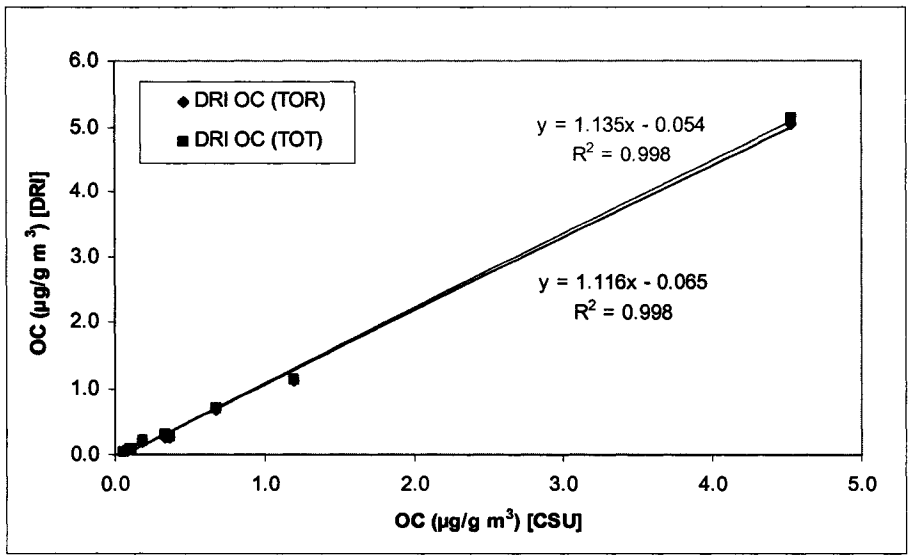

Figure 4-8. Correlation of normalized OC emissions for the combustion of various types of biomass based on DRI TOR and TOT data, as well as Sunset Labs TOT data not corrected for the adsorption artifact.

Comparison between IMPROVE (TOR) and Sunset Labs TOT carbon data was limited by the number of burns for which IMPROVE data were collected. Due to space restrictions on the sampling platform during stack burns the IMPROVE sampler was operated only during chamber burns. The agreement of OC emissions from chambers burns of four different fuels obtained by the two methods is similar to that between the DRI and Sunset Labs OC data: the IMPROVE data are generally higher than the adsorption artifact corrected Sunset Labs emissions, as demonstrated in Figure 4-9. Again, when comparing the uncorrected Sunset OC emissions with the IMPROVE OC data, the agreement is rather good (22% difference on average, excluding the cottonwood data that would be a factor of two higher). The IMPROVE sampler was not equipped with a denuder and carbon data were not corrected for potential adsorption artifacts unlike the Sunset data. This may at least partially explain the difference between the two data sets.

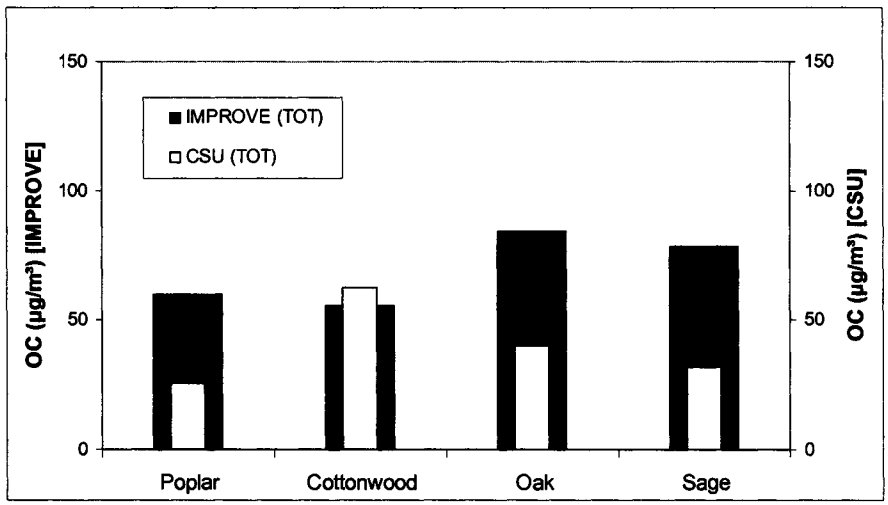

Figure 4-9. Comparison of OC emissions from selected chamber burns obtained by two independent methods: IMPROVE TOR and Sunset Labs TOT protocols.

OC and EC emissions also varied with combustion conditions, such as slope of the fuel bed (which determines the direction of the fire progression) and combustion phase (flaming versus smoldering). Five different types of biomass were investigated regarding their emissions from

heading (up-slope) versus backing (down-slope) fires. While four of these fuels produced more OC during heading burns (roughly double the amount of backing fire emissions), Savannah grass showed the opposite pattern, as illustrated in Figures 4-10 and 4-11.

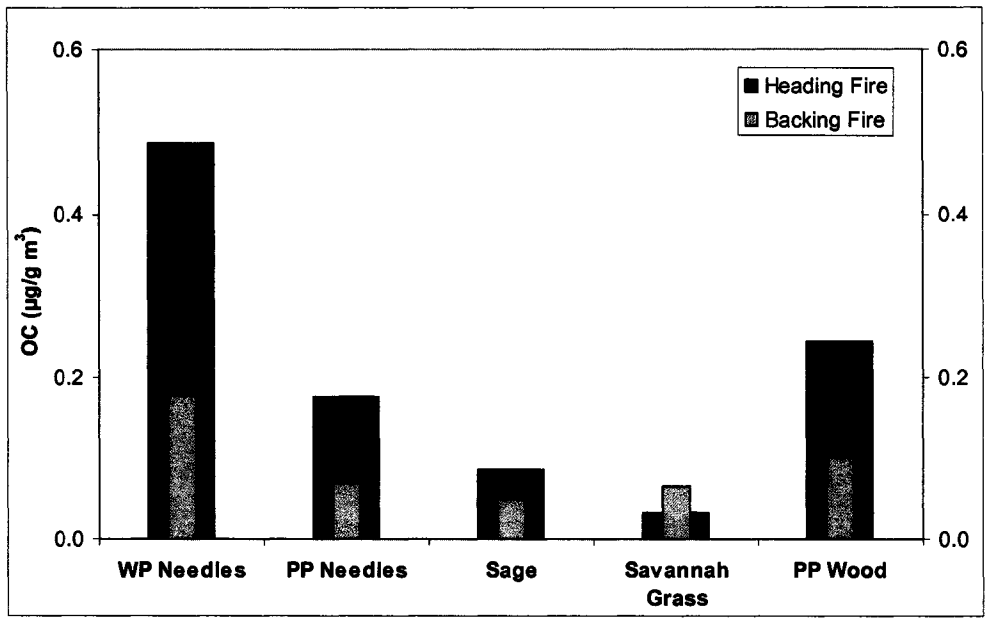

Figure 4-10. OC emissions for selected fuel types as a function of direction of fire progression.

The lower OC emissions for heading fires of Savannah grass coincided with low carbon monoxide (CO) emissions (the lowest of all fuel types investigated). CO emission factors are commonly used to determine the combustion efficiency of a fire. In case of the heading Savannah grass fire, the lower CO emissions indicate relatively high combustion efficiency that is expected to result in reduced emissions of incomplete combustion products, i.e., OC and EC. Heading fires typically spread faster and burn with higher intensity. While the measured emissions from the heading burns of Savannah grass are in agreement with this principle, the other heading burns investigated here did not follow this trend. These observations lead to the postulation that the type of fire propagation (heading or backing) plays a secondary role, while

the nature of the biomass seems to be the main determinant for the magnitude of OC and EC emissions. Additional factors influencing carbon emissions likely include fuel moisture, flame temperature, and stacking of the fuel bed.

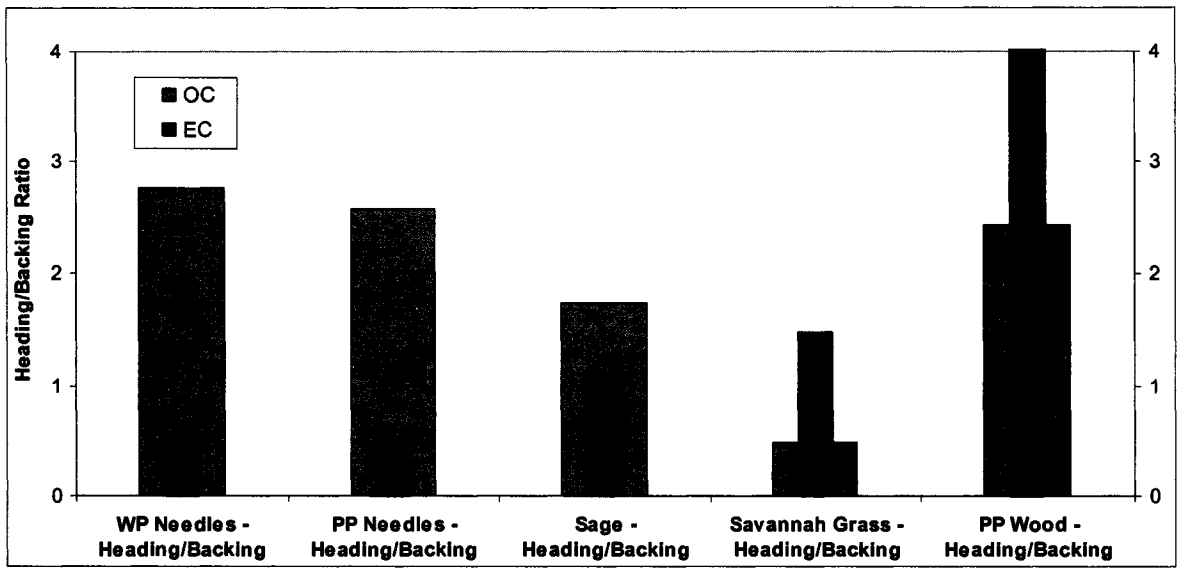

Figure 4-11. Comparison of OC and EC emission ratios for heading versus backing fires.

EC emissions showed a more diverse pattern than OC emissions, as demonstrated by ratios of emission rates for heading versus backing burns (Figure 4-11) and absolute emission values for various fuels and combustion conditions (Figures 4-12 and 4-13). While sage brush and Savannah grass emitted roughly the same amount of EC during heading and backing fires, white pine and ponderosa pine needles were observed with EC emissions half as large for heading fires compared to backing fires. In contrast, ponderosa pinewood smoke was characterized by significantly higher EC emissions from heading relative to backing fires.

EC to OC ratios also did not show any consistent trend as a function of fire propagation (heading versus backing fires) or fuel type (Figures 4-12 and 4-13). While certain types of biomass (e.g.,

white and ponderosa pine needles) produced more OC relative to EC during heading fires, other fuels emitted larger amounts of EC under similar conditions (Figure 4-12). EC/OC emission ratios from backing fires showed similar characteristics (Figure 4-13). Interestingly, smoke from one fuel type, sage brush, contained relatively more EC than OC from both, heading and backing fires, while both, heading and backing fires of white pine needles produced more OC than EC (Figures 4-12 and 4-13).

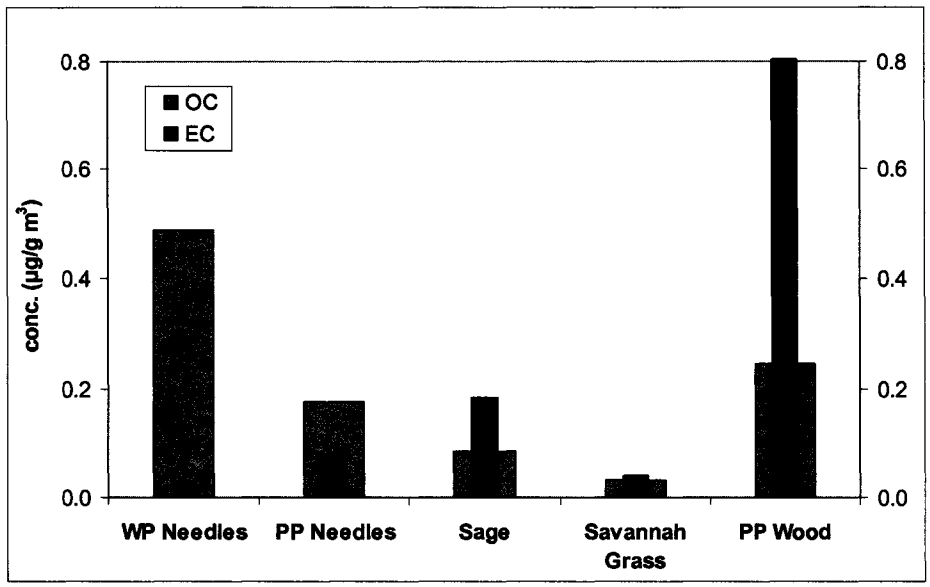

Figure 4-12. OC and EC emissions from heading fires of selected fuel types.

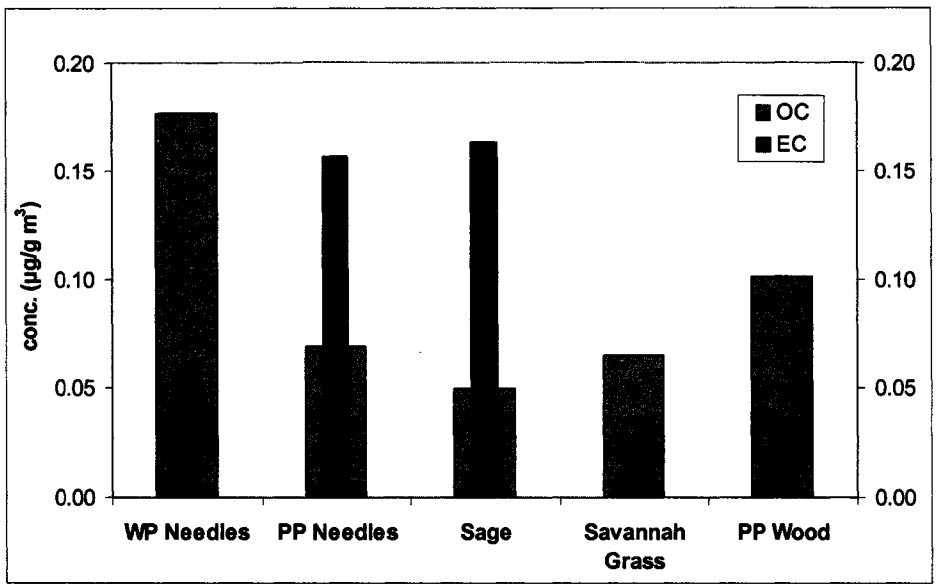

Figure 4-13. OC and EC emissions from backing fires of selected fuel types.

Additional combustion experiments were conducted to evaluate emissions during the flaming versus smoldering fire stages. Two types of biomass were investigated: a hardwood (chestnut oak) and a softwood species (ponderosa pine). OC emissions from oak wood were higher during the flaming fire relative to a smoldering fire (Figures 4-14 and 4-15). Pinewood, on the other hand, generated less OC in the flaming fire compared to the smoldering fire (Figure 4-14). Increased OC concentrations in smoldering fires compared to flaming fires are expected due to lower inherent temperatures after flame pyrolysis has ceased, although previous observations are reported with large variances, primarily due to high uncertainties associated with the OC/EC measurement methods (Reid et al., 2005b). Both fuels produced significantly more EC during the flaming stage compared to the smoldering fire, also in agreement with previous reports (Reid et al., 2005b).

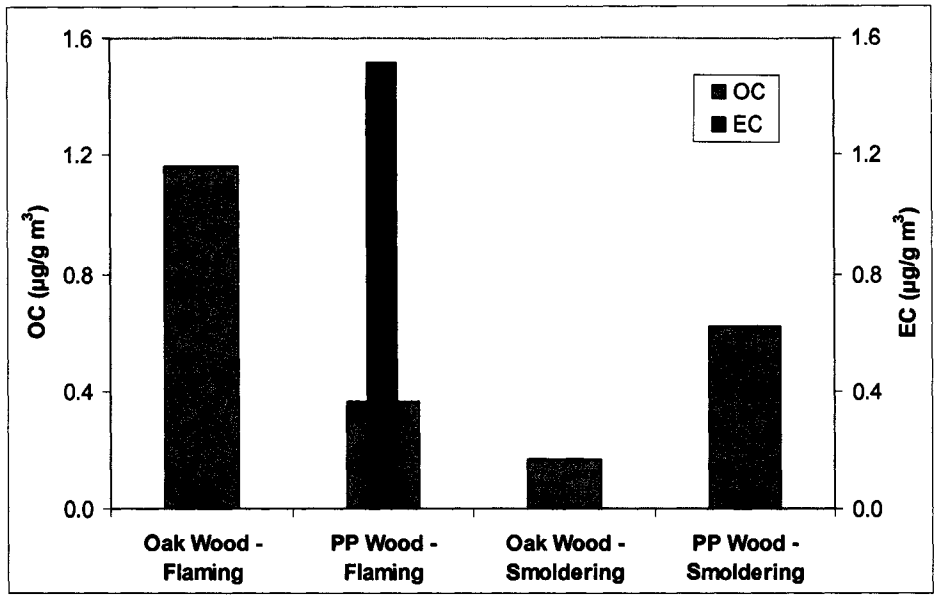

Figure 4-14. OC and EC emissions for flaming and smoldering fires from a hardwood (oak) and softwood (ponderosa pine) species.

EC/OC ratios have been observed in previous studies to range from approximately 0.1 to 0.5 for flaming fires and were typically < 0.1 for smoldering fires (Reid et al., 2005b). While some of the EC/OC ratios observed here fall within the reported range, others are up to one order of magnitude larger. Due to the limited number (two) of experiments that were conducted to distinguish emission characteristics as a function of combustion phases it is difficult to draw conclusions with a large degree of confidence.

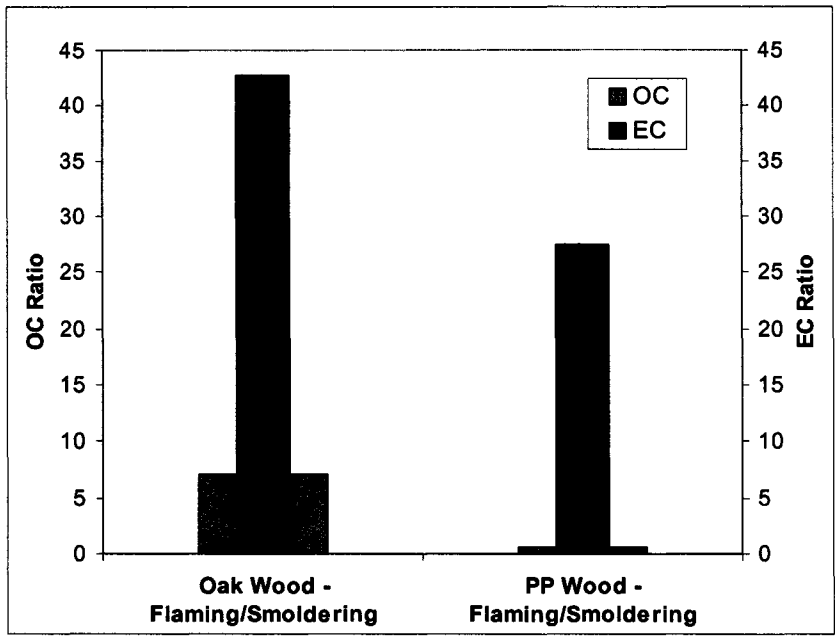

Figure 4-15. Ratios of OC and EC emissions for flaming versus smoldering fires of a hardwood (oak) and softwood (ponderosa pine) species.

While the observation of higher EC emissions relative to OC from the combustion of certain types of biomass under specific conditions is in contrast to EC/OC ratios commonly observed in ambient aerosol particles impacted by biomass combustion (Reid et al., 2005b), one needs to keep in mind that ambient samples include smoke from a mix of fuel types in various configurations, including wood, branches, needles, leaves, brush, and grasses. Therefore, a comparison of source emissions, such as those reported here, with ambient biomass combustion aerosol, may not necessarily be adequate. Furthermore, EC/OC ratios observed in previous biomass combustion source emission studies are typically below 0.5 as well (e.g., Fine et al., 2001, 2004a, Schauer et al., 2001). However, the combustion experiments in most of those studies were carried out in fireplaces or wood stoves, i.e., under confined conditions, whereas the experiments conducted as part of this study simulate open burning that is more typical for wildfires. An additional reason for the high EC content measured here may be an overestimation of EC due to possibly incorrect classification of certain OC components as EC by the analytical (thermal) methods (Iinuma et al.,

2006, Yu et al., 2002). The distinction of OC and EC in biomass combustion aerosol is particularly challenging due to the high carbonaceous content. In addition, higher molecular weight substances in biomass smoke, including biopolymers (e.g., cellulose and lignin), HULIS, and other compounds of secondary origin, may be incorrectly classified as EC (Iinuma et al., 2006, Mayol Bracero et al., 2002). Observations during a recent biomass burning study revealed that up to 70% of the apparent EC (according to thermal analysis) was organic material such as that described above (Mayol Bracero et al., 2002).

4.3.3. Anhydrosugar Emissions

Emission factors of the three isomeric anhydrosugars, levoglucosan, mannosan, and galactosan, were determined for a variety of fuel types and combustion conditions. Measured emission factors for levoglucosan, mannosan, and galactosan varied with fuel type, as shown in Figure 4-16 based on average emissions from one type of biomass under various combustion conditions. The emission factors are reported as the amount of anhydrosugar (expressed in μg) emitted per unit mass of OC (in mg). Average levoglucosan emission factors for the ten biofuels investigated during this study ranged from 110 to 1368 μg/mg OC, with the highest factors from Montana grass and the lowest from sage brush (Figure 4-16).

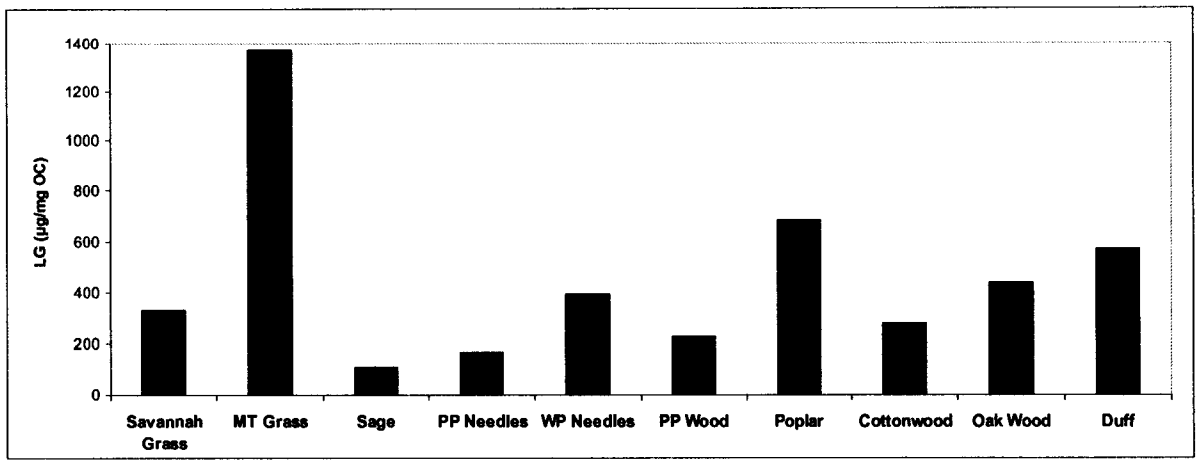

Figure 4-16. Average levoglucosan emission factors for a variety of fuel types (expressed in terms of mass of levoglucosan per unit mass of OC).

The isomeric anhydrosugars mannosan and galactosan were observed with maximum concentrations of 200 and 166 µg/mg OC, respectively, in smoke from duff (Tundra feather moss), as shown Figure 4-17. Minimum concentrations of these anhydrosugars were measured for African Savannah grass with 2 and 3 µg/mg OC, respectively (Figure 4-17).

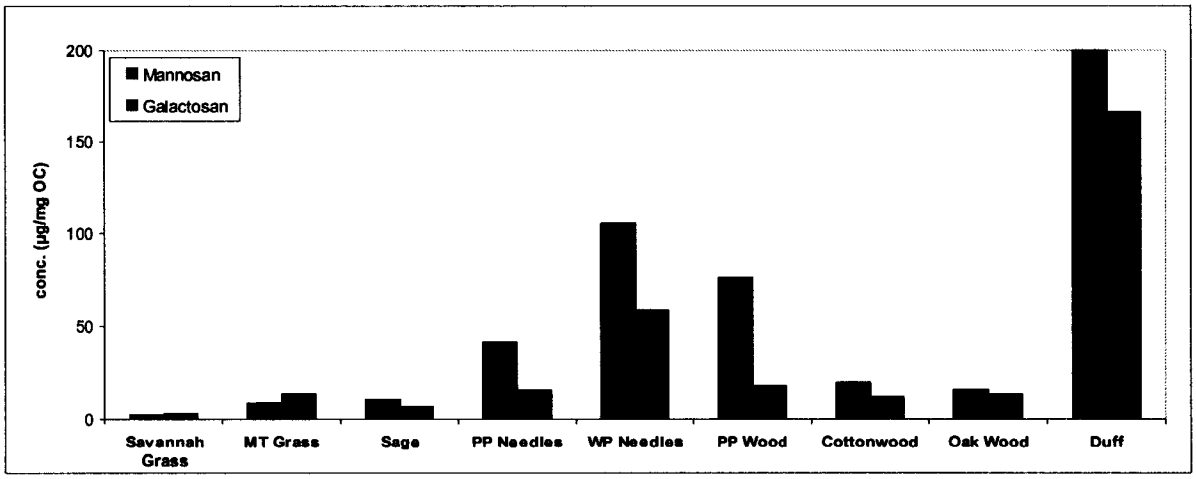

Figure 4-17. Average mannosan and galactosan emission factors for various fuel types.

Emission factors for mannosan and galactosan were generally lower than those of levoglucosan by a factor of three or more, in some cases (e.g., Montana and Savannah grass) by as much as two orders of magnitude, as demonstrated in Figure 4-18. While mannosan and galactosan are derived from hemicellulose, comprising a smaller portion of the total biomass, this alone would not explain the significantly smaller emissions. Hemicellulose is composed of several different sugar monomers, including glucose, xylose, and arabinose, in addition to the "parent" sugars of these anhydrosugars (i.e., mannose and galactose). Thus, mannosan and galactosan are expected to comprise a relatively small fraction of the thermal break-down products, while levoglucosan is released from both biopolymers (cellulose and hemicellulose) contained in wood and other types of biomass. Moreover, the three anhydrosugars (levoglucosan, mannosan, and galactosan) are emitted in varying ratios from different fuel types due to differences in the relative content of cellulose and hemicellulose in different types of biomass. These trends are reflected in ratios of mannosan and galactosan to levoglucosan mass concentrations: the mannosan to levoglucosan ratio was 0.17 on average with a range from 0.005 to 4.1, while the average ratio of galactosan to levoglucosan was 0.08, ranging from 0 (i.e., below detection limits) to 4.0. The observed trends are also are in agreement with previous studies (e.g., Fine et al., 2001, Pashynska et al., 2002, Simoneit et al., 2004, Zdrahal et al., 2002).

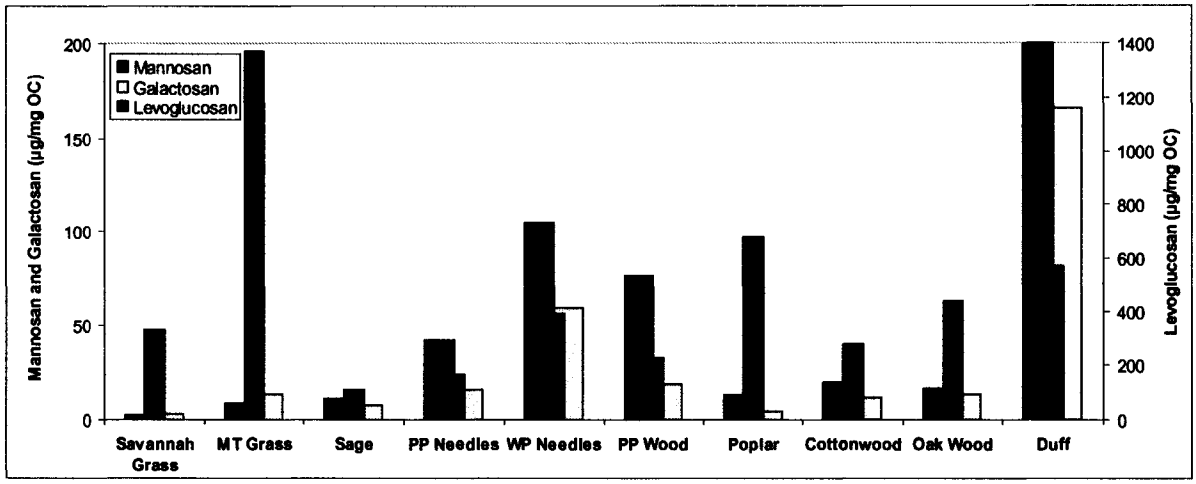

Figure 4-18. Average emission factors for levoglucosan, mannosan, and galactosan from various fuel types (note: levoglucosan emission factors are plotted on a different scale).

Generally, emission factors of the anhydrosugars derived from hemicellulose (e.g., mannosan and galactosan) were larger for softwoods and needles than hardwoods. Hemicellulose in softwoods contains more 6-carbon sugars (e.g., mannose and galactose) compared to hardwoods. Therefore, the combustion of softwoods is expected to release more of the corresponding anhydrosugars, i.e., mannosan and galactosan. The observed trend in the mannosan and galactosan emission factors confirms this theory (Figure 4-18), and is also in agreement with previous findings from residential wood combustion studies (Fine et al., 2001, 2004a, 2004b). Levoglucosan does not follow this pattern, most likely due to the fact that the majority of levoglucosan is released from the thermal degradation of cellulose rather than hemicellulose, unlike its isomers (mannosan and galactosan) that are solely derived from hemicellulose.

Anhydrosugar emission factors were also determined as a function of combustion conditions, i.e., heading versus backing and flaming versus smoldering fires. Table 4-4 summarizes the emission factors for the three anhydrosugars (levoglucosan, mannosan, and galactosan) as a function of fuel type and combustion conditions. Furthermore, emission factors were determined as fractions

of anhydrosugar mass per fine-particle ($PM_{2.5}$) OC mass, as shown for levoglucosan in Figure 4-19, and as fractions of anhydrosugar carbon mass per fine-particle OC mass (Figure 4-20.

Table 4-4. Emission factors for levoglucosan, mannosan, and galactosan (expressed in μg of anhydrosugar per mg of OC).

Type of Biomass	Type of Fire	Levoglucosan (μg/mg OC)	Mannosan (μg/mg OC)	Galactosan (μg/mg OC)
Savannah Grass	Heading	336	3.1	3.1
Savannah Grass	Backing	324	1.6	3.3
Montana Grass	Heading + Backing [a]	1368	8.4	13.4
Sage	Heading	155	14	8.6
Sage	Backing	90	7.7	5.8
PP Needles	Heading	186	50	18.2
PP Needles	Backing	98	15	10.7
WP Needles	Heading	530	144	85.1
WP Needles	Backing	247	66	32.0
PP Wood	Heading	80	26	6.3
PP Wood	Backing	36	7.2	N/D
PP Wood	Flaming	248	97	8.3
PP Wood	Smoldering	539	175	17.6
Cottonwood	Flaming + Smoldering [b]	276	20	11.8
Excelsior (Poplar)	Flaming + Smoldering [b]	680	13	4.3
Oak Wood	Flaming	500	18	17.6
Oak Wood	Smoldering	252	7.8	47.9
Duff	Smoldering	525	216	209

Notes: a.) Sample comprised heading and backing fires; b.) Sampling was conducted during flaming and smoldering fire stages; N/D ... not detected, i.e., below detection limits

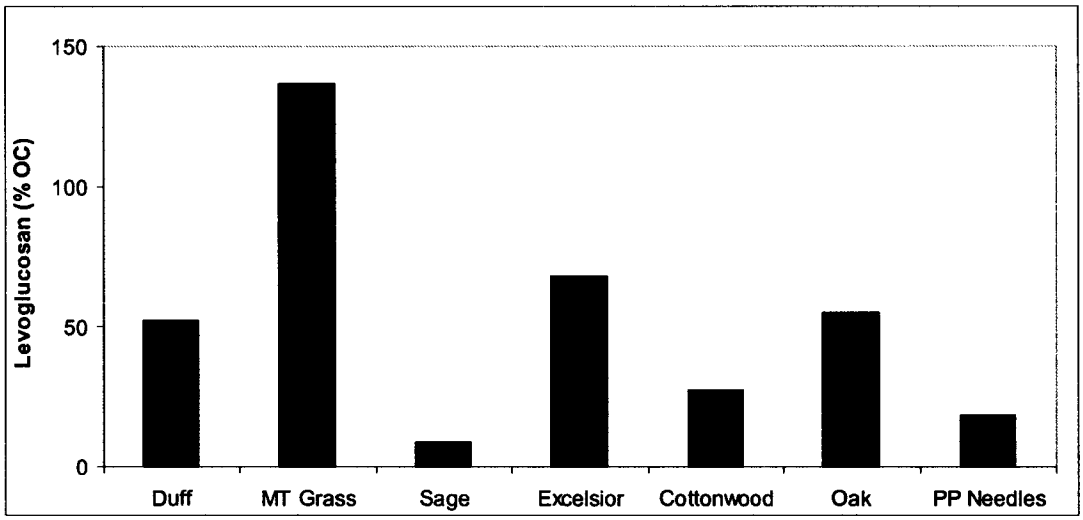

Figure 4-19. Levoglucosan emissions from the combustion of various fuels (expressed as mass percent of OC).

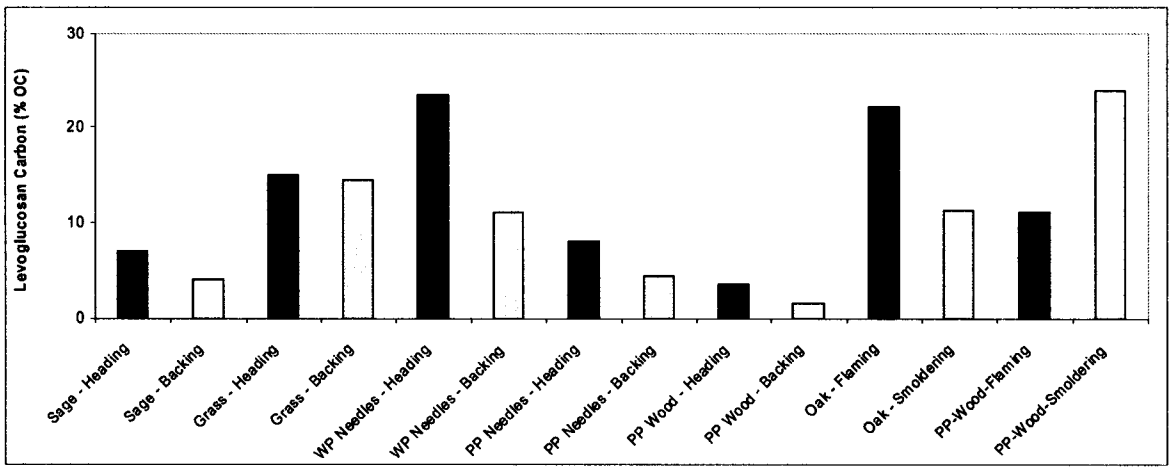

Figure 4-20. Levoglucosan emissions from the combustion of various fuels under different combustion conditions (expressed as percent levoglucosan carbon per OC mass).

The levoglucosan emissions from Montana grass were estimated to be in excess of 100% of OC mass. This is likely due to the fact that OC instead of OM values were used in the computation of the emission factors. OC comprises solely the mass of carbon atoms rather than total organic

mass that includes the mass contributions by heteroatoms (e.g., oxygen, hydrogen, and nitrogen). Because of insufficient information regarding the actual content of the heteroatoms (particularly oxygen) in the organic molecules, OC/OM conversion factors were not determined (other than those for the chamber burns based on mass closure calculations, as described above). OC/OM factors likely vary with type of biomass and combustion conditions.

Different combustion conditions resulted in anhydrosugar emissions that varied with fire phase (flaming versus smoldering combustion stage) and the burn direction (heading versus backing fires). While heading fires of white pine needles, ponderosa pine needles, and sage brush generated higher OC fractions of all three anhydrosugars (levoglucosan, mannosan, and galactosan) compared to backing fires, emission factors for savannah grass were similar for backing and heading fires (Table 4-4 and Figure 4-21). Typical ratios of levoglucosan emission factors for heading versus backing burns were on the order of 2 for pine needles and sage brush. Similar ratios were observed for the isomeric anhydrosugars, mannosan and galactosan. Differences between emission factors from heading and backing fires may be associated with the observation that backing fires burned with slower speeds, possibly resulting in increased flame residence times, while heading fires spread faster and with higher intensity and temperature. The lower levoglucosan emission factors for heading fires of Savannah grass coincided with low OC emissions, as shown above (section 4.3.2.). In addition, carbon monoxide (CO) emissions were lower during the heading fires of this fuel as well, implying higher combustion efficiency that would result in reduced emissions of incomplete combustion products, such as anhydrosugars. It is difficult to draw firm conclusions from these observations, as no burns were conducted during this study to distinguish emissions from flaming versus smoldering fires of Savannah grass. Furthermore, differences in the chemical nature between the individual types of biomass may play an important role in the variation of levoglucosan emission factors. Additional factors influencing emission factors include flame temperature (which is partially determined by the

combustion phase) and fuel moisture. Mannosan and galactosan emission factor ratios for heading versus backing fires followed the same trend as the levoglucosan ratios (Table 4-4 and Figure 4-21). The heading/backing emission factor ratios for the three anhydrosugars were determined as mass ratios described by Equation 4-2:

$$\frac{anhydrosugar_{(heading)} / OC_{(heading)}}{anhydrosugar_{(backing)} / OC_{(backing)}} \qquad (4\text{-}2)$$

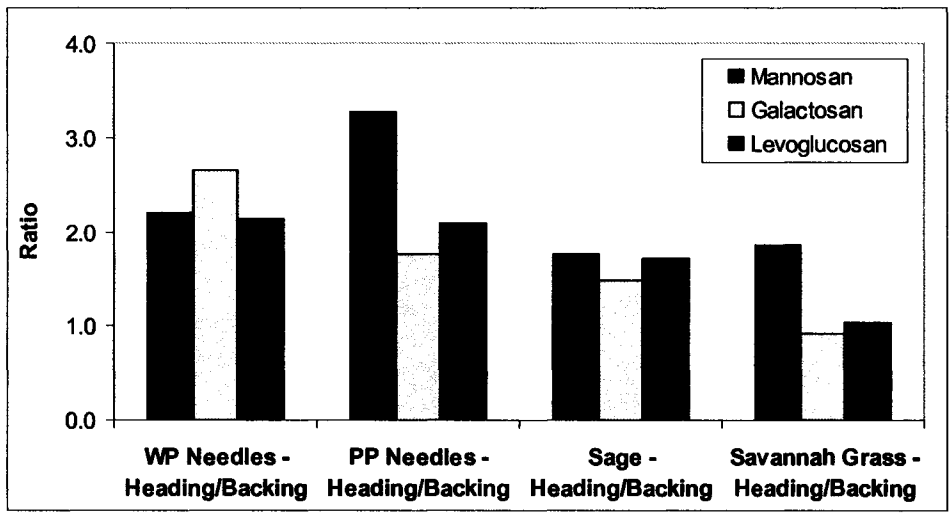

Figure 4-21. Ratios of anhydrosugar emission factors for heading versus backing burns.

As described above (section 4.3.2.), additional combustion experiments were conducted to evaluate emissions from flaming versus smoldering fires of a hardwood (chestnut oak) and a softwood species (ponderosa pine). Flaming fires of oak wood produced roughly twice the mass concentrations of levoglucosan as smoldering burns, expressed by a ratio of approximately 2 for flaming versus smoldering emission factors (Table 4-4 and Figure 4-22). Ponderosa pine wood, on the other hand, generated approximately half the levoglucosan emissions in the flaming phase

compared to the smoldering phase (Table 4-4 and Figure 4-22). Interestingly, changes in emission factor ratios for levoglucosan between the combustion conditions were closely mirrored by changes in mannosan and galactosan ratios (Table 4-4 and Figure 4-22). The flaming/smoldering emission ratios for the three anhydrosugars were determined as mass ratios described in Equation 4-3:

$$\frac{anhydrosugar_{(flaming)} / OC_{(flaming)}}{anhydrosugar_{(smoldering)} / OC_{(smoldering)}} \qquad (4\text{-}3)$$

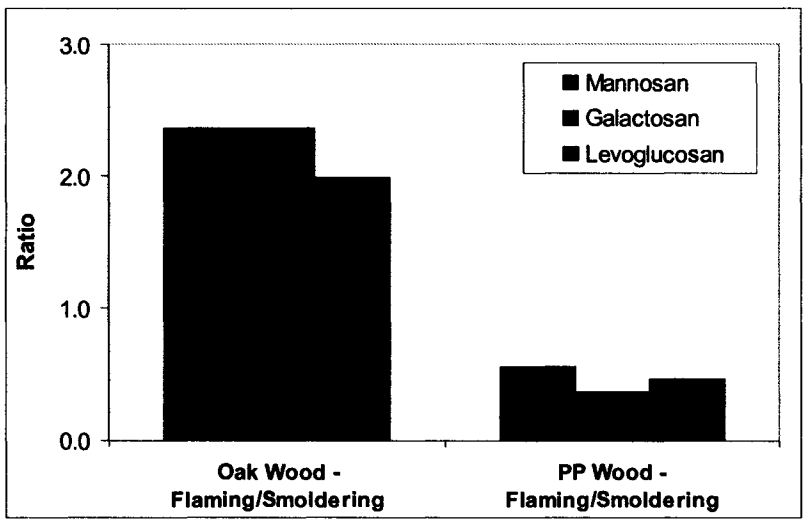

Figure 4-22. Emission factor ratios of anhydrosugars for flaming versus smoldering burns.

The high levoglucosan concentration measured in smoke from the flaming burn of oak wood relative to the smoldering burn (flaming/smoldering ratio = 2.0) is in contrast to observations from other studies (Gao et al., 2003, Schkolnik et al., 2005). However, OC emissions from oak wood were higher during the flaming burn compared to the smoldering fire as well (Figures 4-14 and 4-15). Due to higher combustion efficiency (defined by the ratio of CO to CO_2) common to

flaming fires, primary organic compounds, such as anhydrosugars, potentially decompose to smaller secondary species, whereas the milder combustion conditions associated with smoldering burns in addition to an oxygen-rich environment have been shown to produce higher mass concentrations of PM in general and of anhydrosugars in particular (Gao et al., 2003, Schkolnik et al., 2005). Perhaps the burn temperatures during flaming fires in this study were still below those observed in wildfires or prescribed burns, resulting in higher anhydrosugar emissions than expected for flaming combustion. Unfortunately, the absolute flame temperatures were not measured during this study. On the other hand, the relatively low anhydrosugar (and OC) emission factor ratios observed here for flaming versus smoldering burns of ponderosa pine wood are in good agreement with previous studies (Gao et al., 2003, Schkolnik et al., 2005). The combustion efficiency of the flaming pine wood fires during this study was particularly high relative to flaming fires of other fuel types, characterized by low CO and PM emissions.

The influence of fuel moisture on anhydrosugar and OC emission factors was demonstrated by comparing smoke from wet Montana grass (18% moisture based on dry weight) and dry Savannah grass (6% moisture). The wetter Montana grass was characterized by higher emission factors for OC and $PM_{2.5}$ in general and anhydrosugars in particular (Tables 4-3 and 4-4). The higher water content in Montana grass may have contributed to larger emission factors due to inhibition of flaming, while differences in the chemical and physical nature of the two grasses likely influenced the emission factors as well.

Levoglucosan and OC emission factors correlate well, as demonstrated by a scatter plot of levoglucosan versus OC mass concentrations (Figure 4-23). The correlation factor (R^2) for a linear regression was 0.71, influenced by a rather high levoglucosan mass concentration for Montana grass ($R^2 = 0.89$ when Montana grass is excluded from the data set). Independent measurements by researchers from DRI show the same qualitative trend. Emission factors of

mannosan and galactosan, on the other hand, show weaker correlations with OC emission factors (R^2 = 0.63 and 0.50, respectively).

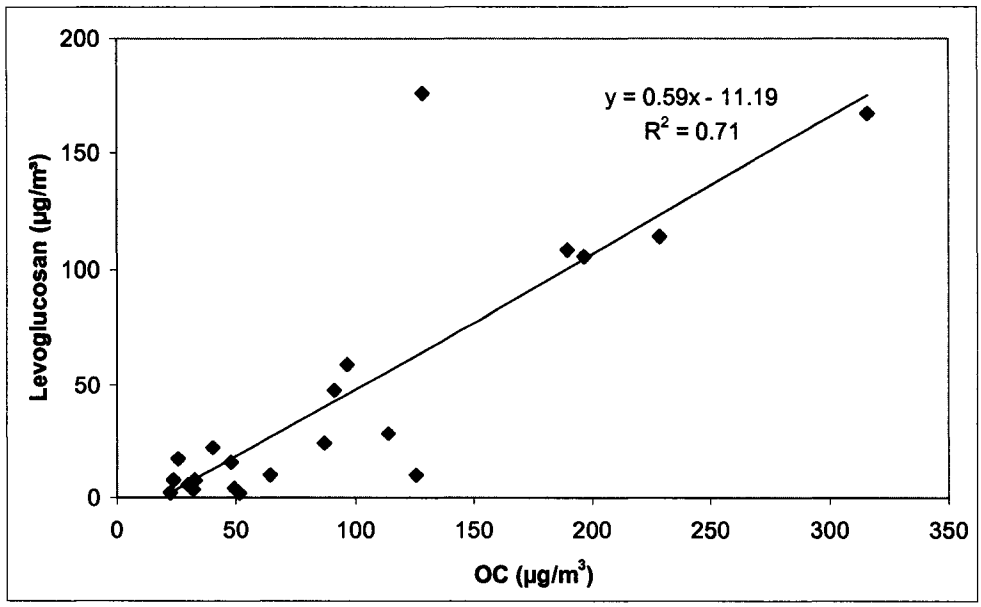

Figure 4-23. Correlation of levoglucosan with OC mass concentrations based on the entire suite of burns conducted during the biomass combustion study.

Soluble potassium (K^+), not of soil or sea salt origin (i.e., present in the fine particle fraction), has been frequently used as indicator of biomass burning (Andreae, 1983, Leslie, 1981, Lewis et al., 1986, Morales et al., 1996, Zweidinger et al., 1990). However, several additional sources for K^+ have been reported, including meat cooking and vegetation (Lawson and Winchester, 1979, Morales et al., 1996, Schauer et al., 1999a, 2002b). Some of these sources may produce K^+ in the fine particle fraction as well. Therefore, the association of K^+ observed in ambient fine particles solely with biomass burning may not necessarily be warranted in all cases. On the other hand, K^+ measured in fine smoke particles, such as those collected during this source sampling study, can exclusively be attributed to biomass burning. However, correlation of levoglucosan with K^+ measured during this study shows no systematic relationship between the two species, as demonstrated in Figure 4-24.

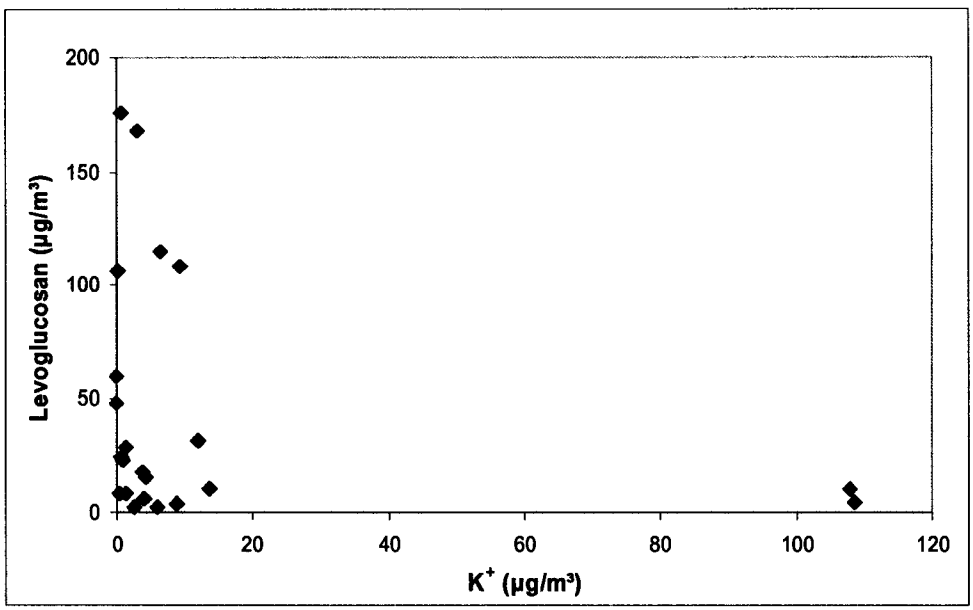

Figure 4-24. Correlation of levoglucosan and K^+ mass concentrations based on the entire suite of measurements from the biomass combustion study.

Levoglucosan and K^+ emission factors may be influenced by combustion conditions, particularly the combustion phase (flaming or smoldering fire), based on different formation mechanisms. Although concentrations of inorganic ions observed in a previous study appeared to be independent of the combustion phase (Gao et al., 2003), emission factors of potassium in particular have been shown to increase significantly with fire temperature (Khalil and Rasmussen, 2003). Moreover, a diurnal variation of levoglucosan/K^+ ratios has been observed which may, in fact, also be related to the combustion phase, as flaming fires tend to prevail during daytime, whereas burning during the night appears to continue as primarily smoldering fires (Schkolnik et al., 2005). While concentrations of inorganic species, such as K^+, are affected to a certain degree by changes in burn temperature (within the limits of typical biomass fires), levoglucosan may be subject to significant thermal alteration at higher temperatures (> 400 °), either due to decomposition to smaller molecules or re-polymerization (Gao et al., 2003, Kawamoto et al.,

2003, Schkolnik et al., 2005). Additional factors may influence the relative concentrations of levoglucosan and K^+ in biomass smoke that are subject to future investigations. Mannosan and galactosan showed a similar relationship to K^+, as demonstrated in Figure 4-25.

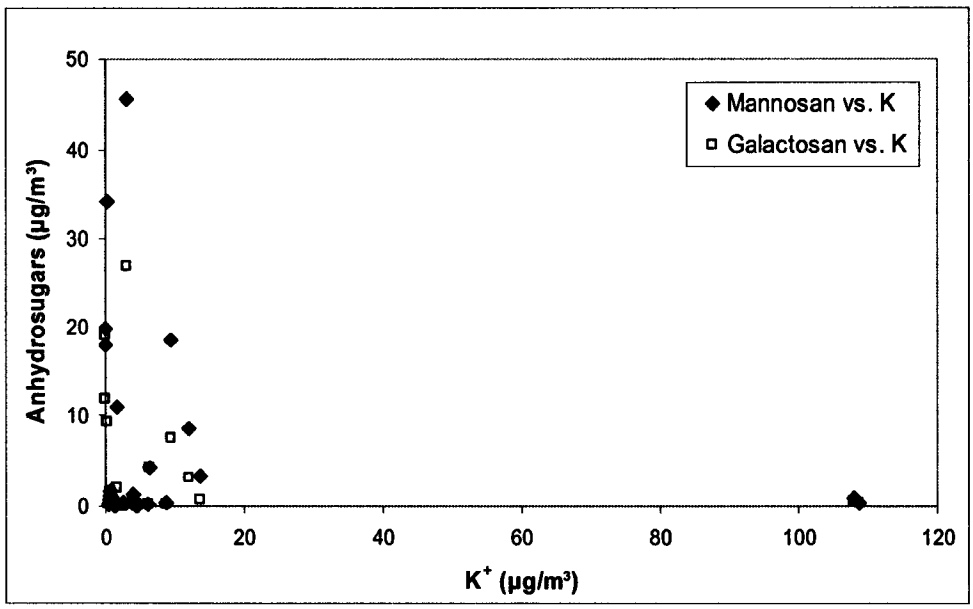

Figure 4-25. Correlation of mannosan and galactosan with K^+ mass concentrations based on the entire suite of measurements from the biomass combustion study.

Emission factors determined in this study were compared to those reported in the literature. Source profiles representative of wildfires and prescribed burns in terms of combustion conditions show a rather narrow range of levoglucosan emission factors (Hays et al., 2005, Hays et al., 2002). Hays et al. (2002) report average levoglucosan emission factors of 4.8% (with a range of 4.3 to 5.6% for three different fuels) for softwoods and 3.6% for mixed hardwoods (Table 4-5). These findings compare reasonably well with the heading (8.0%) and backing burn (3.6%) emission factors for pine wood from this study (Table 4-5), especially when considering that the data reported by Hays et al. (2002) are average emission factors comprising a variety of combustion conditions. However, the flaming and smoldering burns conducted here were characterized by significantly higher levoglucosan emissions (25 and 54%, respectively, for

ponderosa pinewood), as shown in Table 4-5. Likewise, levoglucosan emissions determined in this study from hardwood combustion are higher as well, ranging from 25% (smoldering of oak wood) to 68% (poplar), compared to an emission factor of 3.6% for mixed hardwoods measured by Hays et al. (2002), as demonstrated in Table 4-5.

Table 4-5. Comparison of levoglucosan emission factors from this study with literature source profiles (values are expressed in % fraction of levoglucosan per equivalent of OC).

Type of Biomass	Type of Fire	This Study (% OC)	Hays et al. (2002) (% OC)	Schauer et al. (2001) (% OC)	Fine et al. (2004) (% OC)
PP Needles	Heading	19			
PP Needles	Backing	10			
PP Wood	Heading	8.0	4.3[a]	26[c]	7.1[e]
PP Wood	Backing	3.6			
PP Wood	Flaming	25			
PP Wood	Smoldering	54			
Oak Wood	Flaming	50	3.6[b]	24[d]	
Oak Wood	Smoldering	25			

Notes: a.) value was reported for ponderosa pinewood for mixed-phase (flaming + smoldering) fires; b.) emission factor was reported for mixed hardwoods (predominantly oak); c.) value was reported for combustion of ponderosa pinewood in a residential fireplace; d.) value based on fireplace combustion of oak wood; e.) value was based on fireplace combustion of ponderosa pinewood.

Factors influencing emission factors of levoglucosan (and other anhydrosugars as well as OC in general) include fuel type, combustion phase, fuel bed configuration, time (i.e., duration of a certain fire phase), propagation direction, flame temperature, aeration, fuel moisture content, and the presence of other substances (e.g., acids, bases or salts, either catalyzing or inhibiting the formation of certain combustion products). While the source sampling study conducted by Hays et al. (2002) was based on open combustion of various types of biomass (similar to this study), no distinction was made regarding combustion phase and slope of the surface. Furthermore, the total mass of fuel burned ranged from approximately 5 to 10 kg, whereas the typical fuel mass burned

in this study was 250 g. An additional difference between the two studies was the composition of the fuel: while Hays et al. (2002) used mixtures of fuel components, including branches, needles, and leaves, this study utilized fuel of one configuration only, i.e., either needles or wood from a certain type of biomass. Therefore, emission factors are expected to differ between the two studies. Additional data are shown in Table 4-5 from fireplace and wood stove burning (Fine et al., 2004a, Schauer et al., 2001). The confined combustion environment during these burns contributes an additional factor to those mentioned above, influencing emission factors of anhydrosugars and other organic smoke constituents. In general, emissions from burns under such confined conditions were higher. For instance, levoglucosan emission factors for fireplace combustion of oak or pinewood were reported to be higher than those observed in this study by a factor of approximately six (Table 4-5).

In order to obtain sufficient PM loadings on each filter, sampling was typically conducted to generate composite samples comprised of three burns performed under identical conditions. Thus, the majority of the $PM_{2.5}$ data reported here is characterized by a unique set of conditions (e.g., fuel type, combustion phase, and fire propagation). However, three separate $PM_{2.5}$ samples were collected during one series of combustion experiments (burns 65 - 68: heading fires of ponderosa pine needles) in order to investigate the variability in emission factors between individual burns conducted under the same nominal conditions. Levoglucosan emission factors for these three burns varied from 161 to 205 μg/mg OC. Similarly, OC emission factors had a 30% variability between these burns. Furthermore, a variety of gas-phase chemical species, including CO, CO_2, NO, NO_2, and VOC, measured during each individual burn also showed sizeable differences (in some cases up to 50%) between replicate burns of one fuel type under the same combustion conditions. This phenomenon may be due to several factors, including differences in fuel array and configuration (i.e., how uniformly the fuel is packed), depth of the fuel bed, or composition and dimensions of branches, bark, and leaves. More precise control of

these variables and more replicate burns would be important considerations for future studies. On the other hand, the observed differences in emission factors between replicate burns of the same fuel type may emulate real-world wildfires and prescribed burns more closely, as they are naturally subject to large variability in fuel composition and configuration, as well as combustion conditions.

4.3.6. Anhydrosugar Size Distributions

In addition to the fine-particle (i.e., $PM_{2.5}$) samples, coarse (> 2.5 μm aerodynamic diameter) smoke particles were collected during the majority of the burns. Furthermore, size-segregated samples were collected during the chamber burns, using a multi-stage Hi-Vol impactor. Anhydrosugar mass sampled during stack burns was observed predominantly in fine particles (< 2.5 μm aerodynamic diameter), as shown in Figures 4-25 and 4-26 for levoglucosan and galactosan. On average the levoglucosan fraction measured in coarse particles was approximately 1.2% of that in fine particles ($PM_{2.5}$). The fraction of mannosan and galactosan observed in the coarse fraction was somewhat higher with 6% and 8%, respectively (Figure 4-26).

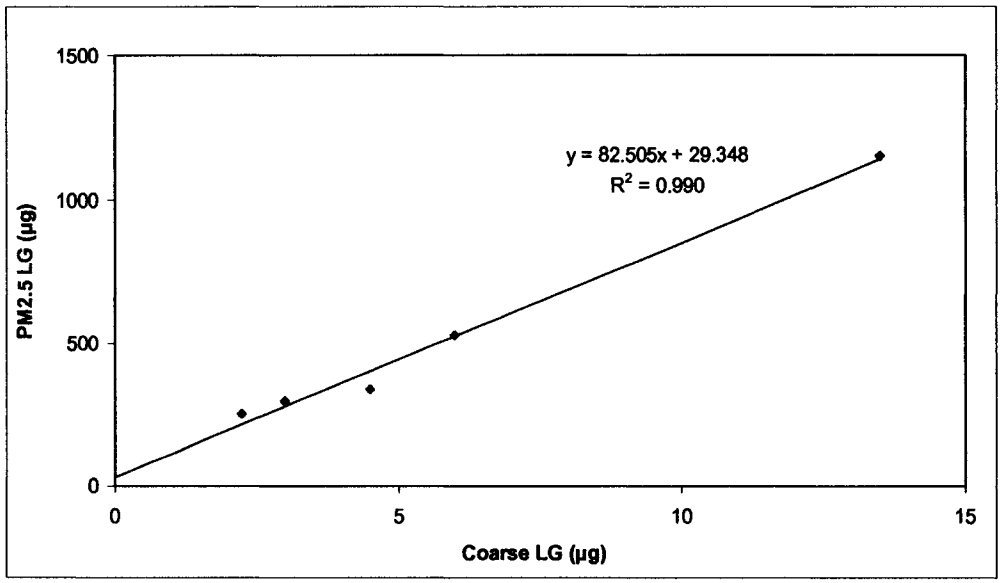

Figure 4-26. Correlation of levoglucosan mass in fine particles ($PM_{2.5}$) versus coarse (> 2.5 µm aerodynamic diameter) particles from burns of white pine needles, sage, and Savannah as well as Montana grasses.

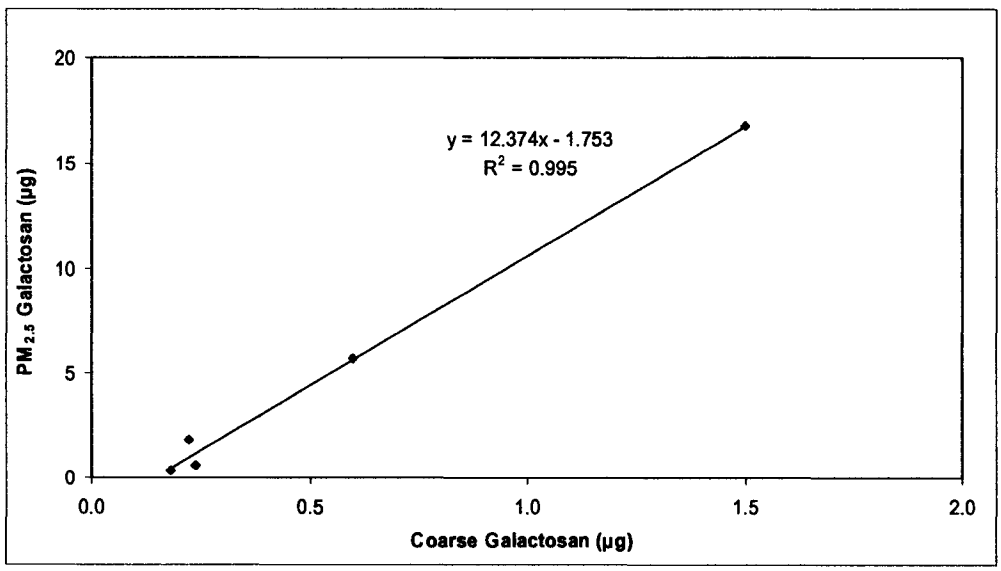

Figure 4-27. Correlation of mannosan mass in fine particles ($PM_{2.5}$) versus the coarse-fraction (> 2.5 µm aerodynamic diameter).

Additional information about the size distribution of levoglucosan in biomass combustion particles was obtained from multi-stage Hi-Vol impactor measurements during the three chamber burns: burns #84 (sage), #85 (duff), and #87 (oak wood). These observations also reveal a predominance of levoglucosan in sub-micron particles (Figures 4-27 and 4-28). In the case of duff smoke slightly higher levoglucosan mass concentrations were measured in the coarse-particle fraction than observed for sagebrush and oak wood, while the majority of the levoglucosan mass was still found in the accumulation mode (Figure 4-28). The slight shift to larger particle sizes may be related to the fact that duff burned in form of a smoldering fire. As smoldering burns are characterized by lower temperatures and thus have lower combustion efficiency, they release more un-combusted condensable products, resulting in the production of larger smoke particles (Reid et al., 2005b). Field measurements of both fairly fresh and aged smoke have also found levoglucosan predominantly present in the fine-particle fraction (Herckes et al., 2005, Schkolnik et al., 2005, Yttri et al., 2005) and chapter 3 of this dissertation.

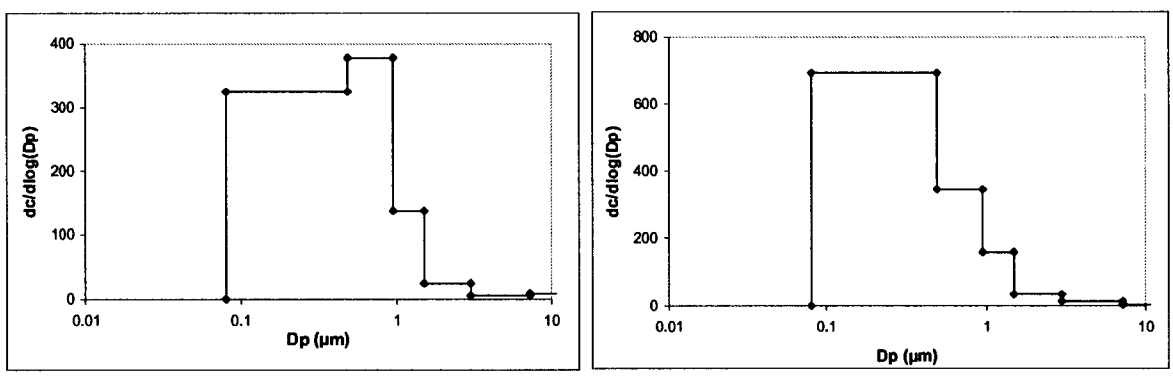

Figure 4-28. Size distributions of levoglucosan for sage brush (left) and oak wood (right).

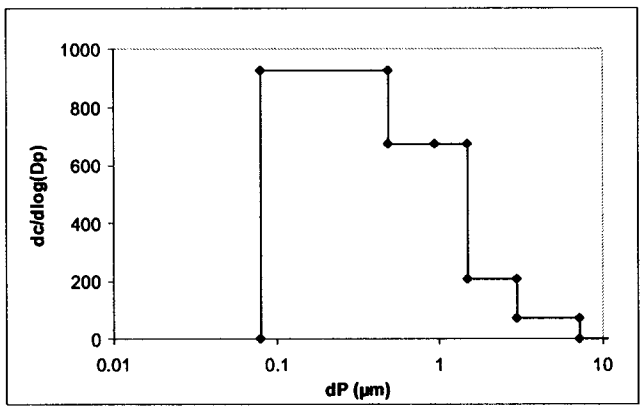

Figure 4-29. Size distributions of levoglucosan for duff (Alaskan feather moss).

4.4. CONCLUSIONS

Emissions from the combustion of biomass differ between controlled, residential burning and wildfires or prescribed burns. Moreover, emissions from different wildfires and prescribed burns exhibit unique chemical and physical characteristics due to differences in the types of biomass burned and the nature of the combustion. During this study various biofuels, including hardwood and softwood, needles, and grasses, were burned in a large combustion chamber under a variety of combustion conditions representative of wildfires and prescribed burns. The emission signatures of individual molecular source tracers were determined as emission factors for several fuel types and combustion conditions. EC/OC emission ratios varied with type of biomass as well as with combustion conditions. Likewise, emission factors for levoglucosan and its isomers (mannosan and galactosan) showed a wide range of values as a function of biomass type and combustion conditions. Levoglucosan emission factors for the same combustion conditions differed from one type of biomass to another type, ranging over an order of magnitude, while

combustion phase (flaming or smoldering) and burn direction (heading or backing) generally produced variations of a factor of 2 to 3 in emission factors for the same fuel type. However, some caution should be used in interpreting these results. Interestingly, anhydrosugar emission factors varied between burns of the same type of biomass and similar combustion conditions, possibly due to differences in fuel array and configuration. Furthermore, the collection of particle-phase organic carbon was likely affected by loss of semivolatile organic compounds (SVOC) and the adsorption of vapor-phase organic compounds, a common set of problems in organic aerosol sampling. Also, some OC may be mis-interpreted as EC depending on the analytical method used. Moreover, differences in analytical methods utilized in this study compared to other source sampling studies, such as for carbon analysis (e.g., optical correction for OC/EC split), may affect the comparability of emission factors.

While both fuel type and combustion conditions were clearly shown to impact emissions characteristics of carbonaceous material, the nature of the fuel appeared to be the dominant factor influencing emission factors. Additional factors include the relative duration of a combustion phase (flaming and smoldering), fuel moisture, and flame temperature (not measured during this study). Furthermore, physical characteristics of the biomass, such as density, can vary between different samples of the same type of biomass and thus influence the speed of propagation of the combustion. Production of condensable organic species that would lead to particle formation can occur in the flaming phase of a burn as well as during the smoldering stage. Also, particle formation may be correlated to CO, both being indicative of incomplete combustion, although due to the influence of various other factors we observed that PM is produced even at low CO emissions (i.e., when CO is being converted to CO_2).

These findings suggest that future source apportionment studies need to utilize detailed emission profiles representative of smoke sources from wildfires and prescribed burns, as emission factors

may vary by a factor of up to 20 between types of biomass burned and combustion conditions. In real-world dynamic fires the combustion processes comprise a wide range of fuel characteristics and combustion conditions (many occurring simultaneously). Even in fires of predominantly one type of biomass, the diversity within that fuel type in terms of the age of individual trees, nature of branches and leaves, moisture content, and physical configuration of the fuel, may result in varying emission characteristics.

While the results from this study give some insight into these variables, further research is necessary to better understand variations of emission factors as a function of biomass type and combustion conditions for wildfires and prescribed burns. Future biomass combustion studies particularly need to include replicate burns and better characterization of the combustions conditions, including flame temperature.

CHAPTER 5 CONCLUSIONS

5.1. SUMMARY and CONCLUSIONS

Organic aerosol constituents in ambient and source samples were successfully determined by GC-MS. Due to the high sensitivity of GC-MS, trace-level organics within various compound classes were accurately measured. Nearly two hundred individual organic compounds were identified and quantified as part of the studies discussed here.

Additionally, three alternative analytical approaches were explored to provide complementary information regarding the composition of fine atmospheric particles based on relatively simple and fast, yet precise and accurate methods: high performance anion exchange chromatography (HPAEC), micro-chip capillary electrophoresis (CE) and an enzyme biosensor. The three methods utilize electrochemical detection techniques (amperometry), providing high sensitivity and selectivity. While the number of analytes amenable to these methods is limited, the resulting selectivity allows for accurate and precise detection and quantification of specific compound classes. In light of the important contributions of biomass combustion to ambient aerosol concentrations, improved measurements are needed to determine the impact of biomass smoke on air quality on regional scales as well as with higher time resolution. The methods discussed here were optimized for the determination of the biomass burning tracers levoglucosan, mannosan, and galactosan.

HPAEC with pulsed amperometric detection (HPAEC-PAD) is a rather new analytical approach for aerosol samples that is capable of measuring various carbohydrates in addition to the anhydrosugars levoglucosan, mannosan, and galactosan over a wide range of concentrations in aqueous extracts of aerosol particles from ambient and source samples. The method was shown to be highly sensitive (MDL for levoglucosan < 0.002 μg/mL) and precise (5% measurement uncertainty for levoglucosan in PM extracts), yet relatively simple without need for chemical derivatization or other complex sample preparation prior to analysis. Due to the high sensitivity of the method, HPAEC-PAD may also be suitable for semi-continuous measurements of fine-particle levoglucosan and other carbohydrates and for routine analyses of biomass combustion tracers in samples from aerosol monitoring networks, such as IMPROVE. Because the technique works well for aqueous solutions, it can also be utilized for direct analyses of atmospheric water samples, including cloud/fog drops and precipitation.

Similar to HPAEC-PAD, the CE-PAD method is characterized by short analysis times and high sensitivity. The method is capable of separating several carbohydrates, including the biomass combustion tracers levoglucosan, mannosan, and galactosan, in less than two minutes. Moreover, the instrumentation is easy to operate and it is less expensive than GC-MS and HPAEC-PAD systems. In addition, CE-PAD and HPAEC-PAD may potentially be interfaced with on-line aerosol collection systems, such as the particle into liquid sampler (PILS), for semi-continuous aerosol characterization, possibly providing important information about chemical constituents in the atmosphere that are subject to rapid changes which can not be measured by current methods.

The biosensor method may be a useful supplemental technique to conventional detection methods for levoglucosan in atmospheric aerosol samples. Due to selective enzyme-catalysis, short response times (< 2 min.), and inexpensive instrumentation, the method may be employed for field applications or screening of large sample sets. However, because of the rather low precision

and sensitivity of the biosensor method in its current state of development, further optimization is needed for the method to be utilized as viable screening tool for ambient aerosol samples influenced by biomass combustion.

The alternative analytical methods described above can provide significant improvements to air pollution and air quality measurements, particularly in determining biomass combustion contributions to ambient PM. Furthermore, these methods may constitute an important step towards closure of the PM mass balance by giving additional insights into the composition of the water-soluble OM fraction. Overall, these methods provide the capability for relatively simple, inexpensive, and sensitive analyses complementary to GC-MS determination of molecular tracers for biomass combustion and other sources.

Detailed chemical analyses, in addition to measurements of physical and aerosol optical properties, during the Yosemite Aerosol Characterization Study (YACS) in the summer of 2002 revealed new insights into aerosol composition and source contributions to regional haze at a western U.S. site with historically high summertime concentrations of carbonaceous aerosol. $PM_{2.5}$ during the timeframe of YACS was dominated by carbonaceous material with an average OM content of 70% (6.3 $\mu g/m^3$ based on an OM/OC multiplier of 1.8), and a peak concentration of 17 $\mu g/m^3$, which is significantly above the long-term (1988-2004) average. More than 90% of the fine OM was derived from contemporary carbon sources rather than fossil fuel combustion, according to radiocarbon measurements (Bench and Herckes, 2004). Additionally, the predominance of biogenic carbon sources was demonstrated by an n-alkane average CPI value of 3.3. Low fossil carbon contributions were further confirmed by estimates of vehicle emission contributions to fine particle OC of approximately 10% on average, using hopane/OC ratios.

Local and regional haze in the western United States, particularly during the summer months, is often influenced by smoke from wildfires. While several smaller fires within Yosemite National Park were responsible for smoke measured during night-time drainage flow out of Yosemite Valley on selected days, two regional haze episodes during YACS were associated with wildfires in California and southern Oregon (McMeeking et al., 2005c), resulting in elevated $PM_{2.5}$ levels for extended periods of time (several days). Molecular source tracers were used in conjunction with measurements of OC and BC, satellite data, and back trajectories to confirm the sources and source regions of the observed regional haze.

Several classes of primary biomass combustion tracers, including anhydrosugars, methoxyphenols, and resin acids, were determined as weekly averages with levoglucosan also measured on a daily basis. Levoglucosan was the dominant tracer species with peak concentrations of 234 ng/m^3 measured during a local fire in Yosemite National Park towards the end of the study and 219 ng/m^3 observed during the regional haze episode in mid August. Primary contributions of biomass smoke to $PM_{2.5}$ organic carbon were estimated to be as high as 65% during the last week of the study (based on weekly average data), using ratios of levoglucosan to OC, and 100% on selected individual days due to the influence of local fires during that time. In addition to smoke from biomass combustion, high concentrations of monoterpene oxidation products and other organic compounds of secondary origin, such as dicarboxylic acids, indicated a significant contribution of secondary organic aerosol (SOA) to fine OM. An important fraction of secondary species was likely associated with smoke from biomass combustion due to enhanced VOC emissions.

Most of the emission source profiles for biomass combustion reported in the literature are based on burning of wood in residential stoves and fireplaces. However, emissions from the combustion of biomass differ between controlled, residential burning and wildfires or prescribed

burns. Moreover, smoke emissions from different wildfires and prescribed burns exhibit unique chemical and physical characteristics due to differences in the types of biomass burned and the nature of the combustion. Various biofuels, including hardwood, softwood, needles, and grasses, were burned in a large chamber under a variety of combustion conditions representative of wildfires and prescribed burns. Emission signatures of OC and EC as well as emission factors (mass of tracer per mass of OC) for individual molecular source tracers were determined for several different fuel types and combustion conditions.

Ratios of EC to OC varied with type of biomass and with combustion conditions. Likewise, emission factors for levoglucosan and its isomers (mannosan and galactosan) showed a wide range of values as a function of biomass type and combustion conditions. Levoglucosan emission factors for the same combustion conditions differed from one type of biomass to another type by one order of magnitude, while combustion phase (flaming or smoldering) and burn direction (heading or backing) generally caused variations in emission factors on the order of 2 to 3 for the same fuel type. While biomass type and combustion conditions were clearly shown to impact emissions characteristics of carbonaceous material, additional factors may have influenced emission factors, including the relative duration of a combustion phase (flaming versus smoldering), flame temperature, air motions, fuel moisture, nature of branches and leaves, and physical configuration of the fuel.

Successful application of receptor-based source apportionment methods requires accurate source profiles that are representative of the emission sources influencing the receptor site. Moreover, the observations from this study demonstrate the need for more detailed emission profiles of molecular source tracers, reflecting the various combustion conditions that are characteristic for wildfires and prescribed burns. Nevertheless, the combustion processes in real-world wildland

fires are complex and comprise a wide range of fuel characteristics and combustion conditions (many occurring simultaneously), complicating accurate assessment of source contributions.

5.2. FUTURE RESEARCH RECOMMENDATIONS

The three alternative analytical methods for biomass smoke tracers described above are at various stages of development. Although the HPAEC-PAD method has been optimized in terms of chromatographic resolution, selectivity, and sensitivity for anhydrosugars, modifications to the method can be made in order to better separate additional carbohydrates, including glucose and mannose, for instance by modifying the eluent gradient. Furthermore, sugar alcohols and other polyols have recently been observed in ambient aerosol particles and may constitute novel indicators for biogenic SOA (Claeys et al., 2004a, Simoneit et al., 2004, Wang et al., 2005). Initial investigations with selected polyols, including arabitol, xylitol, threitol, and erythritol, have shown strong detector response. Additional research is needed to improve the chromatographic separation of these species, particularly the optical isomers, e.g., L-arabitol and D-arabitol. This may be accomplished by changing the eluent pH or by using a chiral HPLC column, although such columns are not available for ion-exchange separations. Chiral columns could be used with HPLC-MS which would simultaneously provide the possibility for identification of additional unidentified polyols and other SOA species.

Coupling HPAEC-PAD with on-line particle collection systems, such as PILS, would provide measurements of biomass smoke tracer concentrations with significantly higher time resolution compared to common filter sampling. With sampling periods potentially as low as 30 minutes (vs. Hi-Vol sampling with 12 or 24-hour sampling times) changes in source contributions that may occur within timeframes of hours could readily be observed. Additional analyte

concentration, for instance on a selective sorbent cartridge, may be required in order to ensure adequate sensitivity, although the intrinsic sensitivity of the HPAEC-PAD method should provide excellent capability for the isomeric anhydrosugar measurements under a wide range of conditions. The total chromatographic run time per injection on the HPAEC system may also be reduced by eliminating or decreasing the length of the column regeneration step and consequently the re-equilibration step by addition of a modifier to the eluent (Cataldi et al., 1999).

While levoglucosan and, presumably, its isomers (mannosan and galactosan) are considered to be stable in the atmosphere over typical fine particle transport times, significant degradation may occur in aqueous media, imposing two major challenges: 1.) the need for preservation of levoglucosan in fog/cloud water samples and aqueous filter extracts. 2.) levoglucosan concentrations may decrease in fine particles due to selective loss of levoglucosan upon scavenging of aerosol particles by atmospheric hydrometeors. As the latter process cannot be influenced, it needs to be better understood and considered in interpreting ambient concentrations of source tracers. On the other hand, attempts were made to preserve levoglucosan in related studies by using chloroform as a biocide. However, application of this method was discontinued because of reduced levoglucosan PAD response due to interference of chloroform or its hydrolysis product (HCl) with levoglucosan or with the detection scheme. Alternatively, preservation of levoglucosan in aqueous filter extracts and fog/cloud samples can possibly be accomplished by destroying microorganisms through exposure with UV light. However, other mechanisms, such as acid or base catalyzed hydrolysis, may be responsible for the degradation of levoglucosan in aqueous samples, instead of or in addition to microbial processes. In such cases the addition of a buffer may minimize the problem, although it may alter other properties of the sample.

Future optimization of the CE-PAD technique should include minimizing potential matrix interferences with anhydrosugar peaks due to differences in conductivity between ambient aerosol sample extracts and CE buffer solution. This could potentially be accomplished by adding a modifier (buffer) to the extract or by extracting directly with buffer solution. Furthermore, additional carbohydrates and polyols may be separated and detected by micro-chip or conventional CE-PAD. Similar to the HPAEC method, micro-chip CE-PAD also has the potential for on-line coupling with semi-continuous aerosol sampling systems, such as PILS, allowing for even higher sampling frequencies due to the short analysis times and small internal volumes.

While the biosensor method has shown promising initial results, further method development is necessary before its useful field application. In particular, the sensitivity and precision of the sensor require improvements. For instance, the use of more sensitive, custom-made electrodes may further lower the detection limits.

Additional evaluations of the detailed chemical speciation data from YACS may include the estimation of source contributions at the valley site, using the molecular marker approach, although the sample set from the valley is relatively small compared to the Turtleback Dome sampling site. Furthermore, the investigation of patterns in the concentrations of certain classes of organic compound may provide useful information regarding source contributions. For instance, the relative abundance of methoxyphenolic acids (in comparison to the corresponding methoxyphenols) may give insight into transport and aging (i.e., stability) of biomass smoke tracers. Additionally, potential patterns in the PAH concentrations may help distinguish contributions from biomass combustion versus vehicle emissions.

Emission signatures of additional biomarkers can be obtained from GC-MS analyses from organic solvent extracts of filters collected during the biomass combustion study. Emission factors of n-alkanes and PAH may be obtained from the neutral extracts, while methoxyphenolic acids, resin acids, and other carboxylic acids can be determined in the methylated portions. In addition, the silylated aliquots may be used to compare concentrations of anhydrosugars with those determined by HPAEC-PAD. Moreover, additional carbohydrates, including sugar alcohols, for which authentic standards are not available may be identified as trimethyl silyl (TMS) derivatives by GC-MS. Furthermore, soluble potassium (K^+) concentrations may be determined in the size-segregated (multi-stage impactor) samples and compared to levoglucosan concentrations in order to gain insight into potential relationships between these biomass smoke tracers. As additional analytical methods become available in our laboratory, such as LC-MS, a more comprehensive characterization of the organic smoke components may be possible. Compound classes to be investigated include polyols, peroxy acids, polyfunctional compounds, water-soluble organic carbon (WSOC) species, and higher molecular weight organic compounds.

While the results from the biomass combustion study give some insight into the variables influencing EC/OC rations and smoke marker emissions, further research is necessary to better understand variations of emission signatures as a function of combustion conditions for wildfires and prescribed burns. Future biomass combustion studies need to include several replicate burns and additional characterization of the combustion conditions. One specific goal of such experiments might be to constrain marker/OC ratios in relevant mixes of fuel types burned under various conditions to better represent real-world wildfires. In addition, it would be very useful to determine the relative importance of fuel characteristics, such as fuel type and moisture content, and burn parameters, including flame temperature, on the emission factors. Moreover, source sampling near actual wildfires would be useful for better assessment of the variability in emission characteristics under real-world conditions.

In order to investigate the formation of SOA during biomass combustion, field experiments may be designed that would track changes in particle composition as the smoke plume from a wild or prescribed fire ages. Such experiments would also give insight into the stability of individual marker species. Possible sampling approaches may include airborne measurements in addition to ground-based observations in order to better track the evolution of the smoke plume over larger distances. Initial sampling would need to be conducted on the order of hours (or fractions of an hour) with sampling intervals becoming longer as the plume ages (e.g., every six hours). Diurnal trends in smoke composition may also be examined by sampling during the night and daytime. In addition to traditional filter-based sampling, novel measurement methods, such as those described above, may be employed in conjunction with semi-continuous sampling in order to monitor the smoke composition with higher time resolution. This is important, as the chemical and physical characteristics are likely to evolve over short periods of time (e.g., hours). The types of smoke constituents to be monitored may include various SOA species, such as terpene oxidation products, dicarboxylic acids, polyacidic and multifunctional compounds, polyols, other WSOC species, and higher molecular weight species, such as HULIS. The examination of the production of SOA and the loss of marker species would be very helpful to better understand long range impacts of biomass smoke on regional air quality, visibility, cloud properties, and climate forcing.

REFERENCES

Abas, M. R. B., Oros, D. R., Simoneit, B. R. T., 2004a. Biomass burning as the main source of organic aerosol particulate matter in Malaysia during haze episodes. Chemosphere 55, 1089–1095.

Abas, M. R. B., Rahman, N. A., Omar, N. Y. M. J., Maah, M. J., Samah, A. A., Oros, D. R., Otto, A., Simoneit, B. R. T., 2004b. Organic composition of aerosol particulate matter during a haze episode in Kuala Lumpur, Malaysia. Atmospheric Environment 38, 4223-4241.

Alessio, G. A., Lillis, M. d., Fanelli, M., Pinelli, P., Loreto, F., 2004. Direct and indirect impacts of fire on isoprenoid emissions from Mediterranean vegetation. Functional Ecology 18, 357–364.

Allen, G. A., Babich, P., Poirot, R. L., 2004. Evaluation of a new approach for real time assessment of wood smoke PM, In: Proceedings of the Regional and Global Perspectives on Haze: Causes, Consequences and Controversies - Visibility Specialty Conference. A&WMA, Asheville, NC.

Allen, J. O., Dookeran, N. M., Taghizadeh, K., Lafleur, A. L., Smith, D. F., Sarofim, A. F., 1997. Measurement of oxygenated polycyclic aromatic hydrocarbons associated with a size-segregated urban aerosol. Environmental Science & Technology 31, 2064-2070.

Allen, J. O., Mayo, P. R., Hughes, L. S., Salmon, L. G., Cass, G. R., 2001. Emissions of size-segregated aerosols from on-road vehicles in the Caldecott tunnel. Environmental Science & Technology 35, 4189-4197.

Alves, C. A., Pio, C. A., Duarte, A. C., 2000. Particulate size distributed organic compounds in a forest environment. Environmental Science & Technology 34, 4287-4293.

Alves, C. A., Pio, C. A., Duarte, A. C., 2001. Composition of extractable organic matter of air particles from rural and urban Portuguese areas. Atmospheric Environment 35, 5485-5496.

Alves, C. A., Carvalho, A., Pio, C. A., 2002. Mass balance of organic carbon fractions in atmospheric aerosols. Journal of Geophysical Research - Atmospheres 107, Art. No. 8345.

Andreae, M. O., 1983. Soot carbon and excess fine potassium - long-range transport of combustion-derived aerosols. Science 220, 1148-1151.

Anttila, P., Hyotylainen, T., Heikkila, A., Jussila, M., Finell, J., Kulmala, M., Riekkola, M. L., 2005. Determination of organic acids in aerosol particles from a coniferous forest by liquid chromatography-mass spectrometry. Journal of Separation Science 28, 337-346.

Baldwin, R. P., 1999. Electrochemical determination of carbohydrates: Enzyme electrodes and amperometric detection in liquid chromatography and capillary electrophoresis. Journal of Pharmaceutical and Biomedical Analysis 19, 69-81.

Baldwin, R. P., 2000. Recent advances in electrochemical detection in capillary electrophoresis. Electrophoresis 21, 4017-4028.

Baldwin, R. P., Roussel, T. J., Crain, M. M., Bathlagunda, V., Jackson, D. J., Gullapalli, J., Conklin, J. A., Pai, R., Naber, J. F., Walsh, K. M., Keynton, R. S., 2002. Fully integrated on-chip electrochemical detection for capillary electrophoresis in a microfabricated device. Analytical Chemistry 74, 3690-3697.

Bench, G., Herckes, P., 2004. Measurement of contemporary and fossil carbon contents of PM2.5 aerosols: Results from Turtleback Dome, Yosemite National Park. Environmental Science & Technology 38, 2424-2427.

Birch, M. E., Cary, R. A., 1996. Elemental carbon-based method for monitoring occupational exposure to particulate diesel exhaust. Aerosol Science and Technology 25, 221-241.

Birch, M. E., 1999. Elemental Carbon (Diesel Particulate): Method 5040, NIOSH.

Bond, T. C., Streets, D. G., Yarber, K. F., Nelson, S. M., Woo, J. H., Klimont, Z., 2004. A technology-based global inventory of black and organic carbon emissions from combustion. Journal of Geophysical Research - Atmospheres 109, Art. No. D14203.

Brown, S. G., Herckes, P., Ashbaugh, L., Hannigan, M. P., Kreidenweis, S. M., Collett, J. L., Jr., 2002. Characterization of organic aerosol in Big Bend National Park, Texas. Atmospheric Environment 36, 5807–5818.

Bushby, B., Fernandes, A., Wallace, D., Kibblewhite, M., 1993. Determination of trace organic micropollutants in atmospheric deposition. Science of the Total Environment 135, 81-94.

Calull, M., Marce, R. M., Borrull, F., 1992. Determination of carboxylic acids, sugars, glycerol and ethanol in wine and grape must by ion-exchange high-performance liquid chromatography with refractive index detection. Journal of Chromatography 590, 215-222.

Carrico, C. M., Kreidenweis, S. M., Malm, W. C., Day, D. E., Lee, T., Carrillo, J., McMeeking, G. R., Collett, J. L., Jr., 2005. Hygroscopic growth behavior of a carbon-dominated aerosol in Yosemite National Park. Atmospheric Environment 39, 1393–1404.

Carrico, C. M., Kreidenweis, S. M., McMeeking, G. R., Sample, L., Engling, G., Wold, C., Lincoln, E., Babbitt, R. E., Day, D. E., Malm, W. C., Collett, J. L., Jr., 2006. Primary biomass smoke dry aerosol optical properties from laboratory combustion of forest fuels. in preparation.

Cass, G. R., 1998. Organic molecular tracers for particulate air pollution sources. Trends in Analytical Chemistry 17, 356-366.

Cataldi, T. R. I., Campa, C., Angelotti, M., Bufo, S. A., 1999. Isocratic separations of closely-related mono- and disaccharides by high-performance anion-exchange chromatography with pulsed amperometric detection using dilute alkaline spiked with barium acetate. Journal of Chromatography A 855, 539-550.

Cataldi, T. R. I., Margiotta, G., Lasi, L., Chio, B. D., Xiloyannis, C., Bufo, S. A., 2000. Determination of sugar compounds in olive plant extracts by anion-exchange chromatography with pulsed amperometric detection. Analytical Chemistry 72, 3902-3907.

Cataldi, T. R. I., Angelotti, M., Bianco, G., 2003. Determination of mono- and disaccharides in milk and milk products by high-performance anion-exchange chromatography with pulsed amperometric detection. Analytica Chimica Acta 485, 43-49.

Chakrabarty, R. K., Moosmüller, H., Garro, M. A., Arnott, W. P., Walker, J. W., Susott, R. A., Babbitt, R. E., Wold, C. E., Lincoln, E. N., Hao, W. M., 2006. Particle emissions from laboratory combustion of wildland fuels: Particle morphology and size. Journal of Geophysical Research - Atmospheres, in press.

Chang, H., Herckes, P., Collett, J. L., 2005. On the use of anion exchange chromatography for the characterization of water soluble organic carbon. Geophysical Research Letters 32, Art. No. L01810.

Charlson, R. J., Schwartz, S. E., Hales, J. M., Cess, R. D., Coakley, J. A., Hansen, J. E., Hofmann, D. J., 1992. Climate forcing by anthropogenic aerosols. Science 255, 423-430.

Chen, L. W. A., Moosmüller, H., Arnott, W. P., Chow, J. C., Watson, J. G., Susott, R. A., Babbitt, R. E., Wold, C. E., Lincoln, E. N., Hao, W. M., 2006. Particle emissions from laboratory combustion of wildland fuels: In-situ optical and mass measurements. Geophysical Research Letters, submitted.

Chow, J. C., Watson, J. G., Pritchett, L. C., Pierson, W. R., Frazier, C. A., Purcell, R. G., 1993. The DRI thermal/optical reflectance carbon analysis system: Description, evaluation and applications in U.S. air quality studies. Atmospheric Environment 27A, 1185-1201.

Christian, T. J., Kleiss, B., Yokelson, R. J., Holzinger, R., Crutzen, P. J., Hao, W. M., Shirai, T., Blake, D. R., 2004. Comprehensive laboratory measurements of biomass-burning

emissions: 2. First intercomparison of open-path FTIR, PTR-MS, and GC-MS/FID/ECD. Journal of Geophysical Research - Atmospheres 109, Art. No. D02311.
Claeys, M., Graham, B., Vas, G., Wang, W., Vermeylen, R., Pashynska, V., Cafmeyer, J., Guyon, P., Andreae, M. O., Artaxo, P., Maenhaut, W., 2004a. Formation of secondary organic aerosols through photooxidation of isoprene. Science 303, 1173-1176.
Claeys, M., Wang, W., Ion, A. C., Kourtchev, I., Gelencser, A., Maenhaut, W., 2004b. Formation of secondary organic aerosols from isoprene and its gas-phase oxidation products through reaction with hydrogen peroxide. Atmospheric Environment 38, 4093-4098.
Crutzen, P. J., Andreae, M. O., 1990. Biomass burning in the tropics - Impact on atmospheric chemistry and biogeochemical Cycles. Science 250, 1669-1678.
Dabek-Zlotorzynska, E., Piechowski, M., McGrath, M., Lai, E. P. C., 2001. Determination of low-molecular-mass carboxylic acids in atmospheric aerosol and vehicle emission samples by capillary electrophoresis. Journal of Chromatography A 910, 331-345.
Dabek-Zlotorzynska, E., Aranda-Rodriguez, R., Graham, L., 2005. Capillary electrophoresis determinative and GC-MS confirmatory method for water-soluble organic acids in airborne particulate matter and vehicle emission. Journal of Separation Science 28, 1520-1528.
Day, D. E., Hand, J. L., Malm, W. C., 2006. Humidification factors from laboratory studies of fresh smoke from biomass fuels. in preparation.
Decesari, S., Facchini, M. C., Fuzzi, S., 2000. Characterization of water-soluble organic compounds in atmospheric aerosol: A new approach. Journal of Geophysical Research - Atmospheres 105, 1481-1489.
Decesari, S., Fuzzi, S., Facchini, M. C., Mircea, M., Emblico, L., Cavalli, F., Maenhaut, W., Chi, X., Schkolnik, G., Falkovich, A., Rudich, Y., Claeys, M., Pashynska, V., Vas, G., Kourtchev, I., Vermeylen, R., Hoffer, A., Andreae, M. O., Tagliavini, E., Moretti, F., Artaxo, P., 2005. Characterization of the organic composition of aerosols from Rondonia, Brazil, during the LBA-SMOCC 2002 experiment and its representation through model compounds. Atmospheric Chemistry and Physics Discussions 5, 5687–5749.
Didyk, B. M., Simoneit, B. R. T., Pezoa, L. A., Riveros, M. L., Flores, A. A., 2000. Urban aerosol particles of Santiago, Chile: Organic content and molecular characterization. Atmospheric Environment 34, 1167-1179.
Eiguren-Fernandez, A., Miguel, A. H., 2003. Determination of semivolatile and particulate polycyclic aromatic hydrocarbons in SRM 1649a and PM2.5 samples by HPLC-fluorescence. Polycyclic Aromatic Compounds 23, 193-205.
Elias, V. O., Simoneit, B. R. T., Cordeiro, R. C., Turcq, B., 2001. Evaluating levoglucosan as an indicator of biomass burning in Carajas, Amazonia: A comparison to the charcoal record. Geochimica et Cosmochimica Acta 65, 267-272.
Engling, G., Carrico, C. M., Kreidenweis, S., Collett Jr., J. L., Day, D. E., Malm, W. C., Hao, W. M., Lincoln, E., Iinuma, Y., Herrmann, H., 2006a. Determination of levoglucosan in biomass combustion aerosol by High Performance Anion Exchange Chromatography with Pulsed Amperometric Detection. Atmospheric Environment, in press.
Engling, G., Herckes, P., Kreidenweis, S. M., Collett, J. L., Jr., 2006b. Composition of the fine organic aerosol in Yosemite National Park during the 2002 Yosemite Aerosol Characterization Study. Atmospheric Environment, in press.
Ervens, B., Feingold, G., Frost, G. J., Kreidenweis, S. M., 2004. A modeling study of aqueous production of dicarboxylic acids: 1. Chemical pathways and speciated organic mass production. Journal of Geophysical Research - Atmospheres 109, Art. No. D15205.
Fanguy, J. C., Henry, C. S., 2002. Pulsed amperometric detection of carbohydrates on an electrophoretic microchip. Analyst 127, 1021-1023.
Figeys, D., Pinto, D., 2000. Lab-on-a-chip: A revolution in biological and medical sciences. Analytical Chemistry 72, 330A-335A.

Fine, P. M., Cass, G. R., Simoneit, B. R. T., 2001. Chemical characterization of fine particle emissions from fireplace combustion of woods grown in the Northeastern United States. Environmental Science & Technology 25, 2665-2675.

Fine, P. M., Cass, G. R., Simoneit, B. R. T., 2004a. Chemical characterization of fine particle emissions from the fireplace combustion of wood types grown in the Midwestern and Western United States. Environmental Engineering Science 21, 387-409.

Fine, P. M., Cass, G. R., Simoneit, B. R. T., 2004b. Chemical characterization of fine particle emissions from the wood stove combustion of prevalent United States tree species. Environmental Engineering Science 21, 705-721.

Fine, P. M., Chakrabarti, B., Krudysz, M., Schauer, J. J., Sioutas, C., 2004c. Diurnal variations of individual organic compound constituents of ultrafine and accumulation mode particulate matter in the Los Angeles basin. Environmental Science & Technology 38, 1296-1304.

Fraser, M. P., Cass, G. R., Simoneit, B. R. T., 1998. Gas-phase and particle-phase organic compounds emitted from motor vehicle traffic in a Los Angeles roadway tunnel. Environmental Science & Technology 32, 2051-2060.

Fraser, M. P., Lakshmanan, K., 2000. Using levoglucosan as a molecular marker for the long-range transport of biomass combustion aerosols. Environmental Science & Technology 34, 4560-4564.

Fraser, M. P., Yue, Z. W., Buzcu, B., 2003. Source apportionment of fine particulate matter in Houston, TX, using organic molecular markers. Atmospheric Environment 37, 2117-2123.

Gao, S., Hegg, D. A., Hobbs, P. V., Kirchstetter, T. W., Magi, B. I., Sadilek, M., 2003. Water-soluble organic components in aerosols associated with savannah fires in Southern Africa: Identification, evolution, and distribution. Journal of Geophysical Research - Oceans and Atmospheres - Atmospheres 108, Art. No. 8491.

Garcia, C. D., Henry, C. S., 2003. Direct determination of carbohydrates, amino acids, and antibiotics by microchip electrophoresis with pulsed amperometric detection. Analytical Chemistry 75, 4778-4783.

Garcia, C. D., Engling, G., Herckes, P., Collett, J. L., Jr., Henry, C. S., 2005. Determination of levoglucosan from smoke samples using microchip capillary electrophoresis with pulsed amperometric detection. Environmental Science & Technology 39, 618-623.

Glasius, M., Duane, M., Larsen, B. R., 1999. Determination of polar terpene oxidation products in aerosols by liquid chromatography-ion trap mass spectrometry. Journal of Chromatography A 833, 121-135.

Glasius, M., Lahaniati, M., Calogirou, A., Di Bella, D., Jensen, N. R., Hjorth, J., Kotzias, D., Larsen, B. R., 2000. Carboxylic acids in secondary aerosols from oxidation of cyclic monoterpenes by ozone. Environmental Science & Technology 34, 1001-1010.

Gogou, A., Stratigakis, N., Kanakidou, M., Stephanou, E. G., 1996. Organic aerosols in Eastern Mediterranean: Components source reconciliation by using molecular markers and atmospheric back trajectories. Organic Geochemistry 25, 79-96.

Gora, R., Hutta, M., 2005. Reversed-phase liquid chromatographic characterization and analysis of air particulates humic (-like) substances in presence of pollens. Journal of Chromatography A 1084, 39-45.

Graham, B., Mayol-Bracero, O. L., Guyon, P., Roberts, G. C., Decesari, S., Facchini, M. C., Artaxo, P., Maenhaut, W., Koll, P., Andreae, M. O., 2002. Water-soluble organic compounds in biomass burning aerosols over Amazonia - 1. Characterization by NMR and GC-MS. Journal of Geophysical Research - Atmospheres 107, Art. No. 8047.

Grosjean, D., Williams, E. L., Grosjean, E., Andino, J. M., Seinfeld, J. H., 1993. Atmospheric oxidation of biogenic hydrocarbons: Reaction of ozone with beta-pinene, D-limonene and trans-caryophyllene. Environmental Science & Technology 27, 2754-2758.

Hand, J. L., Malm, W. C., Laskin, A., Day, D. E., Lee, T., Wang, C., Carrico, C. M., Carrillo, J., Cowin, J. P., Collett, J. L., Jr., Iedema, M. J., 2005. Optical, physical and chemical properties of tar balls observed during the Yosemite Aerosol Characterization Study. Journal of Geophysical Research - Atmospheres 110, Art. No. D21210.

Hansen, A. D. A., Rosen, H., Novakov, T., 1984. The aethalometer — An instrument for the real-time measurement of optical absorption by aerosol particles. The Science of the Total Environment 36, 191-196.

Hatakeyama, S., Ohno, M., Weng, J. H., Takagi, H., Akimoto, H., 1987. Mechanism for the formation of gaseous and particulate products from ozone-cycloalkene reaction in air. Environmental Science & Technology 21, 52-57.

Havers, N., Burba, P., Klockow, D., Klockow-Beck, A., 1998. Characterization of humic-like substances in airborne particulate matter by capillary electrophoresis. Chromatographia 47, 619-624.

Hawthorne, S. B., Miller, D. J., Barkley, R. M., 1987. Identification of Methoxylated Phenols as Tracers of Atmospheric Wood Smoke Pollution, In: Proceedings of the American Chemical Society National Meeting. American Chemical Society, New Orleans, Louisiana.

Hawthorne, S. B., Miller, D. J., Barkley, R. M., Krieger, M. S., 1988. Identification of methoxylated phenols as candidate tracers for atmospheric wood smoke pollution. Environmental Science & Technology 22, 1191-1196.

Hawthorne, S. B., Miller, D. J., Lagenfeld, J. J., Krieger, M. S., 1992. PM-10 high-volume collection and quantitation of semi- and nonvolatile phenols, methoxylated phenols, alkanes, and polycyclic aromatic hydrocarbons from winter urban air and their relationship to wood smoke emissions. Environmental Science & Technology 26, 2251-2262.

Hays, M. D., Geron, C. D., Linna, K. J., Smith, N. D., Schauer, J. J., 2002. Speciation of gas-phase and fine particle emissions from burning of foliar fuels. Environmental Science & Technology 36, 2281-2295.

Hays, M. D., Fine, P. M., Geron, C. D., Kleeman, M. J., Gullett, B. K., 2005. Open burning of agricultural biomass: Physical and chemical properties of particle-phase emissions. Atmospheric Environment 39, 6747-6764.

Hedberg, E., Kristensson, A., Ohlsson, M., Johansson, C., Johansson, P., Swietlicki, E., Vesely, V., Wideqvist, U., 2002. Chemical and physical characterization of emissions from birch wood combustion in a wood stove. Atmospheric Environment 36, 4823-4837.

Heller, A., 1996. Amperometric biosensors. Current Opinion in Biotechnology 7, 50-54.

Helmig, D., Bauer, A., Muller, J., Klein, W., 1990. Analysis of particulate organics in a forest atmosphere by thermodesorption GC/MS. Atmospheric Environment 24A, 179-184.

Herbreteau, B., Salvador, A., Lafosse, M., Dreux, M., 1999. SFC with evaporative light-scattering SFC detection and atmospheric-pressure chemical-ionisation mass spectrometry for methylated glucoses and cyclodextrins analysis. Analusis 27, 706-712.

Herckes, P., Engling, G., Kreidenweis, S. M., Collett, J. L., Jr., 2005. Particle size distributions of organic aerosol constituents during the 2002 Yosemite Aerosol Characterization Study. Environmental Science & Technology, in press.

Hobbs, P. V., Reid, J. S., Kotchenruther, R. A., Ferek, R. J., Weiss, R., 1997. Direct radiative forcing by smoke from biomass burning. Science 275, 1776-1778.

Honda, S., 1996. Separation of neutral carbohydrates by capillary electrophoresis. Journal of Chromatography A 720, 337-351.

Hornig, J. F., Soderberg, R. H., Barefoot, A. C., Galasyn, J. F., 1985. Wood smoke analysis: Vaporization losses of PAH from filters and levoglucosan as a distinctive marker for wood smoke. In: Cooke, M. and Dennis, A. J., Polynuclear Aromatic Hydrocarbons: Mechanisms, Methods, and Metabolism, Batelle Press, 561-568.

Iinuma, Y., Herrmann, H., 2003. Method development for the analysis of particle phase substituted methoxy phenols and aromatic acids from biomass burning using capillary electrophoresis/electro spray ionization mass spectrometry (CE/ESI-MS). Journal of Chromatography A 1018, 105-115.

Iinuma, Y., Boge, O., Gnauk, T., Herrmann, H., 2004. Aerosol-chamber study of the alpha-pinene/O-3 reaction: Influence of particle acidity on aerosol yields and products. Atmospheric Environment 38, 761-773.

Iinuma, Y., Brüggemann, E., Gnauk, T., Andreae, M. O., Helas, G., Müller, K., Parmar, R., Herrmann, H., 2006. Source characterization of biomass burning particles: The combustion of European conifers, African hardwood, savannah grass, German and Indonesian peat. Journal of Geophysical Research - Atmospheres, submitted.

Jandik, P., Cheng, J., Avdalovic, N., 2004. Analysis of amino acid-carbohydrate mixtures by anion exchange chromatography and integrated pulsed amperometric detection. Journal of Biochemical and Biophysical Methods 60, 191-203.

Jang, M., Kamens, R. M., 1999. Newly characterized products and composition of secondary aerosols from the reaction of alpha-pinene with ozone. Atmospheric Environment 33, 459-474.

Jaoui, M., Kamens, R. M., 2003. Gaseous and particulate oxidation products analysis of a mixture of alpha-pinene + beta-pinene/O3/air in the absence of light and alpha-pinene + beta-pinene/NOx/Air in the presence of natural sunlight. Journal of Atmospheric Chemistry 44, 259-297.

Jaoui, M., Kleindienst, T. E., Lewandowski, M., Offenberg, J. H., Edney, E. O., 2005. Identification and quantification of aerosol polar oxygenated compounds bearing carboxylic or hydroxyl groups. 2. Organic tracer compounds from monoterpenes. Environmental Science & Technology 39, 5661-5673.

Jenkin, M. E., Clemitshaw, K. C., 2000. Ozone and other secondary photochemical pollutants: Chemical processes governing their formation in the planetary boundary layer. Atmospheric Environment 34, 2499-2527.

Kavouras, I. G., Mihalopoulos, N., Stephanou, E. G., 1998a. Formation of atmospheric particles from organic acids produced by forests. Nature 395, 683-686.

Kavouras, I. G., Stratigakis, N., Stephanou, E. G., 1998b. Iso- and anteiso-alkanes: Specific tracers of environmental tobacco smoke in indoor and outdoor particle-size distributed urban aerosols. Environmental Science & Technology 32, 1369-1377.

Kavouras, I. G., Mihalopoulos, N., Stephanou, E. G., 1999a. Secondary organic aerosol formation vs primary organic aerosol emission: In situ evidence for the chemical coupling between monoterpene acidic photooxidation products and new particle formation over forests. Environmental Science & Technology 33, 1028-1037.

Kavouras, I. G., Mihalopoulos, N., Stephanou, E. G., 1999b. Formation and gas/particle partitioning of monoterpenes photo-oxidation products over forests. Geophysical Research Letters 26, 55-58.

Kavouras, I. G., Stephanou, E. G., 2002. Particle size distribution of organic primary and secondary aerosol constituents in urban, background marine, and forest atmosphere. Journal of Geophysical Research - Atmospheres 107, Art. No. 4069.

Kawamoto, H., Murayama, M., Saka, S., 2003. Pyrolysis behavior of levoglucosan as an intermediate in cellulose pyrolysis: Polymerization into polysaccharide as a key reaction to carbonized product formation. Journal of Wood Science 49, 469-473.

Kawamura, K., Gagosian, R. B., 1987. Implications of omega-oxocarboxylic acids in the remote marine atmosphere for photo-oxidation of unsaturated fatty acids. Nature 325, 330-332.

Kawamura, K., Kasukabe, H., Barrie, L., 1996. Source and reaction pathways of dicarboxylic acids, ketoacids and dicarbonyls in arctic aerosols: One year of observations. Atmospheric Environment 30, 1709-1722.

Keynton, R. S., Roussel, T. J., Crain, M. M., Jackson, D. J., Franco, D. B., Naber, J. F., Walsh, K. M., Baldwin, R. P., 2004. Design and development of microfabricated capillary electrophoresis devices with electrochemical detection. Analytica Chimica Acta 507, 95-105.

Khalil, M. A. K., Rasmussen, R. A., 2003. Tracers of wood smoke. Atmospheric Environment 37, 1211–1222.

Kiss, G., Gelencser, A., Krivacsy, Z., Hlavay, J., 1997. Occurrence and determination of organic pollutants in aerosol, precipitation, and sediment samples collected at Lake Balaton. Journal of Chromatography A 774, 349-361.

Kjallstrand, J., Ramnas, O., Petersson, G., 2000. Methoxyphenols from burning of Scandinavian forest plant materials. Chemosphere 41, 735-741.

Kleeman, M. J., Schauer, J. J., Cass, G. R., 1999. Size and composition distribution of fine particulate matter emitted from wood burning, meat charbroiling, and cigarettes. Environmental Science & Technology 33, 3516-3523.

Koeber, R., Bayona, J. M., Niessner, R., 1999. Determination of benzo[a]pyrene diones in air particulate matter with liquid chromatography mass spectrometry. Environmental Science & Technology 33, 1552-1558.

Krivacsy, Z., Molnar, A., Tarjanyi, E., Gelencser, A., Kiss, G., Hlavay, J., 1997. Investigation of inorganic ions and organic acids in atmospheric aerosol by capillary electrophoresis. Journal of Chromatography A 781, 223-231.

Krivacsy, Z., Kiss, G., Varga, B., Galambos, I., Sarvari, Z., Gelencser, A., Molnar, A., Fuzzi, S., Facchini, M. C., Zappoli, S., Andracchio, A., Alsberg, T., Hansson, H. C., Persson, L., 2000. Study of humic-like substances in fog and interstitial aerosol by size-exclusion chromatography and capillary electrophoresis. Atmospheric Environment 34, 4273-4281.

Kueckelmann, U., Warscheid, B., Hoffmann, T., 2000. On-line characterization of organic aerosols formed from biogenic precursors using atmospheric pressure chemical ionization mass spectrometry. Analytical Chemistry 72, 1905-1912.

Kutter, J. P., 2000. Current developments in electrophoretic and chromatographic separation methods on microfabricated devices. Trends in Analytical Chemistry 19, 352-363.

Lacher, N. A., Garrison, K. E., Martin, R. S., Lunte, S. M., 2001. Microchip capillary electrophoresis/electrochemistry. Electrophoresis 22, 2526-2536.

Larsen, B. R., Di Bella, D., Glasius, M., Winterhalter, R., Jensen, N. R., Hjorth, J., 2001. Gas-phase OH oxidation of monoterpenes: Gaseous and particulate products. Journal of Atmospheric Chemistry 38, 231-276.

Lawson, D. R., Winchester, J. W., 1979. Sulfur, potassium, and phosphorus associations in aerosols from South-American tropical rain forests. Journal of Geophysical Research - Oceans and Atmospheres 84, 3723-3727.

Lee, S., Baumann, K., Schauer, J. J., Sheesley, R. J., Naeher, L. P., Meinardi, S., Blake, D. R., Edgerton, E. S., Russell, A. G., Clements, M., 2005. Gaseous and particulate emissions from prescribed burning in Georgia. Environmental Science & Technology 39, 9049-9056.

Leslie, A. C. D., 1981. Aerosol Emissions from Forest and Grassland Burnings in the Southern Amazon Basin and Central Brazil. Nuclear Instruments & Methods 181, 345-351.

Lewis, A. C., Askey, S. A., Robinson, R. E., Bartle, K. D., Pilling, M. J., 1995. Identification of polycyclic aromatic compounds in urban air particulate extracts by on-line coupled LC-GC-ITD-MS. Analytical Proceedings Including Analytical Communications 32, 297-300.

Lewis, C. W., Baumgardner, R. E., Stevens, R. K., Russwurm, G. M., 1986. Receptor modeling study of Denver winter haze. Environmental Science & Technology 20, 1126-1136.

Limbeck, A., Puxbaum, H., 1999. A GC-MS method for the determination of polar organic compounds in atmospheric samples. International Journal of Environmental and Analytical Chemistry 73, 329-343.

Lintelmann, J., Fischer, K., Karg, E., Schroppel, A., 2005. Determination of selected polycyclic aromatic hydrocarbons and oxygenated polycyclic aromatic hydrocarbons in aerosol samples by high-performance liquid chromatography and liquid chromatography-tandem mass spectrometry. Analytical and Bioanalytical Chemistry 381, 508-519.

Locker, H. B., 1988. The use of levoglucosan to assess the environmental impact of residential wood-burning on air quality, Ph.D. Dissertation, Dartmouth College, Hanover, NH.

Lopez Hernandez, J., Gonzalez-Castro, M. J., Naya Alba, I., de la Cruz Garcia, C., 1998. High-performance liquid chromatographic determination of mono- and oligosaccharides in vegetables with evaporative light-scattering detection and refractive index detection. Journal of Chromatographic Science 36, 293-298.

Lu, W., Cassidy, R. M., 1993. Pulsed amperometric detection of carbohydrates separated by capillary electrophoresis. Analytical Chemistry 1093, 2878-2881.

Malm, W. C., Sisler, J. F., Pitchford, M. L., Scruggs, M., Ames, R., Copeland, S., Gebhart, K. A., Day, D. E., 2000. IMPROVE (Interagency Monitoring of Protected Visual Environments): Spatial and seasonal patterns and temporal variability of haze and its constituents in the United States: Report III, National Park Service (NPS)/Colorado State University (CSU) - CIRA, Fort Collins, Colorado.

Malm, W. C., Schichtel, B. A., Pitchford, M. L., Ashbaugh, L. L., Eldred, R. A., 2004. Spatial and monthly trends in speciated fine particle concentration in the United States. Journal of Geophysical Research - Atmospheres 109, Art. No. D03306.

Malm, W. C., Day, D., Carrico, C. M., Kreidenweis, S. M., Collett, J. L., Jr., McMeeking, G., Lee, T., Carrillo, J., Schichtel, B. A., 2005a. Intercomparison and closure calculations using measurements of aerosol species and optical properties during the Yosemite Aerosol Characterization Study. Journal of Geophysical Research - Atmospheres 110, Art. No. D14302.

Malm, W. C., Day, D. E., Kreidenweis, S. M., Collett, J. L., Jr., Carrico, C. M., McMeeking, G. R., Lee, T., 2005b. Hygroscopic properties of an organic-laden aerosol. Atmospheric Environment 39, 4969-4982.

Manchester-Neesvig, J. B., Schauer, J. J., Cass, G. R., 2003. The distribution of particle-phase organic compounds in the atmosphere and their use for source apportionment during the Southern California Children's Health Study. Journal of the Air & Waste Management Association 53, 1065–1079.

Mayol Bracero, O. L., Guyon, P., Graham, B., Roberts, G., Andreae, M. O., 2002. Water-soluble organic compounds in biomass burning aerosols over Amazonia - 2. Apportionment of the chemical composition and importance of the polyacidic fraction. Journal of Geophysical Research - Atmospheres 107, Art. No. 8091.

Mazurek, M. A., Cass, G. R., Simoneit, B. R. T., 1989. Interpretation of high-resolution gas chromatography and high-resolution gas chromatography/mass spectrometry data acquired from atmospheric organic aerosol samples. Aerosol Science and Technology 10, 408-420.

McDade, C. E., Eldred, R. A., Ashbaugh, L. L., 2004. Artifact corrections in IMPROVE, In: Proceedings of the Regional and Global Perspectives on Haze: Causes, Consequences and Controversies - Visibility Specialty Conference. A&WMA, Asheville, N.C.

McDonald, R. D., Zielinska, B., Fujita, E. M., Sagebiel, J. C., Chow, J. C., Watson, J. G., 2000. Fine particle and gaseous emission rates from residential wood combustion. Environmental Science & Technology 34, 2080-2091.

McKenzie, L. M., Hao, W. M., Richards, G. N., Ward, D. E., 1995. Measurement and modeling of air toxins from smoldering combustion of biomass. Environmental Science & Technology 29, 2047-2054.

McMeeking, G. R., Kreidenweis, S. M., Carrico, C. M., Collett, J. L., Jr., Day, D. E., Malm, W. C., 2005a. Observations of smoke influenced aerosol during the Yosemite Aerosol

Characterization Study Part II: Aerosol scattering and absorbing properties. Journal of Geophysical Research - Atmospheres 110, Art. No. D18209.
McMeeking, G. R., Kreidenweis, S. M., Carrico, C. M., Lee, T., Collett, J. L., Jr., Malm, W. C., 2005b. Observations of smoke influenced aerosol during the Yosemite Aerosol Characterization Study Part I: Size distributions and chemical composition. Journal of Geophysical Research - Atmospheres 110, Art. No. D09206.
McMeeking, G. R., Kreidenweis, S. M., Lunden, M., Carrillo, J., Carrico, C. M., Lee, T., Herckes, P., Engling, G., Day, D. E., Hand, J. L., Black, N., Malm, W. C., Collett, J. L., Jr., 2005c. Smoke-impacted regional haze in California during Summer 2002. Agricultural and Forest Meteorology, in press.
Miguel, A. H., Eiguren-Fernandez, A., Jaques, P. A., Froines, J. R., Grant, B. L., Mayo, P. R., Sioutas, C., 2004. Seasonal variation of the particle size distribution of polycyclic aromatic hydrocarbons and of major aerosol species in Claremont, California. Atmospheric Environment 38, 3241-3251.
Mogensen, K. B., Klank, H., Kutter, J. P., 2004. Recent developments in detection for microfluidic systems. Electrophoresis 25, 3498-3512.
Morales, J. A., Pirela, D., Durban, J., 1996. Determination of the levels of Na, K, Ca, Mg, Fe, Zn and Cu in aerosols of the western Venezuelan savannah region. Science of the Total Environment 180, 155-164.
Morin-Allory, L., Herbreteau, B., 1992. High-performance liquid chromatography and supercritical fluid chromatography of monosaccharides and polyols using light-scattering detection. Journal of Chromatography 590, 203-213.
Nolte, C. G., Schauer, J. J., Cass, G. R., Simoneit, B. R. T., 2001. Highly polar organic compounds present in wood smoke and in the ambient atmosphere. Environmental Science & Technology 35, 1912-1919.
O'Shea, T. J., Lunte, S. M., 1993. Detection of carbohydrates by capillary electrophoresis with pulsed amperometric detection. Analytical Chemistry 1003, 948-951.
Oefner, P., Chiesa, C., Bonn, G., Horvath, C., 1994. Development of capillary electrophoresis of carbohydrates. Journal of Cap. Elec. 001, 5-26.
Orsini, D. A., Ma, Y. L., Sullivan, A., Sierau, B., Baumann, K., Weber, R. J., 2003. Refinements to the particle-into-liquid sampler (PILS) for ground and airborne measurements of water soluble aerosol composition. Atmospheric Environment 37, 1243-1259.
Palma, P., Cappiello, A., De Simoni, E., Mangani, F., Trufelli, H., Decesari, S., Facchini, M. C., Fuzzi, S., 2004. Identification of levoglucosan and related stereoisomers in fog water as a biomass combustion tracer by ESI-MS/MS. Annali di Chimica 94, 911-919.
Pashynska, V., Vermeylen, R., Vas, G., Maenhaut, W., Claeys, M., 2002. Development of a gas chromatographic/ion trap mass spectrometric method for the determination of levoglucosan and saccharidic compounds in atmospheric aerosols. Application to urban aerosols. Journal of Mass Spectrometry 37, 1249-1257.
Paulus, A., Klockow, A., 1996. Review: Detection of carbohydrates in capillary electrophoresis. Journal of Chromatography A 720, 353-376.
Pearson, J. E., Gill, A., Vadgama, P., 2000. Analytical aspects of biosensors. Annals of Clinical Biochemistry 37, 119-145.
Penner, J. E., Dickinson, R. E., O'Neill, C. A., 1992. Effects of aerosols from biomass burning on the global radiation budget. Science 256, 1432-1433.
Penner, J. E., Charlson, R. J., Hales, J. M., Laulainen, N. S., Leifer, R., Novakov, T., Ogren, J., Radke, L. F., Schwartz, S. E., Travis, L., 1994. Quantifying and minimizing uncertainty of climate forcing by anthropogenic aerosols. Bulletin of the American Meteorological Society 75, 375-400.

Pereira, P. A. D., de Andrade, J. B., Miguel, A. H., 2001. Determination of 16 priority polycyclic aromatic hydrocarbons in particulate matter by HRGC-MS after extraction by sonication. Analytical Sciences 17, 1229-1231.

Plewka, A., Hofmann, D., Mueller, K., Herrmann, H., 2003. Determination of biogenic organic compounds in airborne particles by solvent extraction, derivatisation and mass spectrometric detection. Chromatographia 57, S253-S259.

Plewka, A., Gnauk, T., Brüggemann, W., Neusüss, C., Herrmann, H., 2004. Size-resolved aerosol characterization for a polluted episode at the IfT research station Melpitz in autumn 1997. Journal of Atmospheric Chemistry 48, 131–156.

Poore, M. W., 2002. Levoglucosan in PM2.5 at the Fresno Supersite. Journal of the Air & Waste Management Association 52, 3-4.

Ramdahl, T., 1983. Retene - a molecular marker of wood combustion in ambient air. Nature 306, 580-582.

Reemtsma, T., These, A., 2005. Comparative investigation of low-molecular-weight fulvic acids of different origin by SEC-Q-TOF-MS: New insights into structure and formation. Environmental Science & Technology 39, 3507-3512.

Reid, J. S., Eck, T. F., Christopher, S. A., Koppmann, R., Dubovik, O., Eleuterio, D. P., Holben, B. N., Reid, E. A., Zhang, J., 2005a. A review of biomass burning emissions part III: Intensive optical properties of biomass burning particles. Atmospheric Chemistry and Physics 5, 827-849.

Reid, J. S., Koppmann, R., Eck, T. F., Eleuterio, D. P., 2005b. A review of biomass burning emissions part II: Intensive physical properties of biomass burning particles. Atmospheric Chemistry and Physics 5, 799-825.

Riebau, A. R., Fox, D., 2001. The new smoke management. International Journal of Wildland Fire 10, 415-427.

Rogge, W. F., Hildemann, L. M., Mazurek, M. A., Cass, G. R., Simoneit, B. R. T., 1991. Sources of fine organic aerosol. 1. Charbroilers and meat cooking operations. Environmental Science & Technology 25, 1112-1125.

Rogge, W. F., Hildemann, L. M., Mazurek, M. A., Cass, G. R., 1993a. Sources of fine organic aerosol. 2. Noncatalyst and catalyst-equipped automobiles and heavy-duty diesel trucks. Environmental Science & Technology 27, 636-651.

Rogge, W. F., Mazurek, M. A., Hildemann, L. M., Cass, G. R., 1993b. Quantification of urban organic aerosols at a molecular level: Identification, abundance and seasonal variation. Atmospheric Environment 27A, 1309-1330.

Rogge, W. F., Hildemann, L. M., Mazurek, M. A., Cass, G. R., 1994. Sources of fine organic aerosol. 6. Cigarette smoke in the atmosphere. Environmental Science & Technology 28, 1375-1388.

Samburova, V., Zenobi, R., Kalberer, M., 2005. Characterization of high molecular weight compounds in urban atmospheric particles. Atmospheric Chemistry and Physics 5, 2163-2170.

Sanders, E. B., Goldsmith, A. I., Seeman, J. I., 2003. The model that distinguishes the pyrolysis of D-glucose, D-fructose and sucrose from that of cellulose. Application to the understanding of cigarette smoke formation. Journal of Analytical and Applied Pyrolysis 66, 29-50.

Schauer, J. J., Rogge, W. F., Hildemann, L. M., Mazurek, M. A., Cass, G. R., Simoneit, B. R. T., 1996. Source apportionment of airborne particulate matter using organic compounds as tracers. Atmospheric Environment 30, 3837-3855.

Schauer, J. J., Kleeman, M. J., Cass, G. R., Simoneit, B. R. T., 1999a. Measurement of emissions from air pollution sources. 1. C1 through C29 organic compounds from meat charbroiling. Environmental Science & Technology 33, 1566-1577.

Schauer, J. J., Kleeman, M. J., Cass, G. R., Simoneit, B. R. T., 1999b. Measurement of emissions from air pollutions sources. 2. C1 through C30 organic compounds from medium duty diesel trucks. Environmental Science & Technology 33, 1578-1587.

Schauer, J. J., Cass, G. R., 2000. Source apportionment of wintertime gas-phase air pollutants using organic compounds as tracers. Environmental Science & Technology 34, 1821-1832.

Schauer, J. J., Kleeman, M. J., Cass, G. R., Simoneit, B. R. T., 2001. Measurement of emissions from air pollution sources. 3. C1-C29 organic compounds from fireplace combustion of wood. Environmental Science & Technology 35, 1716-1728.

Schauer, J. J., Kleeman, M. J., Cass, G. R., Simoneit, B. R. T., 2002a. Measurement of emissions from air pollution sources. 5. C1-C32 organic compounds from gasoline-powered motor vehicles. Environmental Science & Technology 36, 1169-1180.

Schauer, J. J., Kleeman, M. J., Cass, G. R., Simoneit, B. R. T., 2002b. Measurement of emissions from air pollution sources. 4. C1-C27 organic compounds from cooking with seed oils. Environmental Science & Technology 36, 567-575.

Schkolnik, G., Falkovich, A. H., Rudich, Y., Maenhaut, W., Artaxo, P., 2005. New analytical method for the determination of levoglucosan, polyhydroxy compounds, and 2-methylerythritol and its application to smoke and rainwater samples. Environmental Science & Technology 39, 2744-2752.

Schnelle, J., Wolf, K., Frank, G., Hietel, B., Gebefugi, I., Kettrup, A., 1996. Particle size-dependent concentrations of polycyclic aromatic hydrocarbons. Analyst 121, 1301-1304.

Schrader, W., Geiger, J., Hoffmann, T., Klockow, D., Korte, E., 1999. Application of gas chromatography-cryocondensation-fourier transform infrared spectroscopy and gas chromatography-mass spectrometry to the identification of gas phase reaction products from the alpha-pinene/ozone reaction. Journal of Chromatography A 864, 299-314.

Schrader, W., Geiger, J., Godejohann, M., Warscheid, B., Hoffman, T., 2001. An analytical approach for a comprehensive study of organic aerosols. Angewandte Chemie International Edition 40, 3998-4001.

Schuetzle, D., Riley, T. L., Prater, T. J., 1982. Analysis of nitrated polycyclic aromatic hydrocarbons in diesel particulates. Analytical Chemistry 54, 265 - 271.

Seinfeld, J. H., Pandis, S. N., 1998. Atmospheric chemistry and physics - from air pollution to climate change, John Wiley & Sons, Inc., New York.

Sheffield, A. E., Currie, L. A., Klouda, G. A., Donahue, D. J., Linick, T. W., Jull, A. J. T., 1990. Accelerator mass spectrometric determination of carbon-14 in the low-polarity organic fraction of atmospheric particles. Analytical Chemistry 62, 2098-2102.

Shimmo, M., Adler, H., Hyotylainen, T., Hartonen, K., Kulmala, M., Riekkola, M. L., 2002. Analysis of particulate polycyclic aromatic hydrocarbons by on-line coupled supercritical fluid extraction-liquid chromatography-gas chromatography-mass spectrometry. Atmospheric Environment 36, 2985-2995.

Shimmo, M., Jantti, J., Aalto, P., Hartonen, K., Hyotylainen, T., Kulmala, M., Riekkola, M. L., 2004. Characterisation of organic compounds in aerosol particles from a Finnish forest by on-line coupled supercritical fluid extraction-liquid chromatography-gas chromatography-mass spectrometry. Analytical and Bioanalytical Chemistry 378, 1982-1990.

Sicre, M. A., Marty, J. C., Saliot, A., 1990. N-Alkanes, fatty acid esters, and fatty acid salts in size fractionated aerosols collected over the mediterranean sea. Journal of Geophysical Research - Atmospheres 95, 3649-3657.

Simoneit, B. R. T., Mazurek, M. A., 1982. Organic matter in the troposphere - II. Natural background of biogenic lipid matter in aerosols over the rural Western United States. Atmospheric Environment 16, 2139-2159.

Simoneit, B. R. T., 1989. Organic matter of the troposphere - V: Application of molecular marker analysis to biogenic emissions into the troposphere for source reconciliations. Journal of Atmospheric Chemistry 8, 251-275.
Simoneit, B. R. T., 1992. Analysis of particulate organics in a forest atmosphere by thermodesorption GC/MS. Atmospheric Environment 26A, 517-519.
Simoneit, B. R. T., Rogge, W. F., Mazurek, M. A., Standley, L. J., Hildemann, L. M., Cass, G. R., 1993. Lignin pyrolysis products, lignans, and resin acids as specific tracers of plant classes in emissions from biomass combustion. Environmental Science & Technology 27, 2533-2541.
Simoneit, B. R. T., Schauer, J. J., Nolte, C. G., Oros, D. R., Elias, V. O., Fraser, M. P., Rogge, W. F., Cass, G. R., 1999. Levoglucosan, a tracer for cellulose in biomass burning and atmospheric particles. Atmospheric Environment 33, 173-182.
Simoneit, B. R. T., Elias, V. O., 2000. Organic tracers from biomass burning in atmospheric particulate matter over the ocean. Marine Chemistry 69, 301-312.
Simoneit, B. R. T., 2002. Biomass burning - a review of organic tracers for smoke from incomplete combustion. Applied Geochemistry 17, 129-162.
Simoneit, B. R. T., Elias, V. O., Kobayashi, M., Kawamura, K., Rushdi, A. I., Medeiros, P. M., Rogge, W. F., Didyk, B. M., 2004. Sugars - Dominant water-soluble organic compounds in soils and characterization as tracers in atmospheric participate matter. Environmental Science & Technology 38, 5939-5949.
Simpson, C. D., Paulsen, M., Dills, R. L., Liu, S., Kalman, D. A., 2005. Determination of methoxyphenols in ambient atmospheric particulate matter: Tracers for wood combustion. Environmental Science & Technology 39, 631-637.
Spanke, J., Rannik, U., Forkel, R., Nigge, W., Hoffmann, T., 2001. Emission fluxes and atmospheric degradation of monoterpenes above a boreal forest: Field measurements and modeling. Tellus 53B, 406–422.
Standley, L. J., Simoneit, B. R. T., 1994. Resin diterpenoids as tracers for biomass combustion aerosols. Journal of Atmospheric Chemistry 18, 1-15.
Temesi, D., Molnar, A., Meszaros, E., Feczko, T., Gelencser, A., Kiss, G., Krivacsy, Z., 2001. Size resolved chemical mass balance of aerosol particles over rural Hungary. Atmospheric Environment 35, 4347-4355.
Turpin, B. J., Lim, H.-J., 2001. Species contributions to PM2.5 mass concentrations: Revisiting common assumptions for estimating organic mass. Aerosol Science and Technology 35, 602-610.
Voegel, P. D., Baldwin, R. P., 1997. Electrochemical detection in capillary electrophoresis. Electrophoresis 18, 2267-2278.
Wang, J., 2001. Glucose biosensors: 40 years of advances and challenges. Electroanalysis 13, 983-988.
Wang, J., 2002. Real-time electrochemical monitoring: Toward green analytical chemistry. Accounts of Chemical Research 35, 811-816.
Wang, W., Kourtchev, I., Graham, B., Cafmeyer, J., Maenhaut, W., Claeys, M., 2005. Characterization of oxygenated derivatives of isoprene related to 2-methyltetrols in Amazonian aerosols using trimethylsilylation and gas chromatography/ion trap mass spectrometry. Rapid Communications in Mass Spectrometry 19, 1343-1351.
Ward, T. J., Smith, G. C., 2005. The 2000/2001 Missoula Valley PM2.5 chemical mass balance study, including the 2000 wildfire season - seasonal source apportionment. Atmospheric Environment 39, 709-717.
Warscheid, B., Hoffmann, T., 2001. On-line measurements of alpha-pinene ozonolysis products using an atmospheric pressure chemical ionisation ion-trap mass spectrometer. Atmospheric Environment 35, 2927-2940.

Weber, R. J., Orsini, D., Daun, Y., Lee, Y. N., Klotz, P. J., Brechtel, F., 2001. A particle-into-liquid collector for rapid measurement of aerosol bulk chemical composition. Aerosol Science and Technology 35, 718-727.

Willeke, K., 1975. Performance of Slotted Impactor. American Industrial Hygiene Association Journal 36, 683-691.

Wilson, R., Turner, A. P. F., 1992. Glucose oxidase: An ideal enzyme. Biosensors & Bioelectronics 7, 165-185.

Wu, W. Z., Wang, J. X., Zhao, G. F., You, L., 2002. The emission soot of biomass fuels combustion as a source of endocrine disrupters. Journal of Environmental Science and Health A37, 579-600.

Yttri, K. E., Dye, C., Slordal, L. H., Braathen, O. A., 2005. Quantification of monosaccharide anhydrides by liquid chromatography combined with mass spectrometry: Application to aerosol samples from an urban and a suburban site influenced by small-scale wood burning. Journal of the Air & Waste Management Association 55, 1169-1177.

Yu, J. Z., Xu, J., Yang, H., 2002. Charring characteristics of atmospheric organic particulate matter in thermal analysis. Environmental Science & Technology 36, 754-761.

Zamfir, A., Peter-Katalinic, J., 2001. Glycoscreening by on-line sheathless capillary electrophoresis/electrospray ionization-quadrupole time of flight-tandem mass spectrometry. Electrophoresis 22, 2448-2457.

Zamfir, A., Vakhrushev, S., Sterling, A., Niebel, H. J., Allen, M., Peter-Katalinic, J., 2004. Fully automated chip-based mass spectrometry for complex carbohydrate system analysis. Analytical Chemistry 76, 2046-2054.

Zdrahal, Z., Oliveira, J., Vermeylen, R., Claeys, M., Maenhaut, W., 2002. Improved method for quantifying levoglucosan and related monosaccharide anhydrides in atmospheric aerosols and application to samples from urban and tropical locations. Environmental Science & Technology 36, 747-753.

Zheng, M., Fang, M., Wang, F., To, K. L., 2000. Characterization of the solvent extractable organic compounds in PM2.5 aerosols in Hong Kong. Atmospheric Environment 34, 2691-2702.

Zheng, M., Cass, G. R., Schauer, J. J., Edgerton, E. S., 2002. Source apportionment of PM2.5 in the Southeastern United States using solvent-extractable organic compounds as tracers. Environmental Science & Technology 36, 2361-2371.

Zook, C. M., LaCourse, W. R., 1995. Pulsed amperometric detection of carbohydrates in fruit juices following high performance anion exchange chromatography. Current Separations 14, 48-52.

Zweidinger, R. B., Stevens, R. K., Lewis, C. W., Westberg, H., 1990. Identification of volatile hydrocarbons as mobile source tracers for fine-particulate organics. Environmental Science & Technology 24, 538-542.

APPENDIX A - List of Standards

Table A-1. Authentic standards used for analyte identification and quantification by GC-MS and HPAEC-PAD.

Compound	Manufacturer	Product No.	CAS No.	Purity	m.w.
Abietic acid	Helix Biotech		514-10-3		302.46
Acetovanillone	Aldrich	A10809	498-02-2	98%	166.18
Adipic acid	Aldrich	24,0524	124-04-9	99+%	146.14
Azelaic acid	Aldrich	24,6379	123-99-9	98%	188.22
20R-Cholestane	Chiron	0622,27	481-21-0	99.9%	372.68
Cholesterol	Aldrich	362794	57-88-5	99%	386.66
2-Decanone	Aldrich	196207	693-54-9	98%	156.27
Dehydroabietic acid	Helix Biotech		1740-19-8		300.44
3,5-Dimethoxy-4-hydroxyacetophenone	Acros	1155400	2478-38-8	97%	196.20
3,5-Dimethoxy-4-hydroxycinnamic acid	Aldrich	D13460-0	530-59-6	97%	224.21
1-Docosanol	Sigma	B-4755	661-19-8	98%	326.61
Dodecanedioic acid	Aldrich	D1009	693-23-2	99%	230.30
Dotriacontane	Acros	11769	544-85-4	99%	450.88
Eicosane	Aldrich	219274	112-95-8	99%	282.55
9,10-Epoxyoctadecanoic acid	Sigma	S812463			298.47
4-Ethylguaiacol	Aldrich	W243604	2785-89-9	98+%	152.19
Eugenol	Aldrich	E51791	97-53-0	99%	164.20
Galactosan	Sigma	A5180	644-76-8		162.14
D-Glucose	Aldrich	G8270	50-99-7	99+%	180.16
Glutaric acid	Aldrich	G3407	110-94-1	99%	132.12

Guaiacol	Acros	12019	90-05-1	99+%	124.14
Hexadecanedioic acid	Fluka	52230	505-54-4	98+%	286.41
Hexatriacontane	Aldrich	H12552	630-06-8	98%	506.98
Homovanillic Acid			306-08-1	98%	182.18
Homovanillyl Alcohol	Aldrich	148830	2380-78-1	99%	168.19
4-Hydroxybenzoic acid	Aldrich	240141	99-96-7	99%	138.12
2-Hydroxyisobutyric acid	Aldrich	16,497-6	594-61-6	98%	104.11
4-Hydroxy-3-methoxycinnamaldehyde	Aldrich	382051	458-36-6	98%	178.18
Isoeugenol	Aldrich	I17206	97-54-1	98%	164.20
Isopimaric acid	Helix Biotech		5835-26-7		302.45
Levoglucosan	Fluka	10390	498-07-7	98+%	162.14
Linoleic acid	Aldrich	23,392-7	60-33-3	99%	280.46
Mannosan	Sigma	A7429	14168-65-1	98%	162.14
D-Mannose	Sigma	D-1502	3458-28-4		180.16
2-Methoxyphenyl acetate	Aldrich	335177	5451-83-2	98%	166.18
4-Methylguaiacol	Aldrich	M6,280-8	93-51-6	99%	138.17
4-Methyl-2,6-dimethoxyphenol	Aldrich	W370401	6638-05-7	97+%	168.19
2-Methylglutaric acid	Aldrich	12,9860	18069-17-5	98%	146.14
(1R)-(+)-Nopinone	Aldrich	327956	38651-65-9	98%	138.21
Octacosane	Acros	12927	630-02-4	99+%	394.77
1-Octacosanol	Sigma	O3379	557-61-9	99%	410.77
2-Octadecanone	Fluka	74733	7373-13-9	97+%	268.48
7-Oxo-dehydroabietic acid	Helix Biotech				314.42
7-Oxooctanoic acid	Aldrich	34,3625	328-51-8	98%	158.20
n-Pentadecanoic Acid	Acros	12983	1002-84-2		242.40
Pimaric acid	Helix Biotech		127-27-5		302.45
Pinic acid	Aldrich	S762792			186.21
cis-Pinonic acid	Aldrich	11,010-8	473-72-3	98%	184.24
Retene	Aldrich	39395-9	483-65-8	81.6%	234.34
Sandaracopimaric acid	Helix Biotech				302.45
β-Sitosterol	Aldrich	S340-2	83-46-5	50%	414.72

Suberic acid	Aldrich	S520	505-48-6	98%	174.20
D-Sucrose	Sigma	S7903	57-50-1	99.5%	342.30
Syringaldehyde	Acros	13288	134-96-3	98%	182.18
Syringic Acid	Aldrich	S800-5	530-57-4	98%	198.18
trans-Cinnamaldehyde	Aldrich	C80687	14371-10-9	99%	132.17
trans-Cinnamic Acid	Aldrich	C80857	140-10-3	99+%	148.16
trans-Norpinic acid	Aldrich	S762806			172.18
6,10,14-Trimethyl-2-pentadecanone	Bedoukian	721	502-69-2		268.48
Vanillic Acid	Aldrich	H3600-1	121-34-6	97%	168.15
Vanillin	Acros	14082	121-33-5	99%	152.15
D-Xylose	Sigma	X3877	58-86-6	99%	150.13

APPENDIX B - Hi-Vol Standard Operating Procedure

$PM_{2.5}$ Sampler: ThermoAndersen GI200-2.5

I. General Instructions

- Do NOT touch the quartz fiber filters with your hands or anything but clean tweezers or aluminum foil.
- Use caution with the quartz fiber filters in order not to damage the fragile substrate.
- Record all observations of any unusual situation or activity or deviations from typical procedures.

II. Changing Filters

In the lab:

1. Inspect new filter for holes and tears; discard if damaged and obtain new filter.
2. Check holder (screen and gaskets) for foreign material and damage.
3. Load new filter onto support screen of the filter holder (centered) with the rough side up.
4. Retain the empty aluminum envelope for the next sample.
5. Re-assemble black frame onto screen (nuts being only slightly hand-tight – do not over tighten).
6. Place protection plate onto holder.

At the collector site:

7. Record the time and any irregular conditions/observations on log sheet.
8. Open collector door + flow event recorder box; record flow (from flow/time disk) on log sheet.
9. Stop flow (on/off switch in timer box).
10. Release the 6 latches on the lower (square) portion of the collector inlet.
11. Open collector inlet by tilting the inlet + locking strut on right side into second position.
12. Loosen black nuts and remove filter holder.
13. If major irregular deposits (bugs) are present on the filter, tilt holder slightly to remove foreign material.
14. Place protection plate on filter holder.
15. Place new filter holder into collector and hand-tighten black nuts (evenly, i.e., diagonally).
16. Close inlet lid + secure with the (6) latches.
17. Raise pen arm on flow event recorder + remove old flow/time disk from recorder.
18. Record sampler name + sampling period on the back of flow/time disk.
19. Insert new flow/time disk.
20. Check time setting on recorder + adjust if necessary by rotating the pin in the center of the recorder with a screwdriver or key.
21. Push pen onto disk + test by manually moving pen up and down drawing a small vertical mark.
22. Record elapsed time (for end + start of sampling periods) on log sheet.
23. Start flow (on/off switch in timer box).
24. Take filter holder back to the lab; handle filter carefully.

In the lab:

25. Remove nuts on black frame and separate the frame from the filter support screen.
26. Label aluminum envelopes (retained from previous filter change) with p-Touch labeling machine.
27. Remove filter with tweezers + place in labeled aluminum envelope.
28. Store filters in freezer.
29. Rinse tips of tweezers with IPA.

APPENDIX C - GC-MS Quantification Sheet - Example

Sample: YS081502HI25SI **Wood Smoke Tracers**

Folder:
Type: Ambient PM2.5 Hi-vol sample + IS WS
Date: GC-MS: 08-13-03; Extr.: 08-12-03
Comments: Silylated Sample

t_R (min.)	Compound	Peak area			Sum	C-28 ratio	C-28 s	LG ratio	LG s	conc. (C28) (ug/mL)	conc. (C28) (ng/m³)	conc. (LG) (ug/mL)	conc. (LG) (ng/m³)
		82	110	112									
7.5	**Benzaldehyde d6**				0								
		77	91	155									
18.0	**Decanoic Acid d19 ME**				0								
		66	82	98									
31.01	**C28D58**	105882	71784	52062	229728								
		240											
29.9	**Chrysene d12**				0								
		206	220	339									
22.02	**Levoglucosan d7 SI**	2269	2048	654	4971								
		329	368	458									
34.9	**Cholesterol**	114	81	65	260	0.00113	0.00702	0.0523	0.00826	0.161	0.081	6.33	3.171
		337	363	468									
35.6	**Ergosterol**				0	0	0.00126	0.0000	0.00149	0	0	0	0
		255	394	484									
36.2	**Stigmasterol**				0	0	0.00321	0.0000	0.00452	0	0	0	0
		204	217	333									
22.06	**Levoglucosan**	751	654	171	1576	0.00686	0.01944	0.3170	0.02915	0.35	0.44	11	13.5
		204	217	333									
22.4	**Galactosan**				0	0.00000	0.01345	0.0000	0.02178	0.00	0.00	0.0	0.00
		204	217	333									
22.6	**Mannosan**				0	0.00000	0.01781	0.0000	0.02285	0.00	0.00	0.0	0.0
	Levoglucosan BLK									0.0570			

APPENDIX D - Molecular Structures of Source Tracers

Vanillin [4-Hydroxy-3-methoxybenzaldehyde]

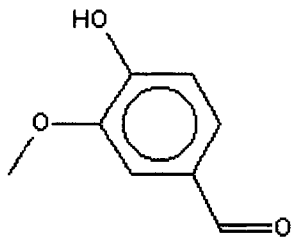

Levoglucosan [1,6-Anhydro-β-D-glucopyranose]

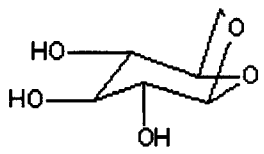

Cholesterol

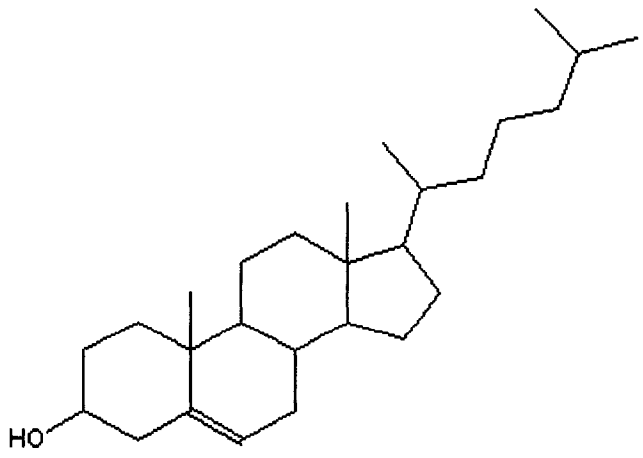

APPENDIX E - YACS Samples

Table E-1. Overview of all individual $PM_{2.5}$ samples collected at Turtleback Dome during the timeframe of YACS.

Sample	Start Date	Start Time	End Date	End Time	Sampling Time (min.)	Flow Rate (m^3/min.)	Sample Volume (m^3)
YS071501HI25	07-14-02	9:05	07-15-02	7:38	1353.0	1.128	1526.2
YS071601HI25	07-15-02	8:49	07-16-02	7:55	1386.0	1.128	1563.4
YS071701HI25	07-16-02	8:12	07-17-02	7:47	1412.0	1.128	1592.7
YS071801HI25	07-17-02	8:17	07-18-02	7:36	1399.0	1.128	1578.1
YS071901HI25	07-18-02	7:56	07-19-02	8:05	1448.0	1.128	1633.3
YS072001HI25	07-19-02	8:45	07-20-02	7:48	1327.0	1.128	1496.9
YS072101HI25	07-20-02	9:12	07-21-02	7:54	1316.0	1.128	1484.4
YS072201HI25	07-21-02	8:30	07-22-02	7:46	1396.0	1.128	1574.7
YS072301HI25	07-22-02	8:29	07-23-02	8:00	1413.0	1.128	1593.9
YS072401HI25	07-23-02	8:26	07-24-02		1354.0	1.126	1524.6
YS072501HI25	07-24-02	8:16	07-25-02	7:45	1409.0	1.126	1586.5
YS072601HI25	07-25-02	8:38	07-26-02	7:45	1389.0	1.126	1564.0
YS072701HI25	07-26-02	8:12	07-27-02	8:57	1424.0	1.126	1603.4
YS072801HI25	07-27-02	8:13	07-28-02	7:05	1373.0	1.126	1546.0
YS072802HI25 [1]	07-28-02	8:41	07-28-02	19:38	656.4	1.126	739.1
YS072901HI25 [1]	07-28-02	19:53	07-29-02	7:37	703.2	1.126	791.8
YS072902HI25 [1]	07-29-02	8:16	07-29-02	19:42	687.0	1.126	773.6
YS073001HI25 [1]	07-29-02	19:56	07-30-02	7:38	701.4	1.126	789.8
YS073002HI25 [1]	07-30-02	8:24	07-30-02	19:13	651.0	1.126	733.0
YS073101HI25 [1]	07-30-02	19:36	07-31-02	7:42	724.8	1.126	816.1
YS080101HI25	07-31-02	8:25	08-01-02	7:44	1398.0	1.126	1574.1
YS080201HI25	08-01-02	8:01	08-02-02	8:00	1440.0	1.126	1621.4

YS080301HI25	08-02-02	8:26	08-03-02	7:42	1395.6	1.126	1571.4
YS080401HI25	08-03-02	8:26	08-04-02	7:53	1407.6	1.126	1585.0
YS080501HI25	08-04-02	8:07	08-05-02	7:52	1426.2	1.126	1605.9
YS080601HI25	08-05-02	8:17	08-06-02	7:54	1415.4	1.126	1593.7
YS080701HI25	08-06-02	8:33	08-07-02	7:46	1392.0	1.126	1567.4
YS080801HI25	08-07-02	8:02	08-08-02	7:41	1419.6	1.126	1598.5
YS080901HI25	08-08-02	8:24	08-09-02	8:02	1420.2	1.126	1599.1
YS081001HI25	08-09-02	8:26	08-10-02	7:51	1405.2	1.126	1582.3
YS081002HI25	08-10-02	8:50	08-10-02	19:52	661.8	1.126	745.2
YS081101HI25	08-10-02	20:04	08-11-02	7:41	696.6	1.126	784.4
YS081201HI25	08-11-02	8:11	08-12-02	7:43	1411.8	1.126	1589.7
YS081301HI25	08-12-02	9:04	08-13-02	8:04	1383.0	1.126	1557.3
YS081302HI25	08-13-02	8:23	08-13-02	19:56	693.0	1.126	780.3
YS081401HI25 [2]	08-13-02	20:08	08-14-02	7:45	697.2	1.126	785.0
YS081402HI25 [2]	08-14-02	8:38	08-13-02	19:28	650.4	1.126	732.4
YS081501HI25 [2]	08-14-02	19:40	08-15-02	7:04	684.0	1.126	770.2
YS081502HI25 [2]	08-15-02	7:44	08-15-02	19:38	714.0	1.126	804.0
YS081601HI25 [2]	08-15-02	19:52	08-16-02	7:56	724.2	1.126	815.4
YS081701HI25	08-16-02	8:33	08-17-02	7:52	1398.6	1.126	1574.8
YS081801HI25	08-17-02	8:15	08-18-02	7:55	1419.0	1.126	1597.8
YS081901HI25	08-18-02	8:35	08-19-02	7:47	1390.8	1.126	1566.0
YS082001HI25	08-19-02	9:02	08-20-02	7:57	1374.6	1.126	1547.8
YS082101HI25	08-20-02	8:32	08-21-02	7:35	1381.8	1.126	1555.9
YS082201HI25	08-21-02	7:52	08-22-02	7:36	1426.8	1.126	1606.6
YS082301HI25	08-22-02	8:41	08-23-02	7:36	1375.8	1.126	1549.2
YS082401HI25	08-23-02	8:06	08-24-02	7:40	1413.6	1.126	1591.7
YS082501HI25	08-24-02	7:53	08-25-02	7:41	1428.6	1.126	1608.6
YS082601HI25	08-25-02	7:45	08-26-02	7:51	1446.0	1.126	1628.2
YS082701HI25	08-26-02	7:56	08-27-02	7:41	1424.4	1.126	1603.9
YS082801HI25	08-27-02	7:47	08-28-02	7:45	1438.2	1.126	1619.4
YS082901HI25	08-28-02	7:51	08-29-02	7:51	1440.0	1.126	1621.4

YS083001HI25	08-29-02	7:55	08-30-02	7:58	1443.0	1.126	1624.8
YS083101HI25	08-30-02	8:04	08-31-02	8:11	1447.8	1.126	1630.2
YS090101HI25	08-31-02	8:21	09-01-02	7:48	1406.4	1.126	1583.6
YS090201HI25	09-01-02	7:52	09-02-02	8:08	1455.6	1.126	1639.0
YS090301HI25	09-01-02	8:12	09-03-02	7:21	1389.6	1.126	1564.7
YS090401HI25	09-01-02	7:25	09-04-02	7:44	1458.6	1.126	1642.4
YS090501HI25	09-01-02	7:48	09-05-02	8:04	1455.6	1.126	1639.0

[1] First intensive haze period; [2] Second intensive haze period

Table E-2. Overview of multi-stage impactor samples collected at Turtleback Dome.

Sample Name	Start Date	Start Time	End Date	End Time	Sampling Time (min.)	Flow Rate (m^3/min.)	Sample Volume (m^3)
YS071401MULA	07-13-02	10:55	07-14-02	7:05	1210	1.13	1367.3
YS071501MULA	07-14-02	9:40	07-15-02	7:41	1321	1.13	1492.7
YS071601MULA	07-15-02	8:36	07-16-02	10:40	1564	1.13	1767.3
YS072001MULA	07-17-02	7:52	07-20-02	7:45	4313	1.13	4873.5
YS072201MULA	07-20-02	9:28	07-22-02	7:03	2690	1.13	3040.2
YS072501MULA	07-22-02	8:31	07-25-02	7:43	4271	1.13	4826.7
YS072801MULA [1]	07-25-02	8:48	07-28-02	7:02	4214	1.13	4761.6
YS072901MULA [1]	07-28-02	8:11	07-29-02	7:32	1400	1.03	1442.4
YS073001MULA [1]	07-29-02	8:44	07-30-02	7:41	1378	1.03	1418.9
YS073101MULA [1]	07-30-02	8:26	07-31-02	7:47	1400	1.03	1442.4
YS080301MULA	07-31-02	8:28	08-03-02	7:47	4246	1.03	4373.0
YS080601MULA	08-03-02	8:56	08-06-02	7:56	4261	1.03	4388.4
YS080801MULA	08-06-02	8:35	08-08-02	7:45	2830	1.03	2914.5
YS081001MULA	08-08-02	8:22	08-10-02	7:54	2849	1.03	2934.3
YS081101MULA	08-10-02	8:24	08-11-02	7:43	1400	1.03	1441.8
YS081401MULA [2]	08-11-02	8:34	08-14-02	7:48	4272	1.03	4400.2
YS081501MULA [2]	08-14-02	8:22	08-15-02	7:07	1366	1.03	1406.6
YS081601MULA [2]	08-15-02	7:40	08-16-02	7:59	1459	1.05	1532.2
YS081901MULA	08-16-02	8:57	08-19-02	7:45	4247	1.05	4459.8
YS082201MULA	08-19-02	9:05	08-22-02	7:42	4233	1.05	4444.7
YS082501MULA	08-22-02	8:53	08-25-02	7:35	4249	1.05	4461.0
YS082801MULA	08-25-02	8:45	08-28-02	7:33	4258	1.05	4470.5
YS083101MULA	08-28-02	8:25	08-31-02	7:43	4274	1.05	4487.5
YS090201MULA	08-31-02	8:16	09-02-02	7:39	2847	1.05	2989.4
YS090501MULA	09-02-02	8:39	09-05-02	8:07	4282	1.05	4495.7

[1] First intensive haze period; [2] Second intensive haze period

Table E-3. Overview of all samples collected in Yosemite Valley (visitors center and Merced River site) during YACS.

Sample Name	Start Date	Start Time	End Date	End Time	Sampling Time (min.)	Flow Rate (m^3/min.)	Sample Volume (m^3)
YVR072401HI10 [1]	07-22-02	14:02	07-24-02	9:13	2268	1.13	2563.0
YVR081501HI10	08-14-02	9:29	08-15-02	11:53	1584	1.13	1789.6
YVR082301HI10	08-22-02	10:07	08-23-02	7:58	1311	1.13	1789.6
YV072901TSPB [2,3]	07-26-02	10:32	07-29-02	9:26	4254	1.07	4551.8
YV080201TSPB	07-29-02	9:35	08-02-02	8:36	5701	1.07	6099.6
YV080401TSPB	08-02-02	8:45	08-04-02	19:20	3515	1.07	3761.5
YV080901TSPB	08-04-02	19:31	08-09-02	20:19	6529	1.07	6985.6
YV081201TSPB	08-09-02	08:45	08-12-02	9:52	4387	1.07	4694.3
YV081601TSPB [4]	08-12-02	9:59	08-16-02	9:34	5735	1.07	6136.9
YV081801TSPB	08-16-02	9:42	08-18-02	19:00	3438	1.07	3678.7
YV082301TSPB	08-18-02	19:12	08-23-02	8:22	6551	1.07	7010.0
YV082601TSPB	08-23-02	8:28	08-26-02	9:29	4382	1.07	4688.5
YV083001TSPB	08-26-02	10:01	08-30-02	8:27	5966	1.07	6383.4
YV090301MULB	08-30-02	8:31	09-03-02	8:18	5446	1.07	5827.4
YV090501MULB	09-03-02	8:49	09-05-02	10:20	2968	1.07	3176.0

[1] YVR ... Visitors center; [2] YV ... Merced River site; [3] First intensive haze period; [4] Second intensive haze period

Table E-4. Overview of $PM_{2.5}$ weekly composite samples from Turtleback Dome.

Composite	Start Date	End Date	Sampling Time (min.)	Flow Rate (m^3/min.)	Sample Volume (m^3)
Week 1	07-14-02	07-20-02	9370	1.128	10569.4
Week 2	07-21-02	07-27-02	9701	1.128	10931.6
Week 3	07-28-02	08-03-02	9730	1.126	10956.4
Week 4	08-04-02	08-10-02	9886	1.126	11131.9
Week 5	08-10-02	07-16-02	8316	1.126	9363.8
Week 6	08-17-02	08-23-02	9767	1.126	10998.1
Week 7	08-24-02	08-30-02	10034	1.126	11298.1
Week 8	08-31-02	09-05-02	8614	1.126	9698.9